

REPUBLIC OF PERU
REPORT ON GEOLOGICAL SURVEY
OF
THE YAURI AREA, SOUTHERN PERU

PHASE III
(VOL. 6)

1960-1961

METAL MINING AGENCY
AND INTERNATIONAL COOPERATION AGENCY
GOVERNMENT OF JAPAN

REPUBLIC OF PERU REPORT ON GEOLOGICAL SURVEY OF THE YAURI AREA, SOUTHERN PERU PHASE III (VOL. 6)

909
55
MP

REPUBLIC OF PERU
REPORT ON GEOLOGICAL SURVEY
OF
THE YAURI AREA, SOUTHERN PERU

PHASE III
(VOL. 6)

JICA LIBRARY



1034938[9]

October 1974

METAL MINING AGENCY
JAPAN INTERNATIONAL COOPERATION AGENCY
GOVERNMENT OF JAPAN

国際協力事業団	
受入 月日 '84. 4. -6	709
	55
登録No. 03075	MP

P R E F A C E

The Government of Japan, in response to the request of the Government of the Republic of Peru decided to conduct a geological survey for mineral exploration in Yauri area, southern part of Peru, and commissioned its implementation to the Overseas Technical Cooperation Agency, which was integrated into the Japan International Cooperation Agency, newly established on August 1, 1974.

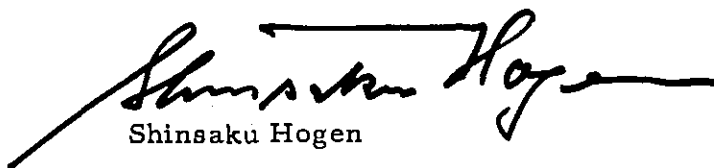
The Agency, taking into consideration of the importance of technical nature of the survey work, in turn, sought the Metal Mining Agency for its cooperation to accomplish the task within a period of three years (1971 - 1973).

This year was the last to complete a series of surveys extending over three years, and as for this current year, a survey team was formed consisting of twenty-four (24) members headed by Mr. Shigeaki Yoshikawa, Mitui Kinzoku Engineering Service Co., Ltd., and sent to the Republic of Peru on October 10, 1973. The team stayed there for seventy-one (71) days from October 11, 1973 to December 20, 1973. During the period of its stay, the team, in close collaboration with the Government of the Republic of Peru and its various authorities, was able to complete survey works on schedule.

This report submitted hereby summarizes the result of the survey performed for the third phase.

I wish to take this opportunity to express my heartfelt gratitude to the Government of the Republic of Peru and the other authorities concerned for their kind cooperation and support extended the Japanese survey team.

October, 1974

A handwritten signature in black ink, appearing to read 'Shinsaku Hogen', with a long horizontal stroke extending to the right.

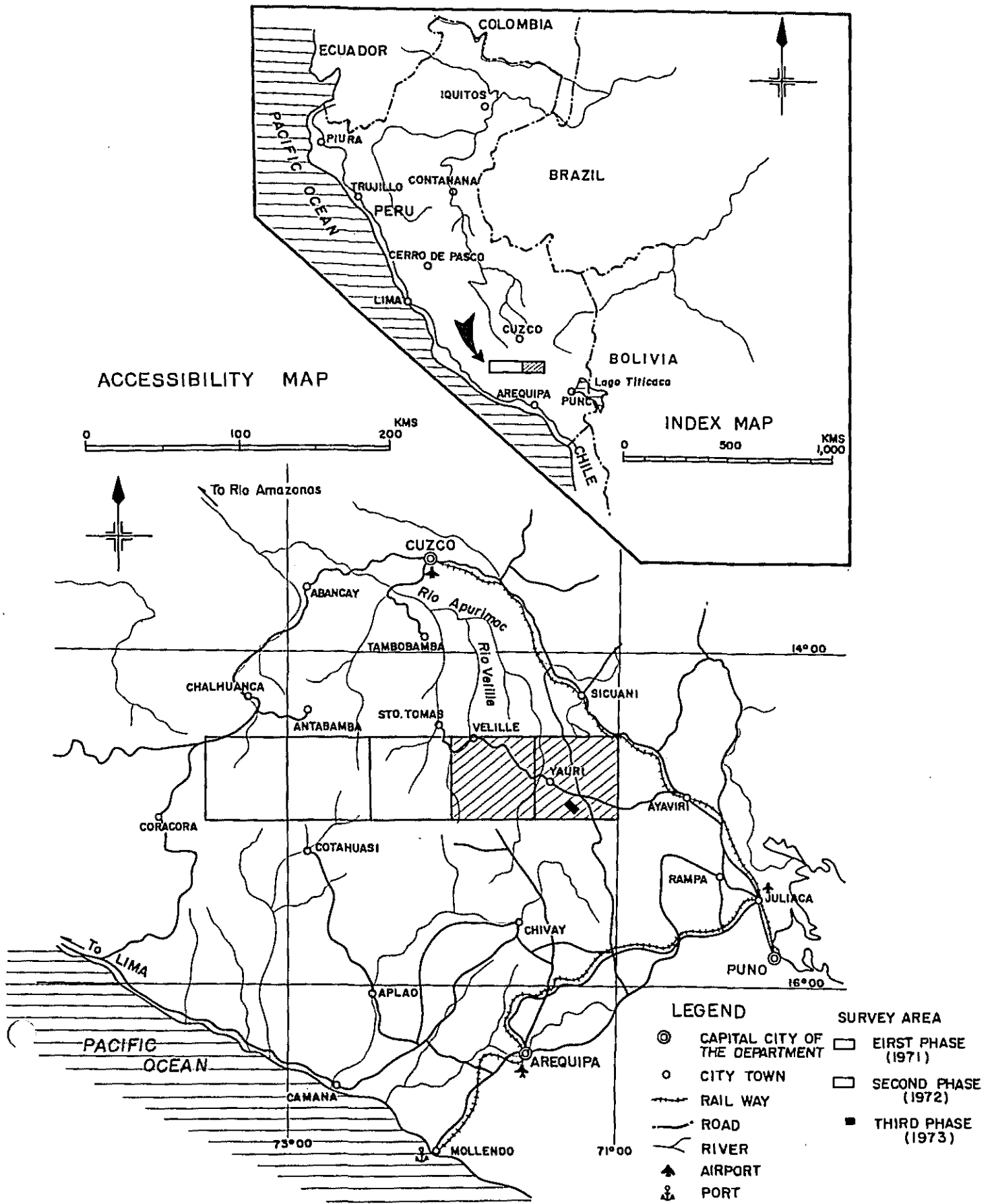
Shinsaku Hogen

President

Japan International Cooperation Agency

Fig. 1

LOCATION MAP OF THE YAURI AREA



GENERAL CONTENTS

PREFACE	i
SUMMARY	v
GENERAL	1

PARTICULARS

PART I	GEOLOGICAL SURVEY	I- 1
PART II	GEOPHYSICAL SURVEY	II- 1
PART III	DRILLING	III- 1

APPENDICES

GEOLOGICAL DATA	A- 1
DRILLING DATA	A-99

ATTACHED MAPS (IN POCKET)

GEOLOGICAL MAPS

GEOPHYSICAL MAPS

SUMMARY

The present survey was carried out in accordance with the program of the third phase of the Yauri area, Republic of Peru.

Based on the geological, geochemical, and gravity surveys of the second phase (1972), both the Coroccohuayco and Huaccollo blocks to the south of Yauri Town were selected as promising areas pregnant with mineral resources.

The object of this survey was to clarify the relation between the subterranean geological structures and the mineralization by conducting geological and geochemical surveys, geophysical survey by IP method, and diamond drillings.

The field works were carried out from October through December, 1973. The principal survey methods adopted were geological mapping of a 1:2,500 scale, geochemical survey by soil sampling (1,681 samples in total) from each point of 200 m x 100 m grid, IP survey in frequency domain with a total extension of measuring lines of 86 km, and in addition, diamond drillings of 6 holes with a total length of 1,503.6 m, in both Coroccohuayco and Huaccollo blocks (an area of 32 square kilometers).

Through these works, data on mineralization zones were newly added to the previous informations on geology and mineralization, and the nature of the mineralized zones could be confirmed in both of the said blocks.

Geology of the surveyed area mainly consists of Mesozoic group and intrusive rocks penetrating it, which are covered by the younger

volcanic rocks, glacial deposits, and alluviums. The geological structure is controlled by a principal direction of NNW-SSE and subordinate one of ENE-WSW rectangular to the former. The surveyed area is divided by a fault crossing at the center in the ENE-WSW direction, and Mesozoic group is prominent in the northern block of the fault (Huaccollo block), while basic plutonic rocks are widely distributed in the southern block (Coroccohuayco block).

The intrusive rocks include plutonic rocks of the earlier intrusion mainly consisting of gabbro and diorite, and acidic to intermediate porphyritic rocks of the later intrusion mostly consisting of quartz monzonite porphyry. The later intrusive rocks are scattered almost throughout the area in the forms of stocks, dikes, sheets, etc., but in the southern block they are distributed from the central to the eastern part, while in the northern block, in the central part, with many of them penetrating in NNW-SSE, the principal structural trend. The mineralization in these blocks is represented by that accompanying network quartz veinlets (confirmed by DDH-4) and that accompanying the copper-bearing skarn around the porphyry (confirmed by DDH-3), and the copper mineralization is directly connected with porphyritic rocks of the later intrusion.

Such alterations related to the mineralization, as silicification, argillization, sericitization, skarnization, chloritization, and epidotization, are predominant, but pervasive association of carbonates may indicate the alteration being different from those of typical porphyry copper type. This may suggest the mineralization of this area has intermediate nature

between skarn copper type (Tintaya ore deposit, for example) and porphyry copper type (Quechua ore deposit, for examples).

The results of age determination on the porphyritic rocks indicated that the age of their intrusion and related alteration is Paleogene, which were added to the data obtained last year.

As a result of precise geochemical survey, copper anomalies were detected predominantly in the surroundings of porphyritic rocks in the Coroccohuayco block, and in the Huaccollo block they were found in the alteration zones of skarnization. Other anomalies were also detected in the northeast of the southern block with possible extension towards east.

Three FE anomalous zones were found by the IP survey. The first zone lies in the center of the northern block (Huaccollo), which seems to be caused by a deep-seated anomalous body. The second one, stretching from the center to the west of the Huaccollo block with a width of 1,500 m, is considered to be ascribed to a blind IP anomalous body, with its possible extension towards Quechua in southwest and in NNW towards Tintaya. The third anomalous zone in the scope of 500 m in width x about 2,500 m in length was detected in the environs of porphyritic rocks along the Qda. Coroccohuayco in the southern block, and DDH-3, which was drilled in the northern outskirts of this zone, has encountered a fairly remarkable copper mineralization of skarn type.

With regard to the drillings, two holes in the Huaccollo block and four holes in the Coroccohuayco block were drilled with a total length of 1,503.6 meters, in which pyritization and copper mineralization

were commonly observed and stronger in and around the porphyritic rocks. Copper ore with skarn was caught in DDH-3, and copper ore accompanying network quartz veinlets in DDH-4; thus, the two types of mineralization were confirmed.

From the results of these surveys, the followings were selected as the areas requiring further investigation:

- (1) Coroccohuayco mineralized zone in the southern block,
- (2) Huaccollo mineralized zone in the northern block,
- (3) The area of eastern extension of the surveyed area and of northern extension of Huaccollo block, where the extended copper mineralization is anticipated with a fair reason of extending tendency of those anomalies obtained through geochemical and IP surveys.

Although Coroccohuayco is the zone where the geological information has been best supplied among the said three, the pilot drillings and trenchings are yet required to investigate the types of intrusion and distribution of porphyritic rocks.

As the geological environments of the Huaccollo block is rather similar to those of the Quechua ore deposit, it is desirable to conduct further pilot drillings in order to clarify the general features of mineralization.

The eastern adjacent of the surveyed area, where high gravity anomaly was detected, would warrant further investigation by such basic surveys as IP and geochemical methods.

It is considered to be an achievement of this survey and a

result of the application of proper methods of investigation, that some potential areas were extracted and selected from a vast area, and both the Coroccohuayco and Huaccollo mineralized zones were finally located, by carrying out a series of fundamental surveys for these three years.

GENERAL

CONTENTS

GENERAL

1.	Introduction	2
1-1	Objects of Surveys	2
1-2	Outline of Surveys	2
2.	General Discussions	7
2-1	Comparison with Survey Results of the Previous Year	7
2-2	Discussions on Geology	8
2-3	Discussions on Geochemical Survey	11
2-4	Discussions on IP Survey	12
2-5	Discussions on Drilling	12
3.	Conclusion and Future Prospect	21
3-1	Conclusion	21
3-2	Comments on Future Surveys	22

CHAPTER 1 INTRODUCTORY REMARKS

1-1 Objects of Surveys

The surveys were drawn up as the third -phase (final phase) survey projects of the Yauri area, and the main objects were to look into the basic conditions of geology controlling the mineralization in the Coroccohuayco and Huaccollo areas, where indications of promising copper mineralization were discovered by the second-phase surveys conducted in 1972, and to examine the general features of ore deposits.

1-2 Outline of Surveys

1-2-1 Scope of Surveys (Refer to Figs. 1 and 2)

The area surveyed lies 25 km to the south-east of Yauri (Fig. 1), and the scope is a block covering an area of 32 square kilometers including both Coroccohuayco and Huaccollo with indications of mineralization as illustrated in Fig. 2.

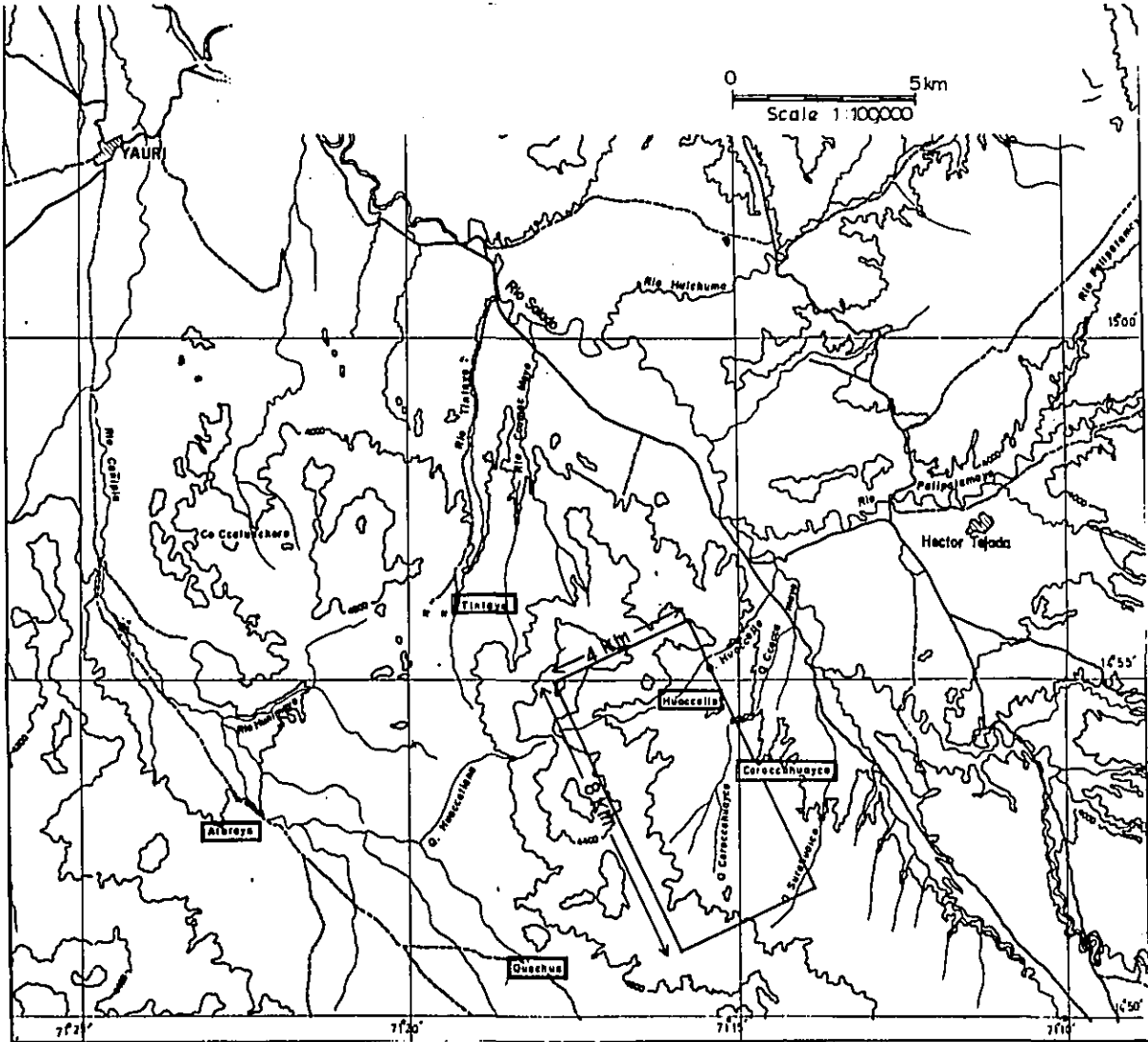
1-2-2 Survey Methods and Period

Geological surveys, geochemical investigations, geophysical investigations by IP method, and structural drillings were carried out.

1) Geological Surveys and Geochemical Investigations

In the whole area surveyed, measuring stations on the grid of 100 m x 200 m were established by transit-tape method and geological mapping of 1:2500 scale was made, and soil samples for geochemical investigations were collected at individual measuring stations (total 1,681 specimens).

Fig. 2 LOCATION MAP OF THE SURVEYED AREA.



The field work required 54 days from October 19 to December 11, 1973.

2) Geophysical Investigations (IP method)

The IP surveys were carried out by the frequency method. The whole block of 27.5 square kilometers equivalent to 85 % of the surveyed area, was covered by 17 measuring lines (with a total length of 68 km) at a spacing of 400 m. In the area including Coroccohuayco and Huaccollo where the indications of mineralization were found in the second -phase geological surveys, 9 measuring lines (with a total length of 18 km) were supplemented in the middle of the 400 m space between the measuring lines, and the surveys were carried out with 26 measuring lines (with a total length of 86 km). The field work required 48 days from October 17 to December 4, 1973.

3) Drilling

The diamond drilling of 6 holes with a total length of 1,503.6 m was carried out at intervals of from 500 m to 2 km, of which 2 holes were drilled in the Huaccollo area and 4 holes in the Coroccohuayco area. The field work required 54 days from October 19 to December 11, 1973.

1-2-3 Constitution of Survey Team

The field surveys and analytical work were conducted by Mitsui Kinzoku Engineering Service Co., Ltd., in cooperation with el Servicio de Geologia y Minería, Republic of Peru.

The constitution of the field survey team was as follows:

1) General Management and Liaison

Head, Shigeaki Yoshikawa	Mitsui Kinzoku Engineering Service Co. , Ltd.
Nobumasa Chiba	Metal Mining Agency
Nobuo Toida	Japan International Cooperation Agency
Hiroshi Sato	Mitsui Kinzoku Engineering Service Co. , Ltd.

2) Geological Survey Party

Koichi Shinoda	Mitsui Kinzoku Engineering Service Co. , Ltd.
Masahiro Kita	Mitsui Kinzoku Engineering Service Co. , Ltd.
Masao Saito	Mitsui Kinzoku Engineering Service Co. , Ltd.
Tsuyoshi Yamada	Mitsui Kinzoku Engineering Service Co. , Ltd.
Tetsuo Sato	Mitsui Kinzoku Engineering Service Co. , Ltd.
Atsushi Takeyama	Mitsui Kinzoku Engineering Service Co. , Ltd.
Julio Acevedo	Servicio de Geologia y Minería, Republic of Peru
Edgar Vardivia	Servicio de Geologia y Minería, Republic of Peru

3) Physical Investigation Party

Shigezo Inuzuka	Mitsui Kinzoku Engineering Service Co. , Ltd.
Takashi Aoyama	Mitsui Kinzoku Engineering Service Co. , Ltd.

Nobuyuki Goto Mitsui Kinzoku Engineering Service
Co., Ltd.

Masaru Hatakeyama Mitsui Kinzoku Engineering Service
Co., Ltd.

Katsuo Sato Mitsui Kinzoku Engineering Service
Co., Ltd.

Akira Kubota Mitsui Kinzoku Engineering Service
Co., Ltd.

Shigeki Asaoka Mitsui Kinzoku Engineering Service
Co., Ltd.

4) Test Drilling Party

Haruo Shimode Mitsui Kinzoku Engineering Service
Co., Ltd.

Yoshiaki Nakagawa Mitsui Kinzoku Engineering Service
Co., Ltd.

Ikuo Tanigawa Mitsui Kinzoku Engineering Service
Co., Ltd.

Koichi Yamashita Mitsui Kinzoku Engineering Service
Co., Ltd.

Mitsuo Nomura Mitsui Kinzoku Engineering Service
Co., Ltd.

Michiyasu Ito Mitsui Kinzoku Engineering Service
Co., Ltd.

Isamu Okazaki Mitsui Kinzoku Engineering Service
Co., Ltd.

CHAPTER 2 GENERAL DISCUSSIONS

2-1 Comparison with Survey Results of the Previous Year

Data on the geology and mineralization of the surveyed area were remarkably increased through the geological surveys of this time, and a great deal of new data on mineralization zones were added to the results of the regional geological surveys conducted last year, by which the following points have been clarified.

- 1) The features of ore deposits and the relation between igneous activity and mineralization was substantially perceived; that is, the mineralization in the areas are represented by that accompanying network quartz veinlets, and that accompanying copper-bearing skarn in the environs of porphyry. Furthermore, with regard to the igneous activity, there are basic rocks of earlier intrusion mainly consisting of gabbro and diorite, and acidic to intermediate porphyritic rocks of later intrusion represented by quartz-monzonite porphyry and others. The copper mineralization is directly connected with the later porphyritic rocks.
- 2) The alteration in the areas is a little different from that of the typical porphyry copper type, and silicification, argillization, sericitization, and biotitization are remarkable, but they are often co-existent with carbonates.
- 3) As a result of age determination of the intrusive rocks in the environs of the mineralized zones, the age of their intrusion or of the

related alteration is Paleogene, which has been supplemented to the data obtained last year.

- 4) As a result of the geochemical investigation, the distribution of anomalies was clarified.
- 5) Three anomalous zones were detected by the IP survey.
- 6) The variation of mineralization in the depths, and especially, the patterns of intrusive rocks were confirmed by drilling.

2-2 Discussions on Geology

From the surveys of this time, the distribution of geological formations and structure in Coroccohuayco and Huaccollo were clarified. Especially, it was clarified that the intrusive rocks were divided into two stages, the earlier and the later stages, and that porphyritic rocks in the later stage was directly connected with the mineralization.

2-1-1 Geology

The distributed rocks largely consist of the Mesozoic sediments and intrusive rocks penetrating it, which are covered with volcanic rocks, glacial deposits, alluvial deposits and the like. The areas are divided by a fault crossing at the center, in the ENE-WSW direction, and the Mesozoic formation is prominent in the northern block of the fault, while basic plutonic rocks are widely distributed in the southern block.

In the northern block, the Mesozoic group is so controlled by an anticlinorium having its axial direction of NNW-SSE, that the oldest Hualhuani formation is widely distributed in the central part, which is

surrounded by the Murco formation, and by the youngest Ferrobamba formation further outside.

In the southern block, plutonic rocks intrude in the center, and the Ferrobamba limestone is distributed on both eastern and western sides.

As intrusive rocks, there are basic plutonic rocks of earlier intrusion mainly consisting of gabbro and diorite, and acidic to intermediate porphyritic rocks of later intrusion represented by quartz monzonite porphyry and others.

The earlier intrusive rocks show a direction of penetration elongated in NNW-SSE in the same way as the main structural direction of the Mesozoic group. The mineralization relating to these rocks is such that only magnetite skarns are formed locally, and no direct connection with copper mineralization is indicated.

The porphyritic rocks of later intrusion form small bodies such as stocks, dikes, sheets, etc., and the direction of penetration is mostly NNW-SSE.

The porphyritic rocks are obviously related to the copper mineralization. In fact, they have brought alterations on the wall rocks of the Mesozoic sediments and the plutonic rocks, as well as on themselves, and the alterations are often associated with copper mineralization.

For the field convenience, the porphyritic rocks were divided into four varieties depending on the degree of porphyritic texture, the quantitative proportion of colored minerals, and the like. They were tentatively named granodiorite, granodiorite porphyry, quartz monzonite porphyry,

and granite porphyry, but there are little difference in the kinds of constituent minerals, and they show in common the features of quartz-monzonitic rocks, rich in alkali feldspars and relatively poor in quartz

These feature are also common in the porphyritic rocks in Tintaya, Quechua, Ataraya, and so on.

Thus, these porphyritic rocks are considered to have substantially solidified from a magma of the same origin, and they are also likely to have been differentiated due to the difference of the conditions of solidification or the period of solidification.

2-2-2 Alteration

The alteration in these areas is considered to have been mainly connected with the intrusion of porphyritic rocks, but it more or less differs from the alteration in the typical porphyry copper. That is, in addition to skarnization and chloritization-epidotization prevailing widely, overlapping carbonatization in the silicification and argillization zones is also often noted. The such peculiarity of alteration is considered to be ascribed, as one of the reasons, to the fact that many of the invaded rocks are those rich in calcium (limestone, calcareous shale, gabbro, and the like); but no clear reason for this is known.

The mineralization in the areas is represented, on a broad view, by that accompanying network quartz veinlets (DDH-4), and copper-bearing skarns in the environs of porphyritic rocks (DDH-3), and is considered to have an intermediate nature between the Tintaya ore deposit dominated by skarn copper-type mineralization and the Quechua ore deposit dominated by porphyry copper-type mineralization.

The mineralization in the "Coroccohuayco alteration zone" in the central part of the southern block is generally poor in the types other than the above two types, and further exploration will be centered on clarifying the potentiality of the silification and skarn zones, and the state of mineralization in these zones.

In the northern block of the areas, the central part is widely covered with gravel layers, and information is insufficient. The geological environment, however, is very similar to those of the Quechua ore deposit, and fractured quartzite zones are likely to be present as in the Quechua ore deposit; therefore, the zone is considered worth exploration.

2-3 Discussions on Geochemical Survey

In the analysis of the results of geochemical survey the threshold values for the anomaly zones, calculated by the following method, were used: the sum of the mean value plus the standard deviation in copper content (about 360 ppm Cu) was fixed as a threshold value for weaker anomalies, and the sum of the mean value plus twice of the standard deviation as that for stronger anomalies. In this connection, the overall mean value of copper content was 104 ppm Cu, and the 5%-value from the highest was 340 ppm Cu and the 10%-value 180 ppm Cu.

The most conspicuous copper anomaly is noted in the "Coroccohuayco alteration zone" in the central part of the southern block. Although they lack in consistency in some degree, the anomaly zones are concentrated in a range of 2.6 km in the NNW-SSE direction and 400 - 800 km in the

ENE-SWS direction, from measuring line P to measuring line I' (PL. I-4), centering on the stocks of quartz monzonite porphyry.

In the skarnized alteration zone around the station 20 on the measuring line G in the northern block, a copper anomaly zone of about 1 km in the NE-SW direction and 200 m in the NW-SE direction was detected.

There is a copper anomaly extending outside the block in the NE direction, starting from the station 37 on the measuring line J at the boundary part, in the eastern part of the southern block. This anomaly is correlated with a copper bearing skarn zone on the ground, and has important significance as an indication of possible extension of copper mineralization to the east of the district.

2-4 Discussions on IP Survey

2-4-1 FE Anomaly Zone

Three zones of FE anomaly were located.

A anomaly zone: It lies in the east of the northern block, and is distributed from the environs of the station 0 on the measuring line G to the environs of the station 15 on the measuring line A. Some anomalies exhibit an FE value of more than 4 %, and the zone has a scope of about 1 km in width, including weaker anomalies of more than 2 % FE value. The general trend of the anomaly zone is NS, but it is considered to be a combination of anomalous sources directed NNW-SE and NE-SW, as there is a flexion point turning to the NE-SE direction in the environs of the measuring line D of the area and it also turns to the same direction

in the environs of the measuring line G, pointing to the FE anomaly zone in Quechua. This anomaly zone is rather similar to the FE anomaly zone in Quechua and exhibits a pattern of a columnar anomaly source with relatively less variation.

Geologically speaking, this anomaly zone is distributed along the western side of the two small anticlinal structures arranged in echelon with their axes in the NNW-SSE direction. The axes of these anticlinal structures plunge south in the southern part and north in the northern part, and locally form small swell-structures. Such swell-structures do not always represent latent intrusive rocks, but at least are considered to be favourable places for the intrusion of igneous rocks, and sub-surface intrusive rocks are expected to exist in this neighborhood. Therefore, this anomaly zone is considered to represent covered zone of the sulphide concentration in and around the possible intrusive rocks.

B anomaly zone: It is an anomaly zone detected (station 16-24 on the measuring line E to station 18-28 on the line G) from the center to the southern part of the northern block, and weak anomaly is recognized rather near to the surface, but the depth of strong anomaly is assumed to be about 300 m deep. The northern half of this anomaly zone is mostly covered with gravel, and the geological condition below the gravel cannot be clarified. There is assumed, however, the existence of an anticlinal structure similar to the case of the A anomaly zone, so that the potential existence of intrusive rocks can well be expected. In this connection, in the neighborhood of station 19 on the measuring line F, a small exposure of

quartz monzonite porphyry exists. In the southern half of the anomaly zone, groups of small stocks of various porphyritic rocks intrude and form a skarn-ization zone geologically and copper anomaly geochemically.

Furthermore, in DDH-2 drilled in this anomaly zone, not only copper mineralization with small dikes of quartz monzonite porphyry has been found, but the universal existence of pyrites has also been recognized, which suggests, therefore, that this anomaly source is at least caused by sulfides.

C Anomaly zone: It is an anomaly zone detected around the central part from the measuring line J' to the measuring line P, in the southern block, and nearly overlaps the alteration zone and geochemically anomalous zone of Coroccohuayco with a scope of about 500 m in width and about 2.5 km in extension. An outstanding feature of the anomaly zone is that considerable changes in the shape and depth of the simulated anomaly sources are recognized, and that FE values of the anomaly sources are low, as compared with those of the anomaly zone in the northern block. It has been nearly clarified from the information drilling conducted lately, that the anomaly sources of the anomaly zone are due to sulfides, but in view of the diversified shape and depth of anomaly sources the geological setting is presumed to be considerably complicated at the depth. Future prospecting, therefore, requires sufficient consideration with regard to these points.

In addition to the three anomaly zones mentioned above, a weak FE anomaly was detected below the copper skarn zone, near the eastern end of the measuring line J (at station 38) which may necessitate future investi-

gations on the eastern side of the surveyed area.

2-4-2 FE Anomaly Zones and Copper Mineralization

If there is no great difference in resistivity and the effects by clay is small, the intensity of FE anomaly should be nearly proportional to the content of sulphides. Accordingly, it is almost certain that FE anomaly zones correspond to concentrated sulphides, and in fact, in DDH-2, DDH-6, etc., where relatively great FE values were detected, greater content of sulphides than the other drill holes were obtained.

The sulphides of copper, however, do not always concentrate in strong FE anomaly zones, but it is known from many examples of prospecting that they rather concentrate in weak anomaly zones some distance apart from the strong FE anomaly zones. For example, in the Quechua ore deposit, the dominant mineralization of copper is recognized in weak anomaly zones where FE values are 2 - 3 %, sometimes in places below 2 %, and it has become clear that the strong FE anomaly zones grown in the surroundings of weak anomaly zones are attributed to pyrite halos.

Also in this area, the FE values at DDH-4 and DDH-3 where relatively dominant mineralization of copper was detected are relatively low; the FE values were about 2 - 3 % near DDH-4, and below 2 % near DDH-3.

That is, the IP anomaly clarifies the state of the existence of latent concentrated sulphide zones formed in connection with mineralization, but does not directly exhibit the location of copper concentration itself. In other words, IP anomaly zones suggest a geological environment suited for the concentration of copper, and means the possible existence of copper

concentration in the neighborhood even where the weaker anomalies exist. In prospecting, therefore, synthetic analyses combining the results of geological surveys, geochemical prospecting, and the like will be indispensable.

2-5 Discussions on Drilling

2-5-1 Locations of the Drill Sites

The locations of drilling were selected in consideration of the rock facies and the features of alteration and mineralization obtained through the surface geological survey, in order to confirm the porphyritic rocks related to the mineralization and states of alteration and mineralization in the depth zones and this drilling with as few as six holes has brought about much information, including two holes locating prominent copper mineralization, and greatly contributed to the assumption of the subterranean structure.

The locations and purposes of the drillings are briefly tabulated as follows:

DDH-1

Location; *Near the Station C¹-18 in Huaccollo Block.

*About 100m south of the outcrop of the mineralized porphyritic rocks along Qda. Huaccollo.

*In the IP A-anomaly.

*Covered with Quaternary sediments.

Object; To confirm suggested latent intrusive rock, and to get hold of

the mode of mineralization and alteration.

DDH-2

Location; *Near the Station F-20 in Huaccollo Block.

*In the IP B-anomaly.

*About 200m north of the skarnized zone coincident to the
geochemical anomaly.

*Covered with Quaternary sediments.

Object; To obtain information of the subsurface geology below Quaternary
sediments, and to check the relation between FE weak anomaly
and sulphide mineralization.

DDH-3

Location; *Near the Station K-26 along the eastern margin of the
Corocchohuayco mineralization zone.

*Covered with Quaternary sediments.

Object; To comprehend outline of the geological structure and the
mineralization in the border zone between eastern limestone
and confluent stock zone of porphyritic rocks.

DDH-4

Location; *Near the Station M-21 in the Corocchohuayco mineralization
zone.

*In the IP C-anomaly.

*In the confluent stock zone of quartz monzonitic porphyries,
associated with remarkable indication of Cu-mineralization.

Object; To check the mode of mineralization in the quartz monzonitic

porphyries, especially its relation to the rock alteration.

DDH-5

Location; *Near the Station M-17 in the Corocohuayco mineralization zone.

*In the IP C-anomaly.

*In the gabbroic rocks showing high geochemical anomaly, in the west flank of the confluent stock zone of porphyritic rocks.

Object; To comprehend the mode of mineralization and its relation to the rock alteration, in the gabbroic rocks around the confluent stock zone of porphyritic rocks.

DDH-6

Location; *Near the Station O'-20 in the Corocohuayco mineralization zone.

*In the IP C-anomaly.

*In the gabbroic rock carrying high geochemical anomaly, in the south of the confluent stock zone of porphyritic rocks.

Object; Same as the object of DDH-6.

2-5-2 Results of Drillings

DDH-1 (250.4 m)

The drill struck the ground rock at a depth of 38 m, these porphyritic rock until 250.4 m where chloritization and partial silicification were observed. An average grade of 0.51 % Cu was shown over the range of 21 m between the depth of 44 m and 65 m.

DDH-2 (250.5 m)

It passed through the such as shale, sandstone and quartzite and quartz monzonite porphyry at four places. The mineralization of copper was found more intense mainly in and around the monzonite porphyry where an average grade of 0.67 % Cu was shown over the range of 23.3 m between the depths of 57.7 m to 80.0 m. The shale appeared to have undergone thermal metamorphism, having been turned phyllitic and undergone silicification, sericitization, chloritization, and hematitization.

DDH-3 (250.2 m)

Gabbro and limestone, and porphyritic rocks penetrating them were found. They have undergone silicification and chloritization, and show particularly conspicuous skarnization.

The skarn consists of garnet, actinolite, epidote, magnetite, etc., and particularly contains large amounts of copper minerals.

The average grade of 0.77 % Cu was shown over the range of 18 m between the depths of 80 m to 98 m, and 1.53 % Cu over the range of 25 m between the depths of 119.4 to 144.0 m.

DDH-4 (250.3 m)

Throughout was quartz monzonite porphyry with conspicuous silicification, argillization and shattering. An average grade of 0.84 % Cu and 0.065 % Mo was shown over the range of 76 m between the depths of 6 m to 84 m. In this zone swarms of network quartz veinlets exist abundantly, and the formation are impregnated with copper minerals. The veinlets are mostly steeply dipped. The average grade of copper throughout the

drill hole was 0.356 %, showing the highest grade of copper among the six holes drilled this time.

DDH-5 (251.1 m)

Gabbro is all through and a small amount of skarn was found near the surface. Silicification and fracturing prevail to a considerable extent in the gabbro. The average grade of copper was 0.55 % between the depths of 7.5 m to 31.0 m, and 0.55 % between 160 m and 176 m, with average grade of 0.226 % throughout the holes.

DDH-6 (251.1 m)

The zone consists of gabbro partially biotitized and skarnized accompanied by silicification, argillization, and chloritization.

The average grade of copper was 0.87 % between the depths of 74 m to 84 m.

The grades of copper and molybdenum of the above six holes are shown below (Table I-8), integrated from the assays of the cores.

From these results, it is understood that the high grade portions of copper are represented by the skarn zone appeared in DDH-3, containing pyrite, chlocopyrite, bornite, and iron minerals, and by the network quartz veinlets traversing the silicified, argillized, and shattered quartz monzonite porphyry as shown in DDH-4.

Either of them exhibits the development of copper mineralization zones in connection with dykes and apophyses of grandiorite porphyry and quartz monzonite porphyry.

CHAPTER 3 CONCLUSION AND FUTURE PROSPECT

3-1 Conclusion

It has become clear as expected, that both areas of Coroccohuayco and Huaccollo, which were selected based on the second -phase survey as areas presenting indications of promising copper mineralization, consist of mineralization zones of porphyry copper-type and copper skarn-type where considerable potentialities as expected.

As the results of surveys of this year, the following three areas have been chosen as the potential areas requiring the further prospectings and investigations:

(1) The area involving an anomaly zone detected by IP survey (hereinafter referred to as "IP anomaly zone") in a scale of about 500 m in width and about 2,500 m in length, spreading in and around the porphyritic rocks distributed along the Qda. Coroccohuayco, which appears to be ascribed to the porphyritic rocks extending in the NNW-SSE direction.

By DDH-3 drilled in the neighborhood of the northern outskirts of the anomaly zone, a mineralization zone of copper-bearing skarn was encountered, and the latency of copper-bearing skarn ore bodies have become more promising in the areas covered with younger gravel beds which lie in the north-eastern outskirts of the IP anomaly zone.

(2) The area represented by an IP anomaly zone detected between the center to the western part of the northern block which is considered to ascribed to a blind sub-surface IP anomalous body, although a mineralized zone

probably due to the porphyritic rocks exposed on the Qda. Huaccollo. The said anomaly has the maximum width of about 1,500 m and its extensions in the SW and NNW directions are considered to stretch towards Quechua and Tintaya situated adjacent to each other.

Another anomaly zone was detected near the center of the northern block, which is considered to be branched out from the IP anomaly zone mentioned above and is considered to be ascribed to an IP anomaly likely to be present in further depths.

(3) The area involving the copper-bearing skarn found at the north-eastern edge of the southern block, which is accompanied by a dominant geochemical anomaly and a weak IP anomaly, and its further extension to the east is expected.

3-2 Comments on Future Surveys

The areas requiring further prospecting from the results of these surveys are:

- (1) The Coroccohuayco altered and mineralized zone in the southern block,
- (2) The Huaccollo altered and mineralized zone in the northern block,
- (3) The area to the east of the surveyed area where the possibility of extended copper mineralization is suggested from the geochemical anomaly, IP anomaly, etc. ,
- (4) The area in the northern extension of the FE anomaly zones in the northern block. The south-western extension of these anomaly zones

is the Quechua area in which prospecting has already been carried out.

Corocchohuayco is the area where geological information has been best obtained among the above areas requiring prospecting and the existence or non-existence of economical ore deposits may be concluded at the earliest time. Accordingly, the first priority should be given to Corocchohuayco for the exploration. With regard to the policy of prospecting in this area, the prospecting should desirably be divided into the following two stages, because the mineralization may still lack in consistency in the present stage of investigation.

The first stage: The examination of the patterns of intrusion of porphyry and its distribution by pilot drilling and trenching to the silicified zones in prophyritic rocks and the assumed skarn zones.

The second stage: The transfer to grid drilling depending on the results of the prospecting in the first stage.

With regard to the policy for prospecting in the Huaccollo zone, the fundamental geological environment of this area is rather similar to those of the Quechua area, and the area has the possibility of the existence of the similar latent deposits as in Quechua, but it is not in the stage of launching full-scale prospecting because geological information is still scarce.

Accordingly, information drilling should be carried out to confirm porphyritic rocks whose potentiality is expected from the IP anomaly and geological structure, and to grasp roughly the relationship between the

mineralization and the IP anomaly.

From the gravity survey of the second-phase the area to the east of the surveyed area is considered to have a geological environment where the possibility of the existence of ore deposits can be expected because a strong local gravity anomaly has been found, from which the latency of intrusive rocks can be anticipated; therefore, area, fundamental investigations such as IP survey, geochemical prospecting, etc. should be tried in this area.

In the area to the north of the surveyed area, further extension of the IP anomaly zone is assumed, but as the nature of the IP anomaly source is unknown, it is desirable to examine whether to expand the scope of investigation to the north according to the results of the future exploration in the surveyed area.

PART I
GEOLOGICAL SURVEY

CONTENTS

PART I GEOLOGICAL SURVEY

1.	Outline of Survey Work	I- 1
1-1	Geological Survey	I- 1
1-2	Geochemical Survey	I- 5
1-3	Examination of Cores of the Pilot Drillings	I- 5
1-4	Age Determination of Rocks	I- 6
2.	Geology	I- 7
2-1	Outline of Geology	I- 7
2-2	Petrography	I-10
2-3	Geological Ages of Intrusive Rocks	I-25
3.	Geological Structure	I-29
3-1	Regional Structure	I-29
3-2	Geological Structure of the Surveyed Area	I-31
4.	Economic Geology	I-34
4-1	Mineralization	I-34
4-2	Alteration.....	I-45
4-3	Results of Geochemical Survey	I-53
5	Geology Indicated by Drillings	I-60
5-1	Selection of Drilling Sites	I-60
5-2	Results of Drilling	I-62

References

List of Tables

Table I-1	Chemical Analysis of Gabbro from the Surveyed Area and the Periphery	I - 14
Table I-2	Chemical Analysis of Intrusive Rocks	I - 18
Table I-3	K-Ar Age Determination for Intrusive Rocks in the Yauri Area .	I - 26
Table I-4	Silica, Lime and Alkali Contents in the Main Earlier Intrusives, Yauri Area	I - 28
Table I-5	Assay Result for Au, Ag and As on the Mineralized Core-Samples from DDH-3 and DDH-4	I - 42
Table I-6	Thickness of Oxidized Zone shown by the Lower Limit of "Clear Limonitization" in the Drill Holes	I - 44
Table I-7a	Qualitative Spectrum Analysis of Drill Cores	I - 58
Table I-7b	Hg Contents in Geochemical Soil Samples	I - 59
Table I-8	Main Copper Mineralizations and Average Sulphur Content in Each Drill Core	I - 63
Table I-9	List of Rock Samples	A - 1
Table I-10	Microscopic Observation	A - 16
Table I-11	Microphotographs	A - 48
Table I-12	Chart of X-ray Diffractive Analysis	A - 86

List of Figures

Fig. 1	Location Map of the Yauri Area	iii
Fig. 2	Location Map of the Surveyed Area	3
Fig. 3	Normative Composition of Porphyries	I - 14
Fig. 4	Histogram and Frequency Curve of Cu Content on the Soil Samples	I - 57
Fig. 5	Copper Grade of Each Drill Hole	I - 69

LIST OF PLATES (are in pocket)

		Scale
PL. I-1.	Geological Map of the Coroccohuayco-Huaccollo Area	1:10,000
PL. I-2.	Geological Profile of the Surveyed Area	1:10,000
PL. I-3.	Alteration Map of the Coroccohuayco-Huaccollo Area	1:10,000
PL. I-4.	Geochemical Map of the Coroccohuayco-Huaccollo Area	1:10,000
PL. I-5.	Sketch Map of Main Mineral showing of the Coroccohuayco Area	
PL. I-6.	Sketch and Sampling Map (3 sheets)	1:5,000
PL. I-7.	Core Log and Assay (6 sheets)	1:200

CHAPTER 1 OUTLINE OF SURVEY WORK

The surveyed area comprises a terrain of 32 square kilometers, as shown in Fig. 2, which includes the mineralized zones of Coroccohuayco and Huaccollo. The area has been so delineated as to form a quadrangle, the long side of which is 8 kilometers in a magnetic bearing of N 23° W parallel to the main trend of geologic structure with its width of 4 kilometers in N 67° E, rectangular to the former.

The works undertaken were mostly geological and geochemical ground surveys and examination of cores obtained from the pilot drillings. Some reviews were made as well, on the geologic ages of some rock units which had been left uncertain in the previous survey of the second phase.

1-1 Geological Survey

Prior to the commencement of geological survey, parallel lines of a magnetic bearing of N 67° E were established at a spacing of 200 meters by a land survey by means of Transit-Compass and measuring tape.

Survey stations were taken at every 100 meters on each of the survey lines.

Taking stations as the base, geological mapping in a scale of 1:2,500 was carried out by means of clinometer and measuring tape. Detailed mapping in a scale of 1:500 and collection of assay samples were made as well on the mineralized outcrops in the Coroccohuayco block. Especially in the vicinity of survey station N¹-21, where small outcrops of altered gabbro, stained with copper-oxide minerals were scattered around,

trenching was added to investigate the features of mineralization.

1-2 Geochemical Survey

Soil samples for geochemical survey, amounting 1,681 in all, were collected at every station spaced in a grid of 200 m. x 100 m.

The samples were taken at the depth from 20 cm to 50 cm below surface. This was deep enough to reach to the B-horizon of residual soil derived from the Mesozoic formations and intrusive rocks, except in the Pampa where the Quaternary sand and gravel beds of a few tens of meters overlie the Mesozoics and intrusives (for instance, about 40 meters thick in the central part of Huaccollo block), and black alluvial soil along the creeks generally has a thickness of several meters.

Indicators of Cu and Mo were used as in the previous year. In view of the development of thick Quaternary formation in this area, some investigation was made on applicability of Hg, as an indicator, which has high penetrability. Chemical analyses were so arranged that Cu and Mo were done by Maria Lau, an experted geochemical analyst in Peru, and Hg by the Central Laboratory of Nippon Mining Co., Ltd.

1-3 Examination of Cores of the Drillings

Geological examination and chemical analyses were made on the cores from 6 drill holes, the length of which reached to 1,506.3 meters in total. Quantitative analyses of total copper, acid-soluble copper, molybdenum and sulphur were made on the cores of all the formations except

the Quaternary rocks. Qualitative analyses were also made on the representative samples of intrusive rocks by means of spectro-photometer (14 samples of the porphyritic rocks; 7 samples of gabbroic rocks).

1-4 Age Determination of Rocks

Age determination was made by means of K-Ar method on 10 samples of the intrusive rocks, 8 of which were porphyritic rocks of later intrusion thought to be related to mineralization. These 8 samples were taken not only in the surveyed area but also from the mineralized zones of Tintaya and Ataraya. The rest 2 were gabbros of earlier intrusion taken in the surveyed area, and were recognized to have been affected by the alteration related to mineralization.

An etching test by fluoric acid was tried on the cherty concretions contained in the Ferrobambe limestone to inspect the existence of fossils of radiolarias and conodontos, etc. An examination was attempted for the presence of pollens, radiolarias, and diatoms in the Coporaque and Puno Formations, the age of which were not determined as no fossils had been found during survey of the second phase.

CHAPTER 2 GEOLOGY

2-1 Outline of Geology

As stated in the previous report of the second phase, the surveyed area lies in the eastern part of Tintaya cupriferous region, and its geology and structure have much similarity to those of Tintaya and Quechua mineralized zones located to the immediate west.

The principal rocks in the said area are the late Mesozoic sedimentary rocks and intrusive rocks invading the former, and they are, in somewhere, covered with the younger volcanic rocks, glacial deposits and alluvium. The Mesozoic formation has a succession of, from the lower upwards, quartzite intercalating shale (the Hualhuani formation), alternation of sandstone and shale (the Murco formation) and limestone (the Ferrobamba formation). The intrusive rocks are grouped into two; the one is a basic plutonic group of earlier intrusion consisting mainly of gabbro and diorite, and the other is a group of porphyritic rocks of later intrusion, acidic to intermediate in chemical composition, represented by quartz monzonite porphyry.

Copper mineralization is obviously brought about by the intrusive activity of the porphyritic rocks as pointed out in the previous survey. The most fundamental and important factors to have controlled the localization, therefore, are considered to be the distribution and forms of the porphyritic rocks. The Mesozoic formation and basic plutonics as invaded rocks, are also controlling the types and emplacement of ore deposits.

Geological age of their intrusion or related alteration have been almost ascertained as Paleogene as a result of age determination by K-Ar method.

The surveyed area is divided into two blocks by a fault passing across the center of the area with a strike of ENE-WSW; the one in the north, the Huaccollo block where the Mesozoic formation is dominating, and the other in the south, the Coroccohuayco block where the basic plutonics are prevailing.

In the Huaccollo block, the Mesozoic formation forms a gentle anticlinorium with its axial trend of NNW-SSE. The central portion of the block is occupied mainly by the oldest Hualhuani quartzite, enclosed by the Murco shale and sandstone. The Murco formation is further surrounded by the youngest Ferrobamba limestone outcropping mainly in the east and west portions of the block. As compared to the Coroccohuayco block, the distribution of basic plutonics is so much less as only a few stock-like bodies are recognized along the western border of the block. The porphyritic rocks are generally scattered rather sparsely as small stocks, dykes and sheets, but more collective intrusions are recognized in the central part of the block. Here, however, a thick covering of Quaternary sands and gravels over the intrusives makes it difficult to indicate their accurate mode of distribution. Intrusions of the basic plutonics as well as porphyritic rocks are aligned in NNW-SSE which is parallel to the principal structural trend of the Mesozoic formation. Intense fracturings accompanying iron-hydroxide stains are often recognized in the quartzite distributed from the center to the west portion of the block.

A fairly large zone of fracturing elongated in NNW-SSE may have been formed, though the fractured quartzite has not been investigated sufficiently.

As stated before, fundamental character of geology and geological structure of the Huaccollo block has much similarity to that of the Quechua mineralized zone. Moreover, an IP anomaly detected in the western part of this block is considered to be continuous to the one obtained in Quechua. It may be fairly anticipated, therefore, some mineralization zone may exist in the Huaccollo block, in view of its geological situation.

As for the Coroccohuayco block, there distribute widely the basic plutonics of gabbro and diorite in the central part, and the Ferrobamba limestone in the east and west parts. Almost none of the Hualhuani and Murco formations has been recognized in this block except a few small outcrops of quartzite, possibly as a form of roof-pendant on the basic plutonics. This may suggest that here the Mesozoic formation also had formed an anticlinal structure, in a general sense, which resembled to the one in the Huaccollo block. Intrusion of the porphyritic rocks is not only concentrated along the eastern border of the basic plutonics, but also recognized more frequently in the eastern limestone. The former part corresponds to "the Coroccohuayco mineralized zone", which has discovered during the survey of second phase. The porphyritic rocks of this mineralized zone were inferred to form a large dyke with its width of 200-800 meters and its elongation of not less than 2.5 kilometers. But the present survey has revealed that they form a converged zone of small stocks. It also has been ascertained that some apophyses split from the

stock have penetrated the limestone lying close to the east of the stock zone. The trend of porphyritic intrusions generally shows NNW-SSE, with a few exceptions showing ENE-WSW, rectangular to the former.

The geological set-up of the Coroccohuayco mineralized zone, as stated above, consists of the basic plutonics, limestone, and porphyritic rocks intruded in the border of the two, which more or less coincides to that of Tintaya mineralized zone. As for the type of mineralization of Coroccohuayco, therefore, not only the mineralization of porphyry copper type, but the copper mineralization related to skarnization, as observed dominant in the Tintaya deposits, may also be important. In fact, a fairly intense copper mineralization of skarn type caught by the drill-hole DDH-3, can be interpreted to have been caused by the porphyry intruded into limestone as sheet-like bodies. This will be noteworthy to suggest the mineralization occurred in a similar geological condition as is found around the East Deposit of Tintaya.

2-2 Rock Descriptions

2-2-1 Mesozoic Formation

The Mesozoic sediments in this area consist of the Hualhuani, Murco and Ferrobamba formations.

The Hualhuani formation, the oldest in this area, is the uppermost of the Yura Group, the age of which is estimated to be lower Cretaceous, mostly distributed in the northern part of the surveyed area, that is, the central part of the Huacollo block. This formation consists of massive

quartzite intercalated with thin layers of shale. The quartzite is poorly stratified, hard and compact, looking white to pale brown in color. Under the microscope, the rock mainly consists of more or less granular quartz grains of 1 mm or so, and the finer quartz grains filling up the interstices of the former with associated feldspar and magnetite grain in minor amounts. The quartzite of this area seem to have been affected by deformation, which may be suggested by the wavy extinction of quartz and its shape often elongated under the microscope. Abundant cracks generally develop in the quartzite, especially the one in the central to the eastern portions of the Huaccollo block, is often fractured heavily. Although the distribution of the fractured quartzite has not been traced sufficiently, it may probably be extended in NNW-SSE with its width of a few hundred meters. The intercalated shale is generally dark grey to black in color, and is calcareous in some parts. It is often converted into slate or hornfels of low grade due to thermal metamorphism. It has been metamorphosed into a reddish orange phyllitic rock, consisting of sericite, chlorite, and hematite in the vicinity of survey station B¹-18 of the northern part of Huaccollo block. This rock, being rich in sericite and quartz, is used as a raw material for pottery by the local people. Most of the hornfels contain parallelly arranged flakes of biotite abundantly and is often associated with garnet.

The Murco formation covers the Hualhuani formation conformably, and is overlain by the Ferrobamba formation with unconformity. This formation is so distributed as to surround the Hualhuani quartzite chiefly

in the eastern, western and southern parts of the Huaccollo block. This consists of an alternation of shale and sandstone, in which more predominant is shale. The shale is generally sandy shale with dark grey to greenish grey color, but partly contains calcareous layers. The sandstone is medium to fine-grained and grey to reddish brown in color. It is generally siliceous in the lower part but arkosic in the upper. The arkosic sandstone is mainly composed of slightly angular grains of quartz, plagioclase and perthitic orthoclase. The shale and sandstone seem to have been subjected under thermal metamorphism of low grade, having fine flakes of secondary siotite arranged parallelly.

The Ferrobamba formation consists mostly of massive and compact limestone distributed mainly in the eastern and western parts of the surveyed area. Generally the limestone is dark grey or bluish grey, fine-grained crystalline limestone, but is converted into yellowish to greyish white, coarse-grained crystalline limestone, near its contact with the intrusive rocks. It often contains small cherty and shaly concretions, and is rarely intercalated with thin layers of light grey shaly limestone and black calcareous shale. An etching test of this cherty concretion by fluoric acid has detected radiolarias, though the radiolarias so far discovered were deformed too much to be properly identified.

2-2-2 Basic Plutonic Rocks

The basic plutonics occupy the most part of the Coroccohuayco block as well as the western fringe of the Huaccollo block as a few small stocks. The alignment of their emplacement is NNW-SSE which is parallel to the

principal structural trend of the Mesozoic sedimentary rocks.

They belong to a plutonic complex varying from gabbro to quartz diorite through diorite, although hornblende gabbro is most redominant.

The gabbro mainly consists of medium-grained, hypidiomorphic, equigranular plagioclase (labradorite to bytownite) and hornblende, the latter showing a poikilitic texture with cadacrysts of olivine, pyroxene, cummingtonite, etc. Most of the pyroxene is monoclinic, but rhombic one is rarely associated. Some isolated, euhedral crystals of orthopyroxene are found in the specimen taken from the cores at the depths of 84.5 m and 98.5 m of DDH-5. The mafic minerals are mostly olivine and clinopyroxene in the specimen from the core at the depth of 175.0 m in DDH-3. The results of chemical analysis of gabbroic rocks are shown on Table 1-1.

Diorite and quartz diorite as well, mainly consists of plagioclase and hornblende, usually showing medium-grained, hypidiomorphic and equigranular texture. But they are deprived of olivine and very poor in pyroxene. Furthermore, they often contain small amounts of potash feldspar, and a little quartz is present in quartz diorite.

The basic plutonic rocks of this area have been more or less affected by thermal metamorphism. Especially, the gabbroic rocks of the Coroccohuayco mineralized zone, may have been subjected to a remarkable metasomatism producing such skarn minerals as garnet, actinolite and epidote. Prior to this metasomatism, however, a sort of thermal metamorphism seems to have taken place, which is evidenced by the

Table 1-1 Chemical Analysis of Gabbro from the Surveyed Area and the Peryphery

Sample No. Rock Name Locality	* 455 Gabbro 1 km South of the Area	36 Metagabbro D-2 in the Area	135 Metagabbro O'-12 in the Area
SiO ₂	46.76	47.93	46.18
TiO ₂	1.18	1.05	1.34
Al ₂ O ₃	19.56	20.85	20.42
Fe ₂ O ₃	5.18	3.92	5.26
FeO	6.73	5.27	5.50
MnO	0.16	0.12	0.17
MgO	5.47	4.35	5.15
CaO	10.42	11.15	11.27
Na ₂ O	2.20	3.09	2.21
K ₂ O	0.53	0.32	0.61
P ₂ O ₅	0.22	0.16	0.10
H ₂ O(+)	1.28	1.28	1.41
H ₂ O(-)	0.19	0.24	0.45
Total	99.88	99.73	100.07
Q	1.08		0.30
C			
or	3.34	1.67	3.34
ab	18.34	26.20	18.86
an	41.98	41.98	43.92
lc	64.74		
ne			
Sal. total	64.74	69.85	66.12
ac			
wo	3.25	5.22	4.64
en	13.70	9.10	12.90
fs	6.34	4.06	3.67
fo		1.27	
fa		0.61	
mt	7.42	5.80	7.66
hm			
il	2.28	1.98	2.58
ap	0.67	0.34	0.34
ti			
Fem. total	33.66	28.38	31.79

* This Sample No. is of the Second-Phase Survey.

replacement of primary brown hornblende and pyroxene by minute brown biotite, together with the pale green to colorless hornblende and cummingtonite. Biotite usually occurs in a form of aggregates of minute flakes. Magnetite is produced abundantly in the concentrated parts of biotite, but sulphides are associated with the later metamorphism than the biotitization. This, therefore, should be treated differently from the biotitization related to the mineralization of the porphyry copper type.

2-2-3 Porphyritic Intrusive Rocks

(1) General Features

In the present field survey, the porphyritic rocks of later intrusion have been classified into four facies based upon grade of progress of porphyritic textures, relative amount of mafic minerals, etc., names of which have been given tentatively as follows:

Granodiorite; Moderately rich in mafic minerals (biotite, hornblende), with faint porphyritic texture by felspar phenocrysts, but closer to plutonic facies due to the coarser groundmass

Granodiorite porphyry; Moderately rich in mafic minerals (biotite, hornblende), with distinct porphyritic texture.

Quartz monzonite porphyry; Poor in mafic minerals (biotite hornblende), fairly rich in felspar phenocrysts, with distinct porphyritic texture.

Granite porphyry; Fairly poor in mafic minerals (biotite hornblende), with distinct porphyritic texture, characterized by a small amount of euhedral phenocrysts of quartz, aside from felspar phenocrysts.

Under the microscope, the granodiorite mainly consists of plagioclase (oligoclase often with a core of andesine), potash feldspar (generally perthitic orthoclase), quartz, green hornblende and brown biotite, associated with sphene, apatite, magnetite, etc. Plagioclase is usually subhedral, short-prismatic and phenocrystic, commonly 2-3 mm, sometimes up to 6 mm in length. Potash feldspar and quartz are anhedral, and occur as fine-grained interstices of less than 1 mm in size.

Granodiorite porphyry generally contains those phenocrysts of subhedral plagioclase of 2-3 mm in length (oligoclase often with a core of andesine), green hornblende of less than 1 mm, and brown biotite in a fine-grained and holocrystalline groundmass mostly composed of quartz and alkali feldspars. Occasionally are recognized the phenocrysts of small amounts of potash feldspar (perthitic orthoclase with fine laminae of albite) and quartz. Sphene, apatite and magnetite are almost usually associated.

Quartz monzonite porphyry mainly consists of those phenocrysts of subhedral, short prismatic plagioclase (generally oligoclase with a core of andesine) of 2-5 mm long and a small amount of brown biotite not more than 2 mm in a fine-grained, holocrystalline groundmass mainly composed of quartz and alkali feldspars. Grain size of groundmass components is less than 0.1 mm. There occurs a small amount of hornblende but not general. The corroded quartz phenocryst is recognized in rare cases. The phenocryst of potash feldspar is generally less in amount than plagioclase, but the reverse cases are also observed in a few thin sections. The common accessories are sphene, apatite and magnetite.

Granite porphyry is characterized by containing euhedral quartz phenocrysts, although its features are so much closer to the quartz monzonite porphyry, as to have been called "quartz monzonite porphyry" in the survey of the second phase. The quartz phenocrysts often reach from 5 mm to 1 mm in diameter. Further, this rock penetrates "the silicified" quartz monzonite porphyry.

Assemblage of rock-forming minerals is common in all these porphyritic rocks, rich in alkali feldspars and rather poor in quartz, which is characteristic usually in such rocks as quartz monzonite. The same character is also recognized commonly in the porphyritic rocks related to the copper mineralization of Tintaya, Quechua and Ataraya. The results of chemical analysis and the normative mineral compositions calculated therefrom on the porphyritic rocks from each of the mineralized zones are shown on Table 1-2. Besides, it has been also clarified that geological age of their intrusion or related alteration is mostly Paleogene, as the results of dating by K-Ar method on each of the samples, the details of which will be given later.

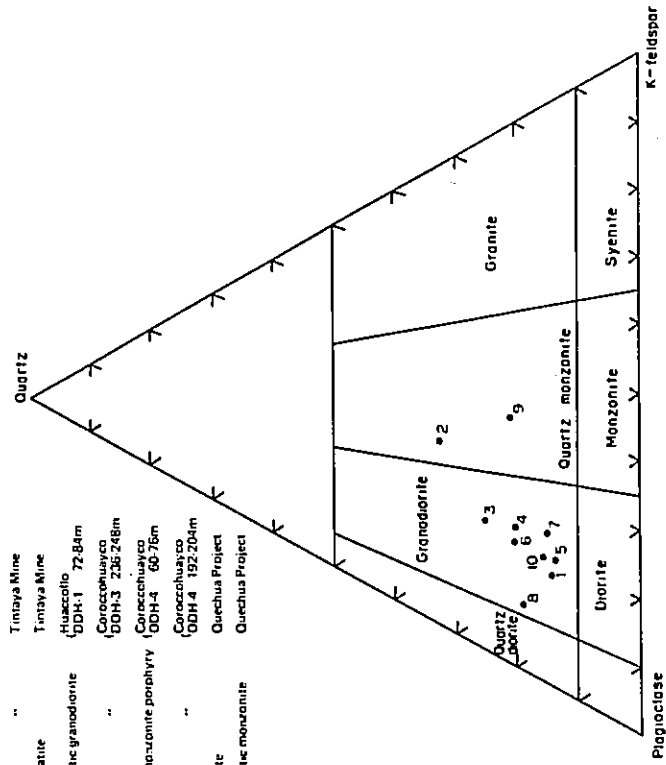
Thus, the porphyritic rocks intruded in this area and in the neighbouring mineralized zones are regarded as comagmatic in origin, but, on the other hand, it is also true that slight differences are always recognized in their properties and appearances. Such differences may probably have been due to slight differences of the conditions of magmatic consolidation, or differences in the differentiation phases caused by slight time lags of periods of intrusion. The porphyritic rocks have been finely classified in

Table 1-2 Chemical Analysis of Porphyries

Sample No.	241 Quartz monzo- nite porphyry Ataraya Mine	242 Quartz monzo- nite porphyry Tintaya Mine	243 Quartz monzo- nite porphyry Tintaya Mine	244 Altered Iaitic Tintaya Mine	236 Porphyritic granodiorite 72m 84m DDH-1	239 Porphyritic granodiorite 236m 248m DDH-3	215 Quartz monzo- nite porphyry 64m 76m DDH-4	240 Quartz monzo- nite porphyry 192m 204m DDH-1	453-(n) Monzonite Quechua	453-(r) Porphyritic monzonite Quechua
SiO ₂	63.45	70.89	66.82	61.50	65.33	66.25	64.32	65.42	62.23	65.12
TiO ₂	0.31	0.21	0.22	0.35	0.26	0.24	0.23	0.22	0.56	0.17
Al ₂ O ₃	16.76	15.16	17.86	18.51	17.05	15.65	17.24	17.35	17.72	18.16
Fe ₂ O ₃	2.66	0.94	1.73	2.28	1.87	1.94	1.36	1.35	0.98	0.43
FeO	1.41	0.69	0.31	0.66	1.36	1.31	1.27	1.27	0.85	0.77
MnO	0.06	0.05	0.04	0.08	0.05	0.04	0.04	0.04	0.08	0.04
MgO	2.24	0.77	1.22	1.22	0.78	0.58	0.61	0.55	0.49	0.36
CaO	4.34	1.72	1.83	3.61	3.04	2.90	3.56	2.49	2.71	2.56
Na ₂ O	4.83	3.39	4.97	4.41	5.96	5.26	5.04	6.25	2.94	5.82
K ₂ O	2.74	4.19	2.94	2.90	2.88	2.82	3.35	1.51	5.38	2.83
P ₂ O ₅	0.04	0.08	0.05	0.24	0.05	0.15	0.12	0.14	3.79	2.16
H ₂ O(+)	0.55	0.93	1.33	3.45	0.44	2.02	2.44	1.74	1.74	1.03
H ₂ O(-)	0.30	0.62	1.26	1.17	0.25	0.41	0.47	0.49	0.13	0.22
Total	99.69	99.64	99.65	99.78	99.84	99.57	100.05	99.60	99.60	99.67
MgO	19.9	8.5	3.4	13.3	7.1	5.8	5.9	5.7	4.7	3.5
FeO	12.6	7.6	3.6	7.2	12.4	13.1	12.4	13.3	16.4	11.4
(Na + K) ₂ O	67.5	83.9	93.0	79.5	80.5	81.1	81.7	81.0	78.9	85.1
Q	13.68	30.30	22.86	17.16	12.66	18.54	14.10	17.04	18.66	14.58
C	2.14	2.14	3.47	3.22	3.22	3.22	3.22	1.22	2.55	1.43
or	16.12	25.02	17.24	17.24	17.24	16.68	20.02	8.90	31.69	16.68
ab	40.87	28.82	41.92	37.20	50.30	44.54	42.44	52.92	24.63	49.27
an	15.85	7.78	8.34	13.34	11.12	10.56	14.46	11.40	12.51	11.12
bc										
me										
Sol. total	(86.52)	(94.06)	(93.83)	(88.16)	(91.52)	(90.32)	(91.02)	(91.48)	(90.04)	(93.08)
ac										
wo	2.09				1.28	1.28	1.04			
en	5.60	1.90	0.70	3.10	2.00	1.50	1.50	1.40	1.20	0.90
fs		0.26			0.66	0.40	0.92	1.06		0.92
fo										
fa	3.94	1.39	0.46	1.39	2.78	2.78	2.09	1.86	1.32	0.70
mi										
hm										
il	0.61	0.46	0.46	0.61	0.46	0.46	0.46	0.46	1.06	0.30
ap	0.34	0.34	0.34	0.34	0.34	0.34	0.34	0.34	0.34	0.67
ti										
fem. total	(12.58)	(4.55)	(3.40)	(6.56)	(7.52)	(6.76)	(6.35)	(5.12)	(3.92)	(3.49)
Or	21.1	40.6	25.5	25.4	21.9	23.2	26.0	12.2	46.0	21.6
Ab	56.1	46.8	62.1	54.9	63.9	62.1	55.2	72.3	35.8	63.9
An	21.8	12.6	12.4	19.7	14.2	14.7	18.8	15.5	18.2	14.5

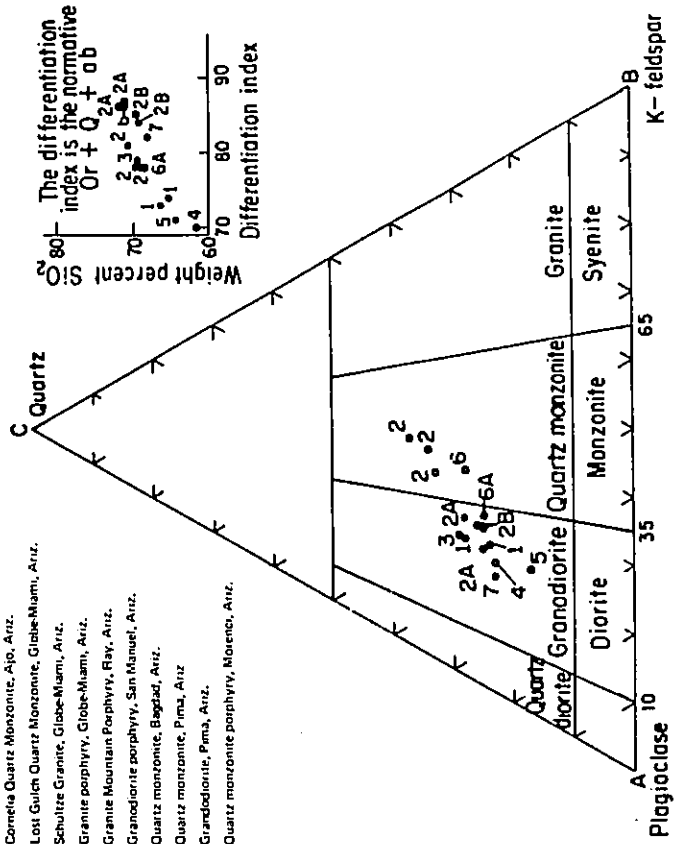
See the Second-Phase Report

1. Quartz monzonite porphyry Ataraya Mine
2. " " Tinaya Mine
3. " " Tinaya Mine
4. Altered latite Huaccollo
5. Porphyritic granodiorite DDH-1 72-84m
6. " " Corcochuyaco DDH-3 235-248m
7. Quartz monzonite porphyry Corcochuyaco DDH-4 60-76m
8. " " Corcochuyaco DDH-4 192-204m
9. Monzonite Quechua Project
10. Porphyritic monzonite Quechua Project



A
Plots of the quartz-K-feldspar-plagioclase triangular diagram of the norms of the norms of porphyries from the Yauri area

1. Cornelia Quartz Monzonite, Ajo, Ariz.
2. Lost Gulch Quartz Monzonite, Globe-Miami, Ariz.
- 2A Schultze Granite, Globe-Miami, Ariz.
- 2B Granite porphyry, Globe-Miami, Ariz.
- 3 Granite Mountain Porphyry, Ray, Ariz.
- 4 Granodiorite porphyry, San Manuel, Ariz.
- 5 Quartz monzonite, Bagdad, Ariz.
- 6 Quartz monzonite, Pima, Ariz.
- 6A Granodiorite, Pima, Ariz.
- 7 Quartz monzonite porphyry, Morenci, Ariz.



B
Plots of the quartz-K-feldspar-plagioclase triangular diagram of the norms of unaltered porphyries from Arizona porphyry copper deposits. Classification from Bateman (4).

Fig. 3. Normative composition of Porphyries

the present survey in view of the importance to discuss the relation of the difference of intrusive condition to mineralization. But the nomenclatures have not been given in strict petrological sense, but have been given rather as field names emphasizing the difference of their features.

(2) Distribution

The porphyritic intrusive rocks have obviously an intimate relation to the copper mineralization, as the intense showings of copper mineralization are limited in the said rocks or in their surroundings.

They occur as such small intrusive bodies as stocks, dykes or sheets. Their distribution is rather sparse in general, but they are more concentrative in distribution from the central to the eastern parts of the Coroccohuayco block and in the central part of the Huaccollo block.

The central part of the Coroccohuayco block corresponds to "the Coroccohuayco mineralized zone" in the previous survey of the second phase, where the porphyritic rocks, quartz monzonite porphyry as principal one, intrude along the eastern fringe of the basic plutonics, forming a converged zone of the porphyritic intrusives in an area of 500 m x 2.5 km extending in NNW-SSE. It has been clarified by the present survey that the porphyritic rocks form an aggregate of many small stocks accompanying those apophyses of dykes and sheets, in stead of forming one single body as reported in the second phase survey. The intrusive sheets penetrate the limestone in a way fairly harmonized to its bedding structure in the area of east side of stocks. Majority of the porphyritic rocks is quartz monzonite porphyry, though there are porphyritic granodiorite,

granodiorite porphyry and granite porphyry. The granite porphyry has intruded after the quartz monzonite porphyry had been silicified. The rest three change one another gradually in rock facies and no definite evidence was found to prove difference of intrusive stages. Most of the porphyritic rocks intrude in a definite alignment of NNW-SSE, but a few are rectangular to them, showing ENE-WSW. The granite porphyry, the youngest of all, shows a trend of NW-SE, slightly deviated from the other ones. In this area, there have been found the most attractive copper mineralization and its related alteration ever found throughout the surveyed area.

In the limestone near the eastern margin of the Coroccohuayco block, the porphyritic rocks intrude as small stocks or sheet-like bodies. The general trend of intrusion shows NNW-SSE, but they are controlled locally by the structure of limestone. They consists of porphyritic granodiorite, granodiorite porphyry, and quartz monzonite porphyry which are transitive one another. There are no predominant facies to be noted, but the granodiorite facies seems to exceed that of quartz monzonite porphyry.

Although the grade of alteration of porphyritic rocks themselves are rather low, some copper-bearing skarn zones are formed along the periphery of altered quartz monzonite porphyry, which can be seen at the eastern terminal of survey line G.

Due to a thick and wide covering of the Quaternary sands and gravels, the distribution of the porphyritic rocks in the area lying between the said two areas of porphyritic rocks has not been clarified. But DDH-3 drilled at the immediate neighbour to the Coroccohuayco mineralized zone

has shown that a few sheets split from a porphyritic stock gave a fairly intense copper mineralization of skarn type to the limestone. This will suggest the possibility of existence of geological conditions similar to the Tintaya ore bodies, especially to its East Ore Body, and will necessitate the further study of the distribution and forms of intrusion of the porphyritic rocks in this boundary zone.

In the central part of the Huaccollo block, the porphyritic rocks expose mostly in its north and south parts.

Exposure in the north can be observed along the bottom of the Qda. Huaccollo, which corresponds to the Huaccollo mineralized zone in the survey of second phase. The porphyritic rocks are capped by a pendant of quartzite along the northern side of the creek and are covered by the Quaternary formation along the south. They consist of porphyritic granodiorite, granodiorite porphyry and quartz monzonite porphyry, among which the porphyritic granodiorite is most predominant. Net-work veinlets and dissemination of pyrite in association with chalcopyrite are recognized in the porphyritic rocks, as reported previously. Similar features of mineralization can also be seen in the quartzite along their contacts.

Small stocks of porphyritic rocks penetrate the Murco shale and sandstone and Ferrobamba limestone surrounding the survey station G-20 in the southern part of the central zone of the Huaccollo block. The stocks consist of porphyritic granodiorite, granodiorite porphyry and quartz monzonite porphyry, which are transitional one another, with a

distinct alignment of NNW-SSE in common. Here, a fairly large skarnized zone has been formed in association with local copper mineralization.

Due to a covering of Quaternary sands and gravels, the distribution of porphyritic rocks is vague in the very center of the Huaccollo block. The area, however, is considered to offer a favourable condition of geological structure for the emplacement of porphyritic rocks as it corresponds to the anticlinal crest of Mesozoic formation. In fact, the drill hole DDH-1 has proved extension of the porphyritic rocks at least 100 meters southwards from their exposures along Qda. Huaccollo. Furthermore, in the vicinity of survey station E-19, a small inlier of quartz monzonite porphyry exposes. DDH-2, located about 400 meters north of small stocks in the southern part of the block, has encountered only a few small dykes of quartz monzonite porphyry, but all of them carry notable copper mineralization. In any case, the geological informations of the central zone of the Huaccollo block are fairly short to clarify the subsurface geology.

2-2-4 Volcanic Rocks

In the southwestern corner of the surveyed area, there distribute dark grey andesitic or basaltic lavas and white rhyolitic tuffs. They are free from alteration and mineralization effects of the porphyritic intrusion, which suggests that they are effusives after the mineralization. Small dykes of olivine-basalt have been recognized in a few localities. DDH-2 has revealed that they penetrated the mineralized quartz monzonite porphyry, showing themselves definitely post-mineralization.

2-2-5 Quaternary Formation

Sand and gravel beds, considered to be glacial deposits, develop from the central to eastern parts of the Huaccollo block. The thickness is estimated about 40 meters based on the results of drill holes DDH-1 and DDH-2.

Sand and gravel beds develop in the east of the Coroccohuayco block, too. They are intercalated with the bedded white tuff and sandstone in the lower horizon. A part of them may belong to the Yauri lake deposits. The thickness of the beds is uncertain but it seems to vary complicatedly, being controlled by the eroded topography of the older formations.

Alluvial soils are developed along the Qdas. Coroccohuayco, Huaccollo and their tributaries. Especially a pampa with rather thick black humas spreads fairly widely along the downstream of the Qda. Coroccohuayco, offering favorite pastures.

2-3 Geological Ages of Intrusive Rocks

The plutonic rocks shown on the geological charts of Yauri and Velille are all younger than the Ferrobamba limestone, as reported in the second phase survey, and geological age of their intrusions has been considered as Late Cretaceous or Early Tertiary. Age determination, however, by K-Ar method done in the said survey suggested the intrusive activity had begun in Late Jurassic and continued intermittently to Early Tertiary. In the present survey, age determination by K-Ar method on the intrusive rocks was done by the Tohoku University upon our request for further discussion of this problem. The results so far determined are shown in Table I-3.

A sample of gabbro taken from the Tintaya intrusive body, the representative plutonic rock of earlier intrusion, gave K-Ar age of 144 m. y. (Late Jurassic) in the second year survey. And 105 m. y. was determined (Late Lower-Cretaceous) from a sample of quartz diorite taken from the Velille batholith. As they all penetrate the Ferrobamba limestone, on the other hand, their geological ages must be obviously younger than the said limestone. Its age of deposition has not been ascertained clearly yet, although it is considered to have been deposited any time between Upper Jurassic and Middle Cretaceous judged from the identified fossils ever found from it. As the Arcurquina limestone of Arequipa Area, which is possibly be correlated to the Ferrobamba limestone stratigraphically, has been admitted to represent the Albian Stage of Middle Cretaceous, age of the intrusion must be post-Albian Stage.

Table 1-3 K-Ar Age Determination for Intrusive Rocks in the Yauri Area

(A) Result in the Second-Phase Survey

Location	Rock Name	Analytical Mineral	Age x 10 ⁶ Y.	Feature of Sample
1 km south of Coroccohuayco	Gabbro	Hornblende	144	Fresh
5 km south of Velille	Quartz Diorite	Biotite + Hornblende	105	"
Puente Santo Domingo, Pichigua	Granodiorite	"	86	"
3.5 km west of Pichigua	Diorite	Biotite	74	"
Quechua	Porphyritic Quartz Monzonite	Whole Rock	57	With weak hydrothermal alteration
Quechua	Monzonite Porphyry	"	37	With strong hydrothermal alteration and weak mineralization

(B) Result in the Present Survey

Location	Rock Name	Analytical Mineral	Age x 10 ⁶ .	Remarks
Coroccohuayco D-2	Metagabbro	Hornblende	53	With weak hydrothermal alteration and mineralization of sulphides
Coroccohuayco O'-12	Metagabbro	Hornblende	30	With marked hydrothermal alteration and weak mineralization of sulphides
Ataraya Mine	Quartz Monzonite Porphyry	Hornblende-Biotite	73	Almost fresh except for very weak Chloritization of mafic silicates
Tintaya Mine	Quartz Monzonite Porphyry	Biotite	40	Sampled near the contact with skarn: fairly altered hydrothermally
Tintaya Mine	Quartz Monzonite Porphyry	Biotite	39	Highly weathered and distinctly altered hydrothermally
Tintaya Mine	Altered Latite	Whole Rock	38	With completely altered mafic silicates
Huaccollo DDH-1 72m - 84m	Porphyritic Granodiorite	Biotite	26	With distinct hydrothermal alteration and mineralization of sulphides
Coroccohuayco DDH-3 236m-248m	Porphyritic Granodiorite	Biotite	43	With commonly chloritized biotite and disseminated pyrite
Coroccohuayco DDH-4 60m - 76m	Quartz Monzonite Porphyry	Biotite	39	With weakly chloritized biotite and abundant chalcopyrite and bornite
Coroccohuayco DDH-4 192m-204m	Quartz Monzonite Porphyry	Biotite	44	With weakly chloritized biotite and fairly abundant pyrite

⁴⁰Ar R radiogenetic argon 40. $\lambda_e = 0.584 \times 10^{-10} \text{ yr}^{-1}$, $\lambda\beta = 4.72 \times 10^{-10} \text{ yr}^{-1}$

The results of re-determination of K-Ar age on the said two samples in present survey were similar to what was done in the previous survey. Samples of gabbroic rocks taken from the area of present survey showed almost similar K-Ar ages to those of the porphyritic rocks, which may be due to hydrothermal alteration accompanied by intrusion of the later porphyritic rocks.

The results of re-determination of K-Ar ages strongly suggest that the earlier intrusive activity began in Late Jurassic, but it is the matter of the first consideration to clarify the age of Ferrobanda limestone definitely. Therefore the problem has not been solved yet.

Many samples of the later porphyritic rocks seem to indicate rather the age of hydrothermal alteration than the age of magmatic consolidation, as they are widely affected by the said alteration. The ages determined on the porphyritic rocks indicated K-Ar ages ranging from Eocene (58 ± 4 --- 37 ± 2 m. y.) to Oligocene (37 ± 2 --- 25 ± 2 m. y.), except the quartz-monzonite porphyry taken from the Ataraya Mine. They almost coincide with those K-Ar ages obtained from the determination on the Tacaza Volcanic Rocks in the second phase survey. The Tacaza Volcanic Rocks are fairly rich in alkali (51.8 alkali-lime index by Peacock), and are accompanied by, though slightly, mineralization, as reported previously. This is an interesting fact as to suggest the later porphyritic rocks have magmatic affinity to the Tacaza Volcanics. The sample of quartz-monzonite porphyry taken from the Ataraya Mine showed 73 m. y. (Late Cretaceous). As the grade of alteration of this sample is very faint, its

K-Ar age is considered to show the very age of its consolidation. This value is fairly close to that of the Pichigua intrusives (86---74 m. y.). This Pichigua intrusives, as mentioned in the previous report, intruded in the latest stage of the earlier intrusive activity, forming a batholithic mode of occurrence of diorite or granodioritic nature, but on the other hand, having remarkable porphyritic texture that shows the shallow intrusion, and accompanying the dissemination of pyrite and alteration such as tourmalinization and silicification. In their chemical composition too, they are richer in alkaline components, especially in potash, in comparison to other earlier intrusive rocks (Table I-4), suggesting an affinity to the later porphyritic rocks.

Thus, the igneous activity in the Yauri Area is considered to be successive one from plutonic to volcanic activities, resulting in producing various rock species and facies in response to magmatic differentiation and physico-chemical conditions of intrusion.

Table I-4 Silica, Lime and Alkali Contents in the Main Earlier Intrusives, Yauri Area

Intrusive Body	Rock Name	SiO ₂ %	CaO %	Na ₂ O %	K ₂ O %	Sample No.
Tintaya	Gabbro	46.76	10.42	2.20	0.53	No. 455 in 2nd-phase survey
	Meta-gabbro	47.93	11.15	3.09	0.32	No. 36' in this survey
	Meta-gabbro	46.18	11.27	2.21	0.61	No. 135 in this survey
Vellile	Quartz diorite	59.48	7.48	3.99	1.31	No. 19 in 2nd-phase survey
	Quartz diorite	58.46	5.95	3.32	1.73	No. 9 in 2nd-phase survey
	Grano-diorite	56.59	7.05	4.78	0.45	No. 4 in 2nd-phase survey
Pichigua	Grano-diorite	59.87	5.74	3.64	2.26	No. 376 in 2nd-phase survey
	Diorite porphyrite	52.89	5.90	3.85	2.10	No. 354 in 2nd-phase survey
	Diorite	52.11	7.69	3.23	2.75	No. 349 in 2nd-phase survey

CHAPTER 3 GEOLOGICAL STRUCTURE

3-1 Regional Structure

The Tintaya region in which the surveyed area is involved, is a terrain of intrusive rocks and the Mesozoic sediments exposing as an inlier of the lake deposits in the southwestern fringe of the Yauri Basin. This basin is a graven formed in between the Western Cordillera and Laramani Massif as reported in the previous survey, and its eastern side is terminated by a great fault of NNW-SSE. The west side of the basin may possibly be bordered by faults, too, as the distribution of lake deposits and topography are more distinctly controlled by the two structural trends of NW-SE and NE-SW, though there are no distinct faults observed on the west side of the basin.

The Tintaya region forms a considerably big hill, getting in between the Rivers Salado and Campia which are flowing down either in NW or NNW. The gravity survey done in the last survey indicated an existence of a fault with downthrow of the east block along the River Salado which borders the eastern side of the region. In this sense, the Tintaya region might be a faulted mountain block in a small scale formed at the periphery of the Yauri Basin.

The Mesozoic formation of Tintaya region shows repeated small and gentle foldings with its axis of NNW-SSE or NW-SE, forming an anticlines are so formed as the one, from Tintaya to Quechua, and the other, from Huaccollo to Coroccohuayco.

The earlier plutonics, being capped by roof-pendants of considerably wider remnants of the Mesozoic formation, spread in an area of 10 km in width and more than 20 km in elongation, intruding with a distinct trend of NNW-SSE parallelly to the main structural axis of the Mesozoic sediments.

The Mesozoic formation and the plutonic rocks are cut by two sets of faults, the one striking in NNW-SSE and the other rectangular to the former. Behavior of the faulting movements have not been clarified satisfactorily, but vertical shifting seems to be leading, with the downthrow of west side in regards to the system of NNW, and with the downthrow of north side in regards to the system of NE or NEN. A shattered zone of NNW system has been formed in Quechua. The similar one is inferred to exist in the Huaccollo block, too.

The intrusion of later porphyritic rocks is controlled by such the structures mentioned above, especially by the structure of NNW system. Three structural trends were estimated in the previous survey, such as Coroccohuayco-Huaccollo line, Quechua-Tintaya line, and Ataraya line, along which intrusion of the porphyritic rocks are seen collectively. The porphyritic rocks occur along these structural lines of NNW in the forms of small stocks and dykes, but they often occur as sheet-like bodies in the Mesozoic formation, being controlled by its bedding structures. The structures of NE or ENE system also control the intrusion of porphyritic rocks, as is seen in the dykes of Tintaya which are parallel to a fault of NE system, but are split out of a stock. Such are recognized in Coroccohuayco, too.

3-2 Geological Structure of the Surveyed Area

It is the matter of course, the fundamental geological structure is similar to that of the Tintaya region as mentioned in the foregoing chapter, consisting of the combination of two sets of structural trends, the one of NNW-SSE as principal factor, and the other, rectangular to the former as subordinate factor.

The trend of NNW system has controlled the structure for long period, as the folding of the Mesozoic formation, elongation and arrangement of the intrusive rocks, fissures and fractured zones associating with quartz veins, are all showing this trend.

The structure of ENE system is well represented by a fault crossing the central part of the area. In the Huaccollo block, the Mesozoic formation dominates in the north of the fault, and, on the contrary, the plutonic rocks expose widely in the south of the fault, Coroccohuayco block. The Huaccollo block was downthrow most probably. There is a few dykes of porphyritic rock intruded parallelly to the fault at about 1 km south of it. Some of the fissures and quartz veins show the similar trend locally. Therefore, the faulting of ENE system, though subsidiary, must have been the structural factors to introduce intrusion of the porphyritic rocks and related mineralization.

3-2-1 Folding Structure of the Mesozoic Formation

The Mesozoic formation of the Huaccollo block forms a wide anticlinorium composed of three small anticlines with an axial trend of NNW-SSE. The axes of these small anticlines are plunging southwards in the

southern part, and northwards in the north, resulting in a formation of local small swell-structure. Such a swell structure was not necessarily caused by the igneous intrusion, but it may safely be said, at least, it offered favorable structural condition to enable the intrusion of igneous rocks.

3-2-2 Forms and Arrangements of Intrusives

In the Coroccohuayco block, the earlier plutonic rocks are widely distributed with a trend of NNW-SSE, centering its distribution in the central part of the block where existence of the anticlinal axial portion of the Mesozoic formation is inferred. The plutonic rocks are less exposed in the Huaccollo block, with a few small stocks arranged in NNW-SSE along the eastern periphery of the block. It is anticipated an existence of large plutonic body hidden in the Huaccollo block similarly to the Coroccohuayco block, but its depth can hardly be guessed as amount of faulting displacement is not determined.

The later porphyritic rocks are intruding collectively in the central zone of the area combining the Coroccohuayco and Huaccollo mineralization zones, and along the eastern periphery of the area. They occur generally as groups of small intrusive bodies, and those intruded in the plutonic rocks form small stocks and dykes, but those intruded in the Mesozoic formation often form sheet-like bodies being controlled by its structure. The general trend of intrusion of the porphyritic rocks, similarly to their general trend of arrangement, show NNW-SSE, but some local variation of ENE-WSW, rectangular to the former, is also observed.

In view of the general habit of intrusion, the porphyritic rocks are considered to have intruded mainly along the structurally weak zones of NNW-SSE, with some exceptions followed the subordinate breakage of ENE-WSW.

3-2-3 Fissuring and Fracturing

Tectonic movement seems to have continued after intrusion of the porphyritic rocks, as there are often recognized the porphyritic rocks showing cataclastic texture. Many quartz veinlets are developed in the porphyritic rocks in the Coroccohuayco and Huaccollo mineralized zones. Most of the quartz veinlets are divided into two groups of their trends, the one having strike of NNW-SSE, dipping 60° - 80° , and the other having strike of ENE-WSW with dips of 60° - 80° , the former being extraordinary predominant. As the mineralization in the porphyritic rocks is mainly in association with quartz veinlets, the mode of development of quartz veinlets may be considered to control the localization of ore deposits.

Fissures and joints are fairly well developed in the quartzite of Huaccollo block, and it is anticipated an existence of fractured zone elongated in NNW-SSE especially from the center westwards in the block. Although the mechanism of formation of the fractured zones have not been solved clearly, the fractured zone of Quechua is considered to have been formed by the intrusive activity of the porphyritic rocks. If the Huaccollo fractured zones have been formed in the similar mechanism to that of Quechua, it must have an important significance to the localization of mineralization.

CHAPTER 4 ECONOMIC GEOLOGY

4-1 Mineralization

4-1-1 General Features of Mineralization

Copper mineralization and its related alteration have been brought along with intrusive activity of the later porphyritic rocks, as reported in the second phase survey.

The type of mineralization, however, is not the "typical" porphyry copper type against the previous anticipation, but is considered to be a combined type of copper mineralization of porphyry copper type and skarn type.

Difference of the types of mineralization mainly depends upon the chemical composition of host rocks. Mineralization of porphyry copper type is observed in the porphyritic rocks or in such non-calcareous sediments as quartzite, sandstone, and sandy shale. Mineralization of skarn type is observed mostly in limestone and calcareous shale. The gabbroic rocks rich in calcium have been affected by metasomatic alteration and mineralization in association with the formation of skarn minerals.

Mineralization seems to have an intimate relation to shattering of the porphyritic rocks, as almost all the remarkable indications of mineralization have been formed in and around the shattered porphyritic rocks. Distribution of the shattered porphyritic rocks are mostly concentrated in the central zone of the surveyed area, the area combining the Coroccohuayco and Huaccollo mineralized zones. The trend of the shattered zone in the

porphyritic rocks is generally NNW-SSE, with a few local exceptions having rectangular trend to the former.

Mineralization has been essentially controlled by such factors of rock facies and structure as stated above. Especially, in the mineralization of porphyry copper type, most of ore minerals are concentrated in the fractures, of which development may render an important factor for ore deposition.

Primary sulphide minerals are pyrite and chalcopyrite with a little amount of molybdenite as an accessory. Spharelite, galena, and tetrahedrite rarely appear. According to assay results of ore samples, minute amounts of gold and silver are also contained. Bornite is the important copper mineral in the Coroccohuayco mineralized zone, but most of it is considered to be of secondary origin. Chalcocite, covellite, cuprite, native copper, malachite, chrysocolla, and azurite, are other secondary minerals mostly distributed near the ground surface. They are considered mostly the products in situ. Magnetite and specularitic hematite are fairly wide spread, characterizing the nature of mineralization of this area.

4-1-2 Principal Indications of Mineralization

(1) Indications in the Coroccohuayco Block

The most prominent mineralization and related alteration in the Coroccohuayco block can be seen in the Coroccohuayco mineralized zone located in the central part of the block. This zone is intruded by the porphyritic rocks frequently in the forms of small stocks and dykes of quartz monzonite porphyry as principal one, and in the limestone of eastern

adjacent some sheet-like apophyses are split from the stocks (cf. PL. I-1 and I-2). Prominent alteration can be observed in and around these porphyritic rocks as shown in PL. I-3, and many copper anomalies have been detected too by geochemical survey in a area covering 400---800 m x 2.6 km. (cf. PL I-4).

Prominent copper mineralization in this area is mostly in association with bunches of quartz veinlets formed in the porphyritic rocks and skarn formed in the limestone. The mineralization encountered by DDH-4 of pilot drillings (0.83 % Cu, 0.065 % Mo in 78 m of core length) is related to one of the quartz veinlet zones in the porphyritic rocks. A fairly intense copper mineralization (1.53 % Cu in 24.6 m of core length, or 0.70 % Cu in 84 m of extended core length including the portions of weak mineralization) was also encountered by DDH-3 in association with skarnization (cf. PL. I-2). Copper minerals in these mineralization are principally chalcopyrite and bornite.

The quartz veinlets usually show two sets of their trends, the one is NNW-SSE in strike with dips of 60° - 80° E, and the other, ENE-WSW in strike with dips of 60° - 80° N, the former being predominant. The quartz veinlets are not distributed uniformly in the porphyritic rocks, but they usually form a zone of 50--20 m in width. Distribution of them in the gabbroic rocks becomes suddenly sparse, showing scattered and uncollective patterns, in those portions where the stocks of porphyritic rocks are terminated by the gabbroic rocks. But in the stock immediate south of DDH-4, a zone of quartz veinlets of 300 m x 500 m has been formed by

the intersection of two systems of them, NNW and ENE (cf. PL. I-3).

DDH-4 is located in the border between the stock groups of porphyritic rocks and eastern limestone, where it has encountered the mineralization of limestone replacement type. This mineralization is considered to have been caused by sheet-like apophyses split from a porphyritic stock (cf. PL. I-2). This bordering zone is widely covered by sands and gravels of Quarternary as shown by PL. I-1, but the results of DDH-3 may suggest a possibility that a mineralization field similar to that of the East Ore Body of Tintaya may have been formed.

In the gabbroic rocks around the porphyritic rocks, metasomatism can be noticed, being represented by actinolite, garnet, and epidote, and its related copper mineralization. So far as the results of DDH-5 and -6 are concerned, it does not seem to be spread widely, but sparse in distribution (cf. PL. I-2). But in the certain Limited area, as can be seen near the survey station N'-22, fairly intense copper mineralization has been brought out in association with this alteration (cf. PL. I-5 and sketch -3).

As for the other indications of mineralization, it may be noticeable that copper anomaly detected by geochemical survey starts from the vicinity of survey station J-37 in the eastern border, and extends northeastwards beyond the limit of surveyed area (cf. PL. I-4). May it be less evaluated for prospecting purpose, this anomaly can be correlated to the copper-bearing skarn zone and may have an important significance to suggest that the mineralization extends eastwards beyond the surveyed area.

4-1-3 Indications in the Huaccollo Block

The fundamental geological environment resembles to that of the Quechua mineralized zone as mentioned in Chapter 2. The central area, where a favorable field for mineralization is highly anticipated, is mostly covered by the Quarternary formation, which makes it difficult to collect exact informations about geology and mineralization amply (cf. PL. I-1).

Considerably prominent alteration and mineralization on the surface are so distributed as to surround the central portion of the block where the Quarternary formation develops (cf. PL. I-3).

There lies the Huaccollo mineralized zone, which was discovered during the survey of the second phase, on the Qda. Huaccollo flowing in the northern border of the Quarternary area. As is already reported, veinlets and dissemination of pyrite in association with chalcopyrite are observed here fairly wide-spread in the porphyritic rocks exposing along the creek, and an existence of a hidden zone of sizable copper mineralization has been anticipated. Through the re-study of the outcrops and core-logging of DDH-1, drilled about 100 m south of the outcrop, during the current survey, however, it has been understood that the mineralization is characterized by pyrite-hematite-chlorite veins, but the silicification related to the copper mineralization (mostly quartz veinlets) is generally weak and more or less localized. Such the features of mineralization and alteration strongly suggest that this portion represents the peripheral zone of mineralization. Besides, fissures and veinlets exhibit a distinct trend of NNW-SSE.

Intensely fractured quartzite with coatings of iron hydrate films are observed abundantly in the western side of the Quarternary formation. Although its relation to mineralization is still uncertain, it has been cleared in Quechua that there is a close relationship between the fractured zone and mineralization, which, consequently, necessitates the study of distribution and origin of the fractured quartzite. In the porphyritic granodiorite exposing in the vicinity of survey station D'-8, a zone of quartz veinlets of approximately 100 m wide is extending in ENE-WSW. The intersectional area of this zone of quartz veinlets and the one noticed in the "Huaccollo mineralized zone" may be noticeable as a promising field for mineralization.

In the southern side of the Quarternary area, group of small stocks of the porphyritic rocks penetrate a formation of alteration of limestone, shale, and sandstone, giving fairly wide effects of skarnization against the said sediments. Some intense but local copper mineralization is recognized in the skarn zone, and geochemical survey has detected a copper-anomalous zone of about 200 m x 1 km (cf. PL. I-4). DDH-2 of pilot drillings located about 200 m north of the skarn zone has encountered only a few small dykes of the porphyritic rocks, but distinct copper mineralization has been recognized in the dykes and in the sediment around their intersections (cf. PL. I-2). This mineralization is of porphyry copper type brought along silicification and argillization, which is noteworthy to indicate a hidden zone of mineralization of porphyry copper type under the Quarternary formation.

4-1-4 Ore Minerals

The principal primary minerals are pyrite, chalcopyrite, and molybdenite, which occur as veinlets and dissemination. A part of bornite might be of primary.

The most abundant sulphide is pyrite, which are observed commonly in all the six drill holes. Its distribution has been obscured very much on the surface due to advanced oxidation and leaching. But distinct dissemination and fissure-filling of pyrite have been recognized, though locally, in the argillized quartz-monzonite porphyry of the Coroccohuayco mineralized zone. A zone of pyrite veinlets has also been noticed, as already mentioned, in the altered porphyritic rocks exposing along the Qda. Huaccollo. Minor amount of pyrite seems to be widely distributed almost all over the surveyed area. (cf. PL. I-3).

The most important copper mineral is chalcopyrite, but some secondary bornite is in association with pyrite in the Coroccohuayco mineralized zone. The copper minerals in the porphyritic rocks mostly occur in and around quartz veinlets, and the typical dissemination is rather sparse. Associated ore minerals are mainly pyrite, molybdenite, magnetite, and hematite. Most magnetite occurs as dissemination, and direct association with copper minerals is rather rare. Magnetite is thought mainly to have been formed prior to the copper mineralization. Paragenesis of hematite and chalcopyrite has been recognized in DDH-1. In the affirmed indications of copper mineralization in the Coroccohuayco block, pyrite is generally dominant to chalcopyrite.

But in the mineralized portions by copper encountered by DDH-4, copper minerals fairly exceed pyrite in amount. In quartzite, sandstone, and shale, too, chalcopyrite occurs more often as fracture-filling and veinlets than as dissemination. In the skarnized limestone and gabbroic rocks, copper minerals occur as dissemination, stringers, or in association with quartz-calcite veins. Pyrite and magnetite are co-existing minerals but magnetite may probably be the product prior to the copper mineralization.

Molybdenite occurs almost always in association with copper sulphides but generally sparse. DDH-4, however, has encountered copper mineralization which contains considerable amount of molybdenite giving assay of 0.065 % Mo. in 78 m of core length.

Seldomly, galena and spharelite occur in association with chalcopyrite and pyrite in the skarnized limestone and gabbroic rocks. Minor amount of tetrahedrite included in chalcopyrite has been recognized in the gabbroic rocks from the core of DDH-6 at the depth of 78.4 m.

Au, Ag, and As have been assayed on 30 samples from the drill-cores of mineralized portions encountered by DDH-3 and -4. The results are shown in Table I-5, telling the ore contains trace amount of gold, minor amount of silver and negligible amount of arsenics harmless for exploitation.

Though the leached zone has been less developed than expected, the secondary alteration of ore minerals is more or less advanced. Effects of oxidation have been recognized in DDH-1 and -2 even below the sand and gravel beds of about 40 m thick which is probably of glacial origin.

Table I-5 Assay Result for Au, Ag and As on the Mineralized Core-Samples from DDH-3 and DDH-4

Hole No.	Sample No.	Au	Ag	As	Remarks		
					Total Cu	Mo	Host rock
DDH-3	3038	ppm tr	ppm 4	ppm 6	% 2.72	% tr	Skarnized limestone
	3040	tr	3	2	0.84	-	
	3042	tr	4	3	0.90	0.001	
	3044	tr	8	6	1.23	0.001	
	3046	tr	4	5	0.48	0.001	
	3048	tr	3	5	0.44	0.002	
DDH-4	4002	tr	6	1	0.92	0.014	Quartz monzonite porphyry
	4004	tr	2	tr	0.48	0.010	
	4006	tr	2	tr	0.32	0.002	
	4008	tr	2	tr	0.29	0.004	
	4010	tr	4	tr	0.66	0.004	
	4011	tr	3	tr	0.61	0.080	
	4012	tr	6	2	1.06	0.025	
	4014	0.2	15	1	3.62	0.600	
	4015	2.0	28	2	5.91	1.56	
	4016	tr	5	tr	0.98	0.043	
	4018	tr	1	tr	0.42	0.005	
	4020	tr	tr	tr	0.48	0.004	
	4022	tr	1	tr	0.32	0.044	
	4024	tr	tr	1	0.18	0.008	
	4026	tr	2	1	0.48	0.004	
	4028	tr	3	2	1.82	0.262	
	4030	tr	9	2	1.83	0.032	
	4032	tr	4	1	1.32	0.011	
	4034	tr	5	1	1.27	0.025	
	4036	tr	2	1	0.48	0.002	
4038	tr	tr	1	0.30	0.005		
4040	tr	tr	2	0.42	0.003		

The oxidation must have advanced deeper than the present water table at least, which may suggest that oxidation might have advanced actively even before the deposition of the sands and gravels.

Bornite, chalcocite, covellite, cuprite, native copper, malachite, chrysocolla, and azurite have been noticed as secondary minerals.

Bornite is ranked as the most important copper mineral with chalcopyrite in the Coroccohuayco mineral with chalcopyrite in the Coroccohuayco mineralized zone.

Bornite here was taken as primary at first, which was, in fact, supported by a texture suggesting as if there were exsolutional relation between chalcopyrite and bornite. But the following evidences may strongly suggest its secondary origin if not all, but at least most of it.

- 1) Bornite replacing chalcopyrite has often been recognized.
- 2) Though minor in amount and localized, some chalcocite and covellite are replacing chalcopyrite and bornite.
- 3) As a general tendency, chalcopyrite is replaced by bornite, and bornite by chalcocite and covellite, showing a gradual decrease of sulphur contents in the copper minerals (oxidation).
- 4) The co-existing magnetite is also replaced by hematite advancedly suggesting intense oxidation.

The depth of the secondary alteration in the Coroccohuayco mineralized zone is still uncertain, but the alteration is considered to have advanced fairly deep, as the occurrence of bornite and chalcocite had been recognized as deep as 250.3 m below the surface, that is, the bottom of DDH-6.

An oxidation zone containing hematite, limonite, and jarosite lies near the surface with associated such copper minerals as malachite, chrysocolla, and azurite. The depth of oxidation zone is fairly variable as shown in Table I-6. Localized occurrence of native copper and cuprite is noticed in the lower portion of oxidized zone. Considering from the frequent existence of copper sulphides mixed with copper oxide minerals, leaching of copper seems not so much advanced, though evidenced affirmedly. One of the reasons may be inferred to the frequent occurrence of calcite in the country rocks. Calcite, as will be explained later, is contained not only in the calcareous sediments but also in almost all the country rocks as a product of carbonatization, which might have prevented migration of large amount of copper.

Table I-6 Thickness of Oxidized Zone shown by the Lower Limit of "Clear Limonitization" in the Drill Holes

Block	Hole No.	Depth from the Surface	Thickness of Oxidized Zone
Huaccollo	DDH-1	38.5m - 55.5m	17.0m*
	DDH-2	41.5m - 62.8m	21.3m*
Coroccohuayco	DDH-3	0m - 62.7m	62.7m
	DDH-4	0m - 6.0m(-)	6.0m(-)
	DDH-5	0m - 22.2m	22.2m
	DDH-6	0m - 33.2m	33.2m

* Thickness without the glacial sediments

4-2 Alteration

4-2-1 Feature of Alteration

The intrusive rocks and the Mesozoic formation have been affected by alteration to some extent. Type of the alteration comprises a complex of the hydrothermal alteration of porphyry copper type and the metasomatic alteration of skarn type, being controlled by the influence of chemical characters of country rocks.

The alteration of porphyry copper type is mostly observed in the porphyritic rocks and non-calcareous sediments. Silicification, argillization, and sericitization are recognized as main processes, but because of the usual accompaniment of carbonatization, the type of alteration may slightly differs from that of the so-called typical porphyry copper.

Limestone and calcareous shale are often skarnized at the contact with the porphyritic rocks, and the gabbroic rocks are also affected by the metasomatic alteration accompanying skarn minerals.

Chloritization and epidotization are recognized quite wide-spread, and most of the gabbroic rocks, shale, and arkosic sandstone have suffered this kind of alteration.

Besides, as has been described in Chapter 2, the porphyritic rocks have given thermal metamorphism to the surrounding sediments and gabbroic rocks prior to these alterations, resulting in producing abundant biotite frequently in the gabbroic rocks, shale, and sandstone.

4-2-2 Description of Each Alteration

(1) Silicification

Silicification of this area is recognized as bunches of quartz veinlets in the porphyritic rocks but the so-called "massive" silicified rocks are not recognized.

1) Silicified Zones of the Coroccohuayco Block

The most well-defined silicified zone can be seen in a group of small stocks of quartz-monzonite porphyry in the Coroccohuayco mineralized zone as outline in 4-1.

In a stock directly south of DDH-4, a zone of net-work quartz veinlets of approximately 300 m x 500 m has been formed, in which the station N'-20 being about the center. General trends of the quartz veinlets are in two system, the one is NNW-SSE in strike with dips of 60° - 80° E; and the other; ENE-WSW in strike with dips of 60° - 80° N, the former being predominant. Quartz veinlets have generally the width ranging from 1 mm to 1 cm at spacing from less than 5 cm to about 30 cm. Any direct sign of mineralization can hardly be recognized on the surface, but small spots of iron hydroxide after sulphides are commonly recognizable along the quartz veinlets in most cases. The iron hydroxide may be a mixture of limonite and jarosite, presenting dull yellow to pale maroon. Weak impregnation of copper oxides are often recognized in the periphery of silicified zone. Besides, there occur a few small dykes of "unsilicified" granite porphyry intruding into the silicified quartz-monzonite porphyry. The granite porphyry contains minor amount of chalcopyrite and pyrite, indicating that its intrusion took place succeedingly to the silicification.

Another such silicified zone by quartz veinlets also exists in the

quartz-monzonite porphyry, which lies in the northern side of the silicified rocks above-mentioned. Mineralization encountered by DDH-4 is related to one of such silicified zones as already mentioned. The silicified zone here is emplaced in the argillized porphyritic rocks as narrow zones with distinct trend of NNW-SSE. The silicified zone consists of numerous parallel quartz veinlets with a general strike of NNW-SSE with dips of 60° - 80° E. The quartz veinlets generally have the width of a few millimeters to approximately 1 cm at the spacing of a few centimeters to 20 cm or so with some of rare exceptional quartz veins of more than 5 cm wide. Almost none of copper mineral can be recognized on the outcrops of these silicified zones except the one near DDH-4, but there exist the "relief" iron hydrates similarly to that silicified zone described before. In the silicified zone near DDH-4, as shown in the Sketch-1, PL. I-5, a distinct mineralization is presented by copper oxide ores as well as an old adit. The quartz veinlets are often in association with carbonate minerals. Many copper quartz veinlets in DDH-4 are usually associated with calcite of small amount, considerably wide-spread throughout the porphyries with sericite, clay minerals, and chlorite.

2) Silicified Zones of the Huaccollo Block

The silicification seen on the ground surface in this block is generally local and weak with the following exceptions;

- (a) Bunches of quartz veinlets of NNW system in the porphyritic rocks along the Qda. Huaccollo, especially near the station C-17.

- (b) Bunches of quartz veinlets of ENE system in the porphyritic granodiorite near the station D'-8.

In the exposures of the porphyritic rocks along the Qda. Huaccollo, chloritization and weak argillization are generally dominant, with the characteristic development of pyrite-hematite-chlorite-quartz veins. But small amount of pyrite-quartz veinlets are also observed commonly, and they are specially concentrated near the station C-17. Many quartz veinlets associate a small amount of chlorite, calcite, and hematite. More calcite is contained in the chlorite veinlets. According to the core log of DDH-1, the chlorite veinlets are either cutting the quartz veinlets or being cut by them. Chalcopyrite seem to be associated with the quartz veinlets and the earlier chlorite veinlets. Many of the sulphides disseminated in the porphyritic rocks are replacing the chloritized mafic minerals. Plagioclase has often been turned into pink along chlorite stringers, but none of the conversion of plagioclase into potash feldspar can be seen. Most of the feldspars are partly replaced by calcite, sericite, and clay minerals. Alteration of biotite and common hornblende is mainly represented by chlorite and calcite. Sometimes secondary biotite is formed after the pre-existing mafic minerals, but probably due to unstable condition, it is further converted into chlorite. The alteration here has the nature of propylitization somehow as stated above, but such alterations as silicification, argillization, and sericitization are distinct though local. The outcrops of this zone are considered to correspond to transitional zone from the propylitization to argillization zones of alteration of por-

phyry copper.

A zone of quartz veinlets of about 100 m wide has been formed in the porphyritic granodiorite near the station D'-8, filling up a breakage zone of ENE trend. Most of the veinlets are a few millimeters to 1 cm wide, arranged parallelly in a very compact spacing of 2 or 3 cm. The quartz veins are pure white in color and poor in the "relief" iron hydrates. So it may be difficult to expect any intense mineralization from this very portion. There seems, however, a high possibility that the intersectional portion of this zone with that of the Qda. Huaccollo, a zone of quartz veinlets of NNW system, would offer a favorite field for mineralization.

4-2-2 Argillization and Sericitization

Generally speaking, the porphyritic rocks have been more or less affected by argillization and sericitization. Such can be noticed in the sediments too, as shown by DDH-2 of pilot drillings. But such alterations are generally so faint that distinct megascopical recognition is limited almost in the surroundings of the silicified zones of earlier stage.

In the argillized porphyritic rocks of the Coroccohuayco mineralized zone, feldspars have generally been replaced, though partially, by clay minerals, sericite, and calcite. Halloysite and montmorillonite occur as clay minerals. Mafic minerals are mostly chloritized, but partly replaced by epidote, too. Sometimes biotite is altered into aggregates of calcite and leucoxene. Such paragenesis of calcite and epidote suggests that this argillization is slightly different from the one represented by "argillized zone" in the mineralization of typical porphyry copper type, but has superimposed

over propylitic alteration. In the argillized porphyritic rocks on the surface, weak impregnation of green copper ores and limonitic boxworks of dark brown to reddish brown are often observed and dissemination and stringers of pyrite are also recognized locally. DDH-4, however, indicates that sulphide contents in the argillized porphyritic rocks are less than that in the silicified porphyritic rocks, and that pyrite is more abundant than copper sulphides. In addition, sulphides occur mostly as dissemination in the argillized porphyritic rocks.

In the mineralized porphyritic rocks encountered by DDH-2, such alterations as sericitization and argillization of feldspars and chloritization of mafic minerals are more distinct, although weak silicification by quartz stringers are recognized. Sometimes minor amount of fine grained biotite replacing after common hornblende are noticed. Epidote occurs in minor amount but no carbonate is recognized. This sort of alteration is considered to be akin to what is represented by "standard" argillization zone in the alteration of porphyry copper type. Principal ore minerals consist of pyrite and chalcopyrite, not only being contained in quartz veins and fractures, but also disseminated fairly abundantly. Shale and sandstone around the porphyritic rocks have been altered into hornfels containing the aligned secondary biotite, and small amounts of garnet, actinolite, and epidote, and the biotite has further been chloritized by the later alteration. Moreover, feldspars have been partly replaced by sericite and clay minerals. Alteration of quartzite may appear feeble, but in a sample taken from the drill core of DDH-2 at the depth of 50.5 m, feldspar grains,

contained in small amount, have been completely altered into aggregates of muscovite. Tourmaline, though very minor in amount, has been recognized as well.

4-2-3 Skarnization

Skarnization or pyrometasomatism has been caused not only by the porphyritic rocks but also by the gabbroic rocks of earlier intrusion. The pyrometasomatism by the gabbroic rocks is represented by the formation of magnetite, accompanying a small amount of quartz but lacking copper mineralization. The pyrometasomatism by the porphyritic rocks, on the contrary, has widely produced such skarn minerals as garnet, actinolite, diopside, and epidote, associating with not only magnetite but also sulphides of copper and iron.

In the Coroccohuayco mineralized zone, DDH-3 has revealed an existence of skarnization accompanying prominent copper mineralization near the border between the group of porphyritic stocks and the eastern limestone. Limestone has been replaced, though not universally, by such skarn minerals as garnet, actinolite, diopside, and epidote. Among the skarn minerals, garnet is most abundant, and actinolite, epidote, and diopside mostly occur in the thin shaly layers intercalated in the limestone. Garnet is intensely fractured, being interfilled by quartz and calcite, and actinilite and diopside are partly chloritized. Such would suggest the effects of hydrothermal alteration after the skarnization. Magnetite is considered or have been formed along with the skarnization but sulphides have been brought about by the later hydrothermal alteration, as they are

associated with quartz and calcite, and often replacing the skarn minerals and magnetite.

In the Corocchohuayco mineralized zone, the gabbroic rocks have also been affected by the metasomatic alteration which accompanies skarn minerals near the intrusion of the porphyritic rocks. Skarn minerals consists mostly of actinolite and epidote accompanying garnet. "Skarnized" gabbros are recognized not only on the ground surface, but also encountered by the drill cores from DDH-3, DDH-5 and DDH-6. They, however, show rather sparse occurrence by presenting irregular "vein-like" or narrow zonal forms in general. Metasomatism in the gabbroic rocks may have advanced only around the fractures. Copper mineralization is almost limited in and around such "vein-like" skarn, but the copper ore itself has been formed with the calcite-quartz-chlorite alteration of post-metasomatism. Besides, the ore-bearing quartz-calcite veins are traversed by barren calcite and zeolite veins, which are considered to have been formed in the latest period of hydrothermal alteration together with the formation of serpentine.

In the Huaccollo block, a considerably large body of skarn has been formed near the survey station of G-20, as already mentioned. Skarn which has replaced limestone consists mostly of magnetite and garnet with local association of green copper ores. Shale and sandstone contain garnet, actinolite, and epidote fairly extensively, and prominent copper mineralization can be seen in the intensely skarnized thin layers of calcareous shale. Copper minerals are mostly green copper minerals, with the local

occurrence of chalcopyrite and secondary copper sulphides.

4-2-4 Chlorite-Epidote Alteration (Propylitization)

This sort of alteration is generally faint but observed vastly. In the Corocochuayco block, greater part of the gabbroic rocks have been suffered by this alteration, and this alteration can be observed in many parts of the gabbro, sandstone, and shale in the Huaccollo block. The standard combination of the alteration minerals is considered as chlorite-epidote-calcite.

In accompaniment of this alteration, sulphides (pyrite mostly, chalcopyrite in less amount, and magnetite in limited case) are recognized though scantily, but none of the prominent indication of mineralization has ever been recognized. The zone of their alteration is considered to correspond to the "propylitization zone" which usually represents the outermost zone of the typical porphyry copper deposit.

4-3 Results of Geochemical Survey (cf. PL. I-4)

The results of geochemical survey are shown in PL. I-4.

Samples are the soils taken at the regularly arranged station in a grid pattern of 100 m x 200 m, and from 20 cm to 70 cm below the surface, amounting to 1,681 in total. About three quarters of the total samples were taken from B bed of residual soils derived from the Mesozoic sediments and the intrusive rocks, and the remaining one quarter are from the Quaternary sand and gravel beds and alluviums along the creeks. The Quaternary sand and gravel beds amount as thick as 40 m or so.

The alluvial soils also reaches for several meters. Such covering formations are distributed dominantly around the mineralized zones as is shown in PL. I-1, which prevents the perfect detection of geochemical anomalies.

Cu and Mo were chosen as indicators similarly to the second phase survey, and chemical analysis was ordered from Maria Lau (Peruvian geochemical analyst). The analytical methods by Maria Lau are quite similar to that of reported in the last phase, applying 2.2' Biquinoline method for Cu and Thiocyanate method for Mo. Check analysis was done by the Central Laboratory of the Nippon Mining Co., Ltd. on some representative samples showing the assay values of each grade-classification, resultantly assays of Mo by Maria Lau showed a tendency of considerably lower in comparison to those by the Nippon Mining. But practically no serious discrepancies were found between the two in Cu assays, which made possible the detection of geochemical anomalies by Cu.

Cu assays showed a frequency distribution as shown in Fig. 4, and its mean value (\bar{x}) was 104 ppm Cu, and standard deviation (σ) was 259 ppm Cu. Among several ways to fix the threshold values of anomalies, here it was set as follows:

Threshold for weak anomaly : $\bar{x} + \sigma \doteq 360$ ppm Cu.

Threshold for intense anomaly : $\bar{x} + 2\sigma \doteq 660$ ppm Cu.

Samples higher than 360 ppm Cu occupy a little less than 5 % of the whole, and those higher than 660 ppm form about 2 % of the whole.

The most prominent copper anomaly can be seen in the Coroccohuayco

mineralized zone. Here the intense anomalies of copper are more less sparse, but many of them have been noticed for 2.6 km in elongation along the direction of NNW-SSE, with the width of 400 to 800 meters ranging from the survey line from I' to P. As one of the causes of dispersed copper anomalies, the black alluvial soil may be pointed out, which is distributed along the Qda. Coroccohuayco flowing through the center of the anomalous zone.

A copper anomaly is observed in the eastern borde of the Coroccohuayco block, which is extending from the vicinity of the survey station J-37 towards the outside of the area. This anomaly is what is correlated to the copper-bearing skarn zone on the surface and has an important significance to suggest possible extension of the copper mineralization eastwards beyond the surveyed area.

A prominent copper anomaly has been noticed around the skarnized zone near the survey station G-20 in the Huaccollo block, which has a length of about 1 km in NE-SW, and a width of about 20 m.

In the central part of the Huaccollo block and in the eastern part of the Coroccohuayco block, any copper anomaly has never been detected, as is a matter of course, being hidden by the Quarternary sand and gravel beds, which have specially wider distribution around there. Hence, analysis of Hg was tried on the 60 soil samples showing various copper contents and from the different origins, in order to deternine the effectiveness of Hg as an indicator. As is shown in Table I-7b, it was recognized that the Hg contents in the samples were very low and even those showing

the higher copper contents did not always show the higher Hg contents.

Further test was tried on the 23 samples of drilled cores qualitatively by photo-spectrometer. The results are tabulated in Table I-7a, which shows that the sensitivity domains are different according to the elements, and the intensity shown in the table could only indicate roughly the relative abundance of each element. Among the minor elements Ga, V, Co, Sr, Pb, and Ag, are frequently detected. Ni. is also fairly well detected, but it has not been detected entirely from the samples of mineralized porphyritic rocks taken from DDH-4. Sn, Cr, B, and Zn, have been detected only occasionally. Interesting is that B was detected only from the mineralized skarn of DDH-3. Ni and Co have been detected usually in the gabbroic rocks, but Cr has never been detected. Specially, the porphyry copper deposits in South America often contain tourmaline as a boron mineral, but almost none of it has been found in this area, and B has been recognized from the analysis only in limited cases. This fact is noteworthy to characterize the nature of mineralization of this area.

Fig. 4 Histogram and Frequency Curve of Cu Content in the Soil Samples

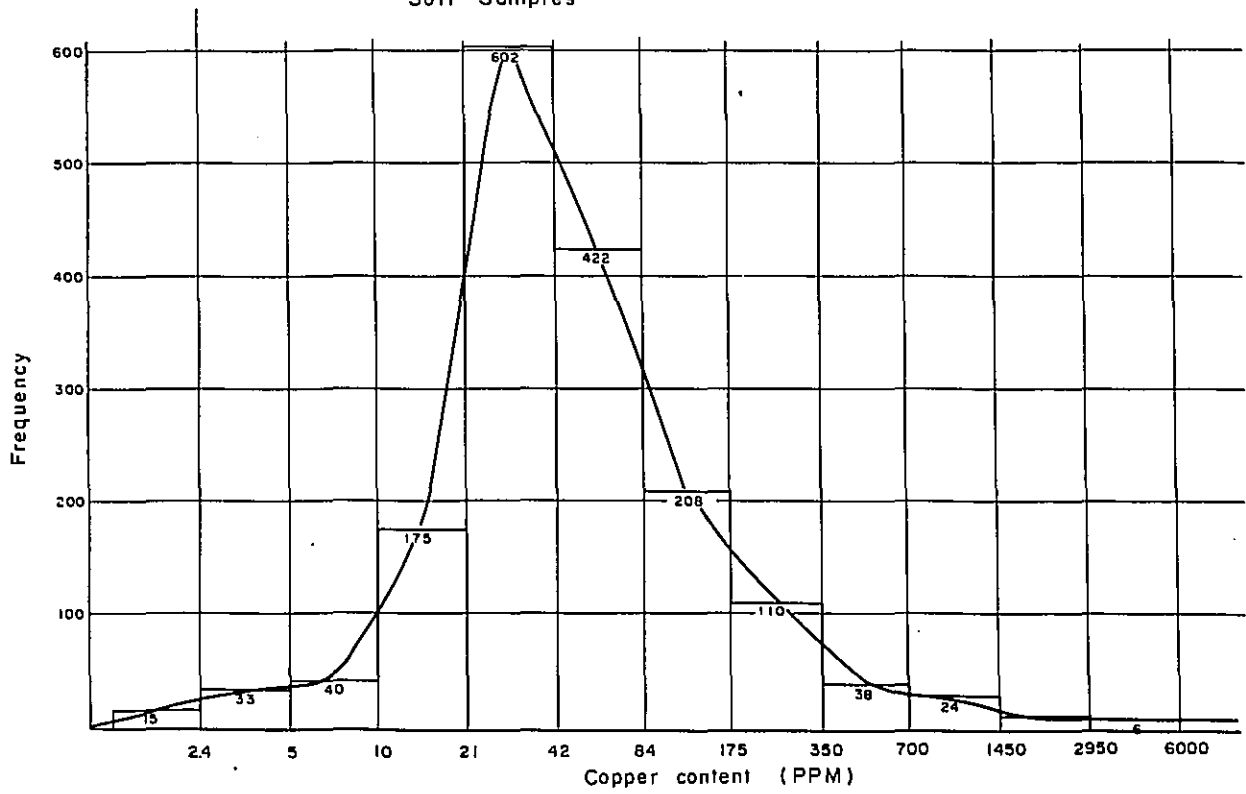


Table I-7a Qualitative Spectrum Analysis of Drill Cores

Sample	Locality	Si	Sn	Ti	V	Al	Ga	Fe	Mn	Ni	Co	Cr	Mg	Ca	Sr	Na	K	B	Ag	Pb	Zn	Cu	Mo
Porphyrific granodiorite	DDH-1 44.0m-46.0m	5	0	3	3	5	3	5	2	1	2	0	3	3	3	5	3	0	2	3	0	4	0
"	DDH-1 57.0m-58.0m	5	2	3	1	4	3	5	0	0	2	0	3	3	0	5	1	0	2	3	0	5	3
"	DDH-1 64.0m-65.0m	5	2	3	2	4	3	5	2	0	3	0	3	3	0	5	3	0	2	3	0	5	0
Quartz monzonite porphyry	DDH-2 57.7m-59.7m	5	0	3	2	5	3	5	1	1	2	0	3	4	3	5	3	0	1	1	0	5	3
Shale	DDH-2 62.8m-64.8m	5	0	3	2	4	3	5	2	3	3	3	3	4	1	5	3	0	2	1	2	5	3
Quartz monzonite porphyry	DDH-2 106.3m-108.3m	5	2	3	1	4	3	5	2	1	0	0	3	3	1	5	1	0	2	3	0	5	2
"	DDH-2 108.3m-110.0m	5	0	3	1	4	3	5	2	1	2	0	3	3	1	5	2	0	2	2	0	5	3
"	DDH-2 135.0m-139.0m	5	0	3	1	4	3	5	2	2	3	1	3	3	3	5	3	0	2	2	0	5	3
Skarn	DDH-3 84.0m-86.0m	5	0	3	0	4	3	5	3	2	3	1	5	5	3	5	3	1	3	0	0	5	0
"	DDH-3 119.4m-122.0m	5	2	3	1	3	3	5	3	2	3	0	3	5	0	5	1	1	3	2	0	5	2
"	DDH-3 130.0m-132.0m	5	1	3	1	4	3	5	3	0	2	0	3	5	3	5	3	1	2	1	0	5	1
"	DDH-3 136.0m-138.0m	5	1	3	1	4	3	5	3	0	3	0	4	5	3	5	3	0	3	1	0	5	1
Quartz monzonite porphyry	DDH-4 14.0m-16.0m	5	0	3	2	5	3	5	2	0	1	0	3	5	3	5	3	0	0	0	0	4	3
"	DDH-4 26.0m-28.0m	5	0	3	3	5	3	5	2	0	0	0	2	5	3	5	3	0	1	0	0	3	3
"	DDH-4 33.0m-34.0m	5	0	3	2	3	3	5	2	0	1	1	2	2	0	5	2	0	3	2	0	5	5
"	DDH-4 68.0m-70.0m	5	0	3	1	5	3	5	2	0	1	1	3	5	3	5	5	0	2	2	0	5	3
Gabbroic rock	DDH-5 12.4m-14.7m	5	0	3	3	5	3	5	3	1	3	0	3	5	3	5	3	0	1	2	0	5	3
"	DDH-5 14.7m-15.1m	5	0	4	3	5	2	5	3	2	3	0	5	5	3	5	2	0	3	3	2	5	4
"	DDH-5 43.0m-45.0m	5	0	4	3	5	3	5	3	2	3	0	5	5	3	5	3	0	2	1	0	5	4
"	DDH-5 124.0m-126.0m	5	0	3	3	4	3	5	2	2	3	0	3	3	1	5	3	0	2	0	0	5	3
"	DDH-5 164.0m-166.0m	5	0	3	3	4	3	5	3	2	3	0	3	5	3	5	3	0	2	0	0	5	3
"	DDH-6 30.0m-32.0m	5	0	3	3	4	3	5	3	2	3	0	3	4	3	5	4	0	2	0	0	5	0
"	DDH-6 78.0m-80.0m	5	0	3	3	5	3	5	2	2	3	0	5	4	3	5	4	0	2	1	0	5	3

Intensity of the Spectral Lines

0; not detected, 1; very weak, 2; weak, 3; moderate, 4; strong, 5; very strong.

Table 1-7b Hg Contents in Geochemical Soil Samples

Sample No.	Hg ppb	Cu ppm	Sample No.	Hg ppb	Cu ppm	Sample No.	Hg ppb	Cu ppm	Sample No.	Hg ppb	Cu ppm
B'-18	30	20	G-21	40	1200	K'-15	30	350	N'-15	30	150
-21	42	20	-24	53	280	-18	30	500	-18	57	60
-24	47	30	H-15	30	15	-21	30	350	-21	30	190
-27	35	200	-18*	30	30	-24	55	400	-24	43	420
C'-18*	47	80	-21*	30	90	-27*	30	60	-27	32	180
-21*	45	120	I'-15	30	75	L'-15	45	5	Q'-15	48	60
-24*	45	90	-18	30	60	-18	30	150	-18	35	1650
-27*	43	30	-21*	30	60	-21	32	200	-21	30	300
E-21*	37	30	-24	40	1200	-24*	30	50	-24	30	250
-24*	33	40	-27*	30	100	-27*	30	75	-27	30	50
F-18*	32	45	J'-15	37	50	M'-15	30	170	P'-15	30	20
-21*	32	60	-18	30	500	-18	30	350	-18	30	150
-24*	40	180	-21	40	300	-21	30	3950	-21	30	30
G-15	100	1900	-24	30	600	-24	30	75	-24	30	100
-18*	45	150	-27	30	800	-27*	30	70	-27	30	N

* Soil sample derived from the Quaternary sediments

CHAPTER 5 GEOLOGY INDICATED BY DRILLINGS

5-1 Selection of Drilling Sites

Six pilot holes, totalling 1,503.6 meters long, have been drilled at various parts of geology spacing some 500 meters to 2 kilometers one another in the central zone of the surveyed area, for the purpose to obtain the basic data on the subsurface geology and mineralization. Location and object of the drill holes are as follows (cf. PL. I-1).

DDH-1

Location; *Near the Station C'-18 in Huaccollo Block.

*About 100 m south of the outcrop of the mineralized porphyritic rocks along Qda. Huaccollo.

*In the IP A-anomaly.

*Covered with Quaternary sediments.

Object; To confirm suggested latent intrusive rock, and to get hold of the mode of mineralization and alteration.

DDH-2

Location; *Near the Station F-20 in Huaccollo Block.

*In the IP B-anomaly.

*About 200 m north of the skarnized zone coincident to the geochemical anomaly.

*Covered with Quaternary sediments.

Object; To obtain information of the subsurface geology below Quaternary sediments, and to check the relation between FE weak anomaly and sulphide mineralization.

DDH-3

Location; *Near the Station K-26 along the eastern margin of the
Coroccohuayco mineralization zone.

*Covered with Quaternary sediments.

Object; To comprehend outline of the geological structure and the
mineralization in the border zone between eastern limestone
and confluent stock zone of porphyritic rocks.

DDH-4

Location; *Near the Station M-21 in the Coroccohuayco mineralization
zone.

*In the IP C-anomaly.

*In the confluent stock zone of quartz monzonitic porphyries,
associated with remarkable indication of Cu-mineralization.

Object; To check the mode of mineralization in the quartz monzonitic
porphyries, especially its relation to the rock alteration.

DDH-5

Location; *Near the Station M-17 in the Coroccohuayco mineralization
zone.

*In the IP C-anomaly.

*In the gabbroic rocks showing high geochemical anomaly, in
the west flank of the confluent stock zone of porphyritic rocks.

Object; To comprehend the mode of mineralization and its relation to
the rock alteration, in the gabbroic rocks around the con-
fluent stock zone of porphyritic rocks.

DDH-6

Location; *Near the Station O'-20 in the Coroccohuayco mineralization zone.

*In the IP C-anomaly.

*In the gabbroic rock carrying high geochemical anomaly, in the south of the confluent stock zone of porphyritic rocks.

Object; Same as the object of DDH-6.

5-2 Results of Drillings

Geology, alteration, and mineralization revealed by them are considerably varying one another as shown in the drill logs (PL. I-7, Sheet I-6). Pyritization is sound commonly in every drill hole, and copper mineralization, though slight and local, has also been encountered by every one of them. This may suggest an existence of considerably large mineralization zone in this area. Major mineralizations encountered by each hole and average sulphur contents of all the rock formations except the Quaternary are shown in Table I-8.

Being located about 100 m south of the porphyritic rocks exposing along the Qda. Huaccollo, DDH-1 has revealed successive existence of the porphyritic rocks under the Quaternary formation. Pyrite-bearing stringers filling up high angled fissures are well developed in the porphyritic rocks. Most of them are pyrite-hematite-chlorite veinlets, but pyrite-quartz veinlets and pyrite-hematite-quartz-chlorite veinlets are also developed extensively. Quartz-bearing veinlets often carry chalc-

Table I-8 Main Copper Mineralizations and Average Sulphur Content in Each Drill Core

Hole No.	Length drilled m.	Depth of ore intersection m.	Length of ore intersection m.	Total Cu %	Soluble Cu %	Mo %	S %	Host rock
DDH-1	250.4	56.0-58.0	2.0	1.21	0.45	0.003		grd.
		63.0-65.0	2.0	1.97	0.16	tr.		"
		(44.0-65.0)	(21.0)	(0.51)	(0.22)	(0.002)		"
DDH-2	250.5	38.5-250.4	211.9	0.09			0.91	
		57.7-80.0	22.3	0.67	0.16	0.005		mz, ss, sh
		106.3-110.0	3.7	0.77		0.003		mz
		135.0-139.0	4.0	0.50		0.038		mz
DDH-3	250.2	182.0-190.0	8.0	0.49		0.011		sh, ss
		41.5-250.5	209.0	0.198			1.05	
		80.0-98.0	18.0	0.77	0.16	0.001		sk (ls, grd)
DDH-4	250.3	119.4-144.0	24.6	1.53		0.001		sk (ls)
		(80.0-164.0)	(84.0)	(0.70)		(0.001)		sk (ls, grd, g)
		0.0-250.2	250.2	0.273			0.66	
DDH-5	251.1	6.0-84.0	78.0	0.84	0.05	0.065		mz
		6.0-250.3	244.3	0.356			0.53	
DDH-6	251.1	7.5-31.0	23.5	0.55	0.24	0.008		g
		118.0-126.0	8.0	0.72		0.008		"
		160.0-176.0	16.0	0.55		0.015		"
DDH-6	251.1	7.5-251.1	243.6	0.226			0.89	
		74.0-84.0	10.0	0.87	0.09	0.003		g
DDH-6		0.0-251.1	251.1	0.143			1.56	

grd; porphyritic granodiorite, mz; quartz monzonite porphyry, ss; sandstone, sh; shale, ls; limestone, sk; skarn, g; gabbroic rock.

pyrite, though usually minor in amount. Mineralization and alteration of this kind are considered to represent the outer zone of mineralization of porphyry copper type as mentioned in Chapter 4. But the abundant development of numerous pyrite-bearing veinlets is noteworthy to suggest an existence of hidden but intense mineralization.

DDH-2 was drilled at about 200 m north of the skarnization zone exposing in the south of central zone in the Huaccollo block. It is about 1 km apart from DDH-1, and the ground between the two is covered with the Quaternary formation. This hole has encountered the Mesozoic formation consisting of shale, sandstone, and quartzite, and some slender dykes of quartz-monzonite porphyry and basaltic rock, after passing through the Quaternary formation of about 40 m thick. The upper part of the Mesozoic formation, down to the depth of 200 m, consists mainly of alternation of sandstone and shale (Murco formation) and the lower, quartzite with intercalating thin layers of shale (Hualhuani formation). Quartz-monzonite porphyry is intruded sparsely as slender dykes with varying width from 10 cm to 10 m. Basaltic rock penetrates the porphyry and sandstone. The porphyry has been affected by alteration represented by the combination of quartz-clay-sericite-chlorite. Alteration of similar kind is observed in the sediments too, but shale and sandstone had been altered into hornfels locally prior to this hydrothermal alteration. Fairly intense copper mineralization is often recognized in the porphyry and the surrounding sediments. Ore minerals are mainly pyrite and chalcopyrite, associated with a small amount of molybdenite. They are

not only contained quartz veinlets and filling up minute cracks, but also are disseminated more or less extensively. Interesting is that the porphyry here has been affected by considerably distinct copper mineralization in spite of its sparse distribution. Four holes from DDH-3 to DDH-6 were drilled in the Coroccohuayco mineralized zone.

Being located in the border between the stock group of porphyry and eastern limestone, DDH-3 has encountered promising copper mineralization of skarn type as already mentioned. Rock formations passed through by this hole are gabbroic rocks down to the depth of 58.0 m, porphyritic rock from 58.0 m to 80.7 m, mostly limestone from 80.7 m to 184.2 m, and mainly porphyritic rock from 184.2 m to the bottom. The contact plane between the porphyritic rock and limestone is inclined with as low angle as that of the bedding of limestone, suggesting its intrusion as a form of intrusive sheet. Limestone and intruding gabbroic rock as narrow dykes are often skarnized, and distinct copper mineralization is often recognized in the skarn of limestone origin. Such will support a possibility of copper mineralized zone of skarn type in the border zone between the stock group of porphyry and eastern limestone.

DDH-4 was so located as to target the stock, where the most prominent copper indications were found on the ground, in order to investigate the features of mineralization in the porphyry stock, which resulted in hitting an intense copper mineralization with bunches of quartz veinlets. It was very feeble in the argillized zone on the contrary. Therefore the zone of copper mineralization may be considered to have been emplaced

in the zone of quartz veinlets. Future prospecting in the porphyry area should be so conducted as to be focussed to investigate the possibility of development of quartz veinlets zone and the features of copper mineralization in the zone of quartz veinlets.

DDH-5 and -6 were drilled for the purpose of securing the features of copper mineralization in the gabbroic rocks around the stock group of porphyritic rocks. In the gabbroic rocks hydrothermal alteration is superimposed over the metasomatic alteration, which is characterized by such skarn minerals as actinolite, epidote, and garnet. In spite of its frequent occurrence, it is not so intense that in most cases skarn is formed in "vein-like" forms along fissures with varying width from a few millimeters to a few centimeters.

Principal hydrothermal alteration consists of carbonatization, and chloritization, accompanying silicification, argillization, and sericitization subordinately. A small amount of zeolite and serpentine are formed too. Silicification, generally weak and local, is represented by quartz-calcite veinlets. Sometimes weak silicification of replacement type can be observed in and around the skarn. Silicification is found more frequently in DDH-5 than in DDH-6. A narrow dyke of porphyry, intruding into the gabbro, has given considerably intense silicification, though local, to the adjacent gabbro, which can be seen in DDH-5 not far deep from the surface. The skarn of gabbroic rock origin exposed on the ground might have also been formed by the intrusion of such dykes of porphyritic rocks. Copper mineralization is observed more distinctly in and around the skarn, but

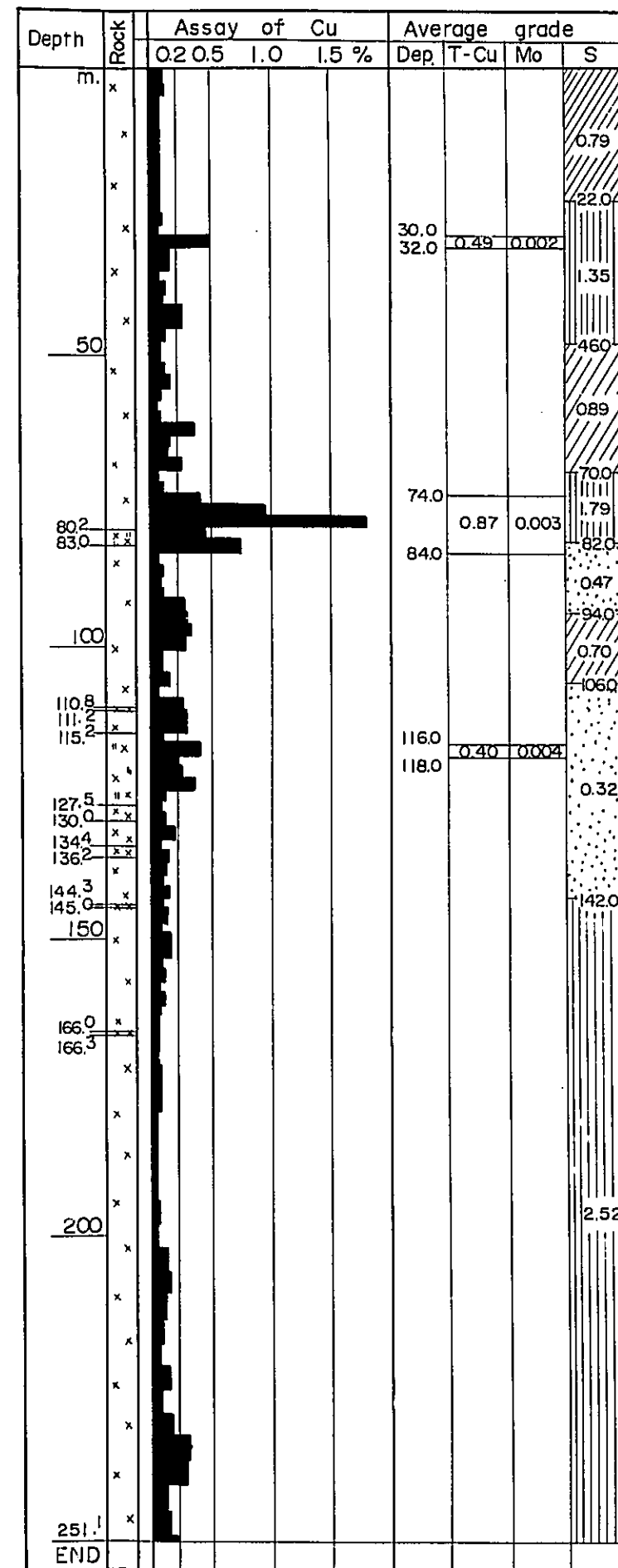
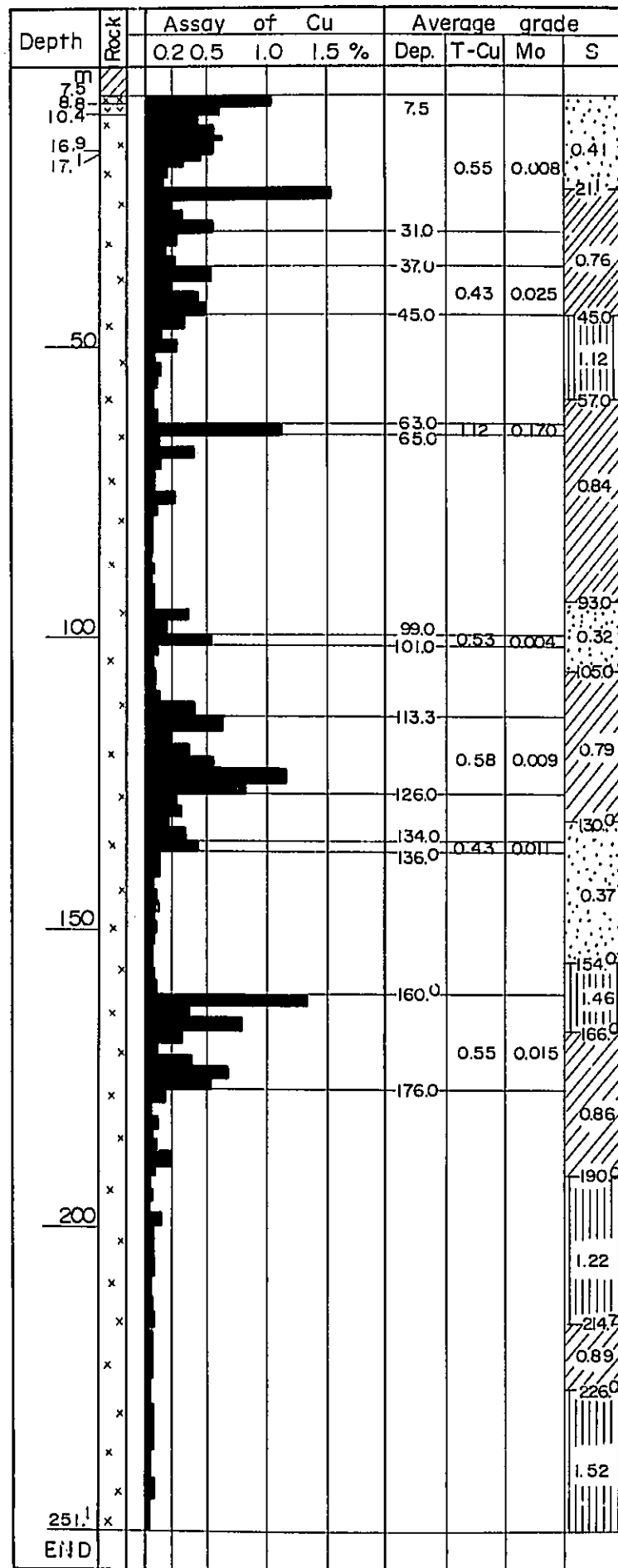
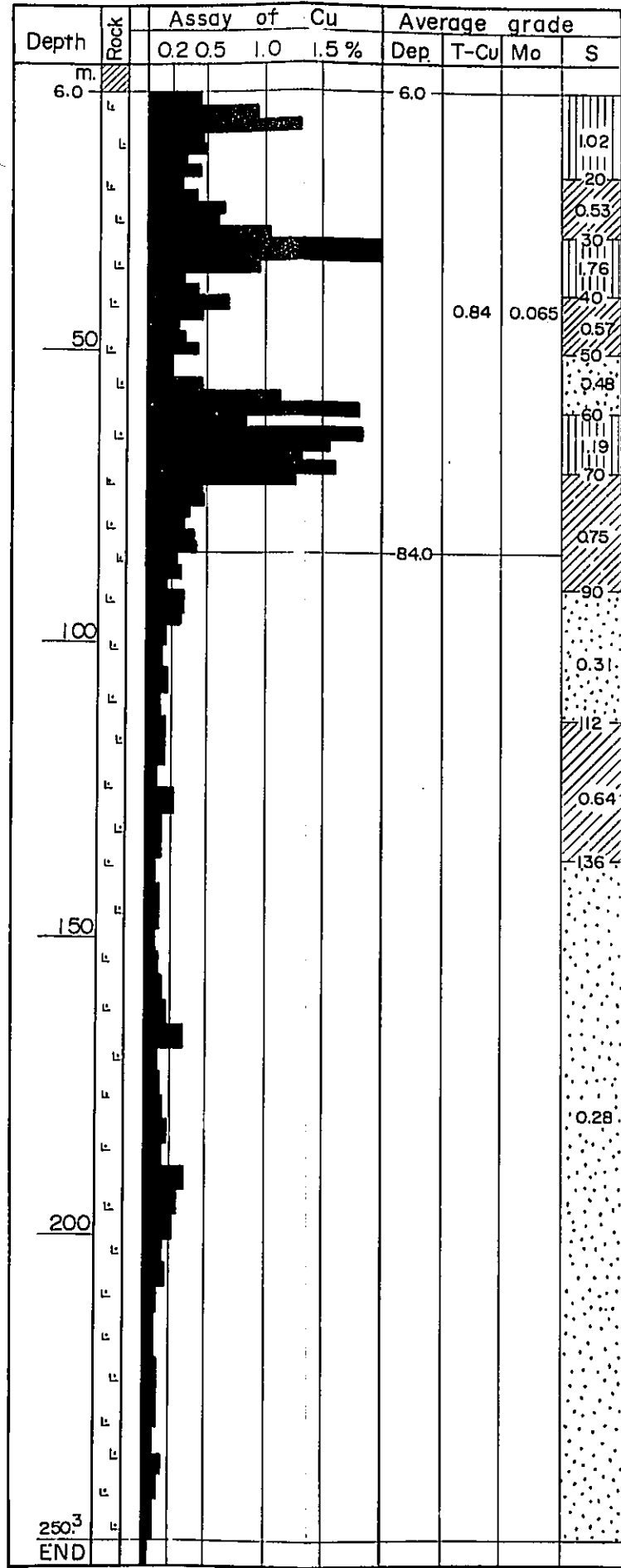
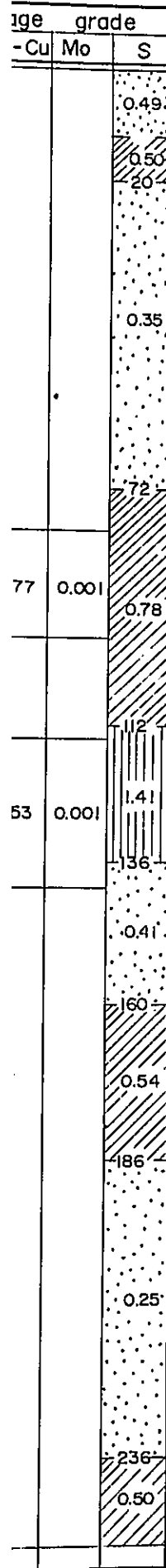
there seems to be no direct relation between skarnization and copper mineralization, as the skarn is often traversed by ore veins. Due to its lithological nature, much more reactive than the unaltered rocks, the skarn is controlling the mineralization as a favorite soaker of ore materials. Main sulphide minerals are pyrite, chalcopyrite and bornite. They are presented either as ore stringers or contained as ore grains in the quartz-bearing veinlets, and as impregnation in the skarn, too.

DDH 4

DDH 5

DDH 6

Fig.5 Copper (



DDH 5

DDH 6

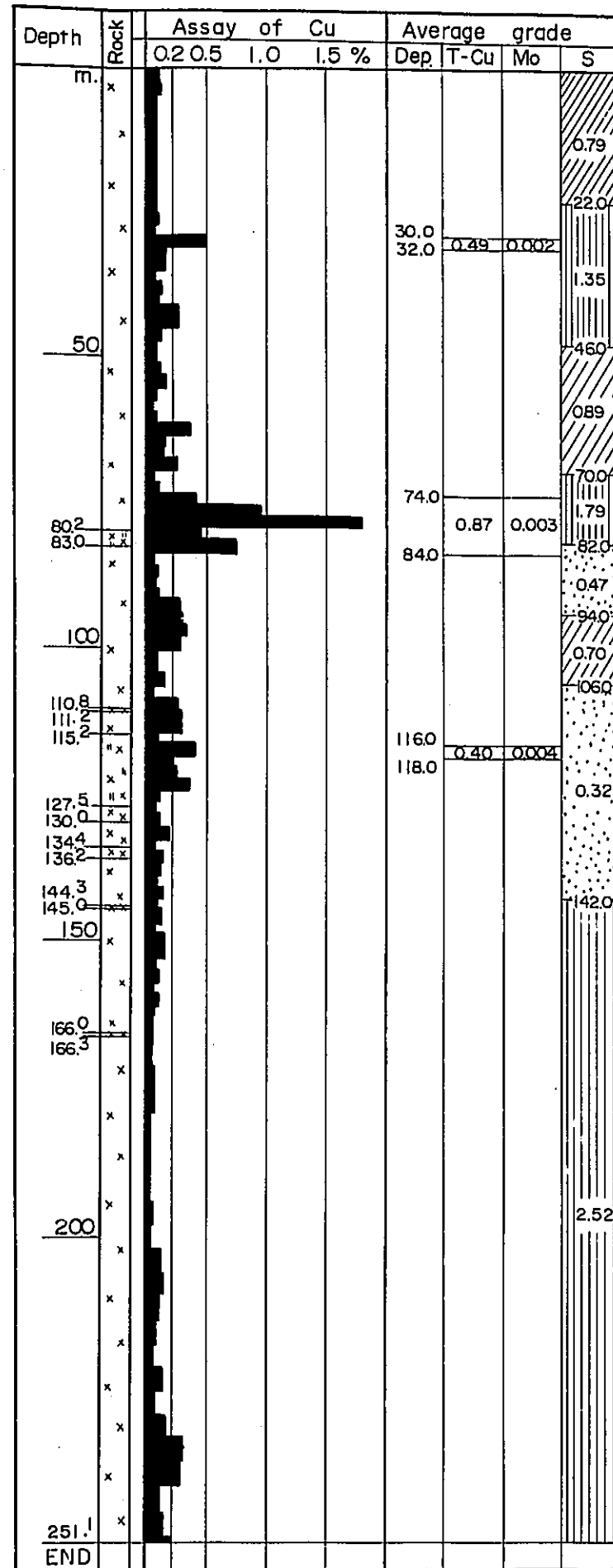
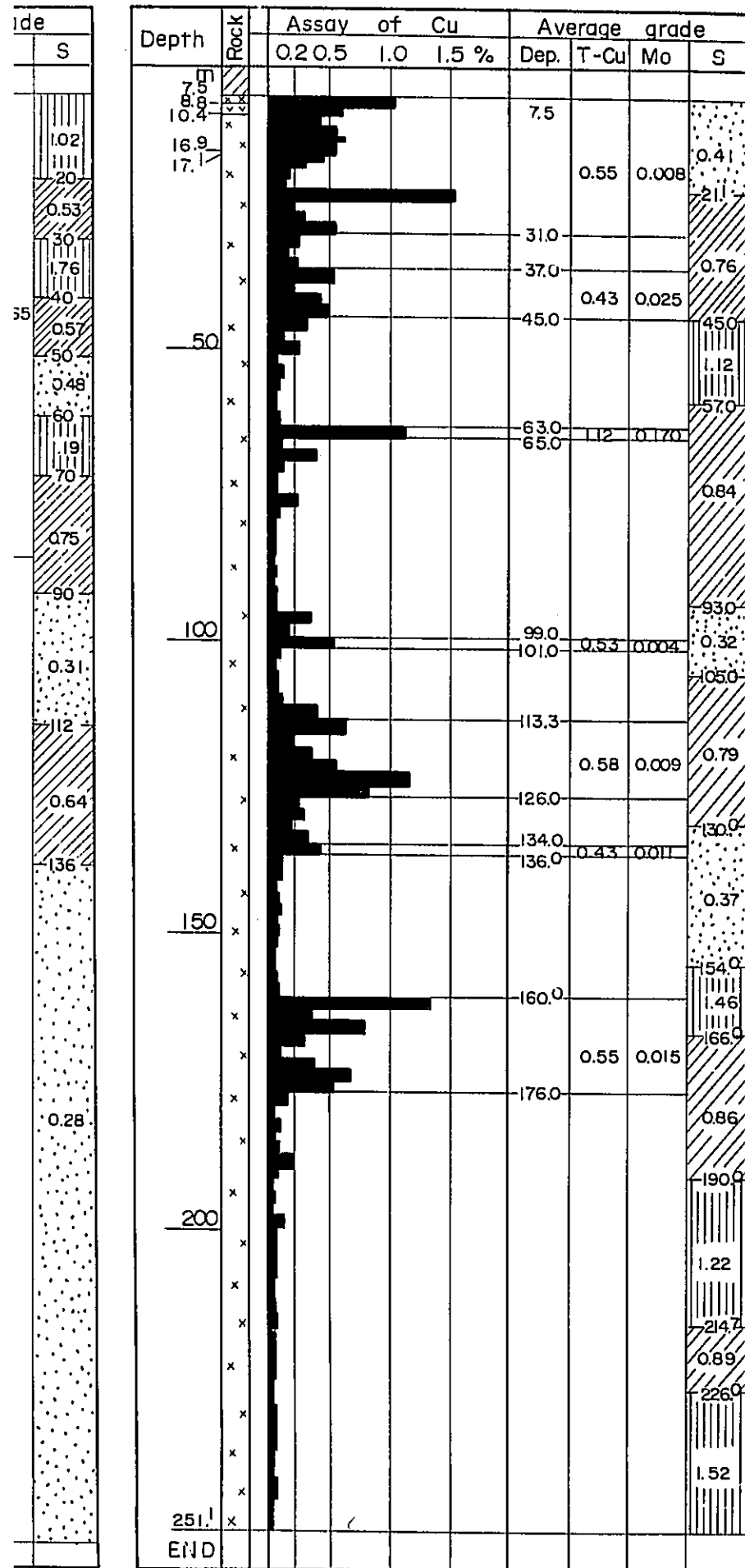


Fig.5 Copper Grade of each Drill Hole

LEGEND

- □ □ Granite porphyry
- ▤ ▤ ▤ Quartz monzonite porphyry
- ▥ ▥ ▥ Granodiorite
- × × × Gabbro - Diorite - Quartz diorite
- ▨ ▨ ▨ Skarn
- ▩ ▩ ▩ Copper showing
- ▽ ▽ ▽ Andesite - Basalt
- ▫ ▫ Rhyolite tuff
- ▬ ▬ ▬ Limestone
- ▭ ▭ ▭ Shale - sandstone
- ▮ ▮ ▮ Quartzite

References

- Bellido, E. B. Others (1972)
Aspectos Generales de la Metalogenia del Peru
Servicio de Geologia y Minería, Peru
- Giletti, B. J. & Day, H. W. (1968)
Potassium-Argon Ages of Igneous Intrusive Rocks in Peru
Nature Vol. 220 November 9
- Hollister V. F. (1973)
Regional Characteristics of Porphyry Copper Deposits of South America
Mining Engineering, August
- James, A. H. (1971)
Hypothetical Diagrams of Several Porphyry Copper Deposits
Economic Geology vol. 66
- Metallic Minerals Exploration Agency of Japan (1972)
Report on Geotectonic Survey of the Southern Peru (in Japanese)
- Overseas Technical Cooperation Agency Metallic Minerals Exploration Agency
Government of Japan (1972, 1973)
Report on Geological Survey of the Yauri Area, Southern Peru
Vol. 1 ~ 5
- Terrones, A. J. (1958)
Structure Control of Contact Metasomatic Deposits in the Peruvian
Cordillera
Mining Engineering, March
- Tifley & Hicks (1966)
Geology of the Porphyry Copper Deposits Southwestern North America
The University of Arizona Press

PART II
GEOPHYSICAL SURVEY

CONTENTS

PART II GEOPHYSICAL PROSPECTING

1.	Introduction	II- 7
1-1	Purpose of the Geophysical Survey	II- 7
1-2	Outline of the Geophysical Survey	II- 7
2.	Surveying Method	II- 8
2-1	Principles of Induced Polarization Method	II- 8
2-2	Field Survey	II-11
2-3	Instruments	II-14
2-4	Survey Methods	II-15
2-5	In-situ and Laboratory Measurements	II-17
2-6	Adjustments and Reliability Considerations of the Results	II-19
2-7	Accuracy Tests	II-23
2-8	Geodetic Survey	II-24
3.	Analyses of the Results	II-25
3-1	Analytical Method	II-25
3-2	General Interpretation	II-27
1)	Apparent Resistivity	II-27
2)	Frequency Effect	II-28
3)	Metal Factor	II-29
4)	Laboratory Measurements	II-30
4)-1	Measuring Apparatus	II-31

4)-2	Results of Laboratory Measurements	II-32
4)-3	Synthetic Considerations of Rock Apecimen Tests ..	II-35
3-3	Detailed Discussion about the Indications	II-39
3-4	Classification of IP Anomalies	II-66
4.	Syntheses	II-68

List of Tables

Table 2-1	IP Values on In-Situ & Laboratory Measurement	II - 18
Table 2-2	Comparison between the Frequency Effects in Percentage, FE and FEY	II - 20
Table 2-3	Comparison between Resistivity Values in Ohm-m, Measured and Calculated	II - 22
Table 2-4	Flow Chart of IP Survey	II - 25
Table 2-5	Laboratory Measurement In-Situ Measurement and Chemical Assay of Samples	II - 34
Table 2-6	Assay & Sulphide Contents Estimated of D D H	II - 38
Table 2-7	Characteristics of the IP Anomalies	II - 66
Table 2-8	Findings of Survey	II - 68

List of Figures

Fig. 2-1	Location Map of the IP Area Surveyed	II - 6
Fig. 2-2	Background or Normal Effect	II - 9
Fig. 2-3	Overvoltage Effect	II - 10
Fig. 2-4	Comparison between the Non-Adjusted and Adjusted Results of FE	II - 21
Fig. 2-5	Sketch of Apparatus	II - 31
Fig. 2-6	Comparison between Field and Simulation of Line - F	II - 44
Fig. 2-7	- ditto -	Line - K
Fig. 2-8	- ditto -	Line - K'
Fig. 2-9	- ditto -	Line - L
Fig. 2-10	- ditto -	Line - L'
Fig. 2-11	- ditto -	Line - M
Fig. 2-12	- ditto -	Line - N
Fig. 2-13	- ditto -	Line - O
Fig. 2-14	- ditto -	Line - O'

List of Plates

PL. II-1-1	Profiles of the Area (FE, AR)	1/20,000
PL. II-1-2	"	1/20,000
PL. II-2-1	Southern profiles of the Area	1/20,000
PL. II-2-2	"	1/20,000
PL. II-3	Assay Map of D D H	
PL. II-3-1	Simulated Model of IP Anomaly on line C & C near D D H - No. 1	1/10,000
PL. II-3-2	" K. K' & L near D D H - No. 3	1/10,000
PL. II-3-3	" L & M near D D H - No. 4 & No. 5	1/10,000
PL. II-3-4	" O & O' near D D H - No. 6	1/10,000
PL. II-4-1	Plan of A. R. 3,900m Level	1/10,000
PL. II-4-2	" 3,800m "	1/10,000
PL. II-4-3	" 3,700m "	1/10,000
PL. II-4-4	Plan of F. E. 3,900m "	1/10,000
PL. II-4-5	" 3,800m "	1/10,000
PL. II-4-6	" 3,700m "	1/10,000
PL. II-4-7	Plan of M. F. 3,900m "	1/10,000
PL. II-4-8	" 3,800m "	1/10,000
PL. II-4-9	" 3,700m "	1/10,000
PL. II-5-1	General Map of IP Area	1/10,000
PL. II-6-1	Profile on Line A	1/5,000
PL. II-6-2	" B	1/5,000
PL. II-6-3	" C	1/5,000
PL. II-6-4	" C'	1/5,000
PL. II-6-5	" D	1/5,000
PL. II-6-6	" D'	1/5,000
PL. II-6-7	" E	1/5,000
PL. II-6-8	" F	1/5,000
PL. II-6-9	" G	1/5,000
PL. II-6-10	" H	1/5,000
PL. II-6-11	" I	1/5,000
PL. II-6-12	" I'	1/5,000
PL. II-6-13	" J	1/5,000

PL. II-6-14	Profile on Line	J'	1/5, 000
PL. II-6-15	"	K	1/5, 000
PL. II-6-16	"	K'	1/5, 000
PL. II-6-17	"	L	1/5, 000
PL. II-6-18	"	L'	1/5, 000
PL. II-6-19	"	M	1/5, 000
PL. II-6-20	"	M'	1/5, 000
PL. II-6-21	"	N	1/5, 000
PL. II-6-22	"	N'	1/5, 000
PL. II-6-23	"	O	1/5, 000
PL. II-6-24	"	O'	1/5, 000
PL. II-6-25	"	P	1/5, 000
PL. II-6-26	"	Q	1/5, 000
PL. II-7-1	Profile on Line	C	1/5, 000
PL. II-7-2	"	C'	1/5, 000
PL. II-7-3	"	D	1/5, 000
PL. II-7-4	"	D'	1/5, 000
PL. II-7-5	"	I'	1/5, 000
PL. II-7-6	"	J	1/5, 000
PL. II-7-7	"	J'	1/5, 000
PL. II-7-8	"	K	1/5, 000
PL. II-7-9	"	K'	1/5, 000
PL. II-7-10	"	L	1/5, 000
PL. II-7-11	"	L'	1/5, 000
PL. II-7-12	"	M	1/5, 000
PL. II-7-13	"	M'	1/5, 000
PL. II-7-14	"	N	1/5, 000
PL. II-7-15	"	N'	1/5, 000
PL. II-7-16	"	O	1/5, 000
PL. II-7-17	"	O'	1/5, 000

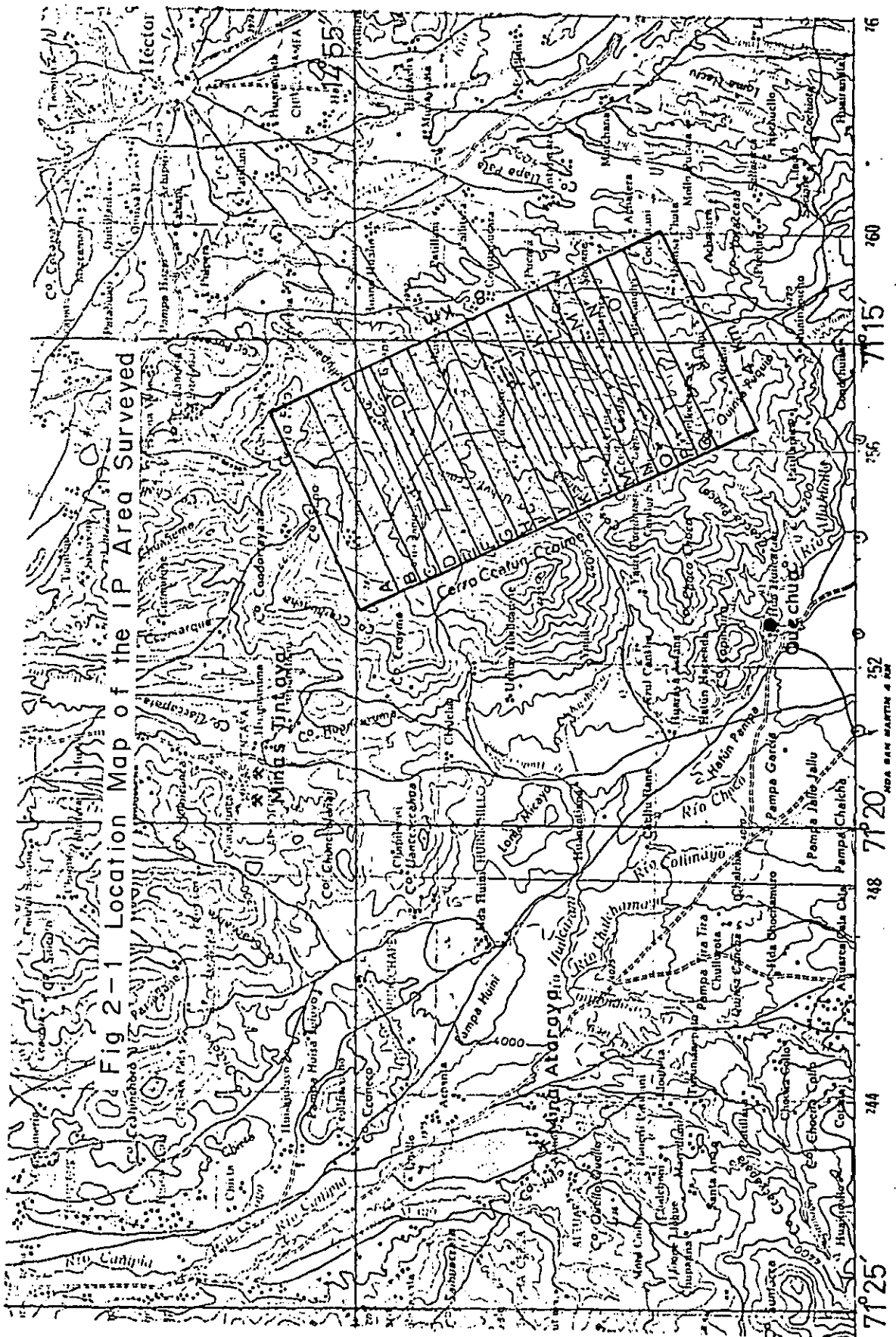


Fig 2-1 Location Map of the IP Area Surveyed

PART II GEOPHYSICAL PROSPECTING

CHAPTER 1. INTRODUCTION

1-1 Purpose of the Geophysical Survey

The present survey covers Coroccohuayco and Huaccollo areas of 32 km², where some promising indications of mineralization have been found by the extensive surveys previously conducted over an area of 15,000 km² during 1971 - 72. These areas are predominantly occupied by Mesozoic formation together with the intrusives, which are covered with relatively newly-formed volcanics, moraines and alluviums. There is a fault zone running through the central area in the NEE-SW direction. The Mesozoics are distributed mainly over the northern part of the fault zone, but in contrast, the southern part is widely dotted with the plutonic rocks. Our purpose of the present geophysical survey is to disclose the geological structures and mineralized zones in these areas by the induced polarization method.

1-2 Outline of the Geophysical Survey

The induced polarization survey has been carried out along 26 surveying lines (shown in PL. II-5-1), which amount to 86 km in total length. The frequency effect and the apparent resistivity have been measured by the dipole-dipole electrode configuration method. The depth effective for the geophysical detection is assumed to be 500 m below the surface.

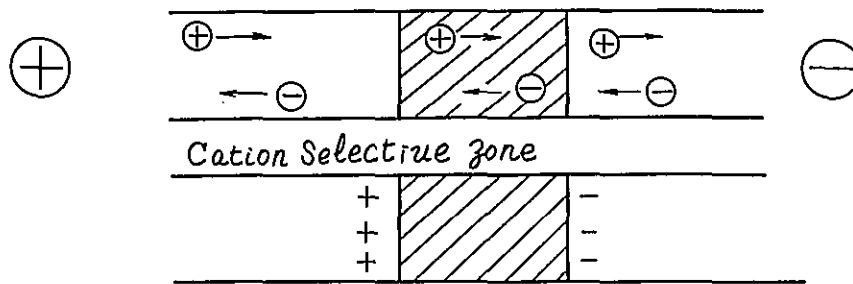
CHAPTER 2. SURBEYING METHOD

2-1 Principles of Induced Polarization Method

Induced polarization method (briefly "IP method") has been recently developed around the geophysical applications of electrical measurements on the basis of an overvoltage phenomenon in terms of electrochemistry. The IP effect is caused by a double-layer of electric charge along the interface between ion- and electron-conductors. All kind of sulphide minerals, a part of oxide minerals and graphite, in general, are strongly polarized even in the cases of low percentage of mineral particles and discontinuous grain distribution. In order to detect the IP effect of mineral deposits in geophysical prospecting, we must have suitable quantitative measures; time domain and frequency domain measures. The IP method is thought to be one of the most effective for detecting disseminated deposits as porphyry-copper, sedimentary copper and lead-zinc deposits in carbonate host rock. The electrochemical phenomena detectable by means of the IP method are as follows:

a) Background or Normal Effect (see Fig. 2-2)

If an electrical current flows through a rock specimen, it exhibits an electrochemical change such as membrane or diffusion polarization. Such a phenomenon is thought to be caused by ion drift in the specimen. This is a common feature to almost all kinds of rock, so that we call "background effect" or "normal effect" of the induced polarization against anomalous IP effects.



b) Overvoltage Effect (see Fig. 2-3)

An external voltage produces the double layer of charge at the surface of sulphide minerals or metallic conductors. When the voltage is removed, a discharge occurs in the direction opposite to the given current. Such a phenomenon can be explained by a combination of ion and electronic conduction. Conductible mineral deposits, in general, are causative of the IP phenomenon and accordingly become objects of prospecting by means of the IP method.

The IP effect can be observable in the following ore minerals; sulphide minerals such as pyrite, pyrrhotite, marcasite, galena, chalcopyrite, molybdenite, pentlandite, cobaltite, argentite, chalcocite, etc., oxide minerals such as magnetite, pyrolusite, cassiterite, etc., and the other kind minerals such as arsenite, nature copper, graphite, clay minerals, etc. It is noticed, however, that the IP phenomenon can not be found in sphalerite because of high resistivity. It has been very often reported that the IP effect caused by graphite or clay deposits disturbs us in the detection of the IP information from the sulphide minerals.

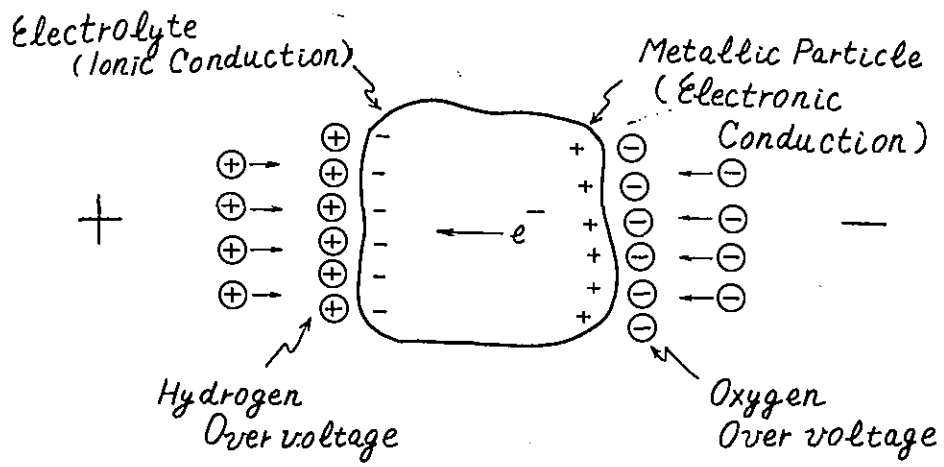


Fig 2-3

2-2 Field Survey

1. Total Length of Surveying Lines

a) 86.0 km with an electrode-separation of 200 m.

b) 34.0 km " " 100 m.

(Both the lines are partially overlapped).

2. Survey Network

a) 200 m electrode-separation lines

Name	Length	Number of Observation Station	Distance from an Adjacent Line	Remarks
LINE A	4.0 km	66		
" B	4.0 "	66	400 m	
" C	"	"	"	
" C'	2.0 km	26	200 m	
" D	4.0 "	66	"	
" D'	2.0 "	26	"	
" E	4.0 "	66	"	
" F	"	"	400 m	
" G	"	"	"	
" H	"	"	"	
" I	"	"	"	
" I'	2.0 km	26	200 m	
" J	4.0 "	66	"	
" J'	2.0 "	26	"	
" K	4.0 "	66	"	

Name	Length	Number of Observation Station	Distance from an Adjacent Line	Remarks
LINE K'	2.0 km	26	200 m	
" L	4.0 "	66	"	
" L'	2.0 "	26	"	
" M	4.0 "	66	"	
" M'	2.0 "	26	"	
" N	4.0 "	66	"	
" N'	2.0 "	26	"	
" O	4.0 "	66	"	
" O'	2.0 "	26	"	
" P	4.0 "	66	"	
" Q	4.0 "	66	400 m	
Total: 26 lines	86.0 km	1,356		

b) 100 m electrode-separation lines

Name	Length	Number of Observation Station	Distance from an Adjacent Line	Remarks
LINE I'	2.0 km	66	200 m	Overlapped with the 200 m lines
" J	2.0 "	66	"	
" J'	"	51	"	
" K	"	54	"	
" K'	"	51	"	
" L	"	45	"	
" L'	"	66	"	
" M	"	51	"	
" M'	"	63	"	
" N	"	51	"	
" N'	"	61	"	
" O	"	51	"	
" O'	"	66	"	
" C	"	66	"	
" C'	"	66	200 m	
" D	"	66	"	
" D'	"	62	"	
Total: 17 lines	34.0 km	1,007		

3. In-situ measurements : 41 Stations.
4. Laboratory measurements of rock specimens : 28 specimens.
5. Surveying periods :
 Field work : Oct. 10 ~ Dec. 21, 1973.
 Data analysis : Dec. 21, 1973 ~ Aug. 1, 1974.
6. Surveyers : 9 surveyers including 2 counterparts.
7. Instruments : 2 sets of the IP surveying apparatus.

2-3 Instruments

The instruments used in the present survey consists of the followings:

Transmitter / McPhar Model 2004

Weight : about 20 kg.

Maximum output power : 2.5 kw.

Output voltage : 0 - 850 V

Output current : 0 - 5 A

Frequencies : 10, 5, 2.5, 1, 0.3, 0.1 Hz and D. C.

Receiver / McPhar Model 29D

Weight : about 10 kg.

Input impedance : 1.9 Mohm.

Sensitivity : 500 micro-V in full scale.

Frequencies : 5, 2.5, 1, 0.3, 0.1 Hz and D. C.

Engine generator / Manufactured by the J. L. O.

Weight : about 34 kg.

Maximum output power : 2.5 kw.

Output voltage : 125 V (400 Hz).

Transmitter / Chiba Electronic Co. Model CH 507 - AB.

Weight : about 25 kg.

Output voltage : 20 - 800 V.

Output current : 0 - 3 A.

Frequencies : 3, 0.3, 1, 0.1 Hz and D. C.

Receiver / Yokohama Electronic Co. Model YN - 504.

Weight : about 7.5 kg.

Sensitivity : 300 micro-V in full scale.

Frequencies : 0.1, 0.3, 1, 3 Hz and D. C.

Input impedance : 10 Mohm.

Generator / McCulloch Model 440

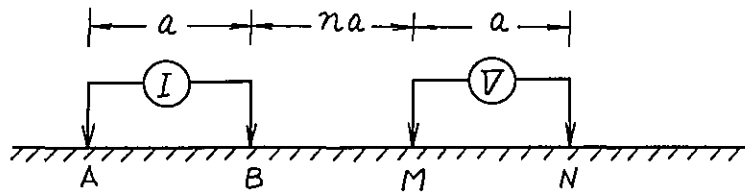
Weight : about 36 kg.

Macimum output power : 2 kw.

Output voltage : 120 V (400 Hz).

2-4 Survey Methods

Two kinds of IP method, frequency domain and time domain, are usually applied to the field survey. We adopted the frequency domain method for the present survey. The frequency domain, which is sometimes called "Wait's method", is a useful method of obtaining an IP effect by comparing the ground impedance for a low-frequency alternating current with that for a high-frequency current. This method is quite different from the time domain from the viewpoint of measuring techniques.



The alternating current to be flown in the ground, in general, has a rectangular wave-form instead of a sine wave. The polarized body such as a sulphide mineral deposit repeats to charge and discharge in accordance with the input wave-form. The quantity of charge or discharge is a function of the frequency.

We used here the dipole-dipole electrode configuration.

In the case that the electrode separation $AB = MN = a = 100\text{m}$, BM is taken as 100, 200, 300 and 400 m long so as to catch the frequency information up to a depth of 250 m below the surface. In the case of 200 m long electrode separation, we adopted 200, 400, 600 and 800 m as a BM distance, where the frequency information from a depth of 500 m below the surface was expected. We surveyed extensively over the whole area with 200 m electrode separation in order to disclose the large-scale underground structures, meanwhile the small-scale variations in geology can be detected by the 100 m spacing surveys.

We should take care of an arrangement of electric power lines for the fear that a careless arrangement sometimes causes an electrical coupling or a leakage. It is of course, therefore, that the voltage line were set up in the distance from the electric line and the quite high insulation resistivity were kept in all cases.

Most of the surveying areas is covered by a dry soil, so that it was difficult to obtain a low ground resistivity. In order to flow a strong current through the earth, it is necessary to keep a ground resistivity low. Therefore, we made holes of 1m x 1m square with depths up to the exposures of fresh rock. When the ground resistivity was still high in spite of the holes, we flowed bentonite into the holes to keep the ground resistivity low.

2-5 In-situ and Laboratory Measurements

In order to know the properties of typical rock in the surveying areas, the in-situ measurements were made from place to place with electrode separation of 5 - 20 m. Furthermore, we made laboratory measurements of the resistivity and IP effect of typical rock specimens. We formed the specimens into parallelepiped of 2 x 4 x 5 cm³ before the measurements. In the following Table 2-1, the measured results are summarized.

Table 2-1 IP VALUES ON IN-SITU & LABORATORY MEASUREMENT

$$FE = \frac{\rho_{0.3} - \rho_{2.5}}{\rho_{2.5}} \times 100$$

Location of Sample	Name of Sample	Apparent Resistivity ρ 25 Hz ($\Omega\cdot m$)										F E (%)																						
		50	100	150	200	250	300	350	400	450	500	1000	2000	3000	4000	5000	6000	7000	8000	1	2	3	4	5	6	7	8	9						
37 39 40 41	Pampas Sediments																																	
48 42 43																																		
13 14 15 12	Lime stone																																	
17 18 19 15 20																																		
35 34 36	Shale																																	
40 28 20	Quartzite																																	
31 32 33	Magnetite Skarn																																	
21 22 23 24 25	Monzonite																																	
4, 5, 11, 12, 3, 6, 7, 8, 9, 10	Diorite																																	

$$FE = \frac{\rho_{0.3} - \rho_{2.5}}{\rho_{2.5}} \times 100$$

Laboratory Measurement

Location of Sample	Name of Sample	Apparent Resistivity ρ 2.5 Hz ($\Omega\cdot m$)										F E (%)																						
		50	100	150	200	250	300	350	400	450	500	1000	2000	3000	4000	5000	6000	7000	8000	1	2	3	4	5	6	7	8	9						
12, 13, 14, 15, 16, 17, 18, 19	Lime stone																																	
28 29	Quartzite																																	
31 32	Magnetite Skarn																																	
21 22 23 24 25 26 27	Monzonite																																	
1 2 3 4 5 6 7 8	Diorite																																	

2-6 Adjustments and Reliability Considerations of the Results

We used two sets of surveying instrument, McPhar Model 29D and Geoscience-type IP meter manufactured by the Yokohama Electronic Co., the characteristics of which may be somewhat different each other. In such a case, a suitable adjustment is required to the results. The adjustment curve were completed by the repetition surveys along LINE K.

Letting FE_x and FE_y be the frequency effects obtained by the Yokohama Electronic Co. instrument and McPhar Model 29D, respectively. Comparing a low frequency alternating current of 0.3 Hz with a high frequency of 3.0 Hz, FE_x is obtained as

$$FE_x = \frac{\rho_{0.3} - \rho_{3.0}}{\rho_{3.0}} \times 100 (\%),$$

Similarly, FE_y is given by

$$FE_y = \frac{\rho_{3.0} - \rho_{2.5}}{\rho_{2.5}} \times 100 (\%),$$

where ρF is the apparent resistivity of a rock for a frequency of F Hz.

The difference between FE_x and FE_y depends on the used frequencies and the frequency responses of electronic circuits such as characteristics of filter, amplifier and integration time of input signals.

Table 2-2 shows the results obtained by the repetition surveys along LINE K.

Table 2-2. Comparison between the Frequency Effects in Percentage, $FE_{(x)}$ and $FE_{(y)}$, obtained with the Yokohama Electronic Co. Model YN-504 (0.3 and 3.0 Hz) and McPhar Model 29D (0.3 and 2.5 Hz), respectively.

Station No. A - B	Station No. M - N	N	FE_x (%)	FE_y (%)	Difference
4 - 6	0 - 2	1	1.7	1.2	0.5
6 - 8	"	2	1.6	1.1	0.5
8 - 10	"	3	2.5	1.9	0.6
10 - 12	"	4	2.7	1.7	1.0
6 - 8	2 - 4	1	2.5	1.9	0.6
8 - 10	"	2	-	2.1	-
10 - 12	"	3	3.4	2.0	1.4
12 - 14	"	4	3.7	3.4	0.3
8 - 10	4 - 6	1	1.6	1.1	0.5
10 - 12	"	2	2.2	1.3	0.9
12 - 14	"	3	2.5	1.2	1.3
10 - 12	6 - 8	1	1.5	1.2	0.3
12 - 14	"	2	2.3	1.4	0.9
12 - 14	8 - 10	1	2.4	1.7	0.7

Note : N indicates the separation factor.

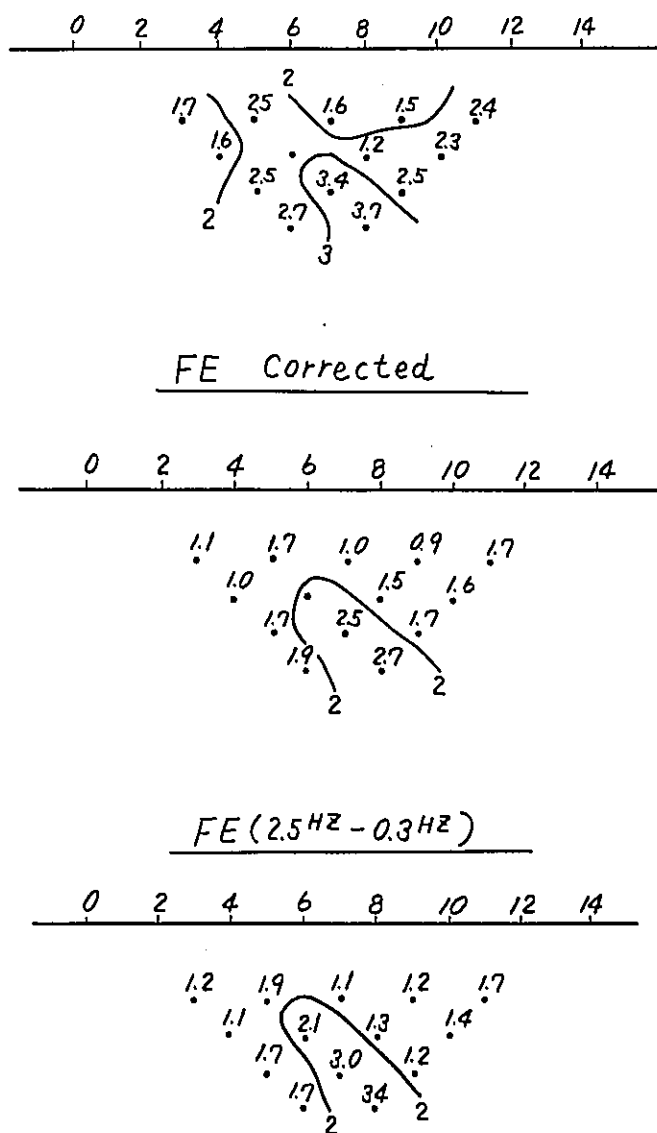
As seen in the above table, FE_x is positively correlated with FE_y . The correlation coefficient computed from the above results becomes 0.67, which is thought to be fairly well correlated each other. Then, the relation

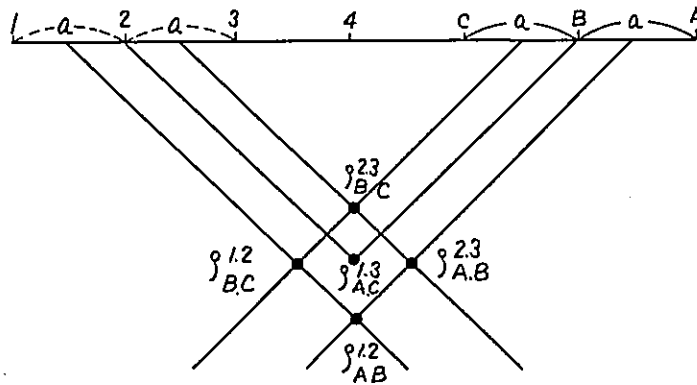
between FE_x and FE_y obtained by means of the least square method is

$$FE_y = 0.80 FE_x - 0.26$$

The IP results measured over the whole surveying areas were adjusted and the IP effects for 3.0 Hz were reduced to those for 2.5 Hz by the above relation.

Fig. 2-4 shows a comparison between the non-adjusted and adjusted results of FE profile obtained at stations along LINE K.





2-7 Accuracy Tests

The ordinary electrode spacing was determined as 200 m. But the detailed surveys with 100 m spacing were used jointly in an area where an anomalous frequency effect was detected, for the purpose of disclosing a small-scale geological structure. Comparison of both the results gives us data for an accuracy consideration of IP measurements.

Assuming that an uniform and homogeneous material forms the earth, a theoretical formula of resistivity in the dipole-dipole electrode configuration as shown in the following figure is given by

$$\rho_{A,C}^{1,3} = \frac{1}{2} \rho_{B,C}^{2,3} + \frac{1}{5} (\rho_{B,C}^{1,2} + \rho_{A,B}^{2,3}) + \frac{1}{10} \rho_{B,C}^{1,2}$$

where $\rho_{A,B}^{M,N}$ denotes the resistivity in the case that current and voltage dipoles are located at stations A and B, and M and N, respectively. The four terms of the right-hand members of the above formula correspond to resistivities measured with a-spacing electrode configuration. In contrast, the left-hand term gives a resistivity of 2a-spacing dipoles. If a set of a-spacing values of resistivity is known, the 2a-spacing value can be estimated from the above formula. Differences between measured values

of resistivity with such calculated ones will become a criterion of an accuracy of resistivity determinations.

The resistivity values, measured and calculated, are tabulated in Table 2-3.

Table 2-3 Comparison between Resistivity Values in ohm-m, Measured and Calculated.

Value $\rho_{A,C}^{1,3}$ Measured	Calculated	Difference	Value $\rho_{A,C}^{1,3}$ Measured	Calculated	Difference
125	125.1	0.1	160	123.9	-36.1
38	37.6	-0.4	95	101.2	6.2
71	67.8	-3.2	61	59.6	-1.4
119	119.8	0.8	66	68.3	2.3
274	262.3	-11.7	92	87	-5.0
87	87.4	0.4	70	68.9	-1.1
90	90.4	0.4	72	79.2	7.2
77	77.3	0.3	54	55.9	1.9
72	60.2	-11.8	70	70.7	0.7
69	67.8	-1.2			

It is noticed in the above table that the differences between the measured and calculated values of resistivity are as small as 3%. Such an error may be mainly caused by non-uniform materials in actuality. Judging from this fact, there is no essential difference between the resistivity values obtained by 100 and 200 m spacing electrode configurations,

and accordingly, the accuracy of resistivity measurements in the present survey holds quite high.

2-8 Geodetic Survey

Based on the topographic map drawn by the geological survey party in 1973, the elevation of Station No. 26 on LINE J' was assumed as 4,000m above sea-level. The concrete block bench mark was then established at the base station, through which the baseline was extended in the direction of 157° . It is off course that the geodetic determination of the baseline was carefully made by repeating surveys. The 26 lines of survey route were established parallel with an interval of 200 m in the direction of $67^\circ - 247^\circ$ on the basis of the baseline. The lengths of the surveying lines were 2 km or 4 km (see PL.II-5-1).

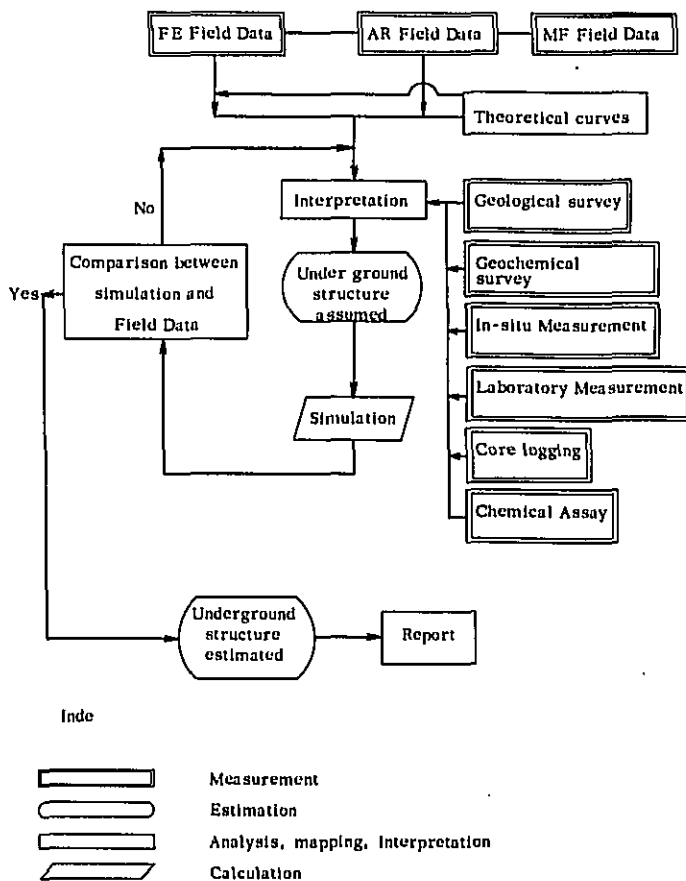
CHAPTER 3. ANALYSES OF THE RESULTS

3-1 Analytical Method

The IP results obtained from the surveys with the surface dipole-dipole electrode configuration were analyzed on the basis of the IP standard curves developed by the geophysicist group of Mitsui Kinzoku Engineering Service Co. The analysing parameters were selected to be compatible with the results of the geological surveys, the drilling data including chemical analyses, and the values of apparent resistivity and FE obtained in laboratory experiments and in-situ measurements.

The outline of the analytical procedure is as follows:

Table 2-4 Flow Chart of IP Survey



AR (apparent resistivity), FE (frequency effect) and MF (metal factor) are effective for estimating the geological structures by means of frequency domain method. These results are represented in the profiles of PLs. II-6-1 ~ II-7-17. PLs. II-5-1 ~ II-5-9 shows the surface distributions of AR, FE and MF. PLs. II-1-2 and II-1-3 are the panel diagrams continuously illustrating the distributions of AR and FE. Here we should bear in mind that AR was measured at a frequency of 2.5 Hz and FE was determined in the unit of percent from resistivity changes for 0.3 and 2.5 Hz alternating current. Meanwhile, MF is given by a ratio $FE/AR \times 10^3$.

The value of FE, which indicates the polarization of underground conductors, has the advantage of essential independence of topographic effects. In contrast, a topographic effect on the value of AR is not so small that terrain correction has to be made to the obtained data. The terrain correction, in general, takes a negative value over the mountain ridge but a positive one over the valley, so that such a correction should be taken into account in an AR survey over the rugged terrain area. For the present survey results of AR which are strongly affected by the terrain, the values of resistivity were determined on the basis of the standard curve developed in Mitsui Kinzoku Engineering Service Co.

FE becomes high but AR low over electrically conductive mineral deposits, where MF is proportional to a ratio FE/AR . In the case of the flat topography having fairly uniform resistivity, similarly to FE, MF is effective for detecting an anomalous zone. In the present survey, we obtained the highly reliable MF data, partially because the background

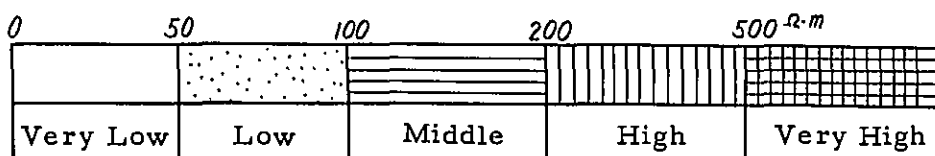
noise is negligibly small and partially because we made every effort on the improvement of the grounding condition. In the following paragraph, the obtained results of AR, FE and MF will be geologically and geophysically interpreted.

3-2 General Interpretation

1) Apparent Resistivity

The value of AR ranges from 20 to 3,000 ohm-m in the survey areas.

In order to understand the regional tendency of AR, the range is divided into five steps : very high, high, middle, low and very low.



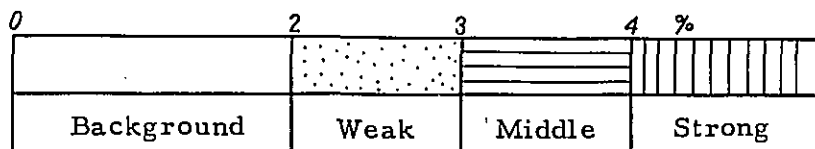
The expressions of these steps are given in the annexed figures as the following classification method. In this case, the resistivity values are based on the results of the in-situ field measurements at 41 stations and the laboratory measurements of 28 rock specimens. The results are summarized in Table 2-1 and 2-5.

The surface distribution of the resistivity is shown in PLs. II-5-1 to II-5-3. We see in the figures that the V.L. (very low resistivity) and L. (low resistivity) zones are arranged over the alluvial zones. Conspicuous zones of V.H. (very high resistivity) are found in the central parts of LINEs A and B and in the eastern parts of LINEs D and E. The former V.H. is thought to be a terrain effect overlapped by an effect of siliceous rock without water content. On the other hand, the latter V.H.

may be caused by the outcrops of strongly-silicified limestone.

2) Frequency Effect

FE takes values ranging from 0.5 to 5.0% in the survey areas. In a fashion similar to the treatment of AR, the range of FE is classified into four steps: weak, middle and strong. In the annexed figures, the following expressions are adopted.



The values of FE were determined from the results of field in-situ measurements at 41 stations and laboratory measurements of 28 rock specimens.

These results are summarized in Table 2-1 and 2-5.

It can be synthetically concluded from the results that there are three anomalous zones of FE in the survey areas. Hence we call them "A", "B" and "C" anomalous zones. The A zone extends widely to the western parts of LINES A - I in the N-S direction. The width of the zone amounts to 1.5 km at maximum. The source of the anomaly is presumed as polarized mineral bodies which are buried in shallow and pillared in shape. The N-S extension of the anomalous zone beyond the survey areas can be expected, judging from the distribution of the anomaly. The survey LINES A - F catches the central part and western margin of the A zone, on the other hand, as the zone is prolonged beyond the survey areas, we cannot grasp the whole shape of this anomaly by the LINES G - I.

The B zone was detected over the area from Station Nos. 16 to 26 on

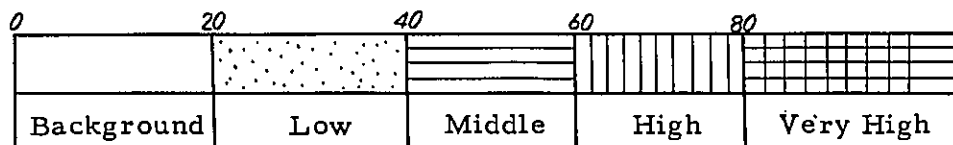
LINEs E - G. Comparing the values of FE of the A zone, those of the B zone are lower. But it is supposed that the northern part of this zone continues to the A zone. The source conductor is so deeply embedded that the corresponding surface anomaly is relatively obscure in shape.

There is another "C" anomalous zone in the southern part of the survey areas. The central part of the C zone is found around LINEs J' - D. The length of this zone amounts to about 2.5 km in the NS direction and the width is about 500 m on an average, though somewhat fluctuated. The source conductor of this FE anomaly may have complicated shapes. The top surface of the conductor are so undulated that the depths estimated from the FE values are different from place to place. It is noteworthy that the C zone coincides with the geochemically anomalous zone. Therefore, the C anomaly is the most promising indication as compared with the other two FE anomalous zones.

Although a small anomalous zone of 2% FE is found at Station No. 36, the eastern end of LINE J, this may not be important. Except the A, B and C anomalies, there is no outstanding FE anomaly (more than 2% FE) over the survey areas.

3) Metal Factor

Similarly to the AR and FE, the values of MF are divided into five steps, background, low, middle, high and very high. The following expressions are adopted in the annexed figures.



The distribution of MF resembles that of FE, i. e. the MF anomalies (MF \cong 20) correspond to the FE anomalies with A, B and C zones. We do not regard as an important MF anomaly, if it is not associated with sometimes caused by very low or low value of resistivity. We call such a value of MF "false anomaly". The MF anomaly distributed east of Station No. 25, LINEs J' - O', is thought to be one of the false anomalies. As a result, the promising anomaly (MF \cong 40 and FE \cong 3 %) are distributed around Stations 13 - 17, LINE C' ; Stations 17 - 21, LINE J' ; Stations 17 - 22, LINE K ; Stations 19 - 21, LINE L' ; Stations 16 - 18, LINE M ; Stations 16 - 20, LINE N and Stations 16 - 22, LINE O'.

4) Laboratory Measurements

It is important for the analyses of the geophysical prospecting results that physical properties of rock samples are determined by means of laboratory experiments. The typical rock specimens were collected over the survey areas, the values of AR and FE are measured together with chemical concentrations of some elements. The physical properties determined by laboratory measurements are compared with the results of the in-situ field measurements.

Although the rock specimens were sampled without exception as uniformly as possible, the values such statistically determined from the samples are not always represent the field-measured values. Moreover, the conditions measuring in a laboratory may be quite different from the natural circumstances. It is impossible, therefore, that the results from the laboratory experiments are substituted into the field-surveyed data.

Notwithstanding, the laboratory data are important for reference to the field data, if the statistical relation between both the data is obtained.

Table 2-5 shows the values of AR and FE determined from the laboratory and in-situ measurements.

4)-1 Measuring Apparatus

One of the most important matters in laboratory experiments is to keep the specimens as it was and ensure the reliability of measured values. The "IP-Characteristics Measuring Apparatus" (see Fig. 2-5) was manufactured by taking the above-mentioned points into consideration. The summary of the apparatus is as follows:

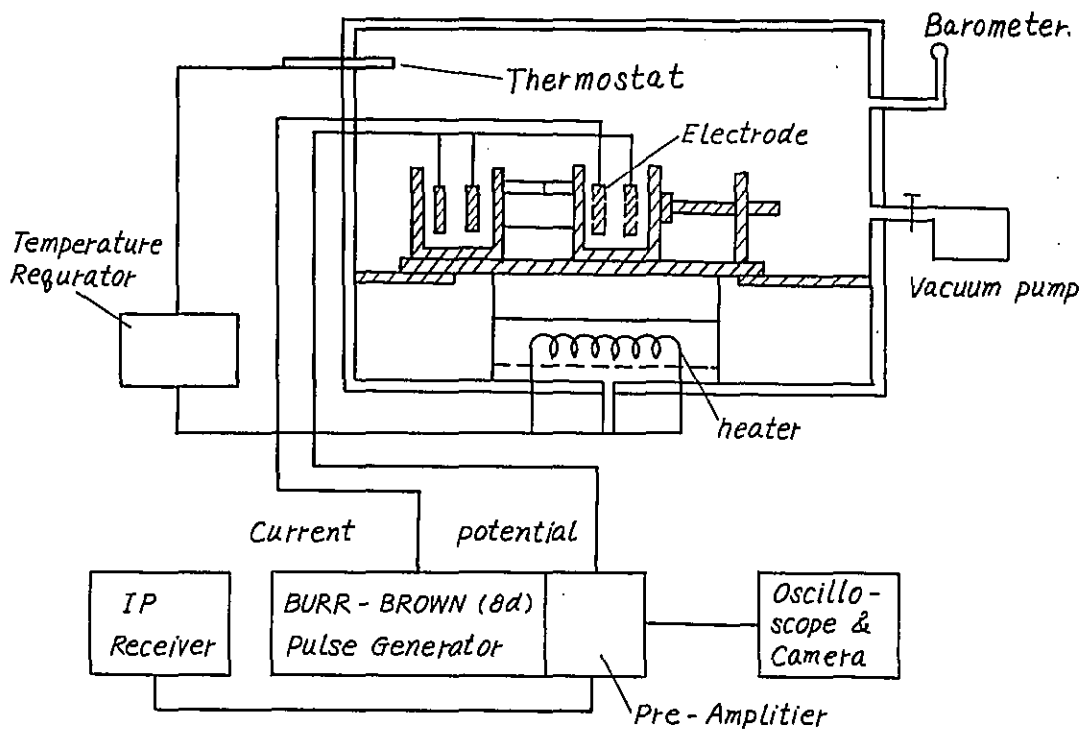


Fig 2-5 Sketch of Apparatus

Thermostat : Iron-made (inner scale 30 x 50 x 30 cm²).

A vacuum pump equipped to decrease inner pressure.

The sample holder can be adjusted with the sample size.

The diameters of the sample contact to the electrolytic bath : 2.5 and 3 cm.

The current electrode made of Ag and the voltage electrode made of AgCl (non-polarized).

Pulse-generator : Burr Brown Co. Model 801

Applicable to time domain and frequency domain methods.

Four output ranges and the corresponding load resistivities as follows:

1 - 11 micro-A Range: 0 - 10.5 Mohm at micro-A

10 - 110 " " : 0 - 10.5 " at "

0.1 - 1.1 mA Range : 0 - 10.5 " at 0.1 mA

1 - 11 mA Range : 0 - 10.5 " at 1 mA

Receiver : Same as the field survey receiver.

4)-2 Results of Laboratory Measurements

The laboratory measurements of AR and FE were made on 28 specimens of typical rock forming the geology of the survey areas. In Table II-5, the measured results are tabulated together with copper and sulphur concentrations. It can be noticed in this table that Sample Nos. 26 and 27, sulphide-disseminated monzonitic rock and Sample Nos. 31 and 32,

magnetite-skarn, indicate very high FE values by the laboratory measurements. The fact that the disseminated monzonitic rock has 8 - 10% FE implies the impregnation with sulphide minerals. The mean value of FE obtained from 8 dioritic rock specimens is 4.2%, on the other hand, that from 7 monzonitic rock samples is 2.4%. It is concluded that dioritic rock indicates an FE higher than monzonitic rock.

We can arrange rock specimens from high to low resistivities in order as quartzite, limestone, dioritic rock and monzonitic rock, but the ranking, in general, is not always kept in actuality.

The resistivity value of Sample No. 14 limestone is 780 ohm-m, but that of Sample No. 15 limestone is 4,810 ohm-m, despite that both the sampled sites are only 100 m apart each other. However, in contradiction to the laboratory measurements, the resistivity values from the in-situ measurements made at the same sites were 250 and 270 ohm-m, respectively. This fact may imply that one of the sampled limestones locally changes in quality, so that we should rather treat them as almost same order of AR on the basis of the in-situ results.

A similar discussion can be made on Sample Nos. 15 and 17. Although the separation of both the sampled sites is 400 m, the former AR is 4,660 ohm-m, but in contrast the latter AR is 36,360 ohm-m, i. e., about ten times higher than the former value. Notwithstanding, the in-situ values of the same sites are almost equal, 185 and 194 ohm-m, respectively.

Sample Nos. 12 and 13 limestone specimens indicated lower resistivity values than those expected from the in-situ results.

Table 2-5 Laboratory Measurement, In-situ measurement and Chemical Assay of Samples

			Laboratory		Chemical assay		In-situ	
			AR ($\Omega \cdot m$)	FE (%)	T-Cu (%)	S(%)	AR ($\Omega \cdot m$)	FE (%)
1	LINE I-4	Dioritic Rock	2,380	4.0			103	0.8
2	" J-20	"	2,540	3.9			82	0.4
3	" L-8	"	1,930	5.0	0.009	< 0.01	128	0.7
4	" M-8	"	1,440	3.2			224	0.6
5	" M-13	"	3,360	4.2			130	1.2
6	" N-10	"	3,230	5.4	0.011	< 0.01	104	1.1
7	" P-12	"	3,510	4.7			136	0.7
8	" Q-14	"	1,790	3.3			110	0.5
9	" O-14	"		(@ 4.2%)			32	0.7
10	" P-10	"					144	0.8
11	" P-14	"					127	1.0
12	LINE B-31	Limestone	32,950	0.7			444	0.3
13	" D-30	"	46,650	0.8			1,510	0.7
14	" G-17	"	780	2.6			250	1.6
15	" G-18	"	4,810	0.1			270	1.1
16	" J-7	"	4,660	3.0	0.003	< 0.01	185	1.4
17	" K-6	"	36,360	0.3	0.002	< 0.01	194	1.3
18	" O-28	"	3,320	1.0			104	1.1
19	" C-4	"	1,590	1.0			131	1.0
20	" A-34	"					483	0.9
21	LINE G-16	Monzonitic Rock	2,690	2.3			85	1.2
22	" M-20	"	694	3.4	0.028	< 0.01	50	1.2
23	" O-18	"	788	2.2			133	1.5
24	" O-20	"	652	3.5	0.006	< 0.01	138	1.3
25	" Q-18	"	747	2.2			73	1.5
26	LINE A	" (py imp)	1,550	9.5	0.090	2.50		
27	C-18 B	" (py imp)	3,110	8.2	0.530	1.42		
				(@ 2.4%)				
28	LINE B-17	Quartzite	6,350	0.6			3,450	1.5
29	" C-12	"	6,230	1.0	0.003	< 0.01	7,500	1.8
30	" C-16	"					103	1.5
31	LINE G-21	Magnetite skarn	1,140	17.0	0.11	0.17	41	1.6
32	" G-22	"	1,980	12.0	0.020	< 0.01	75	1.6
33	" J-36	"					73	1.7
34	LINE C-7	Shale	230	2.3			200	1.1
35	" C-6	"					60	1.2
36	" G-8	"					46	1.2
37	LINE J-24	Pampa					13	0.6
38	" J-26	"					16	0.6
39	" C-28	"					28	0.8
40	" C-17	"					34	0.7
41	" J-29	"					14	0.7
42	" Q-12	"					6	0.5
43	" I-20	"					40	0.9

It is possibly presumed that the limestone around these stations may indicate higher resistivity judging from the in-situ results.

4)-3 Synthetic Considerations of Rock Specimen Tests

The laboratory-experimental results of FE of disseminated monzonitic rock samples were high. As previously mentioned, this fact indicates that such a high FE is due to the sulphite mineral dissemination. This fact was also proved by the chemical analyses as high sulphur concentration ranging from 1.42 to 2.50%. In contrast to the laboratory values, the field-surveyed FE takes weakly anomalous values ranging from 2 to 3%. In other words, the laboratory values of FE are three or four times larger than those of field surveys.

In the case of monzonitic rock Sample Nos. 22 and 24, the laboratory FE values are rather high, 3.4 - 3.5%, in comparison with the field data of about 1.5%, which is as small as background noises. The in-situ measurements were also made on the same sites, and we obtained as 1 - 2% or less. According to the chemical analyses of these samples, the sulphide concentrations were rather small. Judging from the above facts, an FE anomaly should be defined as 6 % FE or more in the case of monzonics rock specimen tests.

The results of laboratory tests of dioritic rock are generally much higher than those of monzonitic rock. However, the FE values obtained by the field survey are almost equal each other, and furthermore, the in-situ values are somewhat higher for the monzonitic rock. The sulphur concentration is rather low for the dioritic rock samples.

The drilling cores sampled from Drilling No. DDH-5, which is located near Station No. 17, LINE M, consist of dioritic rock. The FE values obtained by the field survey around the station were 3 % or more, but we obtained a much lower FE value from the in-situ measurements over dioritic rock zone (Sample No. 20), where is 400 - 500 m apart from the site of DDH-5. The laboratory tests of the drilling cores were desired, but the core-pieces of dioritic rock were unfortunately too small to be provided for laboratory tests. Therefore, we can not make any discussion about the relation between FE's based on laboratory and in-situ tests.

As compared with the cores from DDH-5, the dioritic rock cores from DDH-3 and DDH-4 do not indicate high FE, probably because the DDH-5 cores are abundant in sulphide minerals. The mean value of sulphur concentration in the DDH-5 cores is 0.89 % (see Table 2-6).

In contrast that the magnetite-skarn test-pieces indicate high FE values ranging from 12 to 17 %, the field FE's are 2 - 2.5 %, about 1/6 - 1/7 of the laboratory data, which can not discriminate from the background noises. This fact may be explained as the in-situ value, in general, include effects of the adjacent structures, but in contrast, the laboratory result reflects the pure characteristics of a test-pieces.

The in-situ values of AR over the limestone outcrops (LINEs B and D) in the northern part of the survey areas were 450 and 1,500 ohm-m. These values are well correlated with the AR results of laboratory tests. The locally high AR values over the quartzite distribution are also well correlated with the test-piece results. However, generally speaking, it

is difficult to distinguish rock forming the underground structure on the basis of the in-situ and laboratory tests.

Table 2-6 Assay & Sulphide Contents Estimated of D.D.H

	DDH - NO.1							DDH - NO.2							DDH - NO.3							DDH - NO.4							DDH - NO.5							DDH - NO.6														
	ASSAY			SUIFIDE CONTENTS ESTIMATED				ASSAY			SUIFIDE CONTENTS ESTIMATED				ASSAY			SUIFIDE CONTENTS ESTIMATED				ASSAY			SUIFIDE CONTENTS ESTIMATED				ASSAY			SUIFIDE CONTENTS ESTIMATED																		
	T-Cu%	S-Cu%	S%	Bo%	Cp%	Py%	Total	T-Cu%	S-Cu%	S%	Bo%	Cp%	Py%	Total	T-Cu%	S-Cu%	S%	Bo%	Cp%	Py%	Total	T-Cu%	S-Cu%	S%	Bo%	Cp%	Py%	Total	T-Cu%	S-Cu%	S%	Bo%	Cp%	Py%	Total	T-Cu%	S-Cu%	S%	Bo%	Cp%	Py%	Total								
50														0.09	0.06	0.49	0.01	0.06	0.89	0.96																								0.07	0.04	0.73	0.01	0.06	1.34	1.41
														0.03	0.03	0.50	0	0	0.94	0.94	0.63	0.05	1.02	0.36	1.00	1.09	2.45	0.54	0.41	0.41	0.08	0.23	0.58	0.89	0.07	0.03	0.84	0.03	0.05	1.53	1.61									
														0.04	0.04	0.31	0	0	0.58	0.58	0.61	0.07	0.53	0.35	0.91	0.38	1.64	0.51	0.06	0.69	0.28	0.77	0.66	1.71	0.15	0.09	1.28	0.03	0.11	2.32	2.46									
														0.07	0.04	0.36	0.01	0.06	0.04	0.11	1.89	0.04	1.76	1.16	3.08	0.68	4.92	0.35	0.09	0.82	0.18	0.46	1.13	1.77	0.16	0.09	1.41	0.04	0.11	2.57	2.72									
		0.37	0.39	0.27		0	0.51	0.51	0.05	0.03	0.33		0.06	0.58	0.64	0.05	0.03	0.29	0.01	0.02	0.53	0.56	0.43	0.03	0.57	0.25	0.69	0.51	1.45	0.16	0.05	1.12	0.07	0.20	1.94	2.21	0.10	0.02	0.86	0.04	0.14	1.51	1.69							
		0.32	0.09	1.76		0.66	2.89	3.55	0.64	0.28	0.87		1.03	0.96	1.99	0.04	0.02	0.30	0.01	0.02	0.55	0.58	0.76	0.03	0.48	0.46	1.26	0	1.72	0.30	0.03	0.97	0.17	0.46	1.45	2.08	0.17	0.04	0.92	0.08	0.23	1.55	1.86							
		0.42	0.07	3.88		100	6.66	7.66	0.27	0.02	0.55		0.71	0.57	1.28	0.02	0.02	0.49	0	0	0.92	0.92	1.43	0.05	1.19	0.88	2.34	0.28	3.50	0.09	0.74	0.03	0.03	0.11	1.30	1.44	0.62	0.06	1.79	0.35	0.97	2.57	3.89							
		0.04	0.02	0.67		0.03	1.23	1.26	0.38	0.01	1.45		1.06	2.04	3.10	0.16	0.07	0.87	0.07	0.14	1.51	1.72	0.57	0.04	0.55	0.33	0.91	0.28	1.52	0.29	0.12	0.95	0.11	0.29	1.55	1.95	0.05	0.02	0.81	0.01	0.05	1.49	1.55	0.21	0.05	0.47	0.09	0.29	0.66	1.04
100		0.03	0.02	0.85		0.03	1.58	1.61	0.01	0.01	0.72		0	1.36	1.36	0.64	0.11	0.73	0.33	0.91	0.62	1.86	0.22	0.03	0.36	0.12	0.31	0.42	0.85	0.08	0.04	0.32	0.11	0.29	0.36	0.76	0.20	0.09	0.70	0.06	0.20	1.17	1.43							
		0.04		0.27		0.11	0.45	0.54	0.30		1.60		0.86	2.45	3.31	0.47	0.33	0.74	0.09	0.23	1.21	1.53	0.12		0.26	0.08	0.20	0.32	0.60	0.25		0.90	0.16	0.43	0.87	1.46	0.22		0.48	0.15	0.37	0.58	1.10							
		0.03		0.72		0.09	1.30	1.39	0.17		0.50		0.49	0.62	1.11	1.03		1.11	0.73	1.77	0.45	2.95	0.11		0.63	0.06	0.20	1.02	1.28	0.56		0.94	0.35	0.97	1.15	2.47	0.16		0.29	0.09	0.29	0.32	0.70							
		0.03		0.79		0.09	1.41	1.50	0.21		1.91		0.60	3.21	3.81	1.65		1.70	1.18	2.83	0.58	4.59	0.13		0.65	0.08	0.23	1.03	1.34	0.20		0.36	0.12	0.34	0.40	0.86	0.10		0.20	0.07	0.70	0.23	0.47							
		0.07		1.20		0.20	2.13	2.33	0.07		0.35		0.20	0.53	0.73	0.50		0.48	0.31	0.86	0.19	1.36	0.08		0.22	0.05	0.14	0.30	0.49	0.06		0.38	0.03	0.08	0.62	0.73	0.09		2.91	0.07	0.17	5.34	5.58							
		0.04		0.92		0.11	1.66	1.77	0.14		1.43		0.40	2.43	2.83	0.17		0.33	0.11	0.29	0.38	0.78	0.08		0.27	0.05	0.14	0.40	0.59	0.44		1.46	0.28	0.74	2.13	3.15	0.05		2.77	0.03	0.08	5.15	5.26							
		0.02		0.36		0.06	0.64	0.70	0.15		2.02		0.43	3.53	3.96	0.23		0.57	0.16	0.40	0.74	1.30	0.18		0.30	0.11	0.31	0.34	0.76	0.35		0.80	0.22	0.60	1.00	1.82	0.04		2.52	0.03	0.06	4.70	4.79							
		0.02		0.67		0.06	1.23	1.29	0.33		1.54		0.94	2.28	3.22	0.16		0.51	0.09	0.29	0.74	1.12	0.14		0.20	0.09	0.25	0.19	0.53	0.09		0.91	0.05	0.17	1.58	1.80	0.03		3.22	0.01	0.06	6.04	6.11							
150		0.03		0.52		0.08	0.92	1.00	0.13		1.06		0.37	1.75	2.12	0.03		0.36	0.01	0.06	0.64	0.71	0.23		0.29	0.15	0.40	0.20	0.75	0.06		1.04	0.03	0.11	1.87	2.01	0.04		1.98	0.03	0.06	3.68	3.77							
		0.03		0.97		0.09	1.77	1.86	0.09		1.38		0.26	2.73	2.99	0.06		0.25	0.03	0.11	0.38	0.53	0.16		0.31	0.09	0.29	0.36	0.74	0.04		1.41	0.03	0.05	2.60	2.68	0.13		3.42	0.08	0.23	6.26	6.57							
		0.03		0.66		0.09	1.19	1.28	0.17		0.77		0.48	1.13	1.61	0.04		0.22	0.02	0.06	0.38	0.46	0.06		0.14	0.03	0.11	0.17	0.31	0.06		0.89	0.03	0.11	1.58	1.72	0.09		1.98	0.05	0.17	3.60	3.88							
		0.03		0.70		0.09	1.25	1.34	0.09		0.69		0.26	1.13	1.39	0.06		0.17	0.03	0.11	0.74	0.88	0.07		0.37	0.04	0.11	0.60	0.75	0.05		1.02	0.03	0.09	1.85	1.97	0.17		1.91	0.11	0.29	3.36	3.76							
		0.04		0.47		0.11	0.81	0.92	0.08		0.72		0.23	1.21	1.44	0.02		0.50	0.01	0.02	0.92	0.95	0.07		0.46	0.04	0.11	0.77	0.92	0.02		1.97	0.03	0.09	3.64	3.76	0.18		1.98	0.11	0.31	3.47	3.89							
		0.04		0.65		0.11	1.15	1.26	0.08		0.72		0.23	1.21	1.44	0.02		0.50	0.01	0.02	0.92	0.95	0.07		0.46	0.04	0.11	0.77	0.92	0.05		1.97	0.03	0.09	3.64	3.76	0.18		1.98	0.11	0.31	3.47	3.89							

3-3 Detailed Discussion about the Indications

LINE A PL. II-6-1

High or middle resistivity zone, in general, occupies predominantly LINE A. As seen in PL. II-6-1, there is a roof-shaped pattern of very high resistivity zone beneath Station No. 20, the central part of this line. This may be an effect of mountain topography overlapped by the IP effect of quartzite scarce of water content. We also notice that the low resistivity structure is deepseated beneath Station No. 20. A highly resistive overburden, however, is sometimes recognized as if a deeper structure of low or middle resistivity might exist. It is impossible to judge either of the two cases to be true or not on the basis of IP measurements alone.

An outstanding anticlinal distribution of FE anomaly is found around Stations No. 8 - 18. This is an extension of the anomalous zones recognized in the western parts from LINEs B to I. It is also sure that these zones are prolonged northwards beyond the survey areas.

An explicit MF indication greater than 20 was obtained at three stations. This may imply that this line is generally covered with a highly resistive overburden.

LINE B PL. II-6-2

The downward distribution of AR along LINE B resembles that along LINE A. A roof-shaped pattern of very high resistivity is also found beneath a topographic high around Station 20, and a low AR zone lines between the very high zones. The other low AR zone east of Station No. 32 is possibly due to the alluvial overburden.

There is a roof-shaped FE anomaly distribution between Stations No. 10 and 22. The isoanomaly lines there are not closed near the surface unlike in LINE A. This indicates that the corresponding source is located much shallower, probably shallower than 200 m below the surface. There is no anomalous FE east of Station No. 22. Presumably, any strong sources do not exist in the place shallower than 500 m below the surface.

Unlike the FE anomaly, the corresponding MF anomaly seems to be split into three parts. This may be due to the terrain effects on AR. These three parts of the MF anomaly must essentially be one.

LINE C PLs. II-6-3 and II-7-1

A synclinal structure of low resistivity is explicitly seen in the alluvial zones, west of Station No. 10 and east of No. 26, and in the swamp around Station No. 16. The alluvial zone east of Station No. 26 seems shallowseated, as the associated AR pattern does not extend downwards. The other places are formed by middle or high AR zones. Judging from model computation results, the possible source of the high AR east of Station No. 18 is an underground conductor higher than 200 ohm-m, but the rock can not be identified.

Between Stations No. 8 and 20 is noticed an FE anomaly, which is presumed through the model computations as a pillar-shaped source of high polarization extending to the depth beneath Station No. 6. The dissemination was recognized with the geological survey between Stations No. 10 and 20. The FE anomaly well coincides with the disseminated zone, which is thought to be seated shallower than 100 m. We repeated

the detailed FE surveys between Stations No. 10 and 30 with an electrode separation of 100 m, where the high FE anomaly was recognized in the shallower than 100 m.

A MF anomalous zone is concentrated to an area around Stations No. 14 - 16. This MF anomaly is one of the most conspicuous in the whole survey areas. The high FE and low AR correspond well to this MF.

LINE C' PLs. II-6-4 and II-7-2

Horizontal layers of low AR cover LINE C'. The low AR is caused by the surface alluvial overburden. A FE anomaly extends westwards. The eastern limit of this anomaly is situated at Station No. 18, but the western extension is not explicit beyond LINE C'. This FE anomaly is analyzed as a relatively shallow source by means of FE surveys with an electrode spacing of 100 m, meanwhile, as a deepseated source by means of 200 m spacing surveys. Judging from these facts, the source of the FE anomalies found in the shallow becomes deeper beneath LINE C'.

LINE D PLs. II-6-5 and II-7-3

An anticlinal distribution of high and very high resistivity zones was detected around Station No. 30. This is one of the typical AR distributions explicitly expressing the dipole-dipole characteristics in the present survey. Such a shaped of anomaly appears around a very high AR zone along the anticlinal axis. East of Station No. 30, strongly silicated limestone is outcropped, which indicates high AR values by the in-situ and laboratory measurements (see Tables 2-1 and 2-5).

It is sure, accordingly, that the above-mentioned high AR is caused

by the limestone outcrops. An U-shaped pattern of low AR is detected around Stations No. 10 - 30 by both surveys with electrode separation of 100 and 200 m. This corresponds well to the superficial alluvium.

Comparing the FE anomaly distribution here with those along LINE A - C, we notice that the width of the anomaly source, 200 m deep on an average, becomes narrower under LINE D and the slope of the eastern anomaly becomes more gentle. We presume that the FE anomaly source found in the northern survey lines becomes deeper and wider.

We notice two FE anomaly sources in the MF profile, although only one source is revealed from the corresponding FE anomaly profile. This anomaly is very interesting, on the analogy of the FE anomaly having double sources detected on the southern lines.

LINE D' PLs. II-6-6 and II-7-4

AR is low or middle along this line. There is not any interesting AR feature here. A feeble anomaly is noticed in the depth, but the whole shape of the anomaly is not clear unless this line extends westwards. It is presumed that this anomaly resembles the adjacent anomalies on LINES D and E in shape. The low anomaly of MF corresponds to the feeble FE anomaly.

LINE E PL. II-6-7

AR is high or very high east of Station No. 30. The high AR is caused by strongly-silicified limestone outcrops, the root of which is thought to develop in the depth. The other high distributed west of Station No. 14 may correspond to the quartzite and dioritic rock zones.

Between these two high AR zones, we see a zone of moderate resistivity, downwards extending, which may possibly be caused by the exposed shale.

The FE profile along this line is somewhat different from those along LINES A - D. In contrast to the concentrated anomalous bodies beneath LINES A - D, the anomaly pattern here is split into two parts at least. The west part can be explained as a strongly anomalous source which is shallower than 100 m at minimum below Station No. 6 and inclines eastwards. The east part may be caused by a relatively weak FE source developing in the depth. As previously mentioned, the source is divided into two parts in the MF profile of LINE D, but united in the FE profile. This phenomenon of LINE D corresponds to the FE anomaly pattern here. The double sources may be located between LINES D and E.

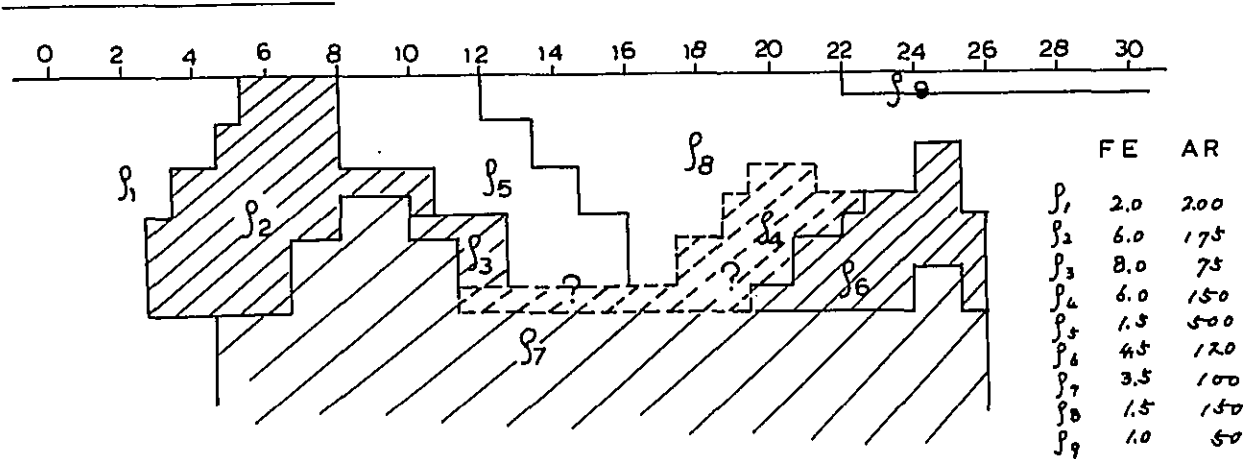
MF anomalies coincide well with the FE anomalies shallowseated under Station No. 6 and deepseated under Station No. 20. The source concerned is also split into two parts.

LINE F PL. II-6-8

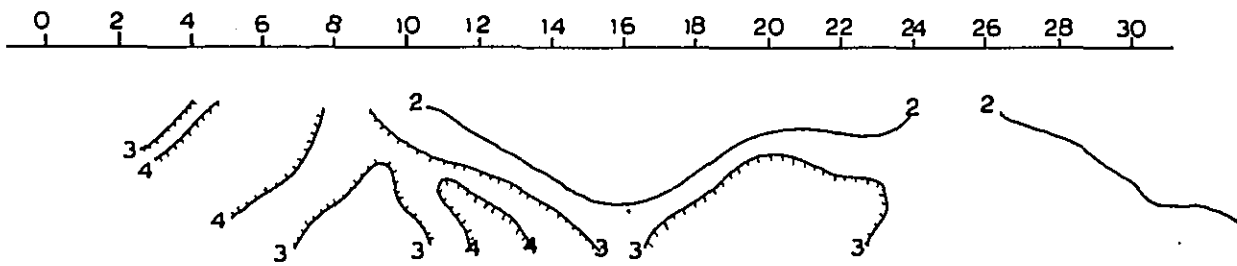
It is very interesting that the high AR is well associated with the surface geology in this profile. An explicit roof-shaped arrangement of high AR between Stations No. 6 and 14 may be due to the topographic upheaval and the distribution of quartzite with small water content. The upheaval zone of moderate AR is also found between the high AR anomalies. This may express the existence of a moderately resistive rock as seen at Stations No. 20, LINES A and B. However, the very high resistivity zone detected east of Stations No. 30, LINES D and E is not recognized here.

LINE - F (a=200 m)

Simulation Model



Field Data



Results of Simulation

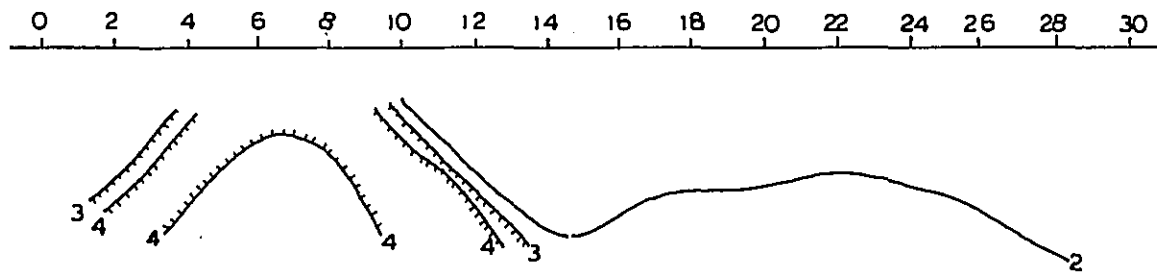


Fig. 2-6

This indicates that the silicified limestone corresponding to the zone is not so deeply developed.

The FE pattern here resembles that in LINE E. Consequently, the source may also be divided into two or more. Combining with the AR result concerned with the western source, an upheaval of moderately resistive rock must be assumed in the depth under Station No. 10. According to the results of model computations simulating the geological structure along this profile, as shown in Fig. 2-6, the associated source of anomaly is embedded on the western slope of the upheaval. The eastern source, meanwhile, is somewhat feeble as compared with the western one, but is relatively deeply developed.

The low MF is well associated with the middle frequency-effective anomaly.

LINE G PL. II-6-0

The pattern of AR along LINE G is very similar to that along LINE F. This indicates the geological resemblance between LINEs F and G. The FE anomaly also has a pattern similar to LINE F. The FE source is surely continued from LINE F. The FE value does not converge in the western margin of this line, so that the corresponding anomaly may be further prolonged. The MF anomalies coincide well with the strongly anomalous FE in the western part and middle-anomalous one in the eastern part.

LINE H PL. II-6-10

The AR values obtained on LINE H range below 200 ohm-m, from

middle to very low resistivity. There is found a low or very low AR zone thickly lying over the east of Station No. 18. The possible cause of this zone is an alluvium distribution there.

The eastern FE anomaly continued from LINE E to G disappears here, so that the anomalous body is discontinuous between LINES G and H. Contrastly, the western FE anomaly is vague. We can expect from the FE distributions previously mentioned that the center of the western anomaly may be located west of Station No. 4. In contrast to the high FE values from LINE A to G, here ranges from low to middle FE. Judging from these facts, the high FE zone will be found on a westward extension of LINE H.

There are three small-scale anomalies of low MF, an anomaly found around Station No. 34, however, is supposed to be a false anomaly because of low AR.

LINE I PL. II-6-11

Similarly to the case of LINE H, AR values here, in general, are middle or lower. There is also a low or very low AR zone corresponding to the alluvium overburden.

A deepseated feeble FE anomaly alone is recognized west of Station No. 12. This anomaly may extend westwards with increasing strength on the analogy of the FE pattern of LINE H. It is impossible, therefore, to determine the exact location of the corresponding source from the FE pattern distributions. The anomaly is merely a part of effects of the source widely westwards distributed beyond the source area.

LINE I' PLs. II-6-2 and II-7-5

No remarkable anomalies of AR FE and MF are picked up along LINE I'. A deeply-embedded weak anomaly is recognized in the central part of this line (from Station No. 16 to 24). This is a coda of the anomaly continuing southwards from LINEs J' and K.

LINE J PLs. II-6-13 and II-7-6

The AR values measured here is, in general, almost low or middle. This implies that the underground consists of relatively low AR structure.

The FE anomaly south of this line is thought to be independent of the source continued from LINE E to I, because the anomalies found in the western parts of LINEs E - I extends seemingly to the west, but in contrast this anomaly converges on the west ends of the forthcoming lines including this line. The shape of the source of this anomaly is presumed as a pillar or a slab.

In the depth west of Station No. 22, there is a weak anomaly. On the other hand, another weak anomaly zone seated below Stations No. 18 - 20 is revealed by means of detailed survey with an electrode separation of 100 m. These sources are presumably the same, embedded south of this line. In addition, there is a feeble anomaly, 2% FE or so, in the eastern end of this line. The cause of the anomaly may be magnetite-skarn out-cropping around there.

The MF pattern has also a feeble anomaly in the eastern end.

LINE J' PLs. II-6-14 and II-7-7

Low or middle AR almost occupies LINE J'. The low AR zone right

under Station No. 20 is continued from LINE J to K. This zone forms an upheaval-shape, which is caused by a deepseated low or middle AR body. On the analogy of the surface geology, we presume the source as monzonitic rock.

We see a roof-shaped FE pattern around Station No. 21. This is also obtained from the detailed survey with an electrode spacing of 100 m around Station No. 22. The source of this anomaly forms a slab lying at a depth of 250 - 300 m below the surface. The FE of the magnetite-skarn outcrop around Station No. 28 was not directly detected by the IP measurements. We obtained there only 1.5% FE even by the in-situ measurements. This means that the outcrop is small-scale, presumably rootless, so that the corresponding FE anomaly is not obtainable.

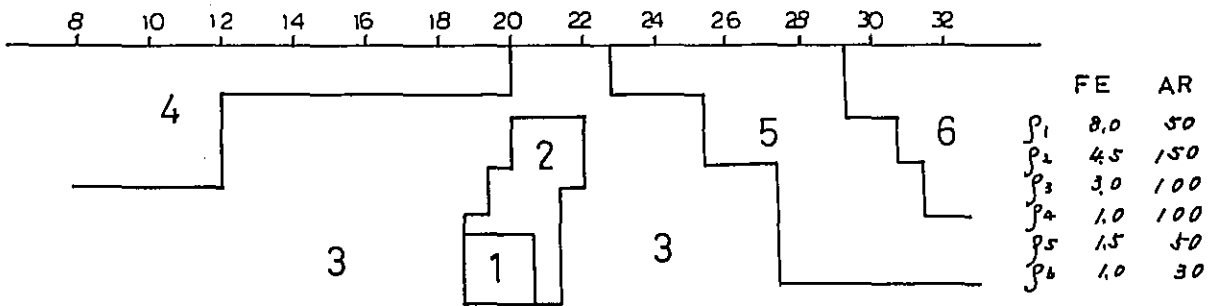
The MF anomaly concentrating to Station No. 20 coincides with the location of the low and middle FE anomalies. It seems likely that the MF values increase with a depth. This fact indicates the source deepseated below the station.

LINE K PLs. II-6-15 and II-7-8

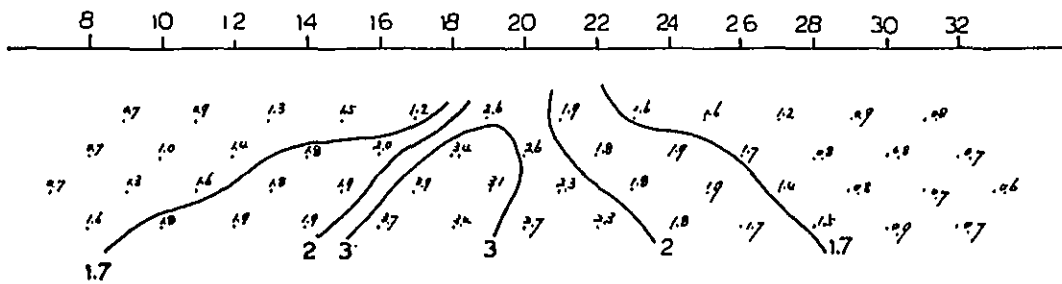
The AR profile of LINE K shows very low, low and middle resistivity zones. The very low zone may correspond to the alluvium overburden. A low zone right under Station No. 20 has relation to the monzonitic rock, which is continued from LINE J'. Another low lying under Stations No. 24 - 29 is also explained by the monzonitic rock as proved in the DDH-4 columnar section. Limestone outcrops just at the high AR around Station No. 4. However, judging from the AR patterns and surface geology, the

LINE-K (a=200M)

Simulation Model



Results of Simulation



Field Data

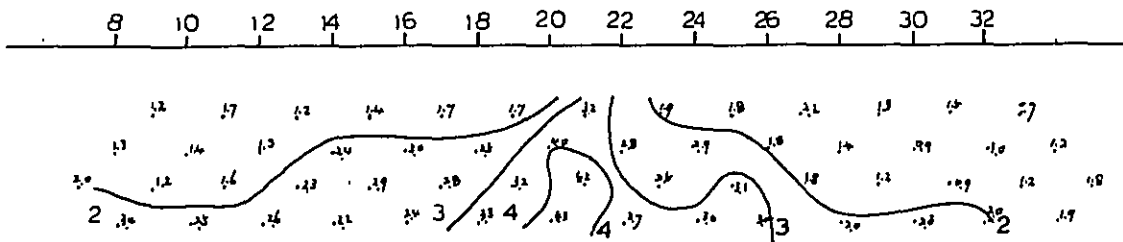


FIG 2-7

limestone deposit is so thin, that the high AR may not be due to the limestone but the deeper-seated dioritic rock.

A gently-sloped roof-shaped FE distribution including middle and high FE values is seen around Station No. 21. According to the simulation model computation, the FE source is a pillar conductor whose head is situated at a depth of about 200 m below the surface around Station No. 22.

DDH-3 near Station No. 26 drilled up mainly monzonitic rock together with skarn including total copper concentrations of 0.77% between -80 and -98 m deep and 1.53% between -119.4 and -144 m deep. Any of FE anomalies corresponding to the skarn zones, however, was not detected. The reason may be given as the followings:

- 1) As compared with deeper sulphide bodies, sulphide minerals in the skarn zones are neither conductible nor polarizable because of the high oxidation.
- 2) The skarn includes ores, whose sulphide concentration is less than the mean value of sulphide concentrations of core samples from the other drilling holes.
- 3) Laboratory tests proved marked differences in FE values between disseminated and non-disseminated monzonitic rocks distributing around DDH-3, whereby they are estimated to be weakly disseminated.
- 4) In-situ measurements proved magnetite-skarn outcrops along LINE G to be low in FE. Analogically, the skarn zone here is also too low in FE to be polarized.

Low or middle value detected at Station No. 20 may indicate some underground sources. MF anomaly east of Station No. 24 is supposed to be a false anomaly associated with low AR.

LINE K'

Generally speaking, AR here is low and middle. Low AR zones under Stations No. 20 and 23 indicate 100 ohm-m conductive underground bodies, which correspond to monzonitic rock on the basis of the source geology. High resistivity measured around Station No. 12 may correspond to diorite on the analogy of indications on LINE K.

A roof-shaped FE pattern, somewhat steep on the west side of the slope, is seen around Station No. 20. The upper part indicates a low FE, but middle and high FEs exist in the lower part. The further downward development of the FE source is presumed from such a pattern. The simulation model computation results in a low FE value in magnetite-skarn around Station No. 23, as shown in Fig. 2-8.

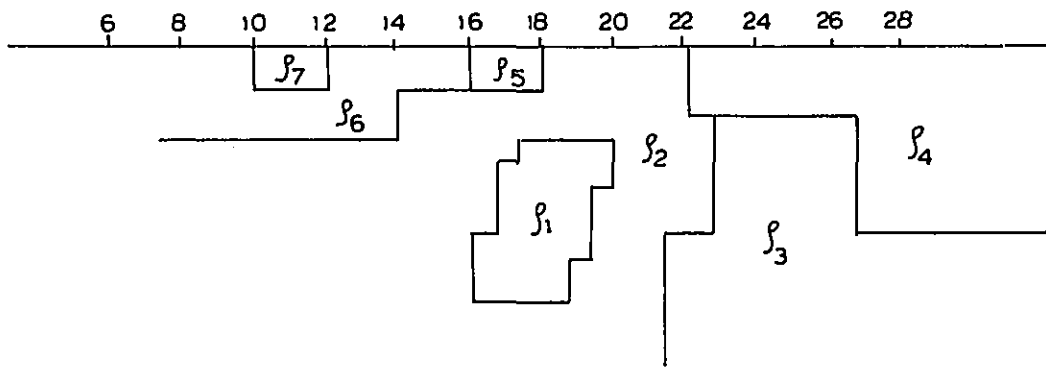
The general aspect of MF anomalies on this line is low but explicit. The centers of the anomalies have a tendency to appear in the eastsides of the FE anomalous centers. Such a deviation may be caused by a highly resistive zone distributing west of LINE K'.

LINE L

The range of AR on LINE L is from very low to high. The low AR zones under Stations No. 5 and 24 have roof-shaped patterns, which are geologically presumed as responses from monzonitic rock. According to the results of the surface geological survey, the zone ranging from middle

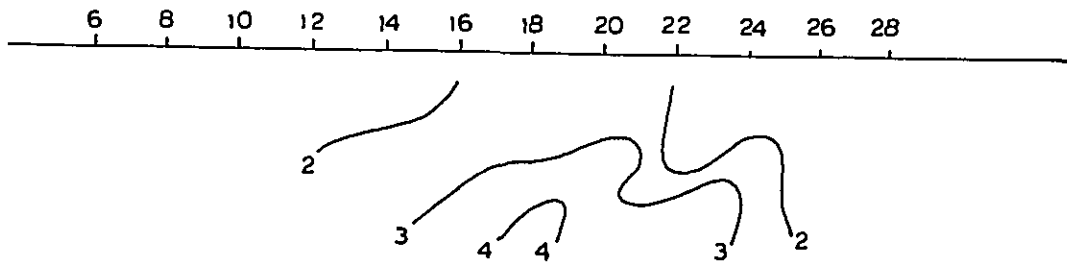
LINE K' (a=200M)

Simulation Model



	FE	AR
p_1	7.0	100
p_2	3.5	100
p_3	3.5	70
p_4	1.5	70
p_5	1.0	70
p_6	1.0	100
p_7	1.0	250

Field Data



Results of Simulation

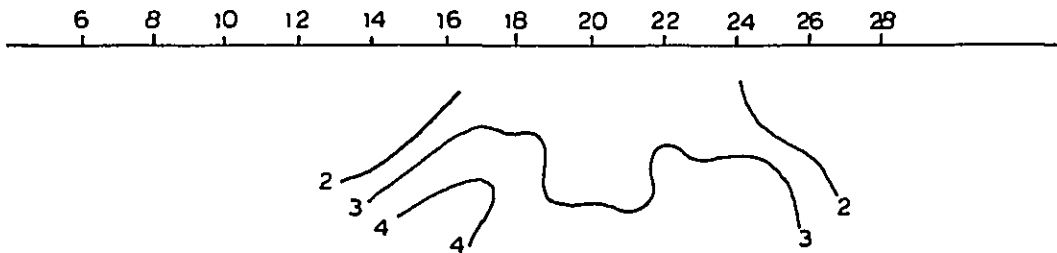
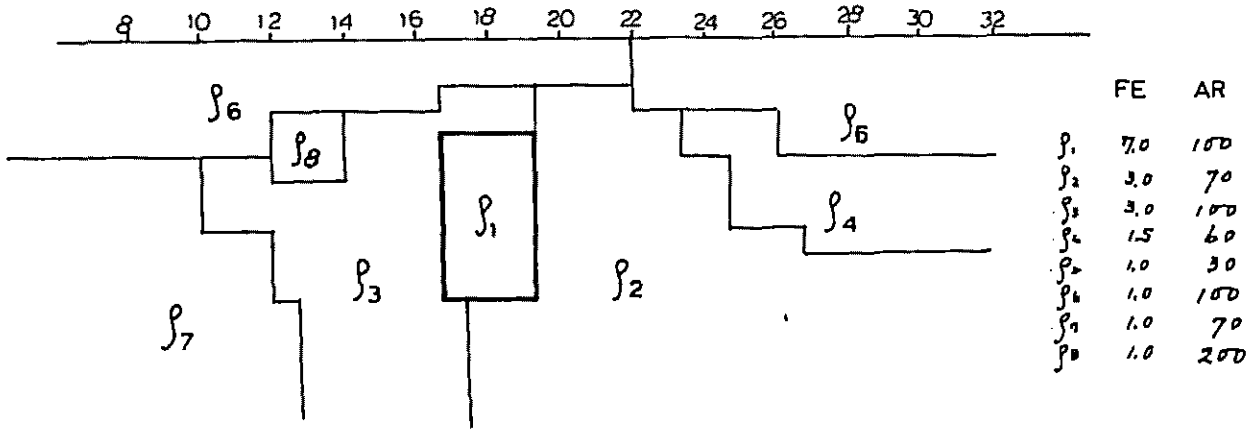


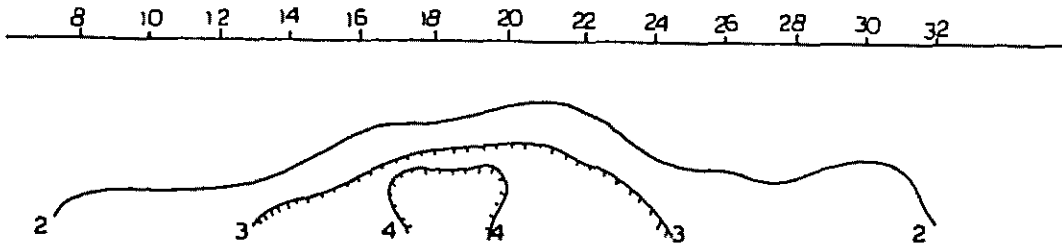
Fig. 2-8

LINE-L (a=200m)

Simulation Model



Field Data



Results of Simulation

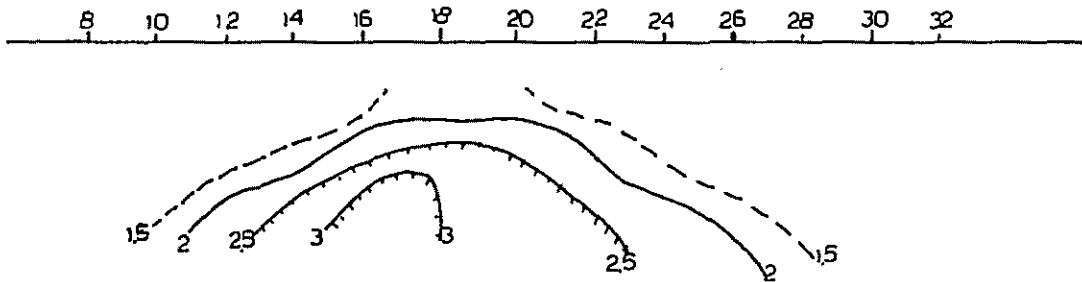


Fig. 2-9

to high AR, which is continued from LINE K, corresponds to diorite, and the very low zone east of Station No. 26 is caused by alluvial layers.

An explicit roof-shaped FE anomaly is found around Station No. 20. The low FE contour ($N = 1$) is gently convex at a depth of 200 m below the surface, and the higher contours lie underneath. The model computation simulating these results gives us a figure as shown in Fig. 2-9, i. e., we see an FE-less zone at a depth of 100 m or so below the surface. In comparison with the adjacent FE anomalies on LINES K' and L', the anomaly source varies discontinuously. The discontinuity is caused by the variation in geological structures.

Extensive low MF anomalies correspond well to the FE anomalies. MF highs which appear at both the sides of this line, i. e., west of Station No. 10 and east of No. 28, are probably false anomalies due to the low AR.

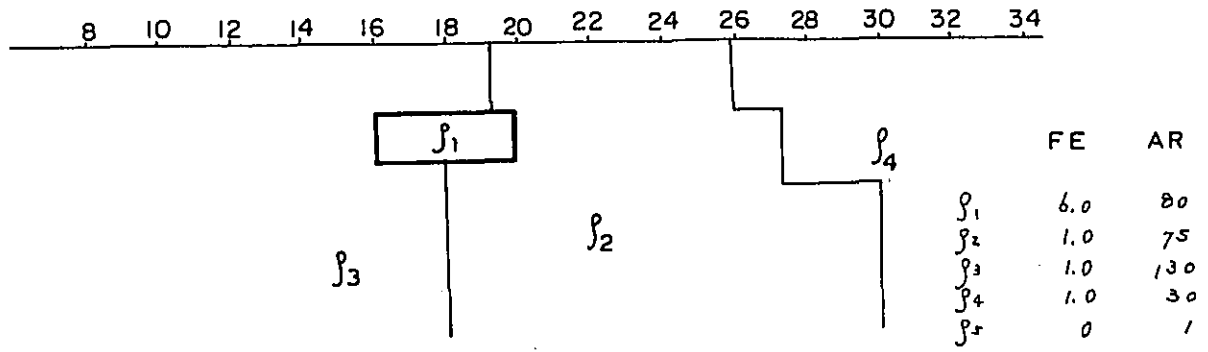
LINE L'

The general electric feature of this line is characterized by low and middle resistivities. The low AR indicates an underground conductor of 100 ohm-m east of Station No. 20, which may be monzonitic rock judging from the geological survey results. A high AR, continued from LINE L, was found by a survey with an electrode spacing of 100 m around Station No. 12, but with a spacing of 200 m the high disappeared. Accordingly, the source is small-scale and shallow. The middle AR zones seen around the station is presumably caused by dioritic rocks.

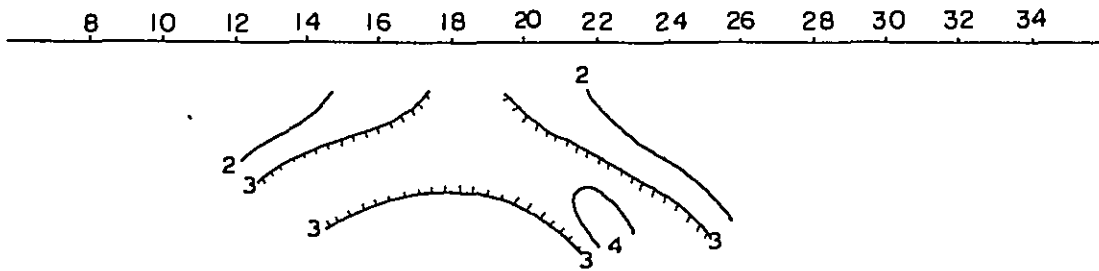
An anomalous FE forms a roof-shaped pattern centering at Station

LINE — L' (a= 200M)

Simulation Model



Results of Simulation



Field Data

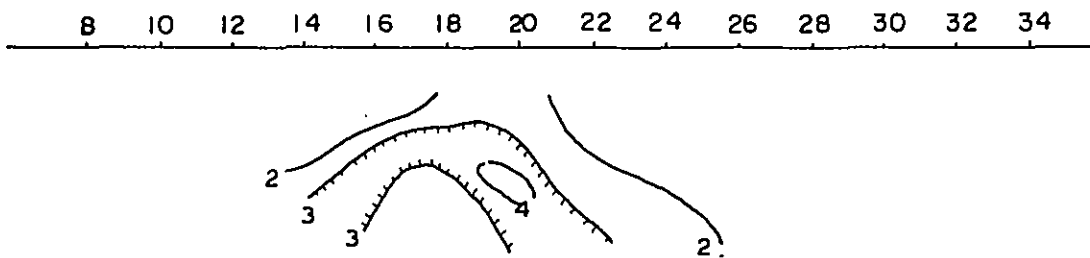


Fig 2-10

No. 18. The middle FE zone is sandwiched between the low FE zones. According to the model computation results, a horizontal slab source is embedded at a depth of about 200 m below the surface. It is interesting that, in contrast to the pillar-shaped FE sources under LINES J' - L, here is found the slab source.

Around Station No. 20, a roof-shaped MF anomaly is explicitly found. This coincides well with the FE anomaly due to the horizontal slab source.

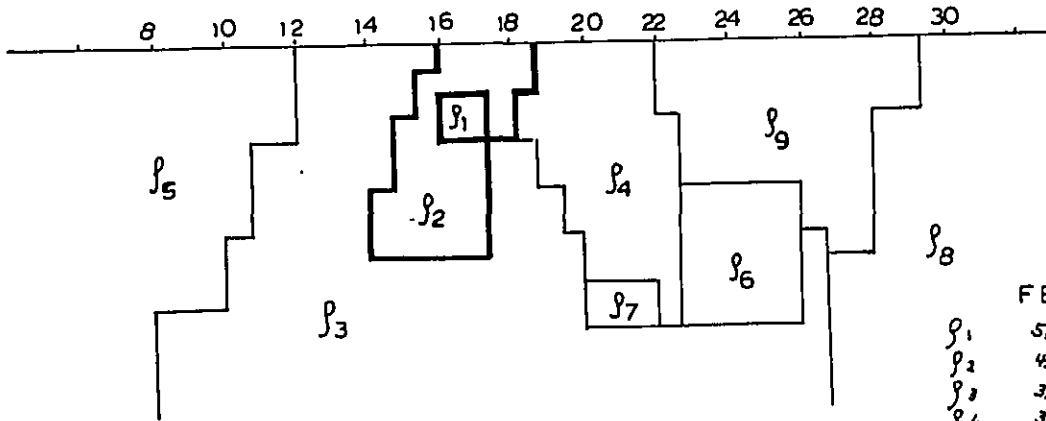
LINE M

A low AR zone occupies predominantly east of Stations No. 15 and 16. The remaining area is covered with middle and high AR's. The cause of the low AR is conductive bodies of 100 ohm-m lying east of Stations No. 15 and 16, meanwhile the high zone is due to high resistive bodies. DDH-4 is located near Station No. 21 on the low AR area, and the drilling core samples wholly consist of monzonitic rock. DDH-5, also located on the low AR area, drilled up cores of dioritic rocks. Generally speaking, dioritic rock produces middle or high AR, but the area of dioritic rock shows low AR near DDH-5, presumably because of superficial water-permeable layers along a stream. A large-scale roof-shaped high AR zone west of Station No. 10 is an effect of dioritic rock which is continued from LINE L.

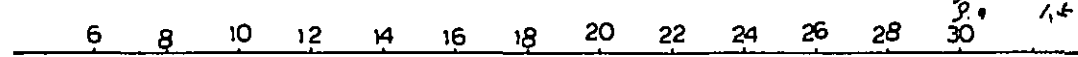
A model computation is made on the basis of the roof-shaped FE anomaly pattern centering at Station No. 18. The simulation model is obtained as a highly anomalous inclined pillar (dipped about 60° west) in the shallow as shown in Fig. 2-11. The mean assaying result of core of

LINE-M (a=200 m)

Simulation Model



Field Data



	FE	AR
ρ_1	5.0	100
ρ_2	4.0	150
ρ_3	3.0	150
ρ_4	3.0	75
ρ_5	1.5	250
ρ_6	1.5	150
ρ_7	1.5	40
ρ_8	1.0	30
ρ_9	1.5	75



Results of Simulation

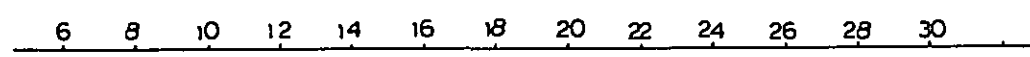


Fig. 2-11

monzonitic rocks of the DDH-4 sampled between 6 and 84 m deep below the surface is total Cu. 0.84% and S. 0.88%. However, according to the simulation model, the monzonitic rock is distributed over a weak FE zone.

Such a tendency may be caused by the following reasons:

- 1) The DDH-4 samples are poor in sulphide minerals.
- 2) A ratio of chalcopyrite to pyrite is approximately one to one on the basis of the assaying result. This indicates that the ratio is too poor in pyrite to be polarized.
- 3) According to the in-situ measurements around Station No. 20, the FE is only 1.2%, probably affected by a low-FE overburden.

In addition, based on the data obtained from a 200 m electrode spacing measurements, another simulation model brings forward that DDH-4 is located in a 3% FE area. This fact may also support the above pre-
sumptions.

A roof-shaped MF anomaly distribution is seen around Station No. 17. The anomaly does not coincide with the strong source of FE anomaly which is presumed from the model. Such an incoincidence is, in general, caused by the space variation in AR. Taking these facts into consideration, it might be concluded that the strong FE anomaly source slopes westwards. MF anomaly east of Station No. 24 is thought to be a false anomaly due to the low resistivity.

LINE M'

The central part of this line is occupied by the low AR, but the outer parts by the middle AR. The very low and low AR zones are situated over Stations No. 14 - 24. This fact implies that low-AR media, lower than 100 ohm-m, exist under the central part of this line. According to the geological survey over there, and comparing with the results from LINE M, we can identify the low-AR media with monzonitic rocks.

On the western tip of this line, an anomaly of 3 % FE or more is recognized. The possible shape of the anomalous source is roof-shaped, but the whole shape is not caught by the present surveys. On an average, the FE values on this line range from 2 to 3 %, low as compared with the FE values on LINE M. The anomalies are possibly continued from those on LINE M.

A high MF anomaly is found around Station No. 18. This is not corresponding to the FE anomaly because of the low AR.

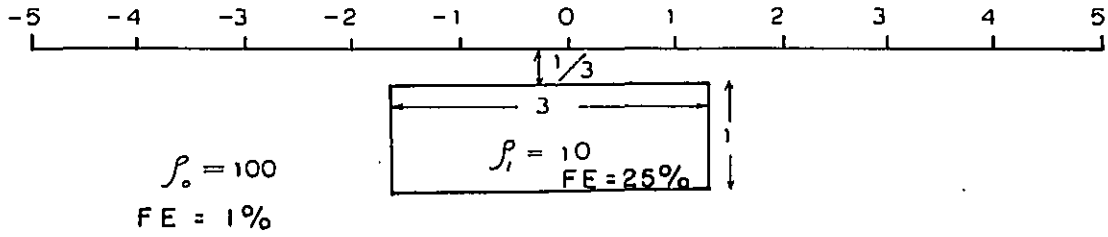
LINE N

The low AR zones around Stations No. 14 - 22 and east of Station No. 26 are presumed as an effect of monzonitic rock. The low and high AR zones west of Station No. 14 are continued from those on LINE M', which are presumed as an effect of dioritic rock.

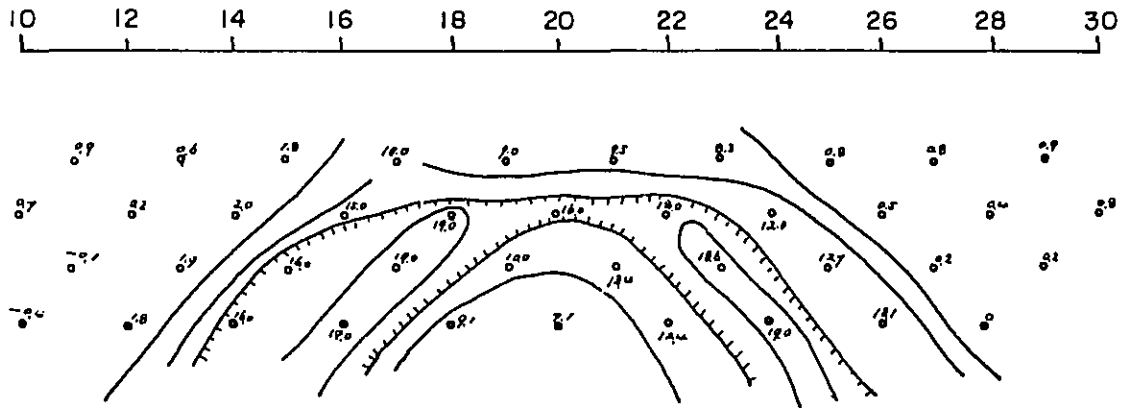
A roof-shaped low FE zone is symmetrically distributed around a middle-FE anomaly at Station No. 20. This distribution resembles that on LINE L' in type. The possible cause of such a distribution is a plate source, as seen in Fig. 2-12, a typical example of two-dimensional section

LINE-N (a=200m)

MODEL (Geoscience Model)



FE (Geoscience)



Field Data (FE)

LINE-N

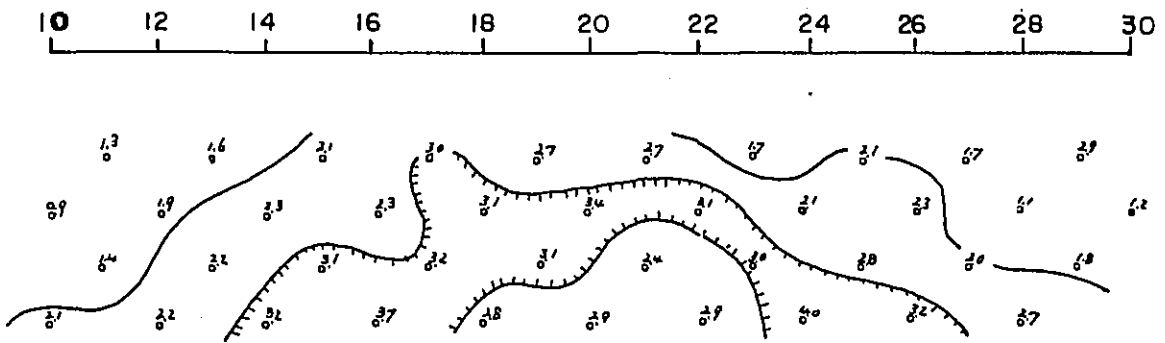


Fig 2-12

analysis. In contrast, the shape of FE sources is not clear in the cases of LINE M'. Meanwhile, the source forms a horizontal slab under LINE N, which is quite different from the structures under LINEs M and M'.

The MF anomaly here shows a roof-shaped pattern well coincident with the FE pattern. A false MF anomaly due to the low AR is found around Station No. 30.

LINE N'

The general aspect of this line is low and middle AR's. According to the geological survey results, the low AR around Stations No. 18 - 20 is presumed as monzonitic rock which is continued from LINE N.

FE anomaly has a roof-shaped pattern around Station No. 20. The source is regarded as a slab horizontally lying at a depth of 200 m below the surface. MF anomaly also has a roof-shaped pattern around Station No. 19, which well coincides with the FE anomaly pattern. The magnitude of the MF anomaly is somewhat small in comparison with that on LINE N.

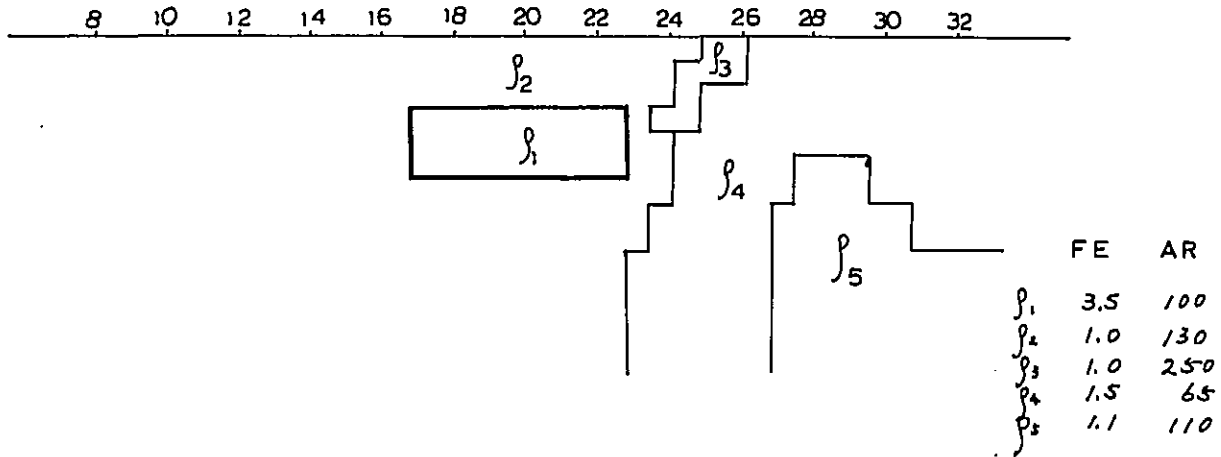
LINE O

Low, middle and high AR's occupy this line. Low AR zones around Station No. 18 and east of No. 28 are presumably caused by monzonitic rocks locally outcropped at Stations No. 18 and from No. 25 to 30. According to the ground geological survey and comparing with the standard curve for analysis, the high AR zone around Station No. 26 is possibly caused by a westwards sloping dioritic rock.

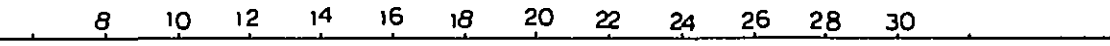
Although FE here, in general, is low, the anomaly is concentrated to a roof-shaped pattern around Station No. 20. As shown in Fig. 2-13, the

LINE-0 (a=200m)

Simulation Model



Field Data



Results of Simulation

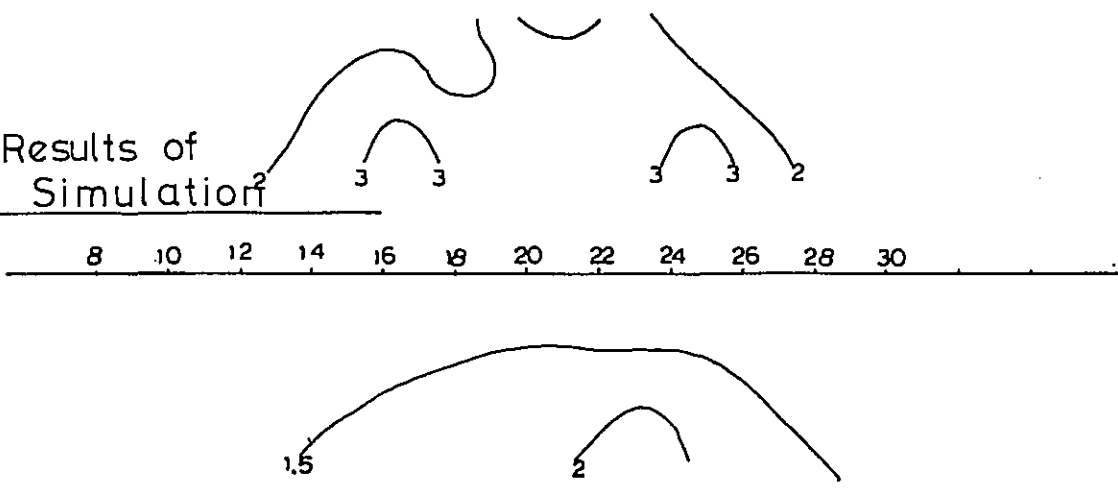


Fig. 2-13

model computation produces an underground structure such as plate source horizontally lying at a depth of about 200 m below the surface.

The associated MF pattern consists of low anomaly zones, concentrating around Station No. 20. Just like the case of LINE N', the MF anomaly is generally weak along this line. The MF anomaly found east of Station No. 26 is regarded as a false anomaly due to the low AR.

LINE O'

A middle AR occupies the main part of this line, but a low AR is found on the eastern tip. According to the model computation results, low AR structures occupy a part east of Station No. 25, while the western part consists of a middle AR structure. Judging from the ground geological survey results, the low AR is supposed to be caused by monzonitic rocks.

As shown in Fig. 2-14, the FE pattern is distributed around Station No. 20. It is concluded from the model computation results that a pillar-shaped high-FE anomaly source, surrounded with lower FE sources, is located at a depth of about 250 m under Station No. 20.

DDH-6 is located nearby Station No. 20. The assaying results show that the mean percentage of sulphide minerals amounts to 3.04 %, which is high as compared with core samples from the other drilling holes. The high FE anomaly on this line may be caused by such an abundance in sulphide minerals. Slab-shaped sources are presumed for the FE patterns of LINES N' and O, while a pillar-shaped source is presumed here. As a whole, the geological structure here may be fairly different from the areas along LINES N' and O.

LINE--O' (a = 200 m)

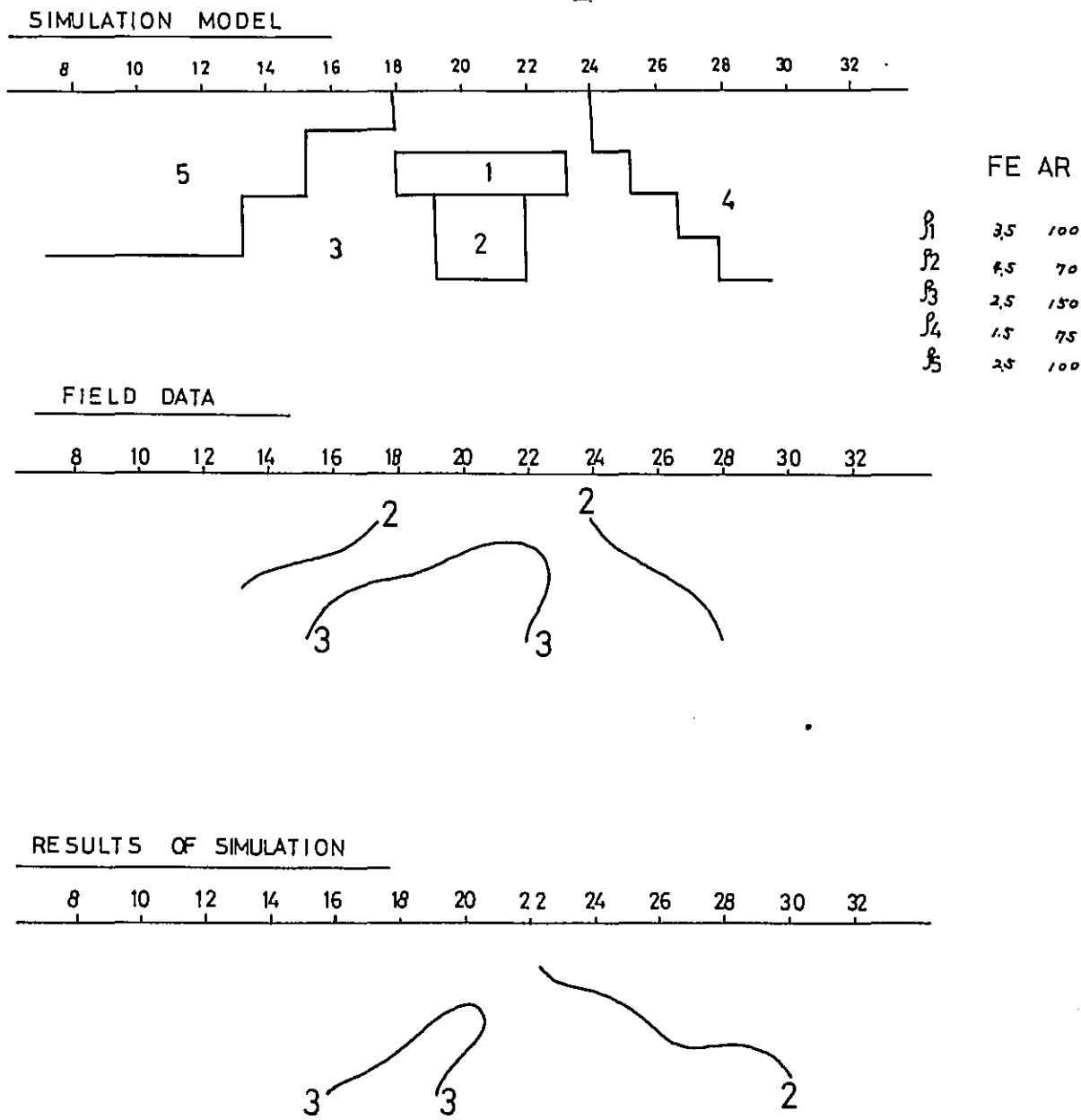


FIG 2-14

An MF anomaly around Station No. 20 well coincides with the associated FE anomaly. The amplitude of the MF anomaly is somewhat larger than that of LINE O.

LINE P

Generally speaking, LINE P consists of low and middle AR zones. According to the ground geological survey results, the low AR zone east of Station No. 22 corresponds to the monzonitic rock distribution, and the middle AR zone west of Station No. 20 to the outcrop of dioritic rocks.

A roof-shaped FE pattern, westwards gently sloping is seen around Station No. 20. An appropriate model for the pattern is an inclined pillar-shaped source, but the inclination angle is not explicitly obtained.

A small-scale anomaly is seen around Station No. 18. The amplitude of the anomaly is also small. MF values east of Station No. 24 show a false anomaly due to the low AR.

LINE Q

The AR values along LINE Q range from low to high. The low AR corresponds to monzonitic rocks. The middle and high AR's west of Station No. 20 correspond to dioritic rocks, similarly to the case of LINE P.

A low FE anomaly is found beneath Station No. 18. The associated source is presumed to be comparatively deep-seated.

MF anomalies here are also small-scale, similarly to the FE anomalies. The amplitude becomes so small that the anomalous zones continued from the above lines diminish here. There may not be any further extension of these zones.

3-4 Classification of IP Anomalies

From the above-mentioned results (3-2 and 3-3), the characteristics of the IP anomalies are summarized as follows:

Table 2-7 Characteristics of the IP Anomalies

Anomaly	FE value & shape of the source	AR	Depth below the surface	Geo-chemical indication	Continuation of the anomaly
A anomaly	5% or less. Almost pillar in shape	Low to very high. Complicated distribution.	From shallow to deep.	Partially coincident.	Continued from LINES A to I. The width is 1.5km at maximum. The northern and SSW extensions are supposed.
B anomaly	4% or less. Shape is not clear.	Middle. Sample distribution.	300 m or deeper.	Almost coincident.	Small-scale. Horizontal extension can not be expected.
C anomaly	5% or less. Pillar or plate in shape.	Ranging from very low to high. Simple distribution.	From shallow to deep.	"	Found in the central parts of LINES J'-P. Lengths of major and minor axes are 2.5km in the NS and 500 m in the EW directions, respectively, Caused by structures complicated in shape and depth.

As seen in the above table, the FE values of A, B and C anomaly zones resemble each other. But in contrast, the AR patterns and the shape of source are different. This fact may possibly indicate that these anomaly

zones are geologically independent and the geological history are different each other. We can conclude, according to the ground geological survey results (PL. II-5-1), that A anomaly is seen around volcanic and sedimentary rocks, meanwhile C anomaly mainly in volcanic areas. That is to say, the most possible cause of such a difference in IP anomaly is space variations in geological structure.

CHAPTER 4. SYNTHESSES

Since the area under survey presented less electric noise and showed better electrode grounding conditions, thereby making it possible to flow large quantities of electric current, the measurement was relatively stable in general and highly reliable results were obtained during the survey.

FE anomalies obtained by the survey are shown in the table below.

Table 2-8 Findings of Survey

Anomalous Zone	Measuring Line	Measuring Station	Estimated Depth of Head	Intensity of Anomaly	Estimated Shape of the Source of Anomaly
A	A	Near station 8 - near station 18	Crop out in the surface on measuring Line C.	Strong anomaly	Columnar
	B	Near station 10 - near station 22	Concealed head and within 300m directly under the surface.	" "	"
	C	Near station 8 - near station 20	"	" "	"
	C'	Near station 18 - westward	"	" "	"
	D	Same as above	"	" "	"
	D'	Near station 14 - near station 22	"	Weak anomaly	Unknown
	E	Near station 4 - near station 10	"	Strong anomaly	Columnar
	F	Near station 10 - westward	"	" "	"
	G	Same as above	"	" "	Unknown
	H	Near station 8 - westward	"	Weak anomaly	"
I	Near station 6 - westward	"	" "	"	
B	E	Near station 16 - near station 24	Within 300m directly under the surface	Weak anomaly	Unknown
	F	Near station 18 - near station 28	The extent of strong anomaly is assumed to be on the order of 300m in depth	Weak anomaly	Unknown
	G	Near station 18 - near station 28	"	" "	"
	H			None	
C	J	Near station 18 - near station 22	Within 300m directly under the surface	Strong anomaly	Unknown
	K	Near station 20 - near station 22	"	" "	Columnar
	K'	Near station 16 - near station 22	"	" "	"
	L	Near station 12 - near station 28	"	" "	"
	L'	Near station 16 - near station 22	"	" "	Tabular
	M	Near station 16 - near station 22	"	" "	Columnar
	M'	Near station 14 - near station 22	"	Weak anomaly	Unknown (Probably columnar)
	N	Near station 16 - near station 26	"	Medium anomaly	Tabular
	N'	Near station 18 - near station 22	"	" "	"
	O	Near station 18 - near station 24	"	Weak anomaly	"
	O'	Near station 16 - near station 24	"	Strong anomaly	Columnar
	P	Near station 16 - near station 24	"	Medium anomaly	"

What causes these FE anomalies is not known at this stage when the pilot drilling is not sufficiently provided yet.

1. A geological survey shows that monzonitic rock with a relatively high content of sulphide minerals exists in anomalous zone C and that the extent of anomalous zone C nearly matches the distribution of this monzonitic rock. The anomaly confirmed by geochemical prospecting also matches nearly the range of anomalous zone C.

2. From the fact that anomalous zones A and B are observed along the axis of anticline as determined by the geological survey and that there is likelihood of existence of intrusive rocks such as monzonitic rock under the ground near the axis, it can be assumed at this stage that the FE anomalies have a correlation with monzonitic rock. The facts that have been clarified and what could have been inferred from the IP Method employed for this survey are indicated below.

- 1) The main structure which is dominant in the Yauri district as determined by the airborne survey, geological survey, and gravity prospecting conducted in 1971 and 1972 has a NNW-SSE trend. With the use of IP Method in this survey, it has been determined that the alignment of anomalous zones A, B and C is nearly in N-S, NNW-SSE and NNW-SSE directions respectively in the survey area and for this reason, the distribution of anomalous zone is presumed to be influenced by the main structure which is dominant in this district.

- 2) According to the data obtained from the six pilot borings performed to date, the section with a high content of copper does not necessarily

correspond to the section with strong FE anomalies, which is the phenomenon often observed also in other areas. In fact, DDH-4 near Station 21 on LINE M, while showing an average 0.8 % copper mineralizing zone in the monzonitic rock extending from several meters below surface to a depth of about 100 m, is located in the weak anomalous zone.

In addition, DDH-3 near Station 26 on LINE K, while showing a skarn zone accompanied by an average 0.6 % copper mineralization extending from a depth of 80 m to a depth of 180 m, is located outside the range of FE anomalous zone. However, the analysis of sulphur content conducted on samples obtained from DDH-2 and DDH-6 located in the area with a high value of FE anomalies shows a relatively high content of sulphide minerals compared with other pilot boring locations. Therefore, the FE anomalies in this area is considered to be due to sulphide minerals.

3) Anomalous zone A is located almost in the center and toward the west on LINES A - I and has a distribution almost in N-S direction in the survey area with the maximum width being 1.5 km. This anomalous zone is presumed to extend further in the north and south-east directions. The shape of a majority of sources of anomaly belonging to this anomalous zone is presumed to be pillared in shape and the distribution of anomalous zone is also along the axis of anticline structure as determined by the geological survey. From a geological point of view, the axis of such anticline structure is considered to have intrusive rocks such as monzonitic rock. It is probable, therefore, that the intrusive rocks and the resultant alteration in the neighbouring area have been detected as the source of anomaly.

4) Anomalous zone B is observed near the center between LINEs E - G. Since this zone shows a distribution of anomalous value which suggests the existance of strong source of anomaly in the depth, the shape of the source of anomaly is not known definitely from the depth of the present prospecting in the survey Area.

As the distribution of this anomaly is also along the axis of anticline structure as in the case with anomalous zone A, this anomaly is considered to be due to the source of anomaly similar to that for anomalous zone A.

5) Anomalous zone C is located near the center between LINEs J - P in the south section of the survey area, and it has a width of about 500 m and a total length of about 2.5 km. Characteristics of anomalous zone C is that its shape and depth have a great variety as compared with anomalous zones A and B. It is also presumed that anomalous zone C has a more complicated subsurface structure than that of anomalous zones A and B.

Judging from the fact that the location of anomalous zone C nearly matches the distribution of monzonitic rock with a relatively strong mineralization and alteration as determined by the geological survey, this anomaly is probably indicating the existence of monzonitic rock and the alteration in the neighboring zone resulting from this monzonitic rock. Also from the fact that the anomaly determined by a geochemical prospecting corresponds well to anomalous zone C, the highest attention should be paid to anomalous zone C from the standpoint of prospecting copper mineralization. However, due consideration must also be given to the fact that the data obtained from pilot borings show that the intensity of FE anomaly and the

extent of copper mineralization do not necessarily have a positive relation between them and that anomalous zone C has a great variety of subsurface structure.

6) In view of the fact that no anomaly has been found other than in the previously mentioned anomalous zones A, B and C except the low FE values which could be compared to skarn zone near Station 38 at the east end of LINE J, it is considered advisable to concentrate the effort of future prospecting in this survey area on anomalous zones A, B and C, including surrounding areas and near Station 38 on LINE J.

PART III
DRILLING

PART III DRILLING

Chapter 1	Outline	III- 3
Chapter 2	Drilling Method and the Machine	III- 5
Chapter 3	Drilling Operation	III-10
3-1	Arrangement	III-10
3-2	Relocation of the Drill Site	III-11
3-3	Withdrawal	III-13
3-4	Coring Conditions and Mudwater Control	III-13
3-5	Excavation Progress	III-15

List of Tables

Table 3-1	Drilling Equipment and Consumed Materials	
	A. Model "TBS-5"	III - 6
	B. Supplies and Drill Parts Consumed	III - 8
Table 3-2	Moving Operations	III - 12
Table 3-3	Summary Record of Drilling Results (DDH-1)	III - 21
Table 3-4	- ditto - (DDH-2)	III - 22
Table 3-5	- ditto - (DDH-3)	III - 23
Table 3-6	- ditto - (DDH-4)	III - 24
Table 3-7	- ditto - (DDH-5)	III - 25
Table 3-8	- ditto - (DDH-6)	III - 26
Table 3-9	Generalized Results of Diamond Core Drilling	III - 27
Table 3-10	(1) Data of Drilling Works (DDH-1)	III - 28
Table 3-10	(2) - ditto - (DDH-2)	III - 29
Table 3-10	(3) - ditto - (DDH-3)	III - 30
Table 3-10	(4) - ditto - (DDH-4)	III - 31
Table 3-10	(5) - ditto - (DDH-5)	III - 32
Table 3-10	(6) - ditto - (DDH-6)	III - 33

Appendices (Drilling)

PL. III-1	Location Map of Drill-Hole of the Coroccohuayco-Huaccollo Area	
Annex 1	Specifications Diamond Bits and Reaming Shells	A - 99
Annex 2	Table Showing Drilling Progress (DDH-1)	A - 101
Annex 3	- ditto - (DDH-2)	A - 102
Annex 4	- ditto - (DDH-3)	A - 103
Annex 5	- ditto - (DDH-4)	A - 104
Annex 6	- ditto - (DDH-5)	A - 105
Annex 7	- ditto - (DDH-6)	A - 106

CHAPTER 1 OUTLINE

Drilling was conducted to investigate the geological conditions of the southern part (Yauri Area) of the Republic of Peru, from 19 October to 11 December, 1973. During this period 6 holes named as DDH-1 to DDH-6, having a combined length of 1,503.6 meters were drilled.

The work was performed by six Japanese drilling engineers, led by a manager. Also, a number of local workers, of the Yauri area, were employed under the cooperation of the Yauri Branch of the Government of Peru. Six crews consisting of 4 local workers each were organized from then, each led by a Japanese engineer. These crews worked in three shifts a day.

The main equipment, consisting of two TBS-5 drilling machines, pumps, rods, drilling tools, etc. were transported from Japan. The drilling was carried by a wire-line method, to improve the core recovery and the drilling efficiency.

Yauri area lies on a plateau, at an elevation of about 4,000 meters, in the Andes Mountains. Because the work was conducted in the season when winter was approaching with a wide variation in daily temperature, it was feared that the water for drilling operations might be frozen. Also, the rainy season was approaching, localized torrential downpours were felt to be encountered occasionally and difficulties were considered to be experienced in the transportation of necessary equipment and personnel.

Though natural conditions were severe, as mentioned above, the Japanese engineers and local employees overcame these difficulties in a very close cooperation, and completed the work nearly within the scheduled period.

The details of the drilling operations are described in the following chapters, and the results of the drilling are shown in the tables below.

Drill hole No.	October		November		December	
	10	20	10	20	10	20
DDH - 1			250.4 m			
DDH - 2				250.5 m		
DDH - 3		250.2 m				
DDH - 4			251.1 m			
DDH - 5				251.1 m	4 th	
DDH - 6					251.1 m	11 th

The drilling order of the holes by each machine was as follows:

No. 1 drilling machine: DDH-1, DDH-2 and DDH-6 3 holes

No. 2 drilling machine: DDH-3, DDH-4 and DDH-5 3 holes

The work was completed in 53 working days, and the average daily drilling depth achieved by one machine was about 14.2 m.

The average core recovery for 6 holes is nearly 100 %, which is an excellent result.

There were no labor problems during the period, and this fact greatly contributed to the shortening of the work schedule.

CHAPTER 2 DRILLING METHOD AND THE MACHINE

The principal part of the rockbeds in the investigated area consists of basic hybrid rocks, porphyritic intrusive rocks, limestone, quartzite and shale. The appearance of fracture and alteration zones were forecast in some parts of the rock strata, so in order to achieve the planned performance, the team used such drilling techniques as mud water method, with bentonite as the basic emulsion material; NQ and BQ wire line method, and NX and BX casing method, after considering the rock condition.

The thickness of the surface soil at DDH-1 and DDH-2 holes was about 40 meters, but at the holes in the southern area it was only about 7 meters.

For these reasons the following drilling procedures were employed. A 101 mm diameter metal bit (type HX) was used for the surface soil layer until the bit hit a hard rock zone, then it was replaced by an NQ diamond bit. At the same time the drilling method was changed to a wire line method, after inserting the NX and BX casing pipes into the drilled hole to stabilize the wall of the hole to improve the drilling efficiency.

The deepest portion of all the holes was drilled with a 60 mm diameter BQ bit. The core recovery for each holes was nearly 100 %, except for the surface soil. This is an excellent achievement.

The type and specification of the drilling machines and other drilling tools used, are listed in the following table.

Table 3-1 DRILLING EQUIPMENT AND CONSUMED MATERIALS

A. MODEL "TBS-5"

MODEL AND NAME		SPECIFICATIONS									
<p>DRILLING MACHINE</p> <p>MODEL, TBS-5 (TONE BORING CO.)</p>	<p>2 SETS</p>	<p>CAPACITY</p> <table border="1" data-bbox="922 432 1366 595"> <thead> <tr> <th data-bbox="922 432 1098 477">ROD SIZE</th> <th data-bbox="1098 432 1366 477">DEPTH (m)</th> </tr> </thead> <tbody> <tr> <td data-bbox="922 477 1098 510">A; AW</td> <td data-bbox="1098 477 1366 510">300</td> </tr> <tr> <td data-bbox="922 510 1098 544">B; BW</td> <td data-bbox="1098 510 1366 544">250</td> </tr> <tr> <td data-bbox="922 544 1098 589">N; NW</td> <td data-bbox="1098 544 1366 589">200</td> </tr> </tbody> </table>	ROD SIZE	DEPTH (m)	A; AW	300	B; BW	250	N; NW	200	<p>OVERALL NET MEASUREMENT; $H \times L \times W = 1,295 \text{ m/m} \times 1,630 \text{ M/M} \times 975 \text{ m/m}$</p> <p>WEIGHT LESS POWER UNIT 700 KG</p> <p>INNER DIA. OF SPINDLE; 80 m/m</p> <p>SPINDLE STROKE; 500 m/m</p> <p>HOIST; PRANETARY GEAR, BAND BRAKE, ROPE SPEED, B SERIES, 12, 24, 40, 58 M/Min</p> <p>MAX. HOISTING CAPACITY 1,500 kg</p> <p>OIL PUMP; TYPE, VARIABLE VOLUME VANE, CAPACITY, 1,800 RPM 0 ~ 26 L/min WARKING PRESURE, 10 ~ 30 kg/cm²; MAX WARKING PRESURE, 35 kg/cm²;</p> <p>POWER UNIT; DIESEL ENGINE, (MITSUBISHI HEAVY INDUSTRIES, LTD.) MODEL, KE-31 HORSE POWER, 2,000 RPM 30.5 P. S. MAX TORQUE, kgm/rpm 11/2, 200 ~ 2,400</p> <p>BORE AND STROKE 79.4 m/m 111.1 m/m</p>
ROD SIZE	DEPTH (m)										
A; AW	300										
B; BW	250										
N; NW	200										
<p>DRILLING PUMP</p> <p>MODEL; 535-RQ (NIPPON LONG YEAR)</p>	<p>2 SETS</p>	<p>OVERALL NET MEASUREMENT; $H \times L \times W = 900 \text{ M/M} \times 2,000 \text{ m/m} \times 1,000 \text{ m/m}$</p> <p>WEIGHT; LESS POWER UNIT 330 kg</p>									

A. (continued)

MODEL AND NAME		SPECIFICATIONS
MUD MIXER MODEL MCE-100A (TONE BORING CO.)	2 SETS	CYLINDER BORE AND STROKE; 70 m/m × 70 m/m DISPLACEMENT; 18 l/min' ~ 140 l/min POWER UNIT; DIESEL ENGINE (YANMER DIESEL CO.) MODEL F-7Y RELATED POWER; 2,000 RPM 7 ps TANK CAPACITY; 125 l EFFECTIVE CAPACITY; 100 l PROPELLER REVOLUTION; 800 ~ 1,000 RPM WEIGHT; LES POWER UNIT 110 kg POWER UNIT; DIESEL ENGINE (YANMER DIESEL CO.) MODEL F-4Y RELATED POWER; 2,000 RPM 4 ps
DERRICK	2 SETS	PIPE DERRICK; HEIGHT, 8.5 m MAX. LOAD CAPACITY; 3 t
GENERATOR MODEL NT-65K (YANMER DIESEL CO.)	1 SET	CAPACITY; 1 kva VOLTAGE; 100 v ELECTRIC CURRENT; 10A
DRILLING TOOLS		DRILL ROD NQ-3 m 60 pcs BQ-3m 120 pcs CASING PIPE NX-3m 20 pcs " 1.5m 10 " " 0.5m 10 " BX-3m 60 " " 1.5m 10 " " 0.5m 10 "
WIRE LINE HOIST		ATTACHED TO BORING MACHINE

B. SUPPLIES AND DRILL PARTS CONSUMED

DESCRIPTION	SPECIFICATIONS	UNITS	QUANTITY						TOTAL
			DDH-1	DDH-2	DDH-3	DDH-4	DDH-5	DDH-6	
LIGHT OIL		ℓ	1,600	2,590	1,520	2,000	1,370	1,530	10,610
MOBIL OIL	ENGINE	ℓ	45	46	77	74	51	45	338
MISSION OIL	GEAR	ℓ	21	27	40	10	15	7	120
TURBINE OIL	OIL PRESSURE	ℓ	25	10	30	10	20	15	110
SPINDLE OIL		ℓ	3	5	5	4	5	3	25
GREASE		kg	19	25	10	15	17	20	106
BENTONITE	25kg/Pack	pack	64	105	96	81	55	104	505
CARBOXY METHYL CELLULOSE		kg	16	30	8	5	10	14	83
METAL CROWN	101m/m	pc	2	3	2	2	1	2	12
SINGLE CORE TUBE	99m/m x 0.5m	set	1		1				2
DOUBLE CORE TUBE	NQ-WL	set	2	1	2	1		1	7
CORE TUBE HEAD	NQ-WL	pc	2	1	2	1	1	1	8
CORE TUBE HEAD	BQ-WL	pc	2	2	2	1	1	1	9
CASING METAL SHOE	NX	pc	1	1	1	1	1	1	6
CASING METAL SHOE	BX	pc	1	1	1	1	1	1	6
DIAMOND BIT	NQ	pc	3	1	2	3	3	5	17
DIAMOND BIT	BQ	pc	5	20	2	4	4	2	38
DIAMOND REAMER	NQ	ps	1	1	1	1	1	2	7
DIAMOND REAMER	BQ	ps	1	2	2	1	2	1	9
CEMENTE	50kg/pack	pack	3	3	2	2	2	3	15
RAG		kg	14	15	15	15	25	25	109
CORE BOX	NX	pc	9	7	23	16	22	34	111
CORE BOX	BX	pc	28	27	23	31	23	15	147
BOARD	30m/m	m ²	4		4				8
SQUARE TINBER		m ³	4		4				8
WIRE	# 10	kg	13	12	15	10	20		70
NAIL		kg	3	3	4	4	10		24
WIRE ROPE	12m/m x 20m	pc	1		1				2
WIRE ROPE	5m/m x 300m	pc	1		1				2

Table 3-1-B. (continued)

DESCRIPTION	SPECIFICATION	UNITS	QUANTITY						TOTAL
			DDH-1	DDH-2	DDH-3	DDH-4	DDH-5	DDH-6	
MANILA ROPE	15m/m x 30m	pc	1		1				2
PIPE WRENCH	900m/m	pc	2		2				4
PIPE WRENCH	600m/m	pc	2		2				4
PIPE WRENCH	450m/m	pc	2		2				4
CORE HAMMER DRIVER		pc	3	4	3	3	3	3	19
BALL BEARING		pc	2	1	1	1	2	3	10
HEAD SHEAVE		pc					1	1	2
CORE LIFTER		pc	4	4	4	4	4	4	24
CORE LIFTER CASE		pc	2	2	3	3	2	2	14
INNER TUBE		pc	2	2	2	2	2	2	12
OUTER TUBE		pc	2		2		1	1	6
V-PACKING		pc	12		12		12	12	48
PISTON ROD		pc		2		2			4
PISTON RUBBER		pc	4	4	4	4			16
VALVE SHEET		pc		8		8			16
CHUCK PEICE		pc	3		3		3	3	12
SUCTION HOSE	50m/m x 3m	pc	1		1			2	4
V-BELT	KE-31 Engines	pc		1		1			2
OIL ELEMENT	"		1	1	1	1	1	1	6
ELEMENT FUEL	"	pc	1	1	1	1	1	1	6
NEEDLE VALVE	F4Y Engine	set	1		1		1	1	4
INTAKE & EXH. VALVE	"	set		1		1			2
SUB & EXH. VALVE	"	set		1		1			2
DELIVERY VALVE	"	set	1	1	1	1			4
NEEDLE VALVE	NT-65K Engine	set	1	1	1	1			4
INTAKE & EXH. VALVE	"	set					1	1	2
SUB & EXH. VALVE	"	set	1		1				2
DELIVERY VALVE	"	set		1		1			2
PRESSURE GAUGE	80kg/cm ²	pc		1			1		2
SPEED METER		pc		1			1		2

CHAPTER 3 DRILLING OPERATIONS

3-1 Arrangement

The 6 Japanese engineers, led by a manager, made a courtesy call to the pertinent Yauri Government Offices to extend greetings, on 19 October, 1973. After this, they started preparatory works such as the reconnaissance of the survey area by jeep, employing local workers, the transportation of the equipment to the drilling sites and arranging the camp accommodations, etc.

The survey area is a comparatively flat plateau, with an altitude of about 4,000 meters. But, a transportation roads were constructed, using bulldozers, among the planned drill sites. Total length of these roads amount to about 14 kilometers.

By use of these roads, the drilling equipment was transported directly from site to site on 2 ton trucks, which greatly contributed to shorten the time for removal. For of the fieldworkers, three camp houses were constructed and used by the advanced team.

Water for drilling operations was obtained by constructing a water supply facility, of small brooks flowing through the pampa and aditch in a wet land. From this facility, water was distributed though pipes of 2"φ x 1,600 meter and 1"φ x 800 meter by utilizing the natural slope and water pumps.

3-2 Relocation of the Drill Site

Relocation of the equipment from a completed hole to another site was effected by small trucks. In using the constructed roads. This enabled the relocation completed in one day. The light and small drilling machines were beneficial for rapid relocation. The details of relocations between two sites are shown in the following table.

Table 3-2 MOVING OPERATIONS

ITEM	DRILL HOLE NO.	DDH-1		DDH-2		DDH-3		DDH-4		DDH-5		DDH-6		TOTAL	
		DAY	MAN DAY	DAY	MAN DAY	DAY	MAN DAY	DAY	MAN DAY	DAY	MAN DAY	DAY	MAN DAY		
MOVING OPERATION	IN	20TH OCT. 1973	8TH NOV. 1973	20TH OCT. 1973	7TH NOV. 1973	23RD NOV. 1973	29TH NOV. 1973								
	OUT	22ND OCT. 1973	8TH NOV. 1973	21ST OCT. 1973	7TH NOV. 1973	23RD NOV. 1973	29TH NOV. 1973								
		6TH NOV. 1973	27TH NOV. 1973	5TH NOV. 1973	21ST NOV. 1973	3RD DEC. 1973	10TH DEC. 1973								
		7TH NOV. 1973	28TH NOV. 1973	6TH NOV. 1973	22ND NOV. 1973	4TH DEC. 1973	11TH DEC. 1973								
PREPARATIONS	HAULAGE	0.5	7	0.5	5.5	0.5	5					0.5	6.5	2	24
	INSTALLATION	1.5	17	0.5	12	1.5	24	0.5	6	0.5	10.5	0.5	8	5	77.5
	TOTAL	2.0	24	1	17.5	2	29	0.5	6	0.5	10.5	1	14.5	7	101.5
	WATER PIPE	0.5	10	1	6	2	18	1.5	12	3	30	1	10	9	88
ACCESS ROAD		8	85	2	73	2	20	5	60	6	60	7	108	38	406
	TOTAL	8.5	95	11	81	4	38	6.5	72	9	90	8	118	47	494
REMOVAL	DISMANTLING	1.5	16.5	1.5	14.5	1.5	24	1.5	20	1.5	19.5	1.5	17.5	9	112
	TOTAL	1.5	16.5	1.5	14.5	1.5	24	1.5	20	1.5	19.5	1.5	17.5	9	112
	PIPE REMOVAL	0.5	10	1	8	0.5	4	0.5	6	0.5	5	1	12	4	45
	HAULAGE			1		12		0.5	12	0.5	16	0.5	18	2.5	58
ROAD REINSTATEMENT	0.5	5	2	24	1	10	2	20	2	14	4	56	11.5	129	
TOTAL	1	15	3	32	2.5	26	3	38	3	35	5.5	86	18	232	
GRAND TOTAL	13	150.5	16.5	145	10	117	11.5	136	14	155	16	236	81	939.5	

3-3 Withdrawal

The two "TBS-5" drilling machines simultaneously began drilling on 20, October. The No. 1 machine drilled three holes, DDH-1, DDH-2 and DDH-6, in total length of 752 meters and completed the drilling on 11, December. The No. 2 machine drilled holes DDH-3, DDH-4 and DDH-5, total length of which amounted to 751.6 meters and completed the drilling on 4, December.

Preparations for storing the casing pipe and the disassembly of the machine, the derrick, and the water supply facility of the last site for the No. 2 machine were done on 6, December, and those for the last site for the No. 1 machine were completed on 11, December. The cleared equipment was transported to Lima by trucks and stored.

3-4 Coring Conditions and Mud Water Control

DDH-1 and DDH-2 holes were found to have a thick surface soil layer. Generally the holes in the northern area had a thick soil layer and those in the southern area had a thin soil layer. The thickness of the soil layer for each hole was as follows:

DDH-1 : 43.4 meters	DDH-4 : 6.0 meters
DDH-2 : 41.5 meters	DDH-5 : 7.5 meters
DDH-3 : 3.0 meters	DDH-6 : 6.8 meters

After the bit cut through the soil layer it reached comparatively homogeneous and stable dioritic and monzonitic rock zones. Accordingly, the drilling could attain as good performance as planned.

Drilling was started using a 101 mm ϕ (HX) bit and continued to as deep as possible with this bit, using mud water. Then NX casing pipes were inserted in the hole, and the NQ wire line method was used in place of the HX drill. BX casing were inserted in the hole drilled by the NQ method, and the drilling was continued.

The insertion depth of BX casing pipes for DDH-1 and DDH-2 holes, having a thick surface soil layer, become 70 to 80 meters. This result was obtained by using the mud water method, especially of it use of bentonite.

The core recovery of about 100 % was achieved chiefly by the use of wire line drilling method. The core recovery of each hole, excluding the surface soil layer, was as follows:

DDH-1 : 100 %	DDH-4 : 100 %
DDH-2 : 100 %	DDH-5 : 99.9 %
DDH-3 : 100 %	DDH-6 : 100 %

The collected core samples were accomodated in the plastic core boxes. The number of core boxes required for each drilling method is 111 in the NQ method and 147 in the BQ method.

The mud water was made by mixing bentonite as the principal emulsion material and carboxyl-methyle cellulose (CMC) as the additive. The pulp density and viscosity of the mud water were maintained by preventing the solidification of the fluid, using a mixer (Type MCE 100A) manufactured by Tone Boring Machine Co., Ltd. of Japan.

The amount of the materials consumed at each hole is as follows:

DDH-1 : Bentonite	1,600 kg	CMC	16 kg
DDH-2 : Bentonite	2,625 kg	CMC	30 kg
DDH-3 : Bentonite	2,400 kg	CMC	8 kg
DDH-4 : Bentonite	2,025 kg	CMC	5 kg
DDH-5 : Bentonite	1,375 kg	CMC	10 kg
DDH-6 : Bentonite	2,600 kg	CMC	14 kg
Total amount of bentonite:			12,625 kg
Amount of bentonite used per meter:			8.4 kg
Total amount of CMC:			83 kg
Amount of CMC used per meter:			0.055 kg

The performances achieved by one shift are shown in Table 3-8, which shows that the maximum rate is 10.69 m, the minimum, 5.83 m and the average 7.63 m.

3-5 Excavation Progress

The excavation operation for each hole is as follows:

3-5-1 DDH-1 Hole

Drilled depth: 250.4 meters Core recovery: 83 %

Starting date: 20 October Completion date: 6 November

On 20 October, 1973, the drilling machine and an 8.5 m high derrick were installed. On 21 October a water distribution piping of 1"φ x 200 m was laid and the cement work for the hole mouth was done. Drilling started on 22 October. We had forecasted beforehand that the thickness of the soil layer would be about 10 meters before starting the drilling, so

we used a 100 mm metal bit for the shallowest portion. In actual drilling, we found that the gravel mixed soil was far thicker than we had expected. We could finally reach the hard rock bed after drilling the surface soil layer for 43.3 meters. The hard rock bed changed to monzonitic rock after drilling 128 meters. Though we encountered water at a depth of about 195 meters, we did not encounter any further abnormality. We continued drilling with a BQ wire line bit, and on 6 November we stopped drilling at a depth of 250.4 meters. The monzonite rock bed continued to the bottom of the hole after the depth of 128 meters.

Because this was the first hole encountering a thick soil layer, we started drilling after making careful preparation. We proceeded drilling, protecting the hole wall with casing, pipes using a mud water method under NQ and BQ wire line drilling. In completing the drilling of the 43 m thick soil layer, we used the casings pipes of only 4.5 meters in NX size and 78 meters in BX size. Accordingly, the special mud water drilling, using bentonite as the basic suspension material, can be said to be successful.

We collected 9 boxes of NQ core samples and 28 boxes of BQ core samples.

3-5-2 DDH-2 Hole

Drilled depth: 250.5 m Core recovery: 100 %

Starting date: 8 November Completion date: 27 November

A 400 m pumping the of 2" diameter and a water tank of 3m x 4m x 1m were prepared for water storage. However, water supply was often

insufficient for our requirements.

By 101 mm NQ wire line method, drilling started on 9 November. Like the DDH-1 hole, there was a thick surface soil, and finally at 41.5m dioritic rock was found.

At around 63 m it turned into shale, and at 99 m quartzite emerged. All 111 m shale came again, at 131 m monzonite, and after around 140 m lay a hard dike. Shale was found again at 164 m, then after 192 m to the hole-bottom quartzite was present.

The length of NX casing pipe used was 22.5 m, and the BX casing pipe 70 m. Core samples of 7 boxes of NQ size and 27 boxes of BQ size were recovered.

3-5-3 DDH-3 Hole

Drilled depth: 250.2 m Core recovery: 100 %

Starting date: 22 October Completion date: 5 November .

Drilling was started with a 101 mm bit. Here the surface soil were extremely thin, and at only 3 m in depth the first rock, diorite, was found. Then at 79.7 m came a skarn of about 2 m thickness. Then thin layers of dioritic rock and shale. And at around 94 m limestone appeared.

This raised some anxiety about such disturbances as anomalous in and out flow of the drilling water. To prevent accidents, caused by such disturbance, we inserted BX casing pipes immediately.

After about 119 m, the lithology became skarnized limestone, whose thickness was confirmed to be about 66 m. From 185.3 m to the final depth it was a series of monzonitic rocks.

A NX casing pipe of 6.1 m and BX casing pipes of 107 m were used. Core samples of 23 boxes of NQ size and 23 boxes of BQ size were recovered.

3-5-4 DDH-4 Hole

Drilled depth: 250.3 m Core recovery: 100 %

Starting date: 7 November Completion date: 21 November

In installing the machinery, a trouble was found in the drilling pump engine, and it was replaced by a Yanmar Diesel "F-7Y" immediately.

The surface soil was only 6 m thick. After that there was no significant change in lithology; that is, there were a series of dioritic rocks all the way to the bottom of the hole.

At around 108 m, the drilling wall collapsed for a while. But by readjusting the viscosity, we could continue drilling without further accident.

The achievements in the already-mentioned four holes gave us confidence in the NQ and BQ wire lines. As a result, a systematic drilling method, with a fairly stable timing of casing insertion, could be established.

Also, various results were obtained in the mixing ratio of bentonite and CMC. Further, it was realized that serious accidents could be prevented with a careful observation on the changes in the air and water temperatures.

The insertion depth of NX casing pipe was 10.5 m and 79 m for the BX pipe. The core recovered amounted to 16 NQ boxes and 31 BQ boxes.

3-5-5 DDH-5 Hole

Drilled depth: 251 m Core recovery: 99.9 %

Starting date: 23 November Completion date: 6 December

This drilling, too, found a shallow soil of only 8 m. Below this depth, there lay a series of dioritic rocks, without notable lithological changes down to the bottom of the hole.

The drilling method was composed of typical casing insertion, mud water circulation, in which NX casing was inserted 9 m from the surface, and BX casing at 105 m.

As for the bit, a 101 mm metal bit was used for the initial drilling, and then the NZ and BQ wire line bits were used successively.

In this hole, the drilling speed showed the maximum value; namely, 10 m per work shift. This may be attributed to the improved skill of the workers in drilling operations and to a relatively stable lithology at the location.

The core recovered amounted to 22 NQ boxes and 23 BQ boxes.

In addition, rainy days increased in late November, and on 29 November there was a torrential rain, which delayed transportation of materials due to the road damage.

3-5-6 DDH-6 Hole

Drilled depth: 251.1 m Core recovery: 100 %

Starting date: 29 November Completion date: 10 December

Rock appeared at a depth of 6.8 m from the surface. Like the DDH-4 and DDH-5 holes, the lithology was a succession of dioritic rocks

all the way to the final depth.

As a result of these 6 hole drillings, it was ascertained that the surface soil of this area is about 7 to 8 m thick in average.

The drilling, the same as the previous ones, showed smooth performance with the 101 mm metal bit for the initial drilling and with the NQ and BQ wire line bit for the residual drilling.

NX casing pipe was inserted at 6.5 m, and BX casing pipe at 163 m. The core recovered amounted to 34 NQ boxes and 15 BQ boxes.

The cores taken from the 6 holes amounted to 111 NQ boxes and 147 BQ boxes. They were carefully sorted and their analytical data collected. Then they were stored in a warehouse.

Cement used for each hole was only 2 to 3 bags (100 to 150 kg), because it was used only for fixing of the hole mouth. None was used for repair measures for troubles in the holes.

The drilling results of each hole are shown in Table 3-2, 3-3, 3-4, 3-5, 3-6 and 3-7, respectively, and their performances are shown in Table 3-8.

SUMMARY RECORD OF DRILLING RESULTS

Table 3-3 DDH-1

DRILLING PERIODS	PERIODS				NUMBER OF DAYS	ACTUAL WORKING DAYS	DAY OFF	TOTAL NUMBER OF WORKERS		
	PREPARATION	20 TH OCT. 1973 - 22 ND OCT. 1973			2.5	2.5		34		
	DRILLING	22 ND OCT. 1973 - 6 TH NOV. 1973			15.0	12.0	3	179		
	REMOVING	6 TH NOV. 1973 - 7 TH NOV. 1973			1.5	1.5		16.5		
	TOTAL	20 TH OCT. 1973 - 7 TH NOV. 1973			19.0	16.0	3	229.5		
DRILLING LENGTH	PLANNED LENGTH	250.00 ^m			CORE RECOVERY FOR EACH 100M SECTION					
	INCREASE OR DECREASE IN LENGTH	0.40 ^m	CORE LENGTH	207.00 ^m	DEPTH OF HOLE	SECTION	TO-TAL	DEPTH OF HOLE	SECTION	TO-TAL
	LENGTH DRILLED	250.40 ^m	CORE RECOVERY	100% (83)	0 - 100 ^m	59%	59%			
WORKING TIME	DRILLING	120°50'	50.8%	45.3%	100 - 200 ^m	100%	78%			
	HOISTING & LOWERING, ROD	16°15'	6.8%	6.1%	200 - 250.40	100%	83%			
	HOISTING & LOWERING I. T.	38°15'	16.1%	14.3%		%	%			
	MISCELLANEOUS	28°00'	11.8%	10.5%	EFFICIENCY OF DRILLING					
	REPAIRING	1°20'	0.6%	0.5%	250.40m/WORK PERIOD			13.2 ^m /DAY		
	OTHERS	33°00'	13.9%	12.3%	250.40m/WORKING DAYS			15.7 ^m /DAY		
	TOTAL	237°40'	100%	%	250.40m/DRILLING PERIOD			16.7m/DAY		
RE-MOVING	PREPARATION	19°50'		7.5%	250.40m/ ^{NET} DRILLING DAYS			20.9m/DAY		
	MOVING	10°00'		3.5%						
CASING PIPE INSERTED	G. TOTAL		29°50'		100%	TOTAL WORKERS/250.40		0.92 SHIFT		
	PIPE SIZE & METERAGE	INSERTED LENGTH DRILLING LENGTH (%)		RECOVERY CASING PIPE	TOTAL DRILLING WORKERS/250.40			0.71 SHIFT		
	NX 4.50	1.8%		100%						
		%		%	HOISTING & LOWERING 10 TIMES		HOISTING & LOWERING I. T. 152 TIMES			
	BX 78.00	31.2%		100%	REMARKS					

SUMMARY RECORD OF DRILLING RESULTS

Table 3-4 DDH-2

DRILLING PERIODS	PERIODS			NUMBER OF DAYS	ACTUAL WORKING DAYS	DAY OFF	TOTAL NUMBER OF WORKERS			
	PREPARATION	8 TH NOV. 1973 - 8 TH NOV. 1973			1.0	1.0		17.5		
DRILLING	9 TH NOV. 1973 - 27 TH NOV. 1973			18.5	15.5	3.0	187.0			
REMOVING	27 TH NOV. 1973 - 28 TH NOV. 1973			1.5	1.5		14.5			
TOTAL	8 TH NOV. 1973 - 28 TH NOV. 1973			21.0	18.0	3.0	219.0			
DRILLING LENGTH	PLANNED LENGTH	260.00 ^m			CORE RECOVERY FOR EACH 100M SECTION					
	INCREASE OR DECREASE IN LENGTH	0.50 ^m	CORE LENGTH	209.00 ^m	DEPTH OF HOLE	SECTION	TO-TAL	DEPTH OF HOLE	SECTION	TO-TAL
	LENGTH DRILLED	250.50 ^m	CORE RECOVERY	100% (83.4)	0 - 100 ^m	59.3%	59.3%			
WORKING TIME	DRILLING	158*10'	43.8%	41.7%	100 - 200 ^m	100%	79.5%			
	HOISTING & LOWERING ROD	57*30'	15.9%	15.2%	200 - 250.50 ^m	100%	83.4%			
	HOISTING & LOWERING I. T.	61*40'	17.1%	16.3%		%	%			
	MISCELLANEOUS	35*30'	9.8%	9.4%	EFFICIENCY OF DRILLING					
	REPAIRING	3*10'	0.9%	0.8%	250.50m/WORK PERIOD			11.9m/DAY		
	OTHERS	45*00'	12.5%	11.9%	250.50m/WORKING DAYS			13.9m/DAY		
	TOTAL	361*00'	100%	%	250.50m/DRILLING PERIOD			13.5m/DAY		
RE-MOVING	PREPARATION	7*00'		1.8%	250.50m/NET DRILLING DAYS			16.2m/DAY		
	MOVING	11*00'		2.9%						
	G. TOTAL	379.00'		100%	TOTAL WORKERS/250.50			0.87 SHIFT		
CASING PIPE INSERTED	PIPE SIZE & METERAGE	INSERTED LENGTH DRILLING %	RECOVERY CASING PIPE	TOTAL DRILLING WORKERS/250.50			0.75 SHIFT			
	NX 22.50 ^m	9.8%	100%							
		%	%	HOISTING & LOWERING 30 TIMES		HOISTING & LOWERING I. T. 264 TIMES				
	BX 70.00 ^m	27.9%	100%	REMARKS						

SUMMARY RECORD OF DRILLING RESULTS

Table 3-5 DDH-3

DRILLING PERIODS	PERIODS				NUMBER OF DAYS	ACTUAL WORKING DAYS	PAY OFF	TOTAL NUMBER OF WORKERS				
	PREPARATION	20 TH OCT. 1973 - 21 ST OCT. 1973							2	2		29
	DRILLING	22 ND OCT. 1973 - 5 TH NOV. 1973							14.5	11.5	3	140
	REMOVING	5 TH NOV. 1973 - 6 TH NOV. 1973							1.5	1.5		24
	TOTAL	20 TH OCT. 1973 - 6 TH NOV. 1973							18	15	3	193
DRILLING LENGTH	PLANNED LENGTH	250.00 ^m			CORE RECOVERY FOR EACH 100M SECTION							
	INCREASE OR DECREASE IN LENGTH	0.20 ^m	CORE LENGTH	247.20 ^m	DEPTH OF HOLE	SECTION	TO-TAL	DEPTH OF HOLE	SECTION	TO-TAL		
	LENGTH DRILLED	250.20 ^m	CORE RECOVERY	100% (98.8)	0 - 100 ^m	97%	97%					
WORKING TIME	DRILLING	94°40'	43.4%	39.0%	100 - 200 ^m	100%	98%					
	HOISTING & LOWERING, ROD	10°20'	4.8%	4.3%	200 - 250.20 ^m	100%	98.8%					
	HOISTING & LOWERING, I. T.	49°20'	22.6%	20.3%		%	%					
	MISCELLANEOUS	28°20'	13.0%	11.7%	EFFICIENCY OF DRILLING							
	REPAIRING	5°30'	2.5%	2.3%	250.20m/WORK PERIOD			13.9m/DAY				
	OTHERS	29°50'	13.7%	12.3%	250.20m/WORKING DAYS			16.7m/DAY				
	TOTAL	218°00'	100%	%	250.20m/DRILLING PERIOD			17.3m/DAY				
	RE-MOVING	PREPARATION	14°00'		5.8%	250.20m/NET DRILLING DAYS			21.8m/DAY			
		MOVING	10°30'		4.3%							
	G. TOTAL	24°30'		100%	TOTAL WORKERS/250.20			0.77 SHIFT				
CASING PIPE INSERTED	PIPE SIZE & METERAGE	INSERTED LENGTH DRILLING % LENGTH	RECOVERY CASING PIPE	TOTAL DRILLING WORKERS/250.20			0.56 SHIFT					
	NX 6.10 ^m	2.4%	100%									
		%	%	HOISTING & LOWERING	9	HOISTING & LOWERING I. T.	187					
	BX 107.00 ^m	42.8%	100%	REMARKS								

SUMMARY RECORD OF DRILLING RESULTS

Table 3-6 DDH-4

DRILLING PERIODS	PERIODS				NUMBER OF DAYS	ACTUAL WORKING DAYS	PAY OFF	TOTAL NUMBER OF WORKERS				
	PREPARATION	7 TH NOV. 1973 - 7 TH NOV. 1973				0.5	0.5		6.0			
	DRILLING	7 TH NOV. 1973 - 21 ST NOV. 1973				14.0	12.0	2.0	141.0			
	REMOVING	21 ST NOV. 1973 - 22 ND NOV. 1973				1.5	1.5		20.0			
	TOTAL	7 TH NOV. 1973 - 22 ND NOV. 1973				16.0	14.0	2.0	167.0			
DRILLING LENGTH	PLANNED LENGTH	250.00 ^m			CORE RECOVERY FOR EACH 100M SECTION							
	INCREASE OR DECREASE IN LENGTH	0.30 ^m	CORE LENGTH	244.30 ^m	DEPTH OF HOLE	SECTION	TO-TAL	DEPTH OF HOLE	SECTION	TO-TAL		
	LENGTH DRILLED	250.30 ^m	CORE RECOVERY	100% (97)	0 - 100 ^m	95%	95%					
WORKING TIME	DRILLING	106°40'	41.3%	39.2%	100 - 200m	100%	96%					
	HOISTING & LOWERING, ROD	22°40'	8.8%	8.3%	200 - 250.30 ^m	100%	97%					
	HOISTING & LOWERING, I. T.	59°30'	23.0%	21.9%		%	%					
	MISCELLANEOUS	30°40'	11.9%	11.3%	EFFICIENCY OF DRILLING							
	REPAIRING	4°50'	1.9%	1.8%	250.30m/WORK PERIOD			15.6m/DAY				
	OTHERS	34°00'	13.1%	12.5%	250.30m/WORKING DAYS			17.9m/DAY				
	TOTAL	258°20'	100%	%	250.30m/DRILLING PERIOD			17.9m/DAY				
	REMOVING	PREPARATION	5°00'		1.8%	250.30m/ ^{NET} DRILLING DAYS			20.9m/DAY			
		MOVING	8°40'		3.2%							
	G. TOTAL	272°00'			100%	TOTAL WORKERS/250.30m			0.67 SHIFT			
CASING PIPE INSERTED	PIPE SIZE & METERAGE	INSERTED LENGTH DRILLING % LENGTH		RECOVERY CASING PIPE	TOTAL DRILLING WORKERS/250.30m			0.56 SHIFT				
	NX 10.50m	4.2 %		100%								
					HOISTING & 14 LOWERING TIMES			HOISTING & 199 LOWERING I.T. TIMES				
	BX 79.00m	31.6%		100%	REMARKS							

SUMMARY RECORD OF DRILLING RESULTS

Table 3-7 DDH-5

DRILLING PERIODS	PERIODS			NUMBER OF DAYS	ACTUAL WORKING DAYS	PAY OFF	TOTAL NUMBER OF WORKERS				
	PREPARATION	23 RD NOV. 1973 - 23 RD NOV. 1973			0.5	0.5		10.5			
	DRILLING	23 RD NOV. 1973 - 3 RD DEC. 1973			10.0	9.0	1.0	104.5			
	REMOVING	3 RD DEC. 1973 - 4 TH DEC. 1973			1.5	1.5		19.5			
	TOTAL	23 RD NOV. 1973 - 4 TH DEC. 1973			12.0	11.0	1.0	134.5			
DRILLING LENGTH	PLANNED LENGTH	250.00 ^m			CORE RECOVERY FOR EACH 100M SECTION						
	INCREASE OR DECREASE IN LENGTH	1.10 ^m	CORE LENGTH	243.10 ^m	DEPTH OF HOLE	SECTION	TO-TAL	DEPTH OF HOLE	SECTION	TO-TAL	
	LENGTH DRILLED	251.10 ^m	CORE RECOVERY	99.9% (97)	0 - 100 ^m	92%	92%				
WORKING TIME	DRILLING	87° 10'	49.7%	45.9%	100 - 200 ^m	100%	96%				
	HOISTING & LOWERING, ROD	7° 50'	4.6%	4.1%	200 - 251.10 ^m	100%	97%				
	HOISTING & LOWERING, I. T.	39° 10'	22.4%	20.6%		%	%				
	MISCELLANEOUS	26° 10'	15.0%	13.8%	EFFICIENCY OF DRILLING						
	REPAIRING	7° 10'	4.1%	3.8%	251.10m/WORK PERIOD			20.9m/DAY			
	OTHERS	7° 30'	4.2%	3.9%	251.10m/WORKING DAYS			22.8m/DAY			
	TOTAL	175° 00'	100%	%	251.10m/DRILLING PERIOD			25.1m/DAY			
CASING PIPE INSERTED	RE-MOVING	PREPARATION	5° 00'		2.6%	251.10m/NET DRILLING DAYS			27.9m/DAY		
		MOVING	10° 00'		5.3%						
	C. TOTAL		190° 00'		100%	TOTAL WORKERS/251.10m			0.54 SHIFT		
	PIPE SIZE & METERAGE		INSERTED LENGTH DRILLING LENGTH	RECOVERY CASING PIPE		TOTAL DRILLING WORKERS/251.10m			0.42 SHIFT		
	NX	9.00m	3.6%	100%							
		%	%		HOISTING & LOWERING TIMES			7 HOISTING & LOWERING I. T. TIMES			
BX	105.00m	41.8%	100%		REMARKS						

SUMMARY RECORD OF DRILLING RESULTS

Table 3-8 DDH-6

DRILLING PERIODS	PERIODS			NUMBER OF DAYS	ACTUAL WORKING DAYS	PAY OFF	TOTAL NUMBER OF WORKERS			
	PREPARATION	29 TH NOV. 1973 - 29 TH NOV. 1973			1	1		14.5		
	DRILLING	30 TH NOV. 1973 - 10 TH DEC. 1973			10.5	8.5	2	107.5		
	REMOVING	10 TH DEC. 1973 - 11 ST DEC. 1973			1.5	1.5		17.5		
	TOTAL	29 TH NOV. 1973 - 11 ST DEC. 1973			13	11	2	139.5		
DRILLING LENGTH	PLANNED LENGTH	250.00 ^m			CORE RECOVERY FOR EACH 100M SECTION					
	INCREASE OR DECREASE IN LENGTH	1.10 ^m	CORE LENGTH	251.10 ^m	DEPTH OF HOLE	SECTION	TO-TAL	DEPTH OF HOLE	SECTION	TO-TAL
	LENGTH DRILLED	251.10 ^m	CORE RECOVERY	100%	0 - 100 ^m	100%	100%			
WORKING TIME	DRILLING	96°20'	47.6%	44.5%	100 - 200 ^m	100%	100%			
	HOISTING & LOWERING, ROD	9°30'	4.7%	4.4%	200 - 251.10 ^m	100%	100%			
	HOISTING & LOWERING, I. T.	40°40'	20.1%	18.7%		%	%			
	MISCELLANEOUS	28°50'	14.3%	13.5%	EFFICIENCY OF DRILLING					
	REPAIRING		%	%	251.10m/WORK PERIOD			19.32m/DAY		
	OTHERS	27°00'	13.3%	12.7%	251.10m/WORKING DAYS			22.82m/DAY		
	TOTAL	202°20'	100%	%	251.10m/DRILLING PERIOD			23.91m/DAY		
RE-MOVING	PREPARATION	7°00''		3.2%	251.10m/ ^{NET} DRILLING DAYS			29.54m/DAY		
	MOVING	6°40'		3.0%						
	G. TOTAL	216°00'		100%	TOTAL WORKERS/251.10 ^m			0.56 SHIFT		
CASING PIPE INSERTED	PIPE SIZE & METERAGE	INSERTED LENGTH DRILLING % LENGTH		RECOVERY CASING PIPE	TOTAL DRILLING WORKERS/251.10 ^m			0.43 SHIFT		
	NX 6.50 ^m	2.6%		100%						
		%		%	HOISTING & 11 LOWERING TIMES			HOISTING & 189 LOWERING I.T. TIMES		
	BX 163.00 ^m	64.9%		100%	REMARKS					

GENERALIZED RESULTS OF DIAMOND CORE DRILLING

Table 3-9

DRILL HOLE NO.	TYPE OF MACHINE	DRILLING PERIOD	DRILLED LENGTH	CORE		NUMBER OF DRILLINGSHIFT			DRILLING SPEED		
				LENGTH	RE-COVERY	DRILLING SHIFT	CASING, ETC.	TOTAL SHIFT	* m/SHIFT	** m/SHIFT	
			m	m	%						
D.D.H-1	TBS-5	COM. OCT. 20, 1973 FIN. NOV. 7, 1973	250.40	(soil=43.40) 207.00	100 (83)	28	5	33	7.59	8.94	
D.D.H-2	TBS-5	COM. NOV. 8, 1973 FIN. NOV. 28, 1973	250.50	(soil=41.50) 209.00	100 (83.4)	43	4	47	5.33	5.84	
D.D.H-3	TBS-5	COM. OCT. 20, 1973 FIN. NOV. 6, 1973	250.20	(soil=3.00) 247.20	100 (98.8)	25	5	30	8.34	10.01	
D.D.H-4	TBS-5	COM. NOV. 7, 1973 FIN. NOV. 22, 1973	250.30	(soil=6.00) 244.30	100 (97)	30.5	3.5	34	7.36	8.21	
D.D.H-5	TBS-5	COM. NOV. 23, 1973 FIN. DEC. 4, 1973	251.10	(soil=7.50) 243.10	99.9 (97)	23	3	26	9.66	10.92	
D.D.H-6	TBS-5	COM. NOV. 29, 1973 FIN. DEC. 11, 1973	251.10	(soil=6.80) 251.10	100 (100)	23.5	3.5	27	9.30	10.69	
TOTAL	6 HOLE	COM. OCT. 20, 1973 FIN. DEC. 11, 1973	1,503.60	1,401.70	100	173	24	197	8.69	7.63	

NOTES: COM : Commenced FIN : Finished

* Drilled length per one shift covering total works conducted.

** Drilled length per one shift covering net drilling operations.

DATA OF DRILLING WORKS

Table 3-10 (1), D.D.H. -1

WORKING TIME & EFFICIENCY DEP- TH OF SECTION	DRILLING		HOISTING & LOWERING ROD		HOISTING & LOWERING I. TUBE		MISCELLANEOUS		REPAIRING		OTHERS		TOTAL		WORKERS TOTAL NUMB- ER OF WORK- ERS	CALCULA- TION PERIOD M	
	WOR- KING TIME	TIME/M KING TIME	WOR- KING TIME	TIME/M KING TIME	WOR- KING TIME	TIME/M KING TIME	WOR- KING TIME	TIME/M KING TIME	WOR- KING TIME	TIME/M KING TIME	WOR- KING TIME	TIME/M KING TIME	WOR- KING TIME	TIME/M KING TIME			
0 - 50	25°30'	0°29'	3°50'	0°04'	1°10'	0°01'	5°10'	0°06'	1°00'	0°01'	8°00'	0°09'	44°40'	0°50'	50	0.94	0 - 53.40
50 - 100	28°00'	0.32'	3°35'	0°04'	7°05'	0°08'	10°10'	0°12'	20'	0°00'4"	7°00'	0°08'	56°10'	1°03'	51.5	0.99	53.40 - 106.6
100 - 150	25°50'	0°31'	1°30'	0°02'	9°10'	0°11'	3°30'	0°04'			6°00'	0°07'	46°00'	0°55'	28.5	0.57	106.60 - 156.50
150 - 200	20°50'	0°29'	3°50'	0°05'	9°10'	0°13'	3°00'	0°04'			6°00'	0°08'	42°50'	0°59'	22.5	0.52	156.50 - 200.00
200 - 250	20°40'	0°25'	3°30'	0°04'	11°40'	0°14'	6°10'	0°07'			5°00'	0°06'	47°00'	0°56'	30.5	0.61	200.00 - 250.4
TOTAL	120°50'	0°29'	16°15'	0°04'	38°15'	0°09'	28°00'	0°07'	1°20'	0°00'3"	32°00'	0°08'	236°40'	0°57'	183	0.73	
	51.0		7.0		16.0		12:0		0.5		13.5		100%				

DATA OF DRILLING WORKS

Table 3-10 (2), D.D.H. -2

WORKING TIME & EFFICIENCY	DRILLING		HOISTING & LOWERING ROD		HOISTING & LOWERING J. TUBE		MISCELLANEOUS		REPAIRING		OTHERS		TOTAL		WORKERS	CALCULATION PERIOD	
	WORKING TIME	TIME/M	WORKING TIME	TIME/M	WORKING TIME	TIME/M	WORKING TIME	TIME/M	WORKING TIME	TIME/M	WORKING TIME	TIME/M	WORKING TIME	TIME/M			TOTAL NUMBER OF WORKERS
0 - 50	9°50'	0°12'	2°10'	0°03'	3°50'	0°05'	3°10'	0°04'	2°00'	0°03'	4°00'	0°05'	25°00'	0°31'	14.5	0.30	0 - 48.50
50 - 100	33°45'	0°38'	5°50'	0°07'	10°45'	0°12'	5°30'	0°06'			8°00'	0°09'	63°50'	1°20'	33.5	0.63	48.50 - 101.0
100 - 150	36°35'	0°41'	6°40'	0°07'	13°15'	0°15'	6°40'	0°07'			9°10'	0°10'	72°20'	1°34'	36.5	0.68	101.90 - 156.0
150 - 200	35°10'	0°46'	24°00'	0°31'	15°30'	0°20'	9°50'	0°13'	30'	0°00'6"	10°50'	0°14'	95°50'	2°07'	50.5	1.09	156.00 - 202.2
200 - 250	42°50'	0°53'	16°10'	0°20'	18°20'	0°23'	6°00'	0°08'	40'	0°00'8"	12°00'	0°15'	96°00'	1°59'	50.0	1.04	202.20 - 250.5
TOTAL	158°10'	0°38'	54°50'	0°13'	61°40'	0°15'	31°10'	0°08'	3°10'	0°00'8"	44°00'	0°11'	353°00'	1°25'	185	0.38	
	44.7		15.4		17.5		9.0		1.0		12.4		100%				

DATA OF DRILLING WORKS

Table 3-10 (3), D.D.H. -3

WORKING TIME & EFFICIENCY DEPTH OF SECTION	DRILLING		HOISTING & LOWERING ROD		HOISTING & LOWERING I. TUBE		MISCELLANEOUS		REPAIRING		OTHERS		TOTAL		WORKERS		CALCULATION PERIOD
	WORKING TIME	TIME/M	WORKING TIME	TIME/M	WORKING TIME	TIME/M	WORKING TIME	TIME/M	WORKING TIME	TIME/M	WORKING TIME	TIME/M	WORKING TIME	TIME/M	TOTAL NUMBER OF WORKERS	WORKERS/M	
0 - 50	15°50'	0°21'	1°00'	0°01'	5°00'	0°07'	3°40'	0°05'	1°30'	0°02'	6°00'	0°08'	33°00'	0°44'	32	0.71	0 - 45.20
50 - 100	22°30'	0°22'	30'	0°00'5"	7°00'	0°07'	5°00'	0°05'			5°00'	0°05'	40°00'	0°39'	30.5	0.49	45.20 - 107.00
100 - 150	15°20'	0°19'	3°50'	0°05'	8°30'	0°11'	7°30'	0°09'			4°50'	0°06'	40°00'	0°50'	22.5	0.47	107.00 - 154.7
150 - 200	17°50'	0°26'	2°00'	0°03'	14°40'	0°21'	3°30'	0°05'	4°00'	0°06'	6°00'	0°09'	48°00'	1°09'	25	0.60	154.70 - 196.3
200 - 250	23°10'	0°26'			14°10'	0°16'	4°40'	0°05'			6°00'	0°07'	48°00'	0°53'	30	0.56	196.30 - 250.2
TOTAL	94°40'	0°23'	7°20'	0°02'	49°20'	0°12'	24°20'	0°06'	5°30'	0°01'	27°50'	0°07'	209°00'	0°50'	140	0.56	
	45.0		3.4		24.0		12.0		2.5		13.1		100%				

DATA OF DRILLING WORKS

Table 3-10 (4) D.D.H. -4

WORKING TIME & EFFICIENCY DEP- TH OF SECTION	DRILLING		HOISTING & LOWERING ROD		HOISTING & LOWERING L. TUBE		MISCELLANEOUS		REPAIRING		OTHERS		TOTAL		WORKERS		CALCULATION PERIOD
	WORKING TIME	TIME/M	WORKING TIME	TIME/M	WORKING TIME	TIME/M	WORKING TIME	TIME/M	WORKING TIME	TIME/M	WORKING TIME	TIME/M	WORKING TIME	TIME/M	TOTAL NUMBER OF WORKERS	WORKERS/M	
0 - 50	21°10'	0°25'	3°00'	0°04'	11°00'	0°13'	7°10'	0°08'	1°40'	0°02'	7°00'	0°08'	51°100'	1°00'	31.5	0.62	0 - 51.10
50 - 100	23°20'	0°29'	3°40'	0°05'	10°50'	0°14'	8°00'	0°10'	3°10'	0°04'	7°00'	0°09'	56°00'	1°17'	30.5	0.64	51.10 - 98.90
100 - 150	22°10'	0°23'	1°10'	0°01'	14°50'	0°15'	3°50'	0°04'			6°00'	0°06'	48°00'	0°49'	25	0.43	98.90 - 157.2
150 - 200	18°50'	0°25'	8°10'	0°10'	10°00'	0°13'	5°00'	0°07'			6°00'	0°08'	48°00'	1°04'	25	0.54	157.20 - 203.3
200 - 250	21°10'	0°27'	6°40'	0°09'	12°50'	0°16'	6°40'	0°09'			7°00'	0°09'	54°20'	1°16'	33.5	0.71	203.30 - 250.3
TOTAL	106°40'	0°26'	22°40'	0°05'	59°30'	0°14'	30°40'	0°07'	4°50'	0°01'	33°00'	0°08'	257°20'	1°03'	151.50	0°61'	
	42.0		9.0		23.0		12.0		0.2		13.0		100%				

DATA OF DRILLING WORKS

Table 3-10 (5) D.D.H. -5

WORKING TIME & EFFICIENCY DEPTH OF SECTION	DRILLING		HOISTING & LOWERING ROD		HOISTING & LOWERING I. TUBE		MISCELLANEOUS		REPAIRING		OTHERS		TOTAL		WORKERS		CALCULATION PERIOD
	WORKING TIME	TIME/M	WORKING TIME	TIME/M	WORKING TIME	TIME/M	WORKING TIME	TIME/M	WORKING TIME	TIME/M	WORKING TIME	TIME/M	WORKING TIME	TIME/M	TOTAL NUMBER OR WORKERS	WORKERS/M	
0 - 50	20°10'	0°23'	2°10'	0°03'	7°30'	0°09'	7°10'	0°08'			6°00'	0°07'	43°00'	0°49'	26.0	0.49	0 - 52.90
50 - 100	17°00'	0°21'			6°00'	0°07'	5°00'	0°06'			4°00'	0°05'	32°00'	0°38'	17.5	0.34	52.90 - 103.90
100 - 150	16°50'	0°20'	3°00'	0°04'	8°40'	0°10'	6°30'	0°08'			5°00'	0°06'	40°00'	0°48'	19.0	0.38	103.90 - 153.90
150 - 200	15°10'	0°18'	1°20'	0°02'	9°20'	0°11'	2°10'	0°03'			4°00'	0°05'	32°00'	0°37'	17.0	0.33	153.90 - 205.40
200 - 250	18°00'	0°24'	1°20'	0°02'	7°40'	0°10'	5°20'	0°07'	7°10'	0°09'	6°00'	0°08'	45°30'	1°00'	29.0	0.64	205.40 - 251.10
TOTAL	87°10'	0°21'	7°50'	0°02'	39°10'	0°09'	26°10'	0°06'	7°10'	0°02'	25°00'	0°06'	192°30'	0°46'	108.5	0.43	
	45.0		4.0		20.0		14.0		4.0		13.0		100%				

DATA OF DRILLING WORKS

Table 3-10 (6) D.D.H. -6

WORKING TIME & EFFICIENCY DEPTH OF SECTION	DRILLING		HOISTING & LOWERING ROD		HOISTING & LOWERING I. TUBE		MISCELLANEOUS		REPAIRING		OTHERS		TOTAL		WORKERS TOTAL NUMBER OR WORKERS	CALCULATION PERIOD	
	WORKING TIME	TIME/M	WORKING TIME	TIME/M	WORKING TIME	TIME/M	WORKING TIME	TIME/M	WORKING TIME	TIME/M	WORKING TIME	TIME/M	WORKING TIME	TIME/M			
0 - 50	17°10'	0°21'	1°10'	0°02'	5°30'	0°07'	4°10'	0°05'			5°00'	0°06'	33°00'	0°41'	19.0	0.39	0 - 48.30
50 - 100	20°30'	0°23'	2°20'	0°03'	8°00'	0°09'	4°10'	0°05'			5°00'	0°06'	40°00'	0°44'	21.0	0.38	48.30 - 103.00
100 - 150	21°45'	0°25'	1°30'	0°02'	12°25'	0°14'	6°20'	0°07'			6°00'	0°07'	48°00'	0°56'	29.0	0.56	103.00 - 154.90
150 - 200	20°45'	0°25'	3°00'	0°04'	9°35'	0°12'	8°40'	0°11'			6°00'	0°06'	48°00'	0°58'	21.0	0.43	154.90 - 204.20
200 - 250	16°10'	0°21'	1°30'	0°02'	5°10'	0°07'	5°10'	0°07'			4°00'	0°05'	32°00'	0°41'	22.0	0.47	204.20 - 251.10
TOTAL	96°21'	0°23'	9°30'	0°02'	40°40'	0°10'	28°30'	0°07'			26°00'	0°06'	201°00'	0°48'	112.0	0.47	
	48.0		5.0		20.0		14.0				13.0		100%				

**APPENDICES
(GEOLOGICAL DATA)**

Table 1-9 List of Rock Samples

Sample No.	Location	Rock name	Thin section	Polished section	Chemical analysis		X-ray analysis	Dating	Fossil	Pollen	Remarks
					Rock	Ore					
1	Z-11	Meta diorite	○								
2	Y-9	Gabbroic diorite									
3	Y-13	Gabbroic diorite									
4	X-18	Limonite ore									
5	X-21N1	Quartzite									
6	X-23N1	Quartzite									
7	X-28(1)	Sandstone									
8	X-28(2)	Sandstone									
9	X-28(3)	Quartz monzonite porphyry	○								
10	X-28(4)	Sandstone									
11	X-28(5)	Sandstone									
12	X-30(1)	Quartz monzonite porphyry									
13	W-10	Gabbroic diorite									
14	W-13	Quartz monzonite porphyry									
15	W-36(1)	Quartz monzonite porphyry									
16	B-7-(1)	Porphyritic granodiorite									
17	B-31N1	Quartz monzonite porphyry									
18	A-1	Gabbro									
19	A-13	Quartz monzonite porphyry									
20	A-27	Shale									
21	B-10R	Granodioritic porphyry									
22	B-19R	Shale	○								
23	B-26R	Quartzite									

Sample No.	Location	Rock name	Thin section	Polished section	Chemical Analysis		X-ray analysis	Dating	Fossil	Pollen	Remarks
					Rock	Ore					
24	B-27R	Porphyritic granodiorite									
25	B-30R	Quartz monzonite porphyry									
26	B'-1R	Gabbro ~ Diorite									
27	B-18	Diorite porphyry	○								
28	C-2	Gabbroic diorite									
29	C-17M	Monzonite porphyry	○			○					
30	C-20R	Granodiorite				○					
31	C-20(2)	Gossan									
32	C-21	Quartz monzonite porphyry									
33	C-26	Porphyritic granodiorite									
34	C'-2	Gabbro									
35	D-5	Shale									
36	D-2	Meta gabbro	○			○		○			
37	D'-3	Porphyritic granodiorite									
38	D'-8M	Skarn									
39	D'-8	Porphyritic granodiorite									
40	E-19	Quartz monzonite porphyry	○								
41	E-27	Quartz monzonite porphyry									
42	E-35	Quartz monzonite porphyry									
43	E-28M	Skarn									
44	E-282M	Metallic mineral									
45	E-34	Limestone									
46	F-4	Quartzite									
47	F'-7	Shale									

Sample No.	Location	Rock name	Thin section	Polished section	Chemical analysis		X-ray analysis	Dating	Fossil	Pollen	Remarks
					Rock	Ore					
48	F'-16	Porphyritic granodiorite									
49	F'-20	Monzonite porphyry									
50	F'-23M	Skarn	○								
51	F'-31	Porphyritic granodiorite	○								
52	F-29	Skarn magnetite ore									
53	F'-34	Monzonite porphyry									
54	F'-34(2)	Monzonite porphyry									
55	F'-37	Grandiorite	○								
56	G-3M	Skarn									
57	G-M	Quartz monzonite porphyry									
58	G'-4	Monzonite porphyry									
59	G'-11	Sandstone (hornfels)									
60	G-15	Limestone									
61	G-152M	Magnetite with copper									
62	G-20	Granodioritic porphyry									
63	G-18M	Limonite									
64	G'-18M	Iron oxide		○							
65	G'-182M	Sandstone - Shale									
66	G-21R	Magnetite skarn	○								
67	G-213M	Monzonite porphyry									
68	G-21M	Copper									
69	G-34M	Skarn									
70	F'-34	Porphyritic granodiorite									
71	G'-34	Granodioritic porphyry									

Sample No.	Location	Rock name	Thin section	Polished section	Chemical analysis		X-ray analysis	Dating	Fossil	Pollen	Remarks
72	H-14	Porphyritic granodiorite									
73	G'-21	Monzonite porphyry									
74	G'-21M	Magnetite skarn		○							
75	G'-23	Porphyritic granodiorite									
76	G'-25	Limestone									
77	H-17	Monzonite porphyry									
78	H'-0	Gabbro									
79	I-6	Shale									
80	I-4	Gabbro									
81	I-62R	Porphyritic Granodiorite									
82	I-10	Shale									
83	I-11	Sandstone									
84	I-14M	Skarn									
85	I-14	Limestone with limonite									
86	I'-16	Monzonite porphyry									
87	I'-24	Skarn	○	○							
88	I'-40M	Skarn									
89	I'-402M	Iron ore		○							
90	I'-41	Granodioritic porphyry									
91	I'-41N	Skarn with magnetite									
92	I'-14	Micro gabbro	○								
93	I'-25M	Magnetite skarn		○							
94	J-11N1	Diorite									
95	J-14S2	Skarn									

Sample No.	Location	Rock name	Thin section	Polished section	Chemical analysis		X-ray analysis	Dating	Fossil	Pollen	Remarks
					Rock	Ore					
96	J-18S1	Quartz monzonite									
97	J-20S1	Porphyritic diorite									
98	J-22S1	Monzonite									
99	J-10S1	Sandstone									
100	J'-14S1	Quartz monzonite porphyry	○								
101	J'-16S1	Diorite									
102	K-14N2	Andesite									
103	K-19S1	Quartz monzonite porphyry	○	○							
104	K-19S2	Hornblende gabbro	○								
105	K-23N1	Skarn									
106	K-23N2	Monzonite									
107	K'-16N1	Quartz monzonite porphyry									
108	K'-21S1	Quartz monzonite porphyry									
109	L-8N1	Diorite									
110	L-14S1	Diorite	○								
111	L-15S1	Porphyritic granodiorite									
112	L-17S1	Diorite									
113	L'-13S1	Gabbro - Diorite									
114	L'-18S1	Skarn									
115	M-15S1	Quartzite									
116	M'-2N1	Olivine Basalt	○								
117	M'-15N1	Diorite	○								
118	M'-15S2	Diorite	○								
119	M'-18S1	Copper									

Sample No.	Location	Rock name	Thin section	Polished section	Chemical analysis		X-ray analysis	Dating	Fossil	Pollen	Remarks
					Rock	Ore					
120	N-13N1	Gabbroic diorite									
121	N-18S1	Gabbroic rock									
122	N-19N1	Quartz monzonite porphyry	○								
123	N-20N1	Meta gabbro	○								
124	N-24S1	Diorite									
125	N-35S1	Quartz monzonite porphyry									
126	N-35N1	Quartz monzonite porphyry	○								
127	N'-21N1	Monzonite									
128	N'-22S1	Magnetite skarn		○							
129	N'-22	Skarn									
130	N'-38S1	Quartz monzonite porphyry									
131	O'-18S1	Gabbroic diorite									
132	O'-19N	Meta gabbro	○								
133	O-26N'	Porphyritic granodiorite									
134	O-28N1	Limestone									
135	O'-12	Meta-gabbro	○		○		○				
136	O'-17N1	Diorite									
137	O'-19	Copper									
138	O'-20S1	Gabbro - Diorite									
139	O'-22S1	Chalcopyrite									
140	O'-23-2	Porphyritic granodiorite									
141	O'-24-1	Porphyritic granodiorite									
142	O'-26S1	Diorite									
143	O'-26S2	Limestone									

Sample No.	Location	Rock name	Thin section	Polished section	Chemical analysis		X-ray analysis	Dating	Fossil	Pollen	Remarks
					Rock	Ore					
144	O'-26S2	Diorite									
145	P-0N1	Gabbro - Diorite									
146	P-9N1	Gabbroic diorite									
147	P-10N1	Diorite									
148	P-10N2	Diorite									
149	P-18N1	Diorite									
150	P-21S2	Limonite									
151	P-21S1	Limonite									
152	P-24N1	Magnetite									
153	P-26N1	Gabbro - Diorite									
154	P-27N1	Limestone									
155	P-30N1	Monzonite									
156	P-34N1	Monzonite									
157	P'-29N1	Quartz monzonite porphyry	○								
158	P-28S1	Magnetite									
159	P'-321N	Diorite									
160	Q-13S1	Gabbroic diorite									
161	Q-15S11	Skarn									
162	Q-14S1	Diorite									
163	Q-19S2	Gabbro	○								
164	Q-19S1	Gabbroic diorite									
165	Q-23N3	Gabbro	○								
166	Q-23N1	Meta gabbro	○								
167	Q-23N2	Quartz monzonite porphyry									

Sample No.	Location	Rock name	Thin section	Polished section	Chemical analysis		X-ray analysis	Dating	Fossil	Pollen	Remarks
					Rock	Ore					
168	Q-24S1	Diorite									
169	Q-25S1	Quartz diorite	○								
170	Q-27S2	Limestone									
171	Q-29-2	Monzonite									
172	Q-31-1	Gabbroic diorite									
173	Q-31S2	Gabbroic diorite									
174	Q'-3-1	Gabbroic diorite									
175	Q-11S1	Gabbroic diorite									
176	Q'-23-1	Monzonite									
177	Q'-39	Quartz monzonite porphyry									
178	Q'-6-1	Monzonite									
179	Q'-6-2	Monzonite									
180	Q'-19-5	Gabbro - Diorite									
181	Q'-20S	Gabbroic diorite									
182	R-23N2	Monzonite									
183	R-24N1	Monzonite									
184	Q'-25-1	Diorite									
185	R-7S1	Monzonite									
186	R-19S1	Diorite									
187	R-24N2	Diorite									
188	R-23N1	Diorite									
189	R-29	Gabbro - diorite									
190	R'-0-1	Rhyolite									
191	R'-1-1	Porphyritic andesite									

Sample No.	Location	Rock name	Thin section	Polished section	Chemical analysis		X-ray analysis	Dating	Fossil	Pollen	Remarks
					Rock	Ore					
192	R'-13-1	Diorite									
193	R'-25	Diorite									
194	R'-31	Diorite									
195	R'-35	Monzonite									
196	S-0	Andesite									
197	S-11	Diorite									
198	S-19	Gabbro - Diorite									
199	S-22	Diorite - Gabbro									
200	S-23	Diorite - Gabbro									
201	Trench	Copper sulphide ore		○							
202	Trench	"		○							
241	Ataraya mine	Quartz monzonite porphyry	○					○			
242	Tintaya mine	Quartz monzonite porphyry	○					○			
243	"	"	○					○			
244	"	Altered latite	○					○			
76'	G'-26R	Quartz monzonite porphyry	○								

DDH-1

Sample No.	Location	Thin section	Polished section	Chemical analysis	X ray analysis	Dating	Remarks
	Depth (m)			Rock			
301	60.5						
302	63.6						
303	64.3	○	○				Porphyritic granodiorite
304	68	○	○				Molybden bearing granodiorite
305	72.8	○		72.0	75.55	72.0	Porphyritic granodiorite
306	75.55			○		○	Granodiorite
307	82.4	○		84.0		84.0	
308	95.5	○					Porphyritic granodiorite
309	141.7	○	○				Cataclastic granodiorite
310	147.8	○					Porphyritic granodiorite
311	231.3	○	○				Cataclastic granodiorite

DDH-2

Sample No.	Location	Thin section	Polished section	Chemical analysis	X ray analysis	Dating	Remarks
	Depth (m)			Rock			
312	50.5	○					Quartzite
313	60.5	○	○		60○		Copper bearing monzonite porphyry
314	74.0	○	○				Copper bearing hornfels of slate
315	93.6	○					Hornfels of sandstone
316	117.5	○	○				Molybden & copper bearing monzonite porphyry
317	152.0	○					Oil ine Basalt
318	158.9	○	○				Copper bearing hornfels of sandstone
319	172.6	○	○				Copper bearing granodiorite

DDH-3

Sample No.	Location	Thin section	Polished section	Chemical analysis Rock	X ray analysis	Dating	Remarks
	Depth (m)						
320	41.1	○	○				Magnetite bearing gabbro
321	50	○					Quartz diorite
322	87.7	○					Lead Copper bearing Limestone Copper bearing skarn
323	91.1	○					
324	91.6	○	○				
325	96.1	○	○				
326	105.0	○					Limestone Copper bearing marble
327	107.7		○				
328	120				○		
329	129.0	○					Skarn
330	136.7	○	○				Copper bearing skarn
331	159.0	○					Skarn
332	164.3	○					Hornfels of calcareous sandstone
333	171.3	○					Aplite
334	175.0	○					Gabbro
335	200	○					Granodiorite
336	211.0	○					Diorite
337	224.8	○					Granodiorite
338	242.4	○		236		236	Porphyritic granodiorite
339	250.0	○		248		248	Granodiorite

DDH-4

Sample No.	Location	Thin section	Polished section	Chemical analysis Rock	X ray analysis	Dating	Remarks
	(Depth (m))						
340					10 ○		Quartz monzonite porphyry
341 342	18.5 20.0	○ ○	○				
343					40 ○		Quartz monzonite porphyry
344 345	49.9	○			53.2 ○		
346 347 348 349	63.5 64.8 68.3 70	○ ○ ○ ○	○ ○	64 74		64 ○ 74	Quartz monzonite porphyry
350	90	○					Quartz monzonite porphyry
351	131.2	○					Quartz monzonite porphyry
352	142.3	○					Copper bearing quartz monzonite porphyry
353	166.3	○	○				
354	177.3	○	○				Quartz monzonite porphyry
355	183.6	○					
356				192	140 ○	192	Quartz monzonite porphyry
357	202	○		204		○ 204	
358 359	220.0 221.1	○ ○	○				Copper bearing quartz monzonite porphyry
360	239.6	○					Quartz monzonite porphyry

DDH-5

Sample No.	Location	Thin section	Polished section	Chemical analysis	X ray analysis	Dating	Remarks
	Depth (m)			Rock			
361					45.60		
362	67.3	o	o				Meta gabbro
363	84.5	o	o				Gabbro
364	98.5	o	o		98.50		Gabbro
365	122.7	o	o				Diorite
366	132.0	o	o				Altered diorite
367 368	172.0	o	o		178.80		Copper bearing gabbro
369	188.9	o	o				Altered gabbro
370	210.0	o					Olivine basalt
371	240.0	o					Altered diorite
372	250.0	o					Diorite

DDH-6

Sample No.	Location	Thin section	Polished section	Chemical analysis	X ray analysis	Dating	Remarks
	Depth (m)			Rock			
373	31.0	○	○				Copper bearing hornblende gabbro
374	74.8	○	○		80○		Calcite vein
375	80.5	○	○			Altered diorite	
376	93.3	○	○			□	Copper bearing hornblende gabbro
377	97.0	○	○				Hornblende gabbro
378	113.7	○○	○		□	Gabbro	
379	114.4	○○	○			Altered diorite	
380	116.0	○○	○				
381	117.0	○○	○				
382	128.0	○			□	Gabbro	
383	135.6	○					
384	166.1	○				Gabbro	
385	234.0	○	○				Gabbro
386	237.3	○					
387					240 ○		Diorite
388	250.3	○	○			Hornblende gabbro	

Table I-10 Microscopic Observations

Sample No.	Location	Rock name	Microscopic observations	Remarks
1	Z-11	Meta-diorite	Subhedral and highly sericitized plagioclase and brownish green hornblende with a distinct poikilitic texture are the main constituents. Colourless to pale greenish hornblende with fibrous shape develops along the mantle of brownish hornblende. Hydrothermal minerals are chlorite after mafics, epidote mainly replacing plagioclase and rarely as veinlets, and ore (only magnetite).	
9	X-28R3	Quartz monzonite porphyry	The rock shows porphyritic texture. Phenocrysts of plagioclase, potassic feldspar, biotite and quartz are in the very fine grained groundmass rich in alkali feldspars. Plagioclase has subhedral shape with a grain size of the order of 2 mm. It sometimes shows Carlsbad twinning and is highly saussuritized and carbonitized with slight sericitization. Biotite is almost completely chloritized. As a phenocryst, also occurs quartz with a spherical shape. Chlorite aggregates replace biotite and carbonates are scattered in the groundmass. As a accessory mineral, apatite, sphene and ore (magnetite only) are observed.	
22	B'-18R	Phyllitic slate	The rock is characterized by the microcrenulation and platy cleavage. Main constituents are quartz, sericite, chlorite and hematite. The rock must be affected by the weak metamorphism.	
27	B-18R	Diorite porphyry	Phenocrysts of plagioclase (subhedral, up to 2 mm, always andesine with acidic mantle), hornblende (subhedral, up to 1 mm, with greenish tint) and sometimes of quartz are scattered in fine-grained groundmass of alkali-feldspar. Feldspar is weakly argillized. Minor accessories are apatite, sphene and ore (magnetite only, fairly rich) to which must be added epidote with normal shape. The rock is weakly altered except for epidotization.	
29	C-17M	Quartz monzonite porphyry	Abundant phenocrysts of plagioclase (euhedral, up to 3 mm, twinned after albite and Carlsbad law) are filled by fine-grained perthitic orthoclase and quartz. Aggregates of fine-grained chlorite may be after biotite. Feldspars are weakly argillized and slightly sericitized. It contains small amounts of sphene, apatite and ore minerals.	

Sample No.	Location	Rock name	Microscopic observations	Remarks
30	C-20R	Quartz monzonite porphyry	The rock has phenocrysts of plagioclase (subhedral, up to 3mm, generally oligoclase sometimes zoned) and potassic feldspar, and brownish biotite (subhedral, up to 1 mm) in a fine-grained equigranular quartz-feldspathic groundmass. Argillization and sericitization of feldspar are weak but universal, and alteration of plagioclase is much intensity than that of potassic feldspar. Biotite has been altered to chlorite from its margin or along the cleavage. The associated minerals are sphene, apatite and later quartz. Pyrite-magnetite dissemination are observed.	
36	D-2	Metagabbro	The rock is medium-grained hypidiomorphic granular in texture, and composed mainly of plagioclase (subhedral, up to 4 mm, twinned after albite, Carlsbad and pericline laws, usually zoned) and hornblende (subhedral prismatic to granular, up to 3 mm, with a pleochroism of X pale brownish yellow, Y brownish yellow and Z brown) with small amounts of cummingtonite, clinopyroxene, apatite, sphene and opaque minerals. Larger crystals of hornblende are commonly poikilitic, enclosing clinopyroxene, plagioclase and opaque minerals. Some hornblendes are partly replaced by small crystals of deep greenish blue-colored hornblende. Cummingtonite occurs commonly as fine-grained aggregates in the core of hornblende. Clinopyroxene is always embraced by hornblende. Small amounts of epidote, chlorite and sericite occur as alteration products.	
40	E-19	Quartz monzonite porphyry	Phenocrysts of plagioclase, potassic feldspar, hornblende and biotite with accessory sphene (fairly rich), apatite and ore, are enclosed in a very fine grained groundmass of alkali feldspars and little quartz. Plagioclase is subhedral, up to 3 mm, sodic andesine, slightly argillized and rarely sericitized. Potassic feldspar is subhedral up to 2 mm, always perthitic orthoclase and in a veinlets. Biotite is chloritized.	
50	F'-23M	Skarn	The rock is mainly composed of epidote (= zoisite), actinolite, calcite with handsome grains of sphene. Actinolite is highly chloritized. Accessories are a little garnet and hematite-limonite. Calcite veinlets are present.	

Sample No.	Location	Rock name	Microscopic observations	Remarks
51	F-31R	Quartz monzonite porphyry	Phenocrysts of plagioclase, hornblende, potassic feldspar and biotite are on a fine-grained groundmass being rich in alkali feldspar. Plagioclase is zoned, weakly argillized and twinned after albite, Carlsbad and pericline law. Biotite is partly chloritized, epidote replacing plagioclase and mafics can be observed and weak epidote-chlorite is present.	
66	G-21R	Quartz monzonite porphyry	Phenocrysts of plagioclase, potassic feldspar and biotite are in the fine-grained holocrystalline groundmass of alkali feldspar and quartz (Phenocrysts of plagioclase > K-feldspar > biotite). Aggregates of biotite and chloritized biotite may be the pseudomorph after essential biotite. Twisted plagioclase and quartz showing wavy extinction may reflect the effect of deformation. Quartz is fragmentally recrystallized (or secondary?). Hematite-sericite concentration can be locally observed.	
76'	G'-26R	Quartz monzonite porphyry	Phenocrysts of plagioclase (subhedral, up to 2 mm, zoned, generally oligoclase) and phenocrysts of colorless and columnar amphibole (subhedral, up to 2 mm, pale greenish in tinge) are scattered in a very fine-grained groundmass of potassic feldspar or alkali-feldspar and quartz. Accessory minerals are a little biotite, sericite, epidote, quartz and opaque minerals. Aggregates and veinlets of epidote-quartz are present, and opaque minerals are hematite and limonite.	
87	I'-24R	Skarn	It is mainly composed of fibrous actinolite, zoned garnet, fine-grained quartz, chlorite, carbonates and ore minerals. Quartz occurs commonly in the form of fine aggregates filling fractures and cavities. Ore minerals are mostly hydrates of iron and copper by the strong supergene alteration.	
92	I'-14R	Microgabbro	The texture is holocrystalline and fine-grained. Idiomorphic hornblende with brownish tint, which sometimes has a core of clinopyroxene, is widely developed. Plagioclase is also idiomorphic with fine-grained shape and may have a composition of Ab30 An70.	

Sample No.	Location	Rock name	Microscopic observations	Remarks
100	J'-14S1	Quartz monzonite porphyry	Phenocrysts of plagioclase (subhedral, up to 4 mm, zoned, with ranging composition from Ab50 An50 in the core to Ab70 An30 in the mantle) and hornblende (subhedral, up to 1 mm, with a pleochroism of X = yellowish green, Y = brownish green, Z = grass green, slightly chloritized) are common in a fine textured crystalline groundmass of alkali feldspars and quartz. Feldspars are weakly argillized but rarely sericitized. Porphyritic quartz with corroded structure is also found, but not so frequent. Biotite also occur in a second stage in place of parts of the hornblende. Common accessories are apatite, sphene (slightly leucoxenized) and ore magnetite only).	Minor amounts of biotite aggregates and cummingtonite are also present. A little sericite-epidote can be seen along fine fracture. Ore (magnetite only) is fairly abundant. The rock is slightly by altered.
103	K-19S1	Quartz monzonite porphyry	Phenocrysts of zoned plagioclase, potassic feldspar, hornblende and biotite occur in a very fine-grained groundmass rich in alkali feldspar. Plagioclase is zoned, weakly sericitized and twisted with a subhedral shape. Greenish hornblende and brownish biotite with twisted habit may be essential. Secondary biotite is common, but not so abundant as fine aggregates. As an accessory minerals, present are sphene, apatite and ore, and recrystallized quartz (or secondary?) can be seen. Chlorite is formed along the cleavage of biotite. This rock is weakly chloritized.	
104	K-19S2	Hornblende gabbro	The texture is holocrystalline, equigranular with medium-grained crystals. Main constituents are plagioclase (subhedral, up to 2 mm, calcic labradorite), handsome crystals of brownish hornblende with poikilitic texture, which are partly altered to cummingtonite and brownish biotite. Hornblende sometimes have a core of clinopyroxene. Sometimes thin veinlets of potassic feldspar can be observed. Accessories are a little sericite, clay and ore (magnetite only). The alteration of this rock is very weak.	

Sample No.	Loca ion	Rock name	Microscopic observation	Remarks
110	L-14S1	Diorite	The rock shows equigranular, holocrystalline and medium-grained texture. Main constituents are plagioclase (subhedral, up to 2 mm, zoned with a ranging composition from basic bytownite to labradorite), potassic feldspar (perthitic orthoclase) and hornblende (sometimes with clinopyroxene core with a pleochroism of X = pale greenish brown, Y = brownish green, Z = brownish green). Fine grained biotite occurs in the part of basic core of plagioclase, which had been saussuritized, may be the product by the thermal alteration. A little chlorite-epidote-sericite are secondary stage products.	
116	M ¹ -2N1	Olivine basalt	In a holocrystalline groundmass of lath-shaped plagioclase and granules of augite with a glassy base, present are phenocrysts of olivine (partly altered to iddingsite), augite (sometimes with ophitic texture) and plagioclase.	
118	M ¹ -15S2	Diorite	The rock, showing fine-textured, and equigranular, is mainly composed of such minerals as follows: plagioclase (subhedral, sometimes porphyritic, up to 1 mm), clinopyroxene with a distinct cleavage, and a little cummingtonite-biotite replacing clinopyroxene. Accessories are sphene and ore. A little epidote (zoisite) and sericite are secondary products after plagioclase. The alteration of this rock is very weak.	
122	N19-n1	Quartz monzonite porphyry	The rock shows porphyritic texture, composed of phenocryst of plagioclase (subhedral, up to 3 mm, zoned with a core of Ab80 An20 having albitic mantle). Potassic feldspar (subhedral, up to 2 mm, almost perthitic with very fine lamellae of albite), columnar hornblende (subhedral, with a pleochroism of X = greenish brown, Y = brownish green, Z = greenish) and brownish biotite scattered in a fine-grained holocrystalline groundmass of quartz and feldspar. As accessories, there occur sphene, apatite, a few hornblende and ore (magnetite). Quartz vein has cut across the rock.	

Sample No.	Location	Rock name	Microscopic observation	Remarks
123	N-20M	Meta-gabbro	The rock shows a hypidiomorphic granular texture, and consists mainly of plagioclase (subhedral, bytownite to labradorite, zoned), hornblende (subhedral, commonly enclosing plagioclase crystals poikilitically, with a pleochroism of pale yellow to brownish green) and clinopyroxene (subhedral, up to 1 mm). Abundant aggregates of fine-grained biotite replace hornblende and clinopyroxene, suggesting that it has been suffered from some thermal effect. A little cummingtonite also replaces hornblende. Plagioclase is weakly argillized and sericitized.	
126	N35-N1	Quartz monzonite porphyry	The rock is slightly cataclastic, but no disturbance of texture, and rich in hematite-limonite (granular, after sulphides?). Constituent minerals are phenocrysts of plagioclase (fairly argillized, a little sericitized), later quartz mainly associated with iron oxides, a little completely chloritized biotite and a little sericite. Groundmass is very fine-grained and composed of alkali-feldspar fairly argillized.	
128	N'-22S1	Skarn	It is mainly composed of diopside, actinolite and magnetite, and contains a small amount of garnet. Actinolite is possibly formed later than diopside. Fine-grained biotite is later than actinolite formation and commonly associated with magnetite and a little quartz. Sericite and clay minerals are fairly commonly produced. It is distinctly weathered and thin veinlets of carbonates fill the fractures.	
129	N'-22	Skarn	The rock is mainly composed of diopside and actinolite (diopside, actinolite), and actinolite is later than diopside. The original rock is may be calcic in composition. Accessory minerals are garnet, sericite, clay, green biotite, ore and quartz. Magnetite-green copper - iron oxide - calcite is latest stage minerals.	
132	0'-19N	Meta-gabbro	The essential minerals are plagioclase, hornblende and clinopyroxene. Plagioclase (subhedral, up to 2 mm, zoned twinned after Carlsbad and albite law, bytownite core with more acid mantle, rare sericitization of plagioclase), and hornblende (subhedral up to 3 mm, with a pleochroism of X = yellowish green, Y = brownish green, Z = brownish green, sometimes with poikilitic texture) are common. Clinopyroxene occur	

Sample No.	Location	Rock name	Microscopic observation	Remarks
135	O'-12	Meta-gabbro	<p>in the core part of hornblende. Secondary cummingtonite in place of hornblende is present. Accessory minerals are a little sericite, biotite and ore (magnetite only). Biotite is also formed perhaps resulting from the replacement of original hornblende.</p> <p>It is medium-grained hypidiomorphic in texture, and composed mainly of plagioclase (subhedral, up to 3 mm, with polysynthetic twinning, distinctly zoned), hornblende (subhedral granular to prismatic, up to 2 mm, with a pleochroism of X pale yellow, Y pale yellowish brown and Z yellowish brown), clinopyroxene and orthopyroxene with very small amounts of cummingtonite and olivine. Hornblende is frequently replaced by green hornblende marginally and/or spottedly. Clinopyroxene, orthopyroxene, cummingtonite and olivine are always enclosed by hornblende. A little biotite occurs as fine-grained and ill-formed flakes. Opaque minerals, apatite and sphene are also present as accessory minerals. Clinzoisite-epidote, chlorite, sericite and carbonates are alteration products. Plagioclase is commonly sericitized and sometimes is altered to clinzoisite-epidote.</p>	
157	P'-29N	Quartz monzonite porphyry	<p>The texture is porphyritic. Phenocrysts are plagioclase, orthoclase, biotite and quartz, enclosed in the fine-grained holocrystalline groundmass of alkali-feldspar. Most abundant are plagioclase with a composition of Ab70 An30. Secondary minerals are calcite, sericite, and chlorite (Calcite > sericite > chlorite). Ore is magnetite only and very poor in amount.</p>	
163	Q-19	Gabbro	<p>The rock is mainly composed of clinopyroxene and plagioclase with accessory minerals of a little sericite, muscovite, chlorite and ore (magnetite only). Cataclastic vein develops. The texture is hypidiomorphic.</p>	
165	Q-23N3	Gabbro	<p>The rock shows medium-grained and hypidiomorphic granular texture. The mineral association is plagioclase (subhedral, up to 4 mm, zoned), clinopyroxene (subhedral, up to 0.5 mm) and hornblende (subhedral,</p>	

Sample No.	Location	Rock name	Microscopic observation	Remarks
166	Q-23	Meta-gabbro	<p>up to 3 mm, sometimes showing poikilitic texture, with a pleochroism of X = yellowish, Y = brownish green, Z = brownish green, occasionally surrounding the core of clinopyroxene). Porphyritic crystals of plagioclase and hornblende sometimes occur. Cummingtonite is also present as a secondary altered products replacing brownish hornblende. Accessory minerals are sphene and ore. Enclaves rich in clinopyroxene are observed.</p> <p>The rock shows a medium-grained and hypidiomorphic granular texture, and consists mainly of plagioclase (subhedral, up to 4 mm, zoned from bytownite to labradorite), hornblende (subhedral, up to 3 mm, with a pleochroism of pale yellow to brownish green) and clinopyroxene (subhedral, up to 0.5 mm, frequently enclosed by hornblende poikilitically). A little cummingtonite replacing hornblende is present. Accessory minerals are sphene and ore minerals. Ore is mostly magnetite, but fairly abundant sulphides occur in small enclaves rich in clinopyroxene.</p>	
169	Q-25S1	Quartz diorite	<p>The texture is equigranular and medium-grained. The main constituent minerals are plagioclase (subhedral, up to 3 mm) and greenish hornblende (partly altered to calcite and epidote) with small amounts of fine grained quartz. Hystorogene minerals are a little sericite, muscovite and chlorite.</p>	
241	Ataraya Mine	Quartz monzonite porphyry	<p>Phenocrysts of plagioclase (euhedral to subhedral, up to 3 mm, showing polysynthetic twinning and strong zoning) and hornblende (euhedral to subhedral, up to 1 mm, with a pleochroism of X = yellow, Y = yellowish green and Z = green) are in a very fine-grained and holocrystalline groundmass of plagioclase, hornblende, potash feldspar, quartz, biotite, opaque minerals, silica minerals and very little glass. Microphenocrysts of opaque minerals are present. Brown biotite and quartz also are rarely found as microphenocrysts. Mafic minerals are weakly chloritized.</p>	

Sample No.	Location	Rock name	Microscopic observation	Remarks
242	Tintaya Mine	Quartz monzonite porphyry	Phenocrysts of plagioclase (subhedral, up to 2 mm, showing polysynthetic twinning and weak zoning), potash feldspar (subhedral to anhedral, up to 1 mm), quartz (anhedral rounded and corroded, up to 1 mm), biotite (rarely tabular flake and commonly fine-grained aggregate, with a pleochroism of X = yellow and Z= Y dark brown) and microphenocrystic hornblende (up to 0.4 mm, pale green) are in a fine-grained and xenomorphic granular groundmass of plagioclase, potash feldspar and quartz with minor amounts of opaque minerals, sphene and apatite. Epidote, sericite and chlorite occur as alteration products. Especially mafic silicates are markedly altered to secondary minerals.	
243	Tintaya Mine	Quartz monzonite porphyry	Phenocrysts of plagioclase (subhedral prismatic, up to 2 mm, with polysynthetic twinning and weak zoning), potash feldspar (subhedral to anhedral, up to 0.6 mm), a little quartz and brown biotite are in a fine-grained groundmass of plagioclase, potash feldspar and quartz with small amounts of apatite and opaque minerals. Quartz is subhedral to anhedral, and large crystals are partially corroded. Most plagioclase crystals are largely altered to sericite and clay minerals. Biotite is rarely fresh and mostly altered to chlorite and epidote.	
244	Tintaya Mine	Altered latite	The rock is highly altered and most of primary minerals are replaced by secondary minerals. It has a porphyritic texture and phenocrysts of plagioclase, potash feldspar and rare quartz are in a fine-grained groundmass of plagioclase lath, potash feldspar and quartz with a small amount of silica mineral. Glass is not recognized at present. A few crystals of apatite are present. Mafic phenocrysts are completely altered to chlorite and sericite, but they may be biotite principally. Feldspars are highly argillized and sericitized.	

Sample No.	Location	Rock name	Microscopic observation	Remarks
302	No. 1. 63.6	Porphyritic granodiorite	The rock is weakly porphyritic and contains plagioclase, potassic feldspar and quartz (plagioclase > K-feldspar > quartz), with veins and veinlets filled in sulphides-- specular hematite-- quartz-- chlorite. Accessories are a little sercite in saussuritized feldspar and leucoxene after sphene.	
304	No. 1. 68.0	Porphyritic granodiorite	The rock is weakly porphyritic and holocrystalline. It contains plagioclase (subhedral, up to 3 mm, always oligoclase with andesine core), quartz (anhedral, interstitial), potassic feldspar (subhedral, up to 2 mm, with a distinct pleochroism of X = pale yellowish green, Y = yellowish green, Z = pale green). (plagioclase > K-feldspar > quartz > hornblende); fairly rich in sphene associated with hornblende and/or magnetite. Weak altered minerals are carbonates, chlorite and sercite (carbonates > chlorite > sercite).	
306	No. 1. 75.55	Porphyritic granodiorite	Porphyritic plagioclase (subhedral, up to 1.5 mm, zoned and twinned after albite, Carlsbad and less abundant pericline laws) are filled by finer-grained and interstitial potash feldspar (up to 0.7 mm, anhedral), quartz (anhedral, up to 0.4 mm) and subordinate brown biotite with a little sphene and opaque minerals. Feldspars are sericitized especially in potash feldspar. Biotite is almost completely altered to chlorite-carbonate aggregates and much less abundantly to clinozoisite.	
308	No. 1. 95.5	Porphyritic granodiorite	The rock shows a fine-grained and porphyritic texture. The main constituent minerals are plagioclase (porphyritic, up to 6 mm, zoned, An% varying from 50 in the core to 30 near the mantle with Carlsbad and albite twinning), potassic feldspar (subhedral, up to 1 mm, always perthitic orthoclase with very fine lamellae of albite), quartz (anhedral, very fine-grained, interstitial), hornblende (subhedral, up to 2 mm, with a pleochroism of X = yellowish green, Y = yellowish green Z = pale green), and biotite (subhedral, up to 2 mm, showing a pleochroism of brownish tinge). Accessory minerals are sphene, apatite and ore. Fine-grained biotites are secondarily formed due to the break down of original biotite and hornblende.	

Sample No.	Location	Rock name	Microscopic observation	Remarks
309	No. 1. 141.7	Cataclastic granodiorite	Chlorite occur along the margin of biotite. Quartz alkali-feldspars in groundmass. Secondary biotite after essential biotite and hornblende are present. Carbonates, chlorite and (sericite) are not so abundant.	
310	No. 1. 147.8	Porphyritic granodiorite	The rock is mainly composed of plagioclase, perthitic orthoclase and quartz, plagioclase > orthoclase >> quartz. It is intensely fractured and cut by the veinlets filled with carbonate, ore and chlorite. Plagioclase shows Carlsbad and albite twinning, being after twisted and destroyed due to the secondary deformation but having weak signs of the saussuritization, very rich in chlorite -specularite stockworks in common along with carbonates.	
311	No. 1. 231.3	Cataclastic granodiorite	The rock is fine- to medium-grained and weakly porphyritic. The main constituents are plagioclase (subhedral, up to 3 mm, with Carlsbad and albite twinning, always andesine, sometimes zoned), potassic feldspar (subhedral, up to 2 mm, often perthitic orthoclase). quartz (anhedral, fine-grained, sometimes showing wavy extinction). The secondary minerals are carbonate (fairly rich), chlorite, biotite (twisted, brownish-secondary chlorite being wavy extinction) and hornblende (subhedral, up to 2 mm, with pale greenish tint). The accessories are sphene, apatite and ore. Aggregates of fine-grained biotite shows the break down of hornblende.	
312	No. 2 50.5	Quartzite	The rock contains quartz, plagioclase and small amounts of potassic feldspar with accessory ore and sphene. Plagioclase is always albite. Potassic feldspar is always perthitic orthoclase. Distinctly discernible are signs of secondary deformation such as fractured grains of quartz and feldspars, twisted plagioclase and elongated quartz. Chlorite is formed in masses of little crystals perhaps resulatory from the replacement of an original biotite. Veins filled with carbonate cut the rock in all directions and very rich ditto in specularite-carbonates veins bearing.	
			The rock, showing cataclastic texture, is composed mainly of quartz. The coarser grained quartz (up to 1 mm) occur 'cemented' by finer-grained quartz. All grains shown wavy extinction and elongated shape,	

Sample No.	Location	Rock name	Microscopic observation	Remarks
313	No.2. 60.5	Quartz monzonite porphyry	Phenocrysts of plagioclase, potassic feldspar and biotite occur in a fine-grained alkali-feldspar rich groundmass. Phenocrysts of plagioclase is zoned, with Carlsbad twinning, biotite have perfectly been altered to chlorite. As an accessory, there are sphene, apatite and ore, to which garnet must be added. Epidote, chlorite and sericite are common hystorogene minerals. Sulphides-quartz veinlets are found.	suggesting the effect of the deformation. A grain of tourmaline (purple in tint) as present. Aggregates of secondary muscovite occur sporadically, forming an pseudomorph after feldspar. A little secondary biotite with brownish tinge is also present. A little hystorogene chlorite is characteristic. Sericite aggregates after feldspar are present.
314	No.2. 74.0	Hornfels of slate	The rock has weak foliation characterized by the parallel arrangement of flaky minerals. It consists of brownish biotite, quartz, plagioclase, colorless amphibole and muscovite. The accessory minerals are garnet, epidote and sphene. The rock must be suffered by the weak thermal alteration. Dissemination of sulphide is rich and latest carbonization are formed.	
315	No.2. 93.6	Hornfels of sandstone	The rock mainly composed of subangular quartz and plenty of feldspar in finer-grained matrix. Feldspars are perthitic orthoclase and plagioclase, both of which are detrital. Fine grains of biotite, which now have been altered to chlorite, is arranged parallel to the effect of weak alteration. Carbonate, sphene and apatite are accessory, and also a little sulphide are present.	
316	No.2. 117.5	Quartz monzonite porphyry	The rock is composed of phenocryst of plagioclase (subhedral, up to 3 mm, zoned, with Carlsbad twinning), potassic feldspar, biotite (completely chloritized, subhedral, up to 2 mm, not so abundant) and a little hornblende. They occur in a fine-grained groundmass of alkali-feldspar and a little quartz. Weak sericitization and marked saussuritizedation of feldspars are observed. Sulphide-quartz-carbonate veins are formed, and also dissemination of sulphides.	

Sample No.	Location	Rock name	Microscopic observation	Remarks
317	No.2.152.10	Olivine basalt	Phenocrysts of olivine (subhedral, up to 4 mm, wholly altered to iddingsite and chlorite), and of augite (subhedral, up to 1 mm, sometimes showing hour glass structure) are in a medium-grained, almost holocrystalline and intergranular groundmass of lath-shaped plagioclase, olivine, augite and ore. Dressy cavities are filled with zeolites.	
318	No.2.158.9	Hornfels of sandston	It is composed of recrystallized quartz and biotite with relict feldspar. Aggregates of fine biotite, epidote and garnet are characteristic, reflecting the thermal effect. Optically negative chlorite with greenish tinge, replacing biotite, is the product of latest alteration process. Spene, apatite and ore are accessory.	
319	No.2.172.6	Foliated granodiorite	The rock shows porphyritic and foliated texture. Phenocrysts of plagioclase (subhedral, up to 2 mm, with Carlsbad and albite twinning, always oligoclase, zoned), potassic feldspar (perthitic orthoclase, up to 2 mm, not so abundant) and hornblende (subhedral, columnar, up to 2 mm, with a pleochroism of X = yellowish green, Y = brownish green, Z = grass green) occur in a foliated groundmass of alkali-feldspar and a little quartz. Twisted twinning planes of feldspar and bending cleavage plane of hornblende, in addition to the foliated texture, may suggest the experienced history of deformation. Secondary products are chlorite, epidote and slight sericite. Accessory minerals are sphene, apatite and ore. Hornblende is partly altered to biotite.	
320	No.3 41.1	Gabbro	The texture is holocrystalline. Main association is plagioclase (subhedral, sometimes porphyritic, up to 4 mm, always with the composition of Ab20 An80 with more acid mantle), hornblende (subhedral, up to 2 mm, originally with greenish brown, partly altered to grass greenish amphibole) and a small amount of biotite (brownish, altered to chlorite from its margin.) Vein filled with carbonate are observed. Sphene and ore are accessories. Ore is magnetite only and fairly abundantly.	
321	No.3. 50.0	Quartz diorite	Large crystals of plagioclase and hornblende from the equigranular texture. Hornblende is sometimes enclosing plagioclase giving a poikilitic texture. Brownish green tint of hornblende is characteristic.	

Sample No.	Location	Rock name	Microscopic observation	Remarks
322	No. 3. 87.7	Limestone	Weak alteration by chlorite-carbonates-sericite (muscovite) and epidote can be observed. Fine aggregates of biotite and a little cummingtonite are seen. Sausurization of plagioclase is found, especially in the basic core of each crystal. Dissemination of magnetite and very poor sulphide are present.	
324	No. 3. 91.6	Limestone	Granulitic crystals of calcite are the main constituent, Also occur muscovite and clinopyroxene, the latter of which has perfectly been changed to chlorite or uralite, by hydroalteration. A little and minute grains of iron oxides are present.	
325	No. 3. 96.1	Skarn	The rock is mainly composed of granular calcite with a little recrystallized quartz and a few quartz veinlets. Holocrystalline texture by granular calcite is seen to be the result of recrystallization. A little sulphides are disseminated.	
327	No. 3. 105.0	Limestone	The rock is separated into the two parts. One part is mainly constructed by tightly cemented calcite with handsome shape. Another part is composed of garnet with many fractures filled by calcite. The transitional zone between two parts are composed of fine-grained calcite.	
329	No. 3. 129.0	Skarn	Main constituents is calcite, with a foliation characterized by the parallel arrangement of crystals (with an average grain size of 0.3 mm). It has banding of alteration of coarser-grained and finer-grained calcite layer. Very small amounts of quartz are also present. A little sulphides are disseminated mainly along with very fine-grained quartz.	
			The mineral association is calcite, iron oxide (magnetite), sulphides, quartz and a little amount of garnet. Quartz occurs in sporadic aggregate. Calcite veins are observed widely.	

Sample No.	Location	Rock name	Microscopic observation	Remarks
331	No. 3. 159. 0	Skarn	The rock is chiefly composed of garnet. Garnet is distinctly fractured filling with calcite and quartz which are associated with ore. Chlorite aggregates possibly after actinolite are found. Magnetite are replaced by hematite and limonite.	
332	No. 3. 164. 3	Hornfels of calcareous sandstone	The rock has a granulitic texture, composed mainly of recrystallized calcite and quartz. Detrital grains of feldspar are also found with irregular habit. Calcite veins are intruding. Leucoxene-sphene are fairly rich, and ore is very poor. A grain of epidote can be found.	
333	No. 3. 171. 3	Aplite	The rock has a fine-grained and granulitic texture, composed of acidic plagioclase, orthoclase and quartz. Fine-grained biotites are also scattered. Apatite is one of the most abundant accessories. Secondary carbonate minerals are widely distributed.	
334	No. 3. 175. 0	Gabbro	The texture is granular. Porphyritic crystals of olivine, which have been hydrated to serpentine mineral, is characteristic. Fine-grained crystals of clinopyroxene are present frequently. Veins filled with carbonates are penetrating.	
335	No. 3. 200. 0	Granodiorite	The texture is medium-grained and weakly porphyritic. Mainly composing minerals are plagioclase (subhedral, up to 3 mm, with a varying composition from Ab70 An30 in the core to Ab90 An10 in the mantle. twinned on Carlsbad, albite and also Periclinal law), greenish hornblende (subhedral, up to 1 mm, partly down graded to biotite) Quartz (interstitial, anhedral), and biotite. Hysterogene minerals are epidote, sericite, and calcite. Sphene, apatite and ore are common as accessories.	
336	No. 3. 211. 0	Diorite	The rock, with an equigranular, holocrystalline and medium-grained texture, is composed of idiomorphic (usually calcic oligoclase) and biotite. Hysterogene minerals are calcite and chlorite, perfectly replacing the grains of biotite. Sphene is the minor accessory.	

Sample No.	Location	Rock name	Microscopic observation	Remarks
337	No. 3. 224. 8	Granodiorite	The rock shows medium-grained, and weakly porphyritic. Main constituents are plagioclase (generally andesine, subhedral, up to 2 mm, with twin lamellation in the albite type often associated by pericline and Carlsbad type), potassic feldspar (subhedral, up to 1 mm, always perthitic orthoclase), quartz (interstitial, anhedral), brownish biotite (subhedral, up to 0.5 mm) and greenish hornblende (subhedral, columnar, up to 1 mm). Hornblende and biotite have usually been decomposed to calcite and chlorite, respectively. Accessory minerals are sphene, apatite and ore minerals.	
338	DDH-3 236m - 248m	Porphyritic granodiorite	The rock is mainly composed of phenocrystic plagioclase (subhedral, up to 2 mm, twinned after albite, Carlsbad and pericline laws, weakly zoned), and finer-grained interstitial minerals such as quartz (anhedral, up to 0.5 mm), potash feldspar (anhedral, up to 0.5 mm), hornblende (subhedral, up to 0.3 mm, with a pleochroism of X = very pale green to colorless, Y = pale green and Z = green) and biotite (subhedral to anhedral, dark brown variety). Accessory minerals are sphene, apatite, zircon and opaque minerals. Feldspars are sericitized. Hornblende is strongly altered to chlorite and epidote. Biotite is mostly altered to chlorite. Carbonate-filled veinlets cut the rock.	
339	No. 3. 250. 0	Granodiorite	The rock, weakly porphyritic texture, is composed mainly of such minerals as plagioclase (subhedral, up to 2 mm, having an content of Ab 30), perthitic orthoclase, quartz, greenish hornblende and brownish biotite. Secondary alteration products are epidote, calcite and chlorite. Apatite, spene and ore are associated.	
341	No. 4. 18. 5	Quartz monzonite porphyry	Phenocrysts of plagioclase, orthoclase and biotite are in the holocrystalline groundmass of quartz and feldspar. The rock is poor in mafic minerals. Large crystal of plagioclase is euhedral, with the grain size up to 3 mm, generally oligoclase to andesine, weakly zoned, and twinning after albite and Carlsbad law. Saussurization is partly seen. As secondary minerals, carbonate is fairly present. A little sericite is also present. Ore-quartz-calcite veinlets are found.	

Sample No.	Location	Rock name	Microscopic observation	Remarks
342	No. 4. 20. 0	Quartz monzonite porphyry	Phenocrysts of plagioclase (subhedral, up to 3 mm, zoned from oligoclase to andesine) and brownish biotite are present in quartz-feldspathic groundmass. Sausseritization is distinctly observed in plagioclase. Accessories are quartz, carbonate and a little amount of sericite-chlorite.	
344	No. 4. 49. 9	Quartz monzonite porphyry	Phenocrysts of plagioclase (subhedral, up to 3 mm, zoned), potassic feldspar (subhedral, up to 2 mm, perthitic orthoclase) and biotite (idiomorphic, brownish) present in the holocrystalline quartz-feldspathic groundmass. Secondary calcite, chlorite, leucoxene and sericite are found.	
346	No. 4. 63. 5	Quartz monzonite porphyry	Relatively large crystals of plagioclase and sometimes of potassic feldspar, with brownish biotite, are enclosed in a fine-grained crystalline quartz-feldspathic groundmass. Plagioclase is zoned with the composition varying from Ab70 An30 to Ab80 An20, and twinned with idiomorphic character. Potassic feldspar is always perthitic orthoclase. Biotite is subhedral, with brownish tinge. Garnet, calcite and ore are frequently present, and also sericite-chlorite are rarely found.	
347	No. 4. 64. 8m	Quartz monzonite porphyry	Phenocrysts of plagioclase (subhedral, up to 2 mm, generally twinned after albite and Carlsbad laws and less commonly after pericline law, weakly zoned), and microphenocrysts of biotite (subhedral to anhedral and rarely tabular flake up to 0.3 mm, with a pleochroism of X = pale yellow and Y, Z = dark brown) and altered hornblende are in a fine-grained holocrystalline groundmass (up to 0.1 mm in size) of anhedral quartz, potash feldspar and plagioclase. Accessory minerals are apatite, sphene and opaque minerals. Feldspars are weakly to moderately carbonitized and sericitized. Hornblende is completely altered to opaque minerals, carbonates and/or epidote. Biotite is weakly chloritized. Frequently carbonate veinlets cut the rock.	

Sample No.	Location	Rock name	Microscopic observation	Remarks
349	No. 4. 70.0	Quartz monzonite porphyry	The mineral association is porphyritic orthoclase and fine grained quartz with small amount of plagioclase. Veins filled with quartz, calcite and ore are penetrating, and rare sericite is present. The rock is affected by weak deformation.	
350	No. 4. 90.0	Quartz monzonite porphyry	Phenocrysts of plagioclase (subhedral, up to 3 mm, with an An content varying from 40 in the core to 20 at the margin of the grains) associated with perthitic orthoclase and brownish biotite is enclosed in a quartz-feldspathic groundmass with a granular texture. Accessory minerals are sphene and apatite.	
351	No. 4. 131.2	Quartz monzonite porphyry	Phenocrysts of plagioclase (subhedral, up to 2 mm) and biotite (subhedral, perfectly altered to chlorite and carbonate) are present in holocrystalline groundmass of quartz and feldspars. Sausuritization of plagioclase is seen to be distinct. As secondary products, calcite, quartz, clay and a little quartz are found.	
352	No. 4. 142.3	Quartz monzonite porphyry	The texture is hypidiomorphic. Main constituents are plagioclase, potassic feldspar and interstitial quartz. Plagioclase is porphyritic, attaining to be 5 mm, with an An content of 30 to 40. Potassic feldspar is always perthitic orthoclase. Biotite could have been present, but is now decomposed to the aggregates of carbonate, sericite and leucoxene.	
353	No. 4. 166.3	Quartz monzonite porphyry	Phenocrysts of plagioclase (subhedral, up to 3 mm, twinned after and pericline law) with minor amount of perthitic orthoclase are in the groundmass. Biotite has perfectly altered to calcite and leucoxene. Secondary calcite is widely developed. The saussuritization of this rock is strong.	
354	No. 4. 177.3	Quartz monzonite porphyry	Enclosed are phenocrysts of plagioclase, perthitic orthoclase and biotite, in the fine-grained holocrystalline groundmass of quartz and feldspar. Hornblende might occur, but has now been altered to calcite. Plagioclase is zoned and twinned. Epidote and sphene are accessory. Some part of secondary biotite is altered to carbonate, and other is completely fresh.	

Sample No.	Location	Rock name	Microscopic observation	Remarks
355	No.4.183.6	Quartz monzonite porphyry	The texture is porphyritic. Fine-grained groundmass composed of quartz, plagioclase and perthitic orthoclase is enclosing phenocrysts of plagioclase with smaller amount of orthoclase. Porphyritic plagioclase is twinned and zoned. Essential ferromagnesian minerals are pale greenish hornblende and biotite, the former of which has partly been altered into calcite and leucoxene. As an accessory, there are sphene, apatite and ore (magnetite).	
356	DDH 4. 192 - 204m	Quartz monzonite porphyry	The petrographic characters are essentially same as those of the specimen No. 335, but the amount of potash feldspar of the former is much less than that of the latter.	
358	No.4.220.0	Quartz monzonite porphyry	Porphyritic plagioclase (subhedral, up to 3 mm) and potassic feldspar (subhedral, up to 5 mm, perthitic orthoclase, sometimes enclosing plagioclase and quartz) with small amounts of ferromagnesian minerals of pale greenish hornblende and biotite are characteristic. Calcite bearing calcite vein in which magnetite is disseminated and found, and pyrite-chalcocopyrite are disseminated along.	
359	No.4.221.1	Quartz monzonite porphyry	Phenocrysts of plagioclase (subhedral, up to 5 mm) and usually oligoclase) and perthitic orthoclase (not so fragment) are enclosed in the fine-grained groundmass of quartz and feldspars. Biotite and pale greenish hornblende, each of which are partly altered to chlorite and calcite, alternatively, are also essential. A little secondary quartz and sericite are present.	
360	No.4.239.6	Quartz monzonite porphyry	The rock is holocrystalline, equigranular and medium-textured. Main constituents are plagioclase (subhedral, up to 3 mm, usually andesine), perthitic orthoclase (up to 2 mm) and interstitial quartz, with brownish and partly chloritized biotite. Apatite and sphene are also associated.	

Sample No.	Location	Rock name	Microscopic observation	Remarks
362	No. 5. 67. 3	Meta-gabbro	The rock can be separated into two parts. One part is holocrystalline and equigranular. Clinopyroxenes (subhedral, up to 4 mm, partly alters to brownish biotite) cummingtonite (subhedral, up to 4 mm, colorless to pale greenish in tint) and plagioclase (subhedral, up to 1 mm) occur. Large crystal of sphene (up to 2 mm) is characteristic. Another part is also holocrystalline. It contains plagioclase (subhedral, up to 2 mm, commonly labradorite), clinopyroxene (up to 2 mm, with the frake of hornblende) and hornblende (subhedral, brownish green) are common. Cummingtonite is formed secondarily. The rock shows an poikilitic texture by plagioclases enclosed in the hornblende. Hystorogene minerals are epidote and chlorite. Sphene and ore are common accessory minerals.	
363	No. 5. 84. 5	Gabbro	The hypidiomorphic equigranular texture is characteristic. Clinopyroxene, brownish green hornblende and plagioclase (subhedral, up to 3 mm) are the main constituent. Epidote-green amphybole-magnetite veins are found, and also a few of latest calcite veins.	
364	No. 5. 98. 5	Gabbro	The texture is equigranular and hypidiomorphic. Widely developed are idiomorphic clinopyroxene, brownish green hornblende and plagioclase. The grained biotite is produced, due to the break down of hornblende. Greenish amphibole is formed near the margin of the crystals of brownish hornblende in the second stage. Basic core of plagioclase is altered to epidote. Veins filled with epidote, green amphybole and magnetite penetrate the rocks. Accessory sphene and ore are found.	
365	No. 5. 122. 7	Diorite	The texture is seen to be hypidiomorphic and equigranular, having an poikilitic texture formed by plagioclase laths enclosed in the brownish hornblende. The most abundant minerals are plagioclase (subhedral, up to 2 mm, zoned), microcline and hornblende (subhedral, up to 4 mm, with a distinct pleochroism of X = yellowish, Y = reddish brown, Z = reddish brown). Greenish hornblende and brownish biotite formed along the cleavage or surrounding the grains of brownish hornblende may be the product of secondary alteration. Secondary carbonates and chlorite are common. Cummingtonite is also formed. As an accessory minerals, it contains sphene apatite and ore.:	

Sample No.	Location	Rock name	Microscopic observation	Remarks
366	No. 5. 132. 0	Altered diorite	The rock is constituted by idiomorphic plagioclase, biotite and quartz. Aggregates of fine-grained biotite which is fairly fresh but partly weak chloritized, show the effect of secondary thermal alteration. The rock has many fractures, sometimes filled with calcite, and has the strong alteration of carbonitization and sericitization. Carbonate is later stage product than biotite and sericite. Fresh sphene and a little epidote are found.	
367	No. 5. 172. 0	Gabbro	The rock is composed chiefly of common hornblende with brownish tinge. Pale greenish to colorless and fibrous amphibole associated with sulphide develop mantling around the brownish hornblende. Minor amount of sericitized and argillized plagioclase is associated. Secondary chlorite and talc is widely present. Veinlets filled with calcite penetrate.	
369	No. 5. 188. 9	Altered gabbro	The texture is equigranular, holocrystalline and medium grained. Main constituents are acidic plagioclase with Carlsbad and Percline twinning. Sausuritization is to be seen distinctly. Quartz does not attain large size. Calcite, epidote and biotite are formed due to secondary alteration. Biotite is fine-grained and frequently aggregate. Accessories are sphene and ore.	
370	No. 5. 210. 0	Olivine basalt	Phenocrysts of olivine (euhedral to subhedral, tabular, up to 0.5 mm altered wholly to iddingsite and carbonate) and augite (more abundant than olivine, subhedral, up to 1 mm, distinctly zoned) are in a holocrystalline, fine-grained groundmass of lath shaped plagioclase, olivine and augite. Zeolite and carbonate are filling the dressy cavities.	
371	No. 5. 240. 0	Altered diorite	The rock with a holocrystalline texture has the mineral association of feldspars, biotite and quartz. Secondary alteration is so distinct that biotites are perfectly decomposed of chlorite and plagioclase are replaced to sericite. As an accessory mineral, there are ore and apatite.	

Sample No.	Location	Rock name	Microscopic observation	Remarks
372	No. 5. 250. 0	Diorite	Medium grained plagioclase and hornblende are the main constituents. Plagioclase is much saussuritized. Hornblende is brownish in tint but altered to greenish from its fringe. Cummingtonite is also present in place of hornblende. Veins filled with calcite and quartz are penetrating. Sericitization and carbonization of plagioclase along veins are observed, and also chloritization of biotite-hornblende.	
373	No. 6. 31. 0	Hornblende gabbro	The texture is equigranular and holocrystalline. Hornblende encloses the feldspar crystals, giving an poikilitic texture. Idiomorphic plagioclase (weak sericitized) is bytownite to labradorite with the twin lamellation of the albite type often accompanied by Carlsbad and pericline types. Individual hornblende crystal is so large as to reach 10 mm, showing distinct pleochroism of X = yellowish, Y = brownish, Z = greenish brown. Cummingtonite also occurs in a second stage. Essential biotite had been presented but must be recrystallized to the masses of fine-grained biotite, which now has partly been altered to chlorite along calcite veinlets. Hysterogene carbonate (crack or parting filling veinlets) and chlorite are present.	
374	No. 6. 74. 8	Calcite vein	It is composed of large amount of calcite and quartz. Secondary chlorite has been scattered. The texture is equigranular. Some sulphides can be observed.	
375	No. 6. 80. 5	Altered diorite	The rock has composed mainly of plagioclase, perthitic orthoclase and fine-grained matrix. It is altered to give the assemblage of biotite and actinolite (biotite > actinolite). As a hysterogene mineral, there occurs greenish chlorite and carbonate. Accessory minerals are sphene and ore.	
376	No. 6. 93. 3	Hornblende gabbro	The rock is holocrystalline, hypidiomorphic-granular texture. Plagioclase is frequently twinned. Subhedral clinopyroxene occur mantled with greenish hornblende. Essential greenish brown hornblende and biotite has partly been decomposed to biotite of fine-grained.	

Sample No.	Location	Rock name	Microscopic observation	Remarks
377	No. 6. 97.0	Hornblende gabbro	Essential constituent minerals are clinopyroxene, hornblende and plagioclase. Large crystal of brownish hornblende always enclosed lath-shaped plagioclase showing poikilitic texture. Clinopyroxene is mantled by greenish hornblende. Plagioclase is twinned after albite, Pericline and Carlsbad law. Commonly developed are fine-grained aggregates of brownish biotite, due to the secondary thermal effect. Cummingtonite also occurs replacing the grain of brownish hornblende. Chlorite, carbonate, epidote and a little sulphide are hyserogene. Secondary biotite and magnetite are fairly rich.	Secondary alteration product of epidote (fairly rich), carbonate, sulphide and chlorite are formed universally. Accessory minerals are sphene, minor amount of sericite, and ore.
378	No. 6. 113.7	Hornblende gabbro	The mineral association is hornblende (with ophitic texture, up to 5 mm, with a pleochroism of X = brown, Y = greenish brown, Z = brown), clinopyroxene (subhedral, altered to hornblende from its margin) and plagioclase (subhedral, with and average grain size of 1 mm, sometimes porphyritic, zoned). Biotite is also essentially present, but not so fragment. Secondary biotite of fine-grained occur, along the veinlets or replacing essential ferromagnesian minerals. Cummingtonite is produced in the second stage. Magnetite is replaced to a little sulphide associated with epidote-chlorite.	
379	No. 6. 114.4	Hornblende gabbro	The rock is equigranular and medium-grained. Some hornblende attain a large size of 6 mm, enclosing of plagioclase. Plagioclase is zoned, mainly labradorite but having the core of bytownite and twinned. Clinopyroxene, sometimes having a "schiller" striation is mantled by brownish green hornblende. Secondary cummingtonite and biotite replace the primary hornblende. The rock may be suffered by the thermal alteration. Two kind of veinlets (one of latest carbonate veinlet, other of sulphide ore-chlorite-(calcite)-(quartz)-veinlet) are observed and chlorite (after biotite) are observed.	

Sample No.	Location	Rock name	Microscopic observation	Remarks
380	No. 6. 116. 0	Gabbro	The rock is composed mainly of orthopyroxene, clinopyroxene and olivine. Widely developed are secondary minerals such as talc and cummingtonite. Fairly amounts of muscovite-sericite are also present. Hysterogene minerals are carbonates-quartz, chlorite and serpentinite.	
381	No. 6. 117. 0	Altered diorite	The rock is equigranular, composed essentially of plagioclase, biotite and hornblende. Fine grained aggregates of biotite occur perfecting essential mafic minerals. It contains minor accessory of sphene and ore (chalcopyrite or bornite). Last stage alteration products are epidote, chlorite and carbonate. The rock is affected by the weak alteration.	
382	No. 6. 128. 0	Gabbro	Hypidiomorphic, granular texture is seen. Most frequently occur clinopyroxene (subhedral to euhedral, up to 10 mm; partly replaced by colorless amphibole), and plagioclase (subhedral, up to 2 mm). A grain of brownish hornblende is also present. Several aggregates of biotite-ore (magnetite) replacing mafic minerals are present, and large sulphide-magnetite and calcite-sulphide-epidote ore, too. Hydrothermal product of the final stage is a little of chlorite, sericite and epidote. A few of this veinlets of calcite cut the ore.	
383	No. 6. 135. 6	Gabbro	The texture is seen to be equigranular, hypidiomorphic and medium-grained. Main constituents are discrete crystals of plagioclase (subhedral, up to 1 mm, having a central core of bytownite decreasing of An content at the edges), clinopyroxene (subhedral, up to 1 mm, sometimes retains in the core of hornblende) and hornblende (enclosing plagioclase to give poikilitic texture, up to 3 mm, with a pleochroism of X = brown, Y = greenish brown Z = greenish brown, down-graded to greenish amphibole). Small amount of secondary biotite and chlorite (after biotite) are observed. Two kind of ore (one of sulphide-calcite-quartz, other of magnetite-secondary biotite). Biotite occurs secondarily, in place of clinopyroxene and hornblende, suggesting the thermal effect.	

Sample No.	Location	Rock name	Microscopic observation	Remarks
384	No. 6. 166. 1	Gabbro	Main constituent mineral is plagioclase, brownish hornblende and clinopyroxene. Plagioclase has an An content of 70. And is some- times enclosed in clinopyroxene. Cummingtonite is widely formed in the second stage. Colorless amphibole is also found. Olivine might have been present, but has now been decomposed. Chlorite and carbonates are hysterozene.	
385	No. 6. 234. 0	Gabbro	The rock is composed mainly of plagioclase (usually labradorite) and brownish hornblende with a poikilitic texture. Essential clinopyroxene and biotite may be present. Secondary biotite and colorless amphibole occur, due to the thermal effect. Sericite, carbonate and chlorite are hysterozene minerals. Quartz bearing sulphide-calcite vein are observed.	
386	No. 6. 237. 6	Gabbro	Main constituents are plagioclase (subhedral, up to 2 mm, zoned), hornblende (subhedral, up to 3 mm, with poikilitic texture enclosing plagioclase, showing a distinct pleochroism of X = brownish, Y = deep brown, Z = greenish brown). Fine grained aggregates of biotite and colorless amphibole (disseminated magnetite with them) are suggested the secondary thermal alteration on the rock. Also discernible are signs of deformation such as penetrating veinlets of twisted plagioclase (montmorillonite and sericitization along veins) quartz with wavy extinction and carbonate. Sausuritization of plagioclase is seen to be distinct. Barren quartz-calcite veins are present.	
388	No. 6. 250. 3	Hornblende gabbro	The most abundant minerals are plagioclase, hornblende and clinopyroxene. Plagioclase has zoned texture and twinning. Hornblende shows brownish tint, with subhedral shape. Greenish hornblende may be secondary. Penetrate veins filled with quartz and carbonate. Ore is magnetite only.	

Sample No.	Location	Rock name	Microscopic observation	Remarks
29	C-17M	Monzonite porphyry	Principal ore mineral is subhedral to euhedral pyrite. As accessory minerals, minor amounts of molybdenite is also present. Subhedral to euhedral pyrite occur as veinlets in acidic volcanics (or plutons).	
29	C-17M(P)	Monzonite porphyry	Principal ore mineral is subhedral to euhedral pyrite. As accessory minerals, chalcopyrite is included in pyrite. Pyrite veinlets with orientation are characteristic of the specimen.	
30	C-20R	Granodiorite	Principal ore minerals are chalcopyrite and magnetite. As accessory minerals, pyrite and hematite, replacing magnetite, are present. Chalcopyrite and magnetite occur as dissemination. Magnetite with minor hematite are euhedral to subhedral.	
55	F'-37M	Granodiorite	Principal ore minerals are galena with minor amounts of covellite rim. Galena occurs as dissemination. Colloform texture displayed by gangue is well-developed.	
64	G'-18M	Iron oxide	Principal ore minerals are chalcopyrite, hematite and pyrite. Chalcopyrite is replaced and rimmed by secondary minerals such as covellite. Bladed hematite occurs as vein-filling materials. Ore textures suggest that specular hematite may be considered to be of late stage than that of chalcopyrite and pyrite.	
66	G-21M	Magnetite skarn	Principal minerals are magnetite and hematite. As accessory minerals, pyrite is present. Magnetite intergrown with hematite by which magnetite is partially replaced. Some magnetite completely replaced by newly-formed bladed hematite.	
74	G'-21M	Magnetite skarn	Principal ore mineral is magnetite. As accessory minerals, hematite is present. Magnetite with euhedral form or bladed shape is partially replaced by hematite along the fracture in magnetite grain.	
87	I'-24R	Skarn	Principal ore mineral is bladed and irregularly-shaped hematite. As accessory minerals, relict of pyrite and magnetite is also observed.	

Sample No.	Location	Rock name	Microscopic observation	Remarks
89	I'-40(2M)	Iron ore	Principal ore minerals are hematite and magnetite. Hematite pseudomorph after magnetite is characteristic. Replace rimnant of magnetite exists in a small amount.	
93	I'-25M	Magnetite skarn	Principal ore mineral is magnetite. As accessory minerals, chalcopyrite and pyrite grains are included in magnetite host. Magnetite occurs as veinlets, spacefilling materials, and as dissemination. Lattice-like hematite in magnetite is characteristic.	
128	N'-22(S1)	Magnetite skarn	As principal ore minerals, hematite and magnetite are present. As accessory minerals, chalcopyrite occurs in a small amounts. Magnetites are observed to be replaced or cross-cut by (secondary) hematite.	
201	Trench	Copper sulphide ore	Principal ore mineral is bornite. As accessory minerals, covellite and supergene minerals are observed to replace bornite. Replace remnant of bornite is a mass with finely rhythmic band is characteristic.	
202	Trench	Copper sulphide ore	Principal ore mineral is bornite. As accessory mineral, covellite and anisotropic phase (unidentified) are present. They occur at the bornite margin, suggestively the secondary formation.	
302	No.1. 63.6	Porphyritic granodiorite	Principal ore minerals are pyrite, specular hematite, and chalcopyrite. Euhedral to subhedral pyrite and bladed hematite are common. Pyrite-hematite veinlet is associating with a small amount of chalcopyrite. Chalcopyrite including small pyrites is cross-cut by chalcocite.	
303	No.1. 64.3	Molybden bearing porphyrite granodirite	Principal ore minerals are specular hematite and pyrite. Molybdenite may be present in small amounts. Because of much difficulty of making polished section of the specimen, microscopic observation was impossible to do.	

Sample No.	Location	Rock name	Microscopic observation	Remarks
309	No. 1. 141. 7	Cataclastic granodiorite	Principal ore mineral is hematite. As accessory minerals, magnetite is also present. Needle-like hematite with a minor amounts of magnetite occurs as vein and dissemination.	
311	No. 1. 231. 3	Cataclastic granodiorite	Principal ore minerals are pyrite and specular hematite. Euhedral to subhedral pyrite with or without bladed hematite occur as veinlets in volcanics. Cataclastic texture is characteristic of hematite.	
313	No. 2. 60. 5	Copper bearing monzonite porphyry	Principal ore minerals are pyrite and chalcopyrite. Pyrite shows euhedral to subhedral. As accessory mineral, covellite is present. Chalcopyrite is replaced and rimmed by tiny covellite, occurring as dissemination.	
314	No. 2. 74. 0	Copper bearing hornfels	Almost all of ore mineral is chalcopyrite in various grain size. Chalcopyrite, obliquely cutting or in part paralleling with the band of wall rock, occurs as veinlet as dissemination.	
316	No. 2. 117. 5	Molybden & copper bearing monzonite porphyry	Principal ore minerals are chalcopyrite and pyrite. As accessory mineral a minor molybdenite is present. They occur as veinlets is present. They occur as veinlets or dissemination. Pyrite is euhedral to subhedral shape.	
318	No. 2. 158. 9	Copper bearing hornfels of sandstone	Principal ore mineral is subhedral to anhedral pyrite. As accessory minerals small amounts of chalcopyrite are present. They occur as dissemination or fine veinlets.	
319	No. 2. 172. 6	Copper bearing granodiorite	Principal ore minerals are pyrite and chalcopyrite. As accessory minerals, hematite and molybdenite are present. A part of euhedral to subhedral pyrite and chalcopyrite in association with small molybdenite occur as dissemination. Molybdenite or hematite with pyrite are filling veinlets.	

Sample No.	Location	Rock name	Microscopic observation	Remarks
320	No. 3. 41. 1	Magnetite bearing gabbro	Principal ore mineral is magnetite. Magnetite is subhedral to euhedral shape. As accessory minerals, hematite is also present. Exsolution-like texture, that is lattice intergrowth of magnetite and hematite is often observed. Such a texture is considered to be formed due to oxidation of magnetite. Magnetite occurs as dissemination or separate grains.	
324	No. 3. 91. 6	Lead & copper bearing gabbro	Principal ore minerals are chalcocopyrite and pyrite. As accessory minerals, a minor amount of galena is present. Chalcocopyrite associating with euhedral to subhedral pyrite occurs as veinlets and dissemination in limestone recrystallized.	
325	No. 3. 96. 1	Copper bearing skarn	Principal ore minerals are bornite and chalcocopyrite. As accessory minerals, minor amounts of secondary phase, chalcocite, is observed to replace bornite. Bornite in association with chalcocopyrite occurs as space-filling materials and as dissemination, often cut by secondary veinlets. Bornite with or without chalcocopyrite is also present in the carbonate vein.	
327	No. 3. 107. 7	Copper bearing limestone	Principal ore minerals are bornite and chalcocite. As accessory minerals, small amounts of covellite replacing bornite is observed. Bornite myrmekitic (?) intergrowth with chalcocite occurs as dissemination in the recrystallized limestone.	
330	No. 3. 136. 7	Copper bearing skarn	Principal ore minerals are bornite, chalcocopyrite and chalcocite. As accessory minerals, a minor covellite is present. Bornite grain with or without chalcocopyrite has rim as a results of replacement, occurring as veinlets or dissemination in the granite, garnet skarn.	
341	No. 4. 18. 5	Quartz monzonite porphyry	Principal ore minerals are bornite, chalcocopyrite and partially oxidized magnetite. Euhedral to subhedral magnetite which is partially or entirely replaced by hematite occur as dissemination. Chalcocopyrite associating with bornite occurs as veinlets and dissemination.	

Sample No.	Location	Rock name	Microscopic observation	Remarks
347	No. 4. 64.8	Quartz monzonite porphyry	Principal ore minerals are bornite and chalcopyrite. As accessory minerals, hematite pseudomorph after magnetite is also present. Small amounts of chalcocite is included in bornite. Bornite with or without chalcopyrite occurs as veinlet and dissemination.	
349	No. 4. 70	Quartz monzonite porphyry	Principal ore minerals are chalcopyrite and bornite. As accessory minerals, minor molybdenite in association with chalcopyrite and bornite is present. Bornite intimately intergrown with chalcopyrite occurs as space-filling materials or veinlets.	
353	No. 4. 166. 3	Quartz monzonite porphyry	Principal ore minerals are chalcopyrite and hematite. Hematite replacing magnetite occurs as separate grain, while chalcopyrite with or without hematite pseudomorph as dissemination.	
354	No. 4. 177. 3	Copper bearing monzonite porphyry	Principal ore minerals are chalcopyrite and magnetite. Magnetite which is partially replaced by hematite occurs as dissemination, while chalcopyrite as dissemination and space-filling materials.	
358	No. 4. 220	Copper bearing quartz monzonite porphyry	Principal ore minerals are chalcopyrite and magnetite. As accessory minerals, small amounts of pyrite is included in chalcopyrite, Hematite occurs as replacement of magnetite. Chalcopyrite with minor pyrite occurs as dissemination, while magnetite with or without chalcopyrite as dissemination and veinlets.	
362	No. 5. 67. 3	Meta-gabbro	Principal ore minerals are bornite, chalcopyrite and magnetite. As accessory minerals, hematite partially replacing magnetite is present. Bornite occurs as veinlets and dissemination, while magnetite as separate grains. Bornite replaced by chalcocite, is characteristic.	
363	No. 5. 84. 5	Gabbro	Principal ore minerals are magnetite and chalcopyrite. As accessory minerals, small amounts of pyrite with chalcopyrite is present. Minor amounts of hematite occurs as replacement of magnetite. Chalcopyrite with or without magnetite occurs as space-filling materials, while magnetite as dissemination and separate grain.	

Sample No.	Location	Rock name	Microscopic observation	Remarks
364	No. 5. 98. 5	Gabbro	Principal ore minerals are chalcopyrite, pyrite and magnetite. As accessory minerals, bornite in association with chalcopyrite is present. Small molybdenite is also found. Magnetite partially replaced by hematite occurs as dissemination, while chalcopyrite with or without magnetite as space-filling materials.	
365	No. 5. 122. 7	Diorite	Principal ore minerals are chalcopyrite, magnetite and pyrite. Magnetite is partially oxidized to hematite. Chalcopyrite with or without pyrite and magnetite occurs as veinlets and dissemination.	
366	No. 5. 132. 0	Altered diorite	Principal ore minerals are bornite, chalcocite and molybdenite. As accessory minerals, small chalcopyrite associating with bornite in present. Bornite-chalcocite with or without molybdenite occurs as veinlets and dissemination.	
367	No. 5. 172. 0	Copper bearing gabbro	Principal ore minerals are pyrite, chalcopyrite and magnetite. Chalcopyrite associating with pyrite and/or magnetite occurs as veinlets and as dissemination.	
369	No. 5. 188. 9	Altered gabbro	Principal ore minerals are chalcopyrite, bornite and magnetite. Myrmekitic intergrowth of chalcopyrite and bornite is observed. Chalcopyrite in association with bornite and or magnetite occurs as dissemination and interstice-filling materials.	
373	No. 6. 31. 0	Copper bearing hornblende gabbro	Principal ore minerals are bornite, magnetite and chalcopyrite. Subhedral to euhedral magnetite occur as dissemination, while bornite with exsolution of chalcopyrite in the form of lamellae as veinlet.	
374	No. 6. 74. 8	Calcite-vein	Principal ore minerals are chalcopyrite, pyrite and hematite pseudomorph after magnetite. As accessory minerals, minor tetrahedrite bleb is included in chalcopyrite. Concentration of euhedral to subhedral pyrite is characteristic of this specimen. Chalcopyrite in association with pyrite occurs as veinlets or as dissemination.	

Sample No.	Location	Rock name	Microscopic observation	Remarks
375	No. 6. 80.5	Altered diorite	Principal ore minerals are chalcopyrite and magnetite. As an accessory mineral, pyrite is present. Chalcopyrite in association with subhedral to euhedral magnetite and/or pyrite occurs as veinlets and dissemination.	
376	No. 6. 93.3	Copper bearing hornblende gabbro	Principal ore minerals are chalcopyrite, magnetite and bornite. As an accessory mineral, a minor amount of hematite replacing magnetite is present. Chalcopyrite associating with magnetite and bornite occurs as vein-filling or interstice-filling materials. Magnetite is euhedral to subhedral in form.	
377	No. 6. 97.0	Copper bearing hornblende gabbro	Principal ore minerals are magnetite, bornite and chalcopyrite. As accessory minerals, small amounts of pyrite, sphalerite and chalcocite are present. Bornite with or without subhedral to euhedral magnetite occurs as veinlet and dissemination. Magnetite is partially replaced by hematite.	
379	No. 6. 114.4	Hornblende gabbro	Principal ore minerals are chalcopyrite, bornite and magnetite. Almost of all chalcopyrite intergrown with bornite occur as veinlets, while subhedral grains of magnetite as dissemination. The stage of deposition of Fe-O assemblage is thought to be different from that of Cu-Fe-S assemblage.	
381	No. 6. 117.0	Altered diorite	Principal ore minerals are chalcopyrite and pyrite. As accessory minerals, a small amount of magnetite is present. Chalcopyrite associating with euhedral to subhedral pyrite occurs as veinlet- or interstice- filling materials.	
385	No. 6. 234.0	Gabbro	Principal ore minerals are magnetite and chalcopyrite. As accessory minerals, bornite and hematite replacing magnetite are present. Subhedral to euhedral magnetite occurs as separate grain, while chalcopyrite with bornite as veinlet and dissemination.	
388	No. 6. 250.3	Hornblende gabbro	Principal ore minerals are magnetite and bornite. As accessory minerals, a small amount of chalcopyrite and chalcocite intergrown with bornite are present. Subhedral to euhedral magnetite with or without bornite occurs as veinlet and dissemination.	

Table I-11 List of photographs

Thin section

Sample No.	Location	Rock name
1	Z-11	Meta diorote
29	C-17M	Quartz monzonite
87	I-24R	Skarn
103	K-19S ₁	Granite porphyry
118	M'-15S ₂	Diorite
165	Q-23N ₃	Meta gabbro
304	No. 1 68.0	Granodiorite
309	No. 1 141.7	Cataclastic granodiorite
312	No. 2 50.5	Quartzite
314	No. 2 74.0	Hornfels of slate
316	No. 2 117.5	Granite porphyry
317	No. 2 152.0	Olivine basalt
319	No. 2 172.6	Granodiorite
321	No. 3 50.0	Quartz diorite
322	No. 3 87.7	Limestone
325	No. 3 96.1	Skarn
332	No. 3 164.3	Hornfels of calcareous sandstone
333	No. 3 171.3	Aplite
334	NO. 3 175.0	Gabbro
367	No. 5 172.0	Gabbro



Sample No. 1

Rock Name
Meta-diorite

Location
Z-11

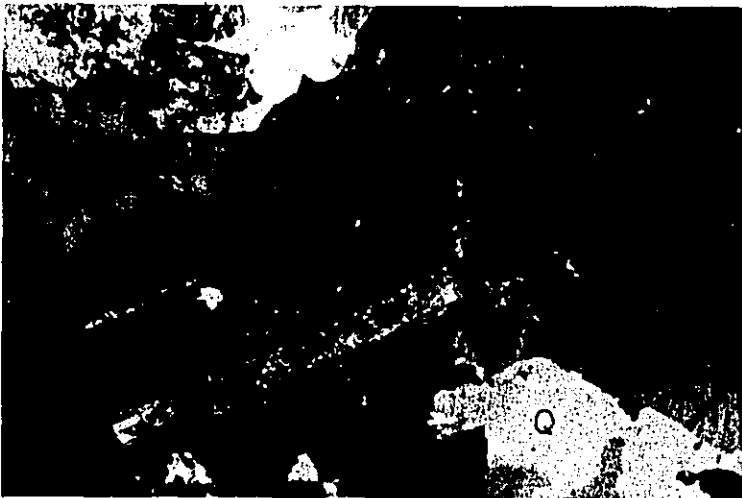
Hb : Brownish
hornblende

P : Plagioclase

A : Colorless
amphibole

Scale 1 mm

Crossed Nicols



Sample No. 29

Rock Name
Quartz monzonite

Location
C-17M

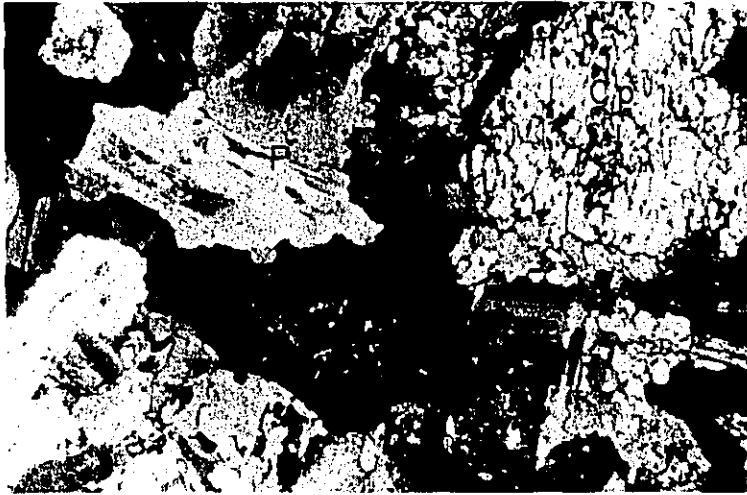
Q : Quartz

P : Plagioclase

K : K-feldspar

Scale 1 mm

Crossed Nicols



Sample No. 118

Rock Name
Diorite

Location
M'-15 S2

P : Plagioclase

Cp : Clinopyroxene

Scale 1 mm

Crossed Nicols



Sample No. 165

Rock Name
Meta-gabbro

Location
Q-23N3

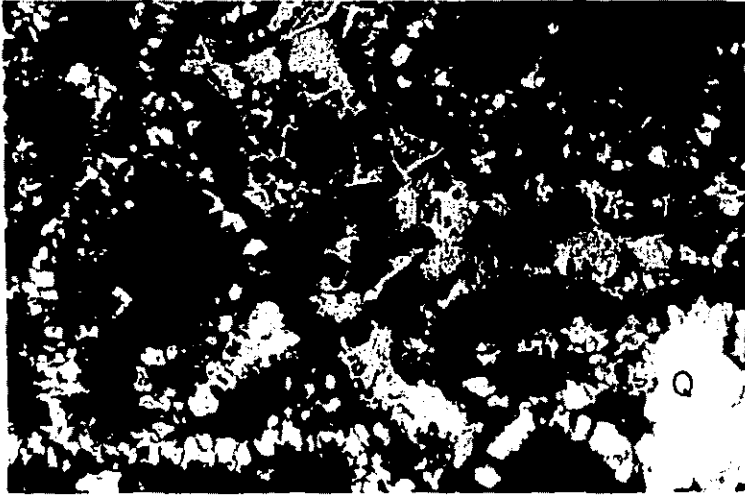
P : Plagioclase

Hb : Hornblende

Cp : Clinopyroxene

Scale 1 mm

Crossed Nicols




Sample No. 87

Rock Name
Skarn

Location
I-24R

Q : Quartz

M : Malachite

Scale  1 mm

Crossed Nicols




Sample No. 103

Rock Name
Granite porphyry

Location
K-19 S1

P : Plagioclase

Hb : Hornblende

Scale  1 mm

Crossed Nicols



Sample No. 304

Rock Name
Granodiorite

Location
DDH 1, 68.0m

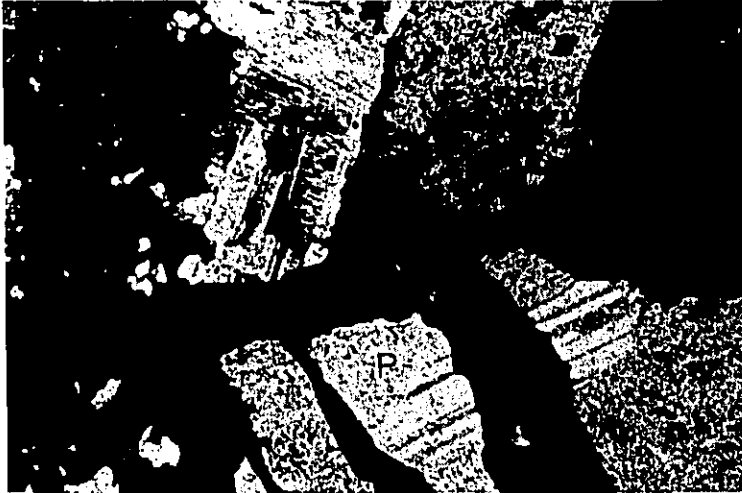
P : Plagioclase

K : K-feldspar

Hb : Hornblende

Scale 1 mm

Crossed Nicols



Sample No. 309

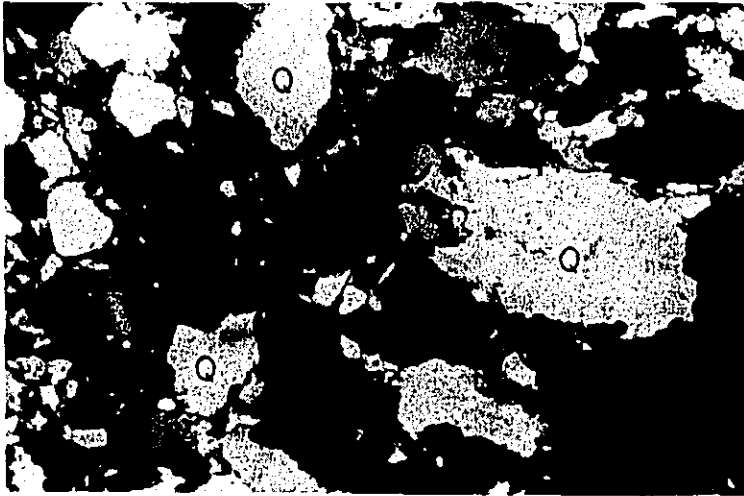
Rock Name
Cataclastic
Granodiorite

Location
DDH 1, 141.7m

P : Plagioclase

Scale 1 mm

Crossed Nicols



Sample No. 312

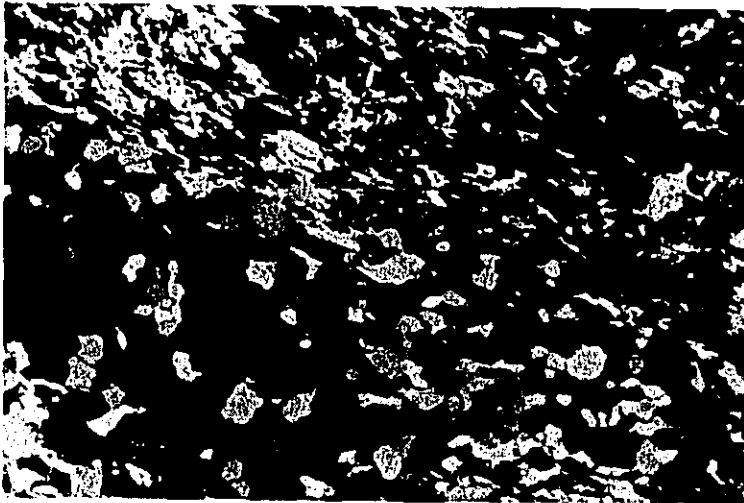
Rock Name
Quartzite

Location
DDH 2, 50.5m

Q : Quartz

Scale 1 mm

Crossed Nicols



Sample No. 314

Rock Name
Hornfels of slate

Location
DDH 2, 74.0m

Q : Quartz

W : White mica

Scale 1 mm

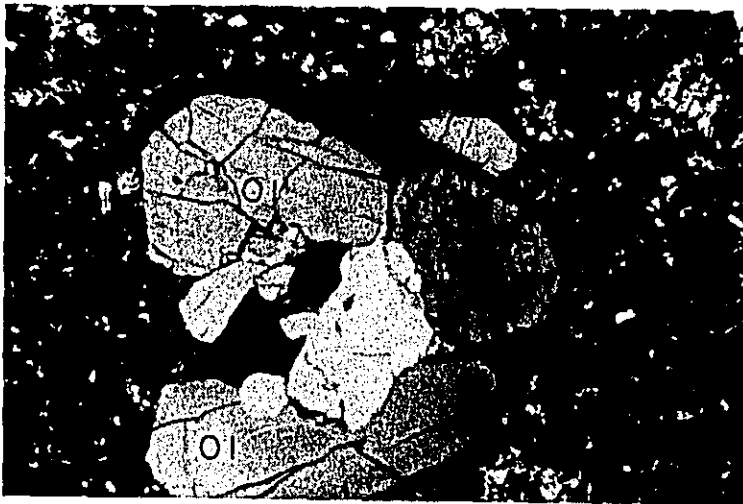
Crossed Nicols



Sample No. 316
Rock Name
Granite porphyry
Location
DDH 2, 117.5m
P : Plagioclase

Scale 1 mm

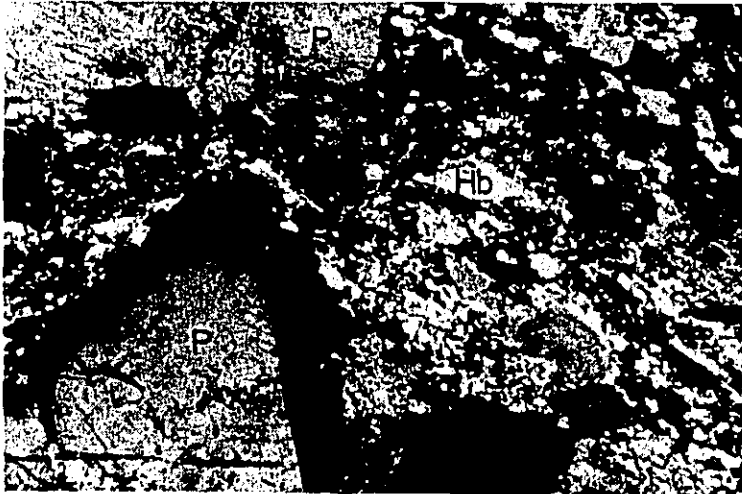
Crossed Nicols



Sample No. 317
Rock Name
Olivine basalt
Location
DDH 2, 152.0m
Cp : Clinopyroxene
Ol : Olivine

Scale 1 mm

Crossed Nicols



Sample No. 319

Rock Name
Granodiorite

Location
DDH 2, 172.6m

P : Plagioclase

Hb : Hornblende

Scale 1 mm

Crossed Nicols



Sample No. 321

Rock Name
Quartz diorite

Location
DDH 3, 50.0m

Q : Quartz

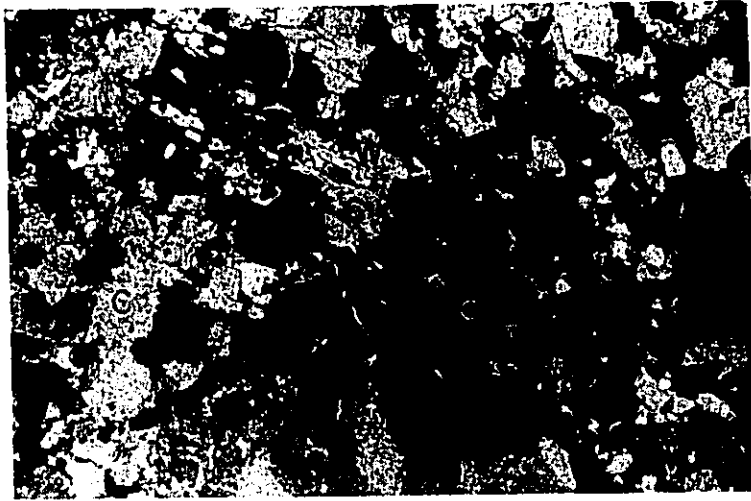
P : Plagioclase

Hb : Hornblende

B : Biotite

Scale 1 mm

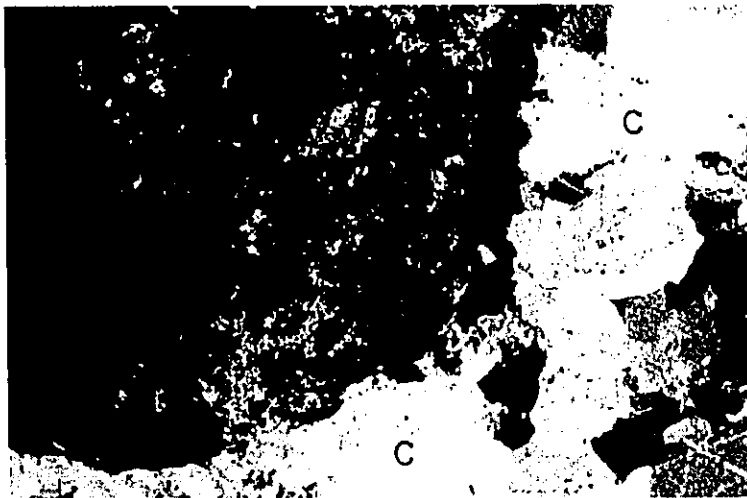
Crossed Nicols



Sample No. 322
Rock Name
Limestone
Location
DDH 3, 87.7m
C : Calcite
W : White mica

Scale 1 mm

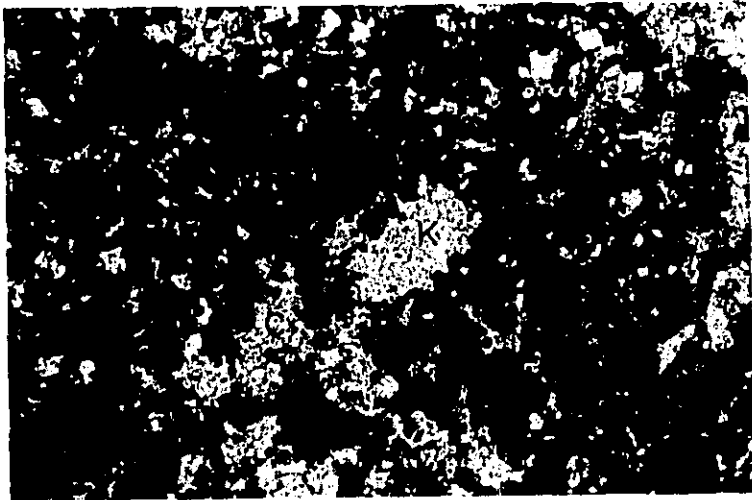
Crossed Nicols



Sample No. 325
Rock Name
Skarn
Location
DDH 3, 96.1m
C : Calcite
G : Garnet

Scale 1 mm

Crossed Nicols



Sample No. 332

Rock Name
Hornfels of
calcareous
sandstone

Location
DDH 3, 164.3m

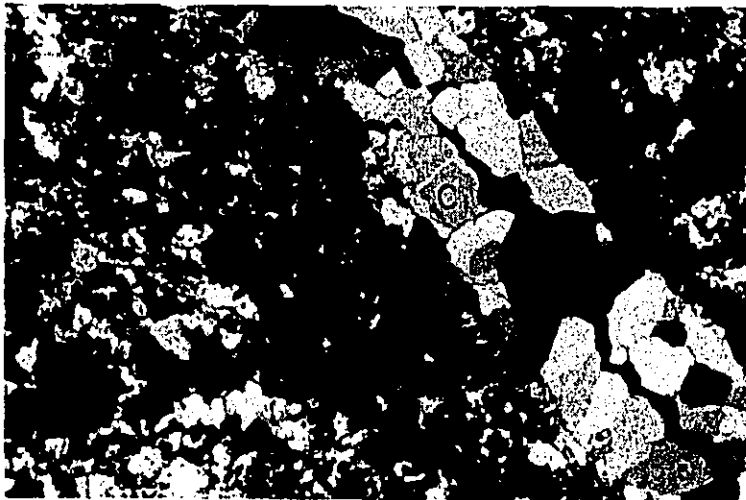
K : K-feldspar

Q : Quartz

C : Calcite

Scale 1 mm

Crossed Nicols



Sample No. 333

Rock Name
Aplite

Location
DDH 3, 171.3m

P : Plagioclase

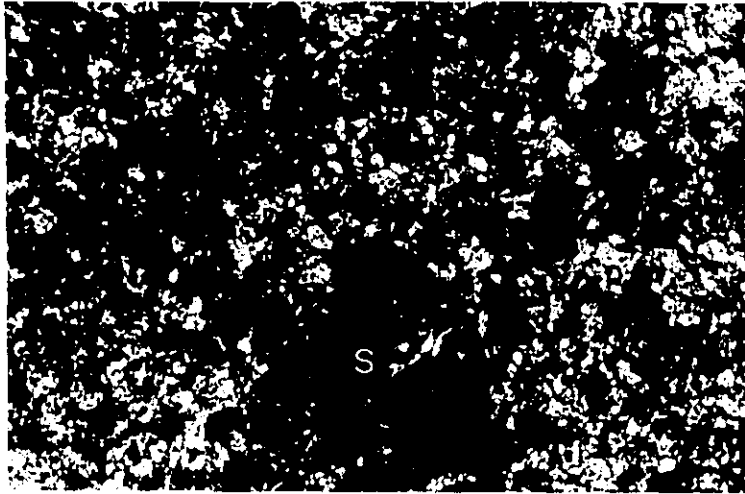
K : K-feldspar

Q : Quartz

C : Calcite vein

Scale 1 mm

Crossed Nicols



Sample No. 334

Rock Name
Gabbro

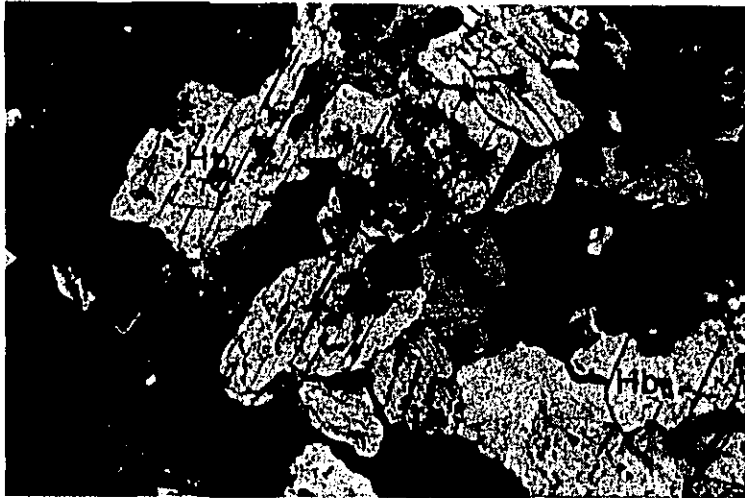
Location
DDH 3, 175.0m

Cp : Clinopyroxene

S : Serpentine
aggregate

Scale  1 mm

Crossed Nicols



Sample No. 367

Rock Name
Gabbro

Location
DDH 5, 172.0m

Hb : Hornblende

P : Plagioclase

Scale  1 mm

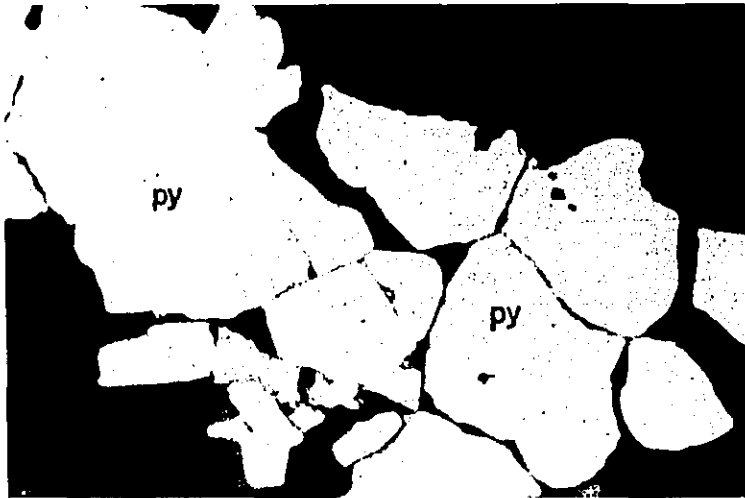
Crossed Nicols

Table I-11 List of microphotographs

Polished section

Sample No.	Location	Rock name
29	C-17M	Monzonite porphyry
29	C-17MP	Monzonite porphyry
30	C-20R	Granodiorite
55	F'-37	Granodiorite
64	G'-18M	Iron oxide
68	G-21M	Green copper
74	G'-21M	Magnetite skarn
74	G'-21(2M)	Magnetite skarn
87	I'-24	Skarn
89	I'-40(2M)	Iron ore
93	I'-25M	Magnetite skarn
128	H'-22S1	Magnetite skarn
201	Trench pit	Copper sulphide ore
202	Trench pit	Copper sulphide ore
302	DDH 1. 63.6	Granodiorite
309	DDH 1. 141.7	Cataclastic granodiorite
311	DDH 1. 231.3	Cataclastic granodiorite
313	DDH 2. 60.5	Monzonite porphyry
314	DDH 2. 74.0	Hornfels of slate
316	DDH 2. 117.5	Monzonite porphyry
318	DDH 2. 158.9	Hornfels of sandstone
319	DDH 2. 172.6	Granodiorite
320	DDH 3. 41.1	Gabbro
324	DDH 3. 91.6	Skarn
325	DDH 3. 96.1	Skarn
327	DDH 3. 107.7	Limestone
330	DDH 3. 136.7	Skarn

Sample No.	Location	Rock name
341	DDH 4. 18.5	Quartz monzonite porphyry
347	DDH 4. 64.8	Quartz monzonite porphyry
349	DDH 4. 70.0	Quartz monzonite porphyry
353	DDH 4. 166.3	Quartz monzonite porphyry
354	DDH 4. 177.3	Quartz monzonite porphyry
358	DDH 4. 220.0	Quartz monzonite porphyry
362	DDH 5. 67.3	Meta gabbro
363	DDH 5. 84.5	Gabbro
364	DDH 5. 98.5	Gabbro
365	DDH 5. 122.7	Diorite
366	DDH 5. 132.0	Altered diorite
367	DDH 5. 172.0	Gabbro
369	DDH 5. 188.9	Altered gabbro
373	DDH 6. 31.0	Hornblende gabbro
374	DDH 6. 74.8	Calcite vein
375	DDH 6. 80.5	Altered diorite
376	DDH 6. 93.3	Hornblende gabbro
377	DDH 6. 97.0	Hornblende gabbro
379	DDH 6. 114.4	Hornblende gabbro
381	DDH 6. 117.0	Altered diorite
385	DDH 6. 234.0	Gabbro
388	DDH 6. 250.3	Hornblende gabbro



Sample No. 29

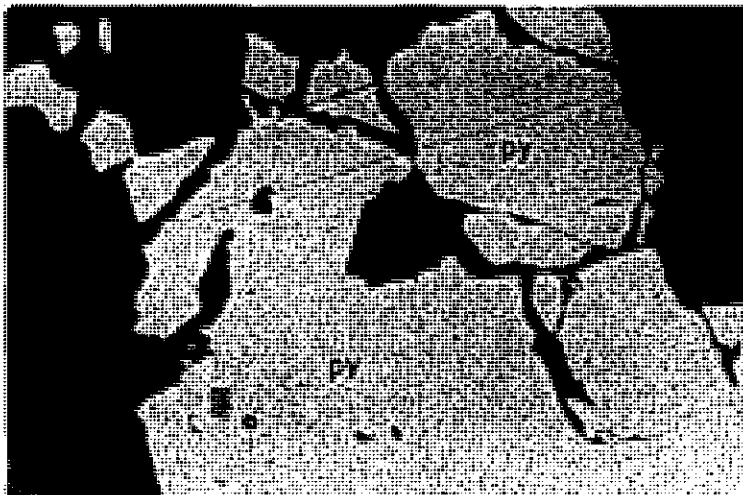
Rock name
Monzonite
porphyry

Location
C-17M

Py : Pyrite

Scale

0.5 mm



Sample No. 29

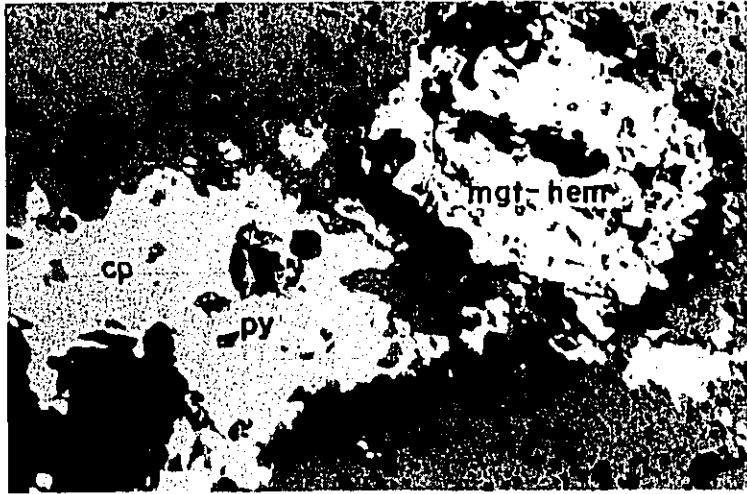
Rock name
Monzonite
porphyry

Location
C-17MP

Py : Pyrite

Scale

0.5 mm



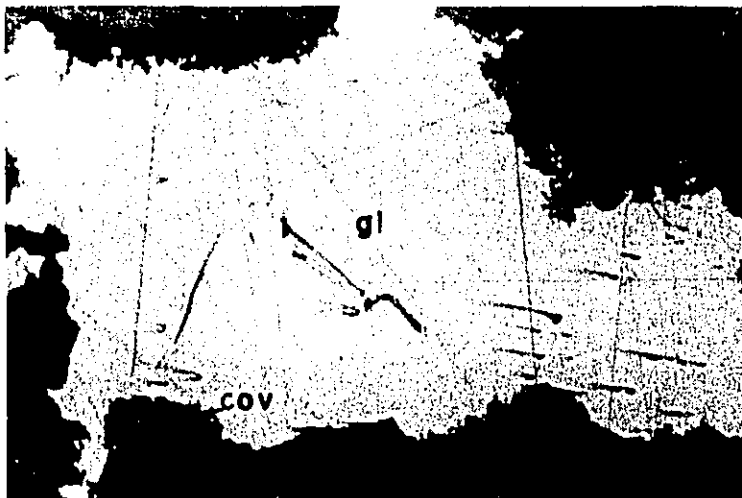
Sample No. 30

Rock name
Granodiorite

Location
C-20R

Cp : Chalcopyrite
Py : Pyrite
Mgt : Magnetite
Hem : Hematite

Scale _____ 0.5 mm



Sample No. 55

Rock name
Granodiorite

Location
F'-37

Gl : Galena
Cov. : Covelline

Scale _____ 0.5 mm



Sample No. 64

Rock name
Iron oxide

Location
G'-18M

Cp : Chalcopyrite

Hem : Hematite

Scale

0.5 mm



Sample No. 68

Rock name
Green copper

Location
G-21M

Hem : Hematite

Mgt. : Magnetite

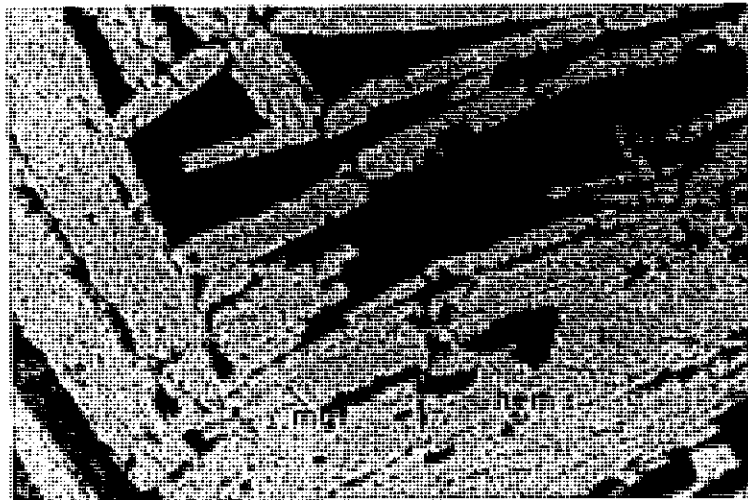
Scale

0.5 mm



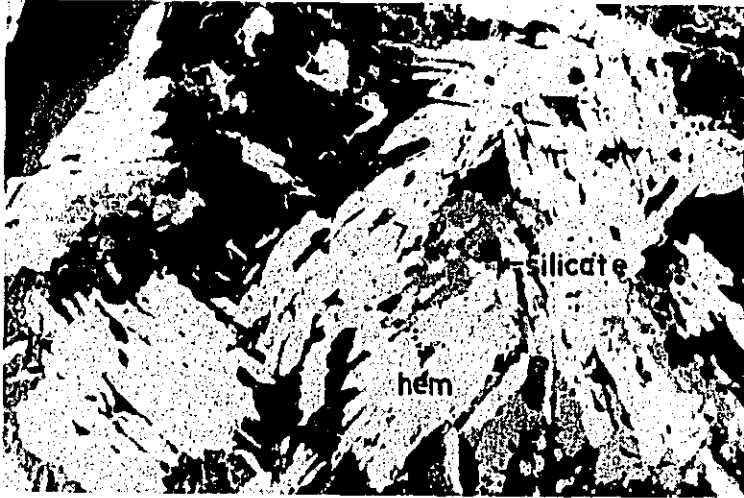
Sample No. 74
Rock name
Magnetite skarn
Location
G'-21M
Mgt : Magnetite
Hem : Hematite

Scale 0.5 mm



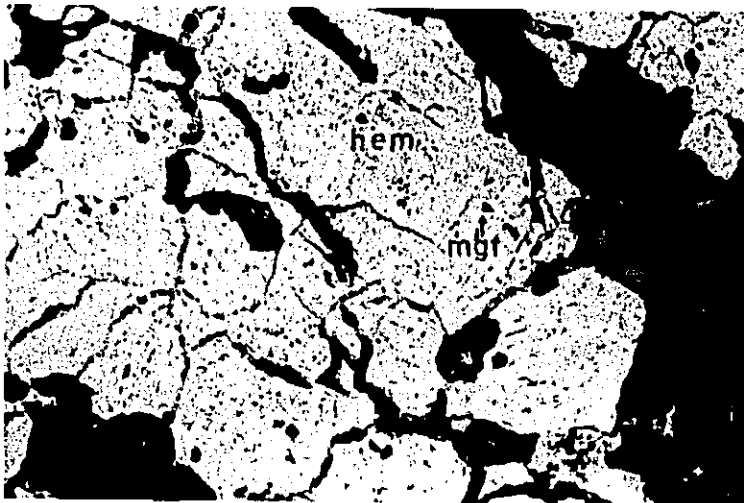
Sample No. 74
Rock name
Magnetite skarn
Location
G'-21M
Hem : Hematite
Mgt. : Magnetite

Scale 0.5 mm



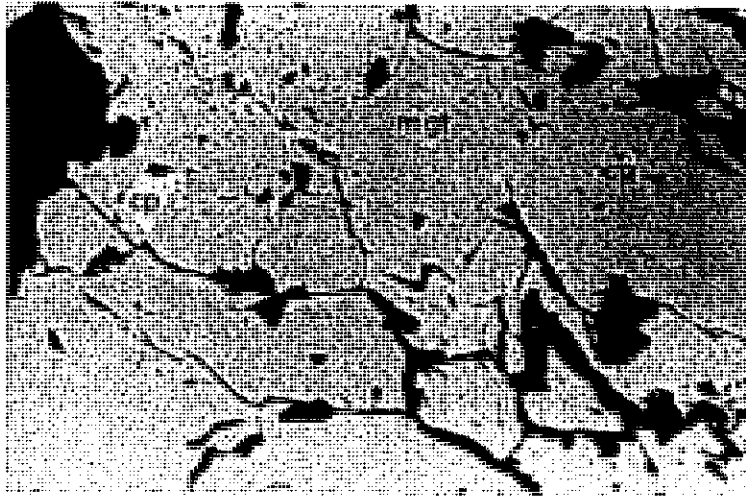
Sample No. 87
Rock name
Skarn
Location
I'-24R
Hem : Hematite

Scale _____ 0.5 mm



Sample No. 89
Rock name
Iron oxide
Location
I'-40(2M)
Hem : Hematite
Mgt. : Magnetite

Scale _____ 0.5 mm



Sample No. 93
Rock name
Magnetite skarn
Location
I'-25M
Cp : Chalcopyrite
Mgt : Magnetite

Scale

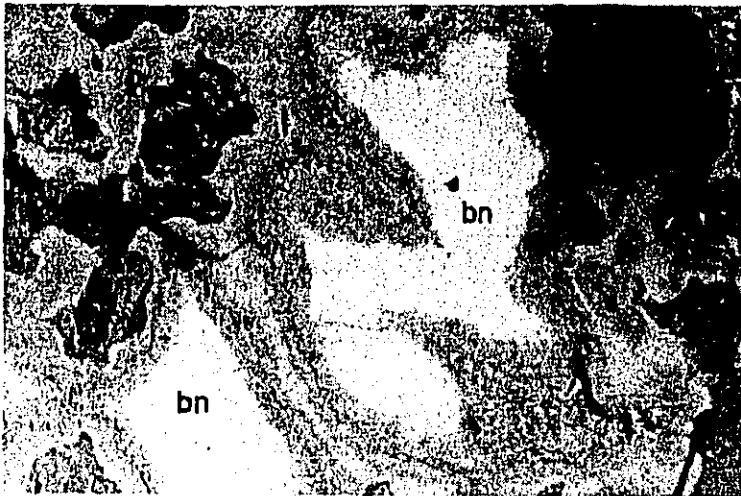
0.5 mm



Sample No. 128
Rock name
Magnetite skarn
Location
N'-22S1
Hem : Hematite
Mgt : Magnetite

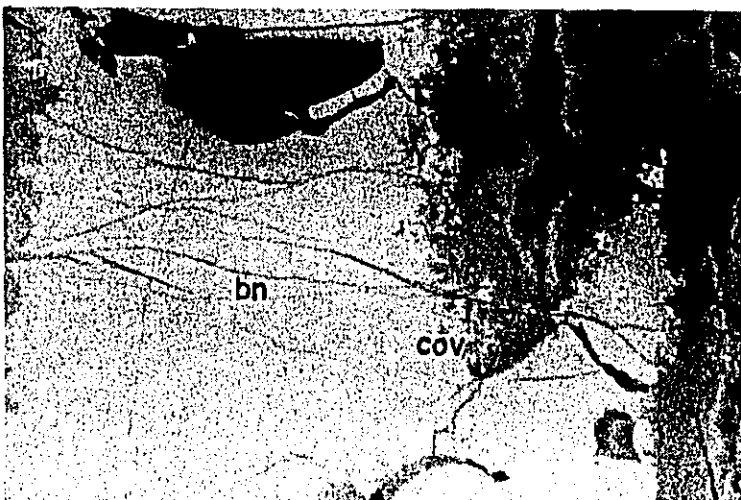
Scale

0.5 mm



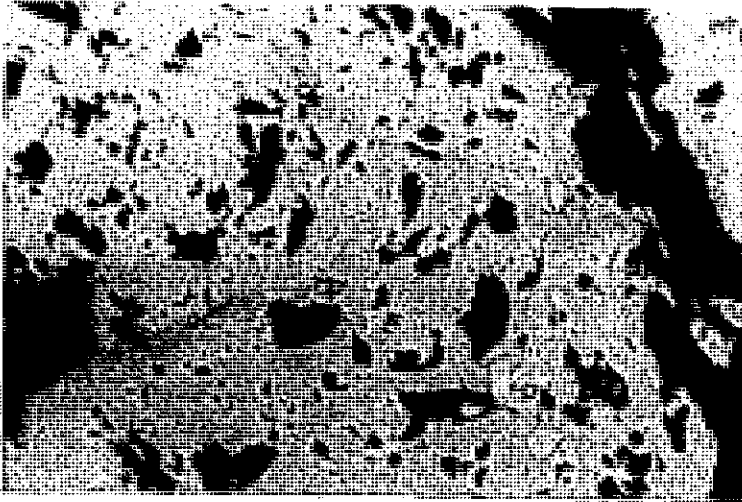
Sample No. 201
Rock name
Copper sulphide
ore
Location
Trench pit
bn : bornite

Scale _____ 0.5 mm



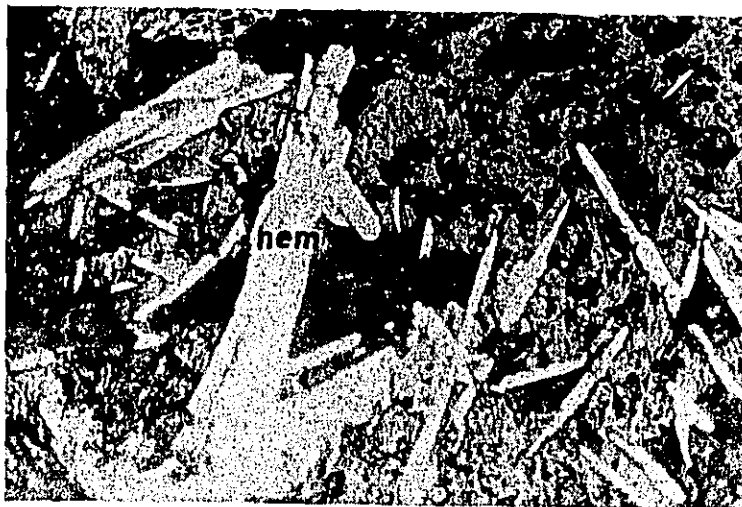
Sample No. 202
Rock name
Copper sulphide
ore
Location
Trench pit
bn : bornite
Cov : Covellite

Scale _____ 0.5 mm



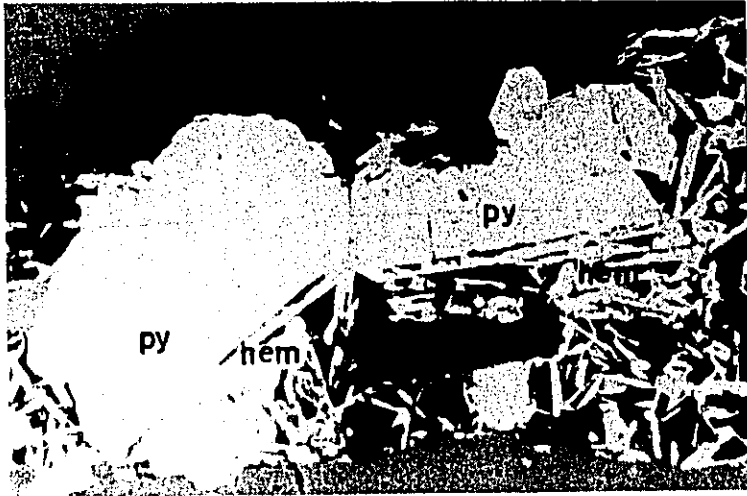
Sample No. 302
Rock name
Granodiorite
Location
DDH 1. 63.6m
Cc : Chalcocite
Py : Pyrite
Cp : Chalcopyrite

Scale _____ 0.5 mm



Sample No. 309
Rock name
Cataclastic
granodiorite
Location
DDH 1. 141.7m
Hem : Hematite

Scale _____ 0.5 mm



Sample No. 311

Rock name
Cataclastic
granodiorite

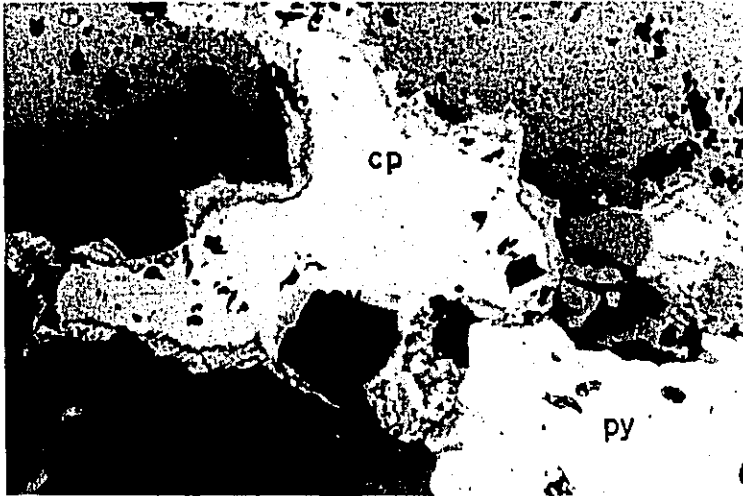
Location
DDH 1. 231.3m

Py : Pyrite

Hem : Hematite

Scale

0.5 mm



Sample No. 313

Rock name
Monzonite porphyry

Location
DDH 2. 60.5m

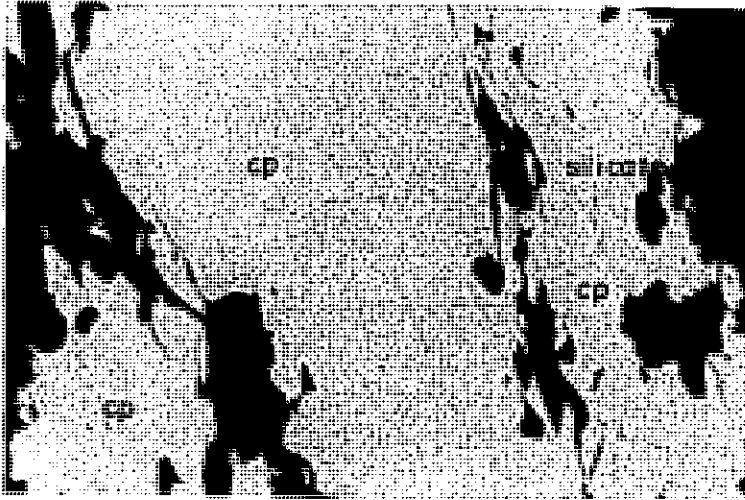
Cp : Chalcopyrite

Py : Pyrite

Cov : Covellite

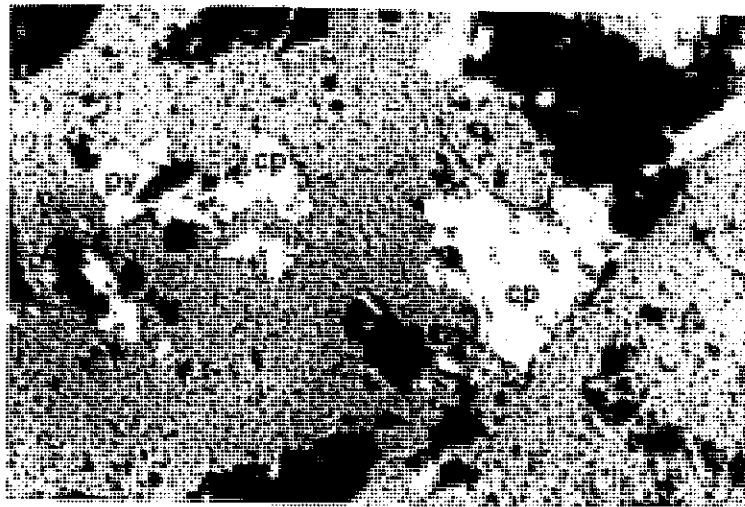
Scale

0.5 mm



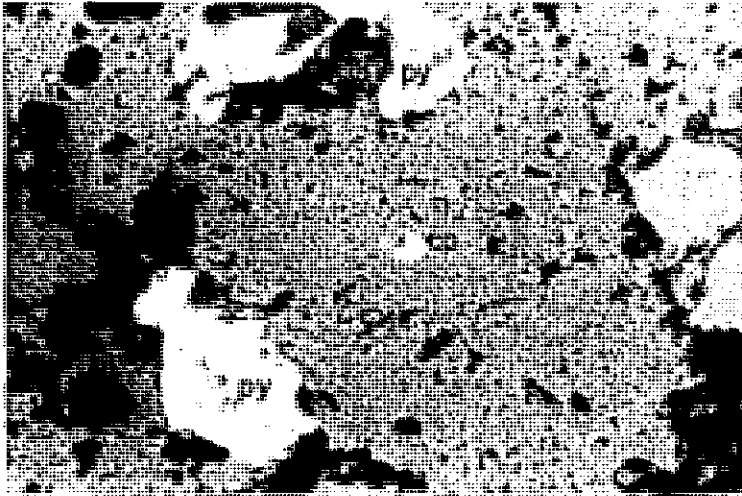
Sample No. 314
Rock name
Hornfels of slate
Location
DDH 2. 74.0m
Cp : Chalcopyrite

Scale 0.5 mm



Sample No. 316
Rock name
Monzonite
porphyry
Location
DDH 2. 117.5m
Cp : Chalcopyrite
Py : Pyrite

Scale 0.5 mm



Sample No. 318

Rock name
Hornfels of
sandstone

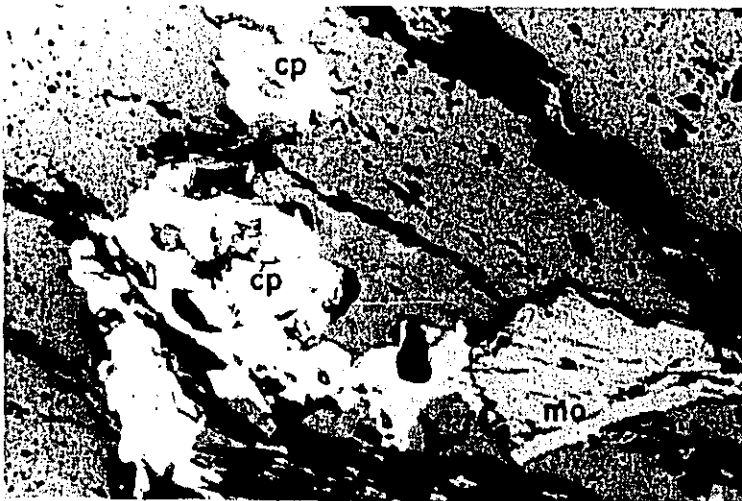
Location
DDH 2. 158.9m

Cp : Chalcopyrite

Py : Pyrite

Scale

0.5 mm



Sample No. 319

Rock name
Granodiorite

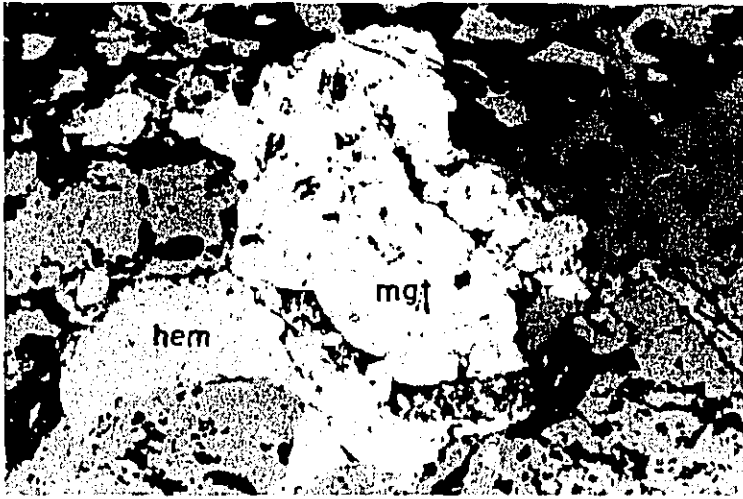
Location
DDH 2. 172.6m

Cp : Chalcopyrite

Mo : Molybdenite

Scale

0.5 mm



Sample No. 320

Rock name
Gabbro

Location
DDH 3. 41.1m

Mgt : Magnetite

Hem : Hematite

Scale

0.5 mm



Sample No. 324

Rock name
Skarn

Location
DDH 3. 91.6m

Cp : Chalcopyrite

Py : Pyrite

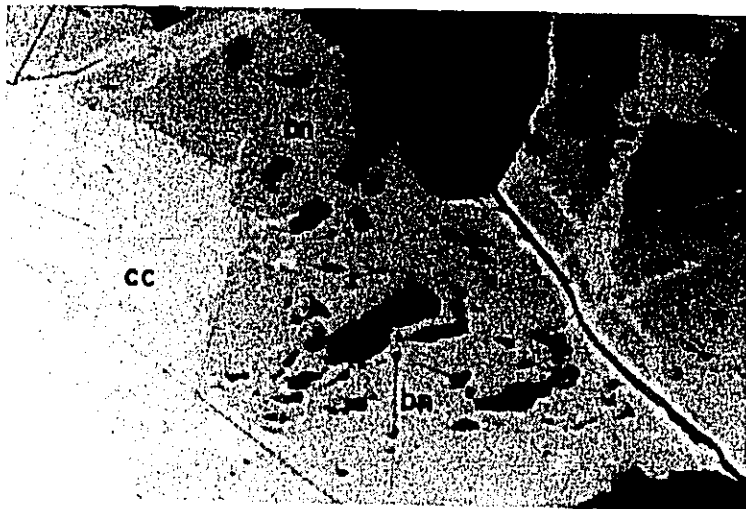
Scale

0.5 mm



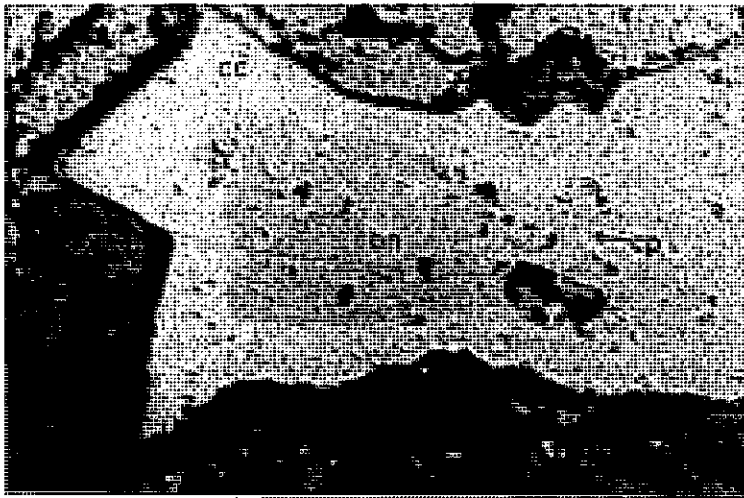
Sample No. 325
Rock name
Skarn
Location
DDH 3. 96.1m
bn : Bornite
Cp : Chalcopyrite

Scale 0.5 mm



Sample No. 327
Rock name
Limestone
Location
DDH 3. 107.7m
bn : Bornite
cc : Chalcocite

Scale 0.5 mm



Sample No. 330

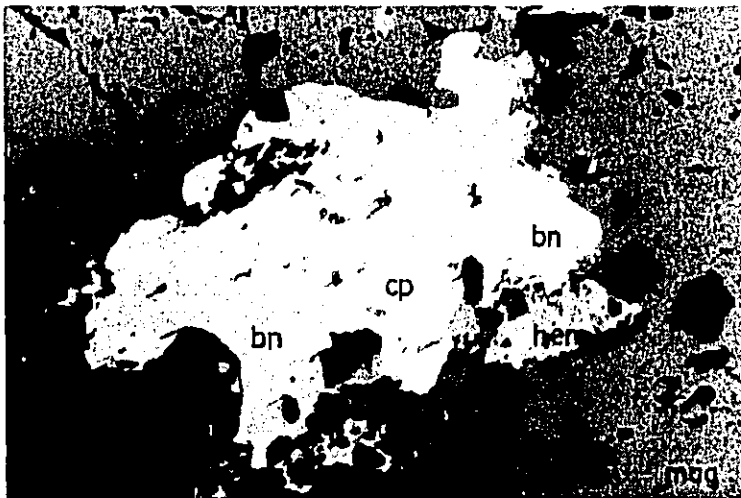
Rock name
Skarn

Location
DDH 3. 136.7m

bn : Bornite
cc : Chalcocite
cp : Chalcopyrite

Scale

0.5 mm



Sample No. 341

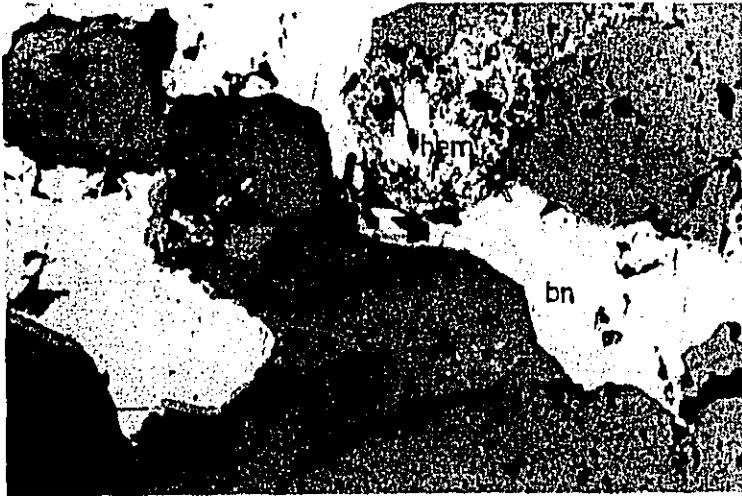
Rock name
Quartz monzonite
porphyry

Location
DDH 4. 18.5m

bn : Bornite
cp : Chalcopyrite
hem : Hematite
mag : Magnetite

Scale

0.5 mm



Sample No. 347

Rock name
Quartz monzonite
porphyry

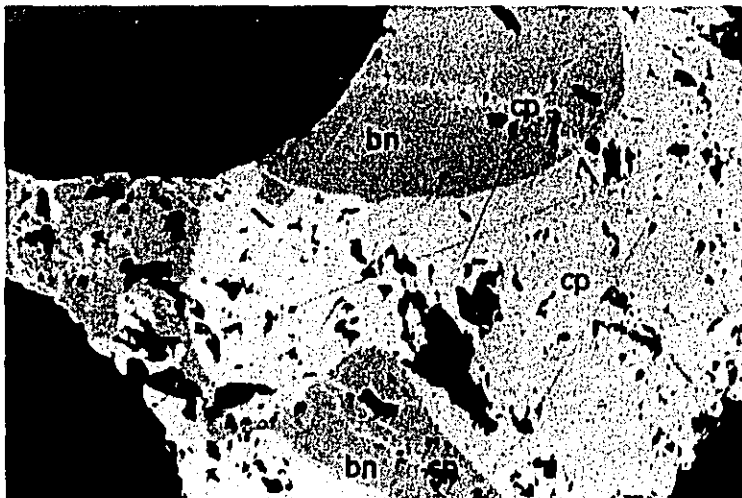
Location
DDH 4. 64.8m

bn : Bornite

cp : Chalcopyrite

Scale

0.5 mm



Sample No. 349

Rock name
Quartz monzonite
porphyry

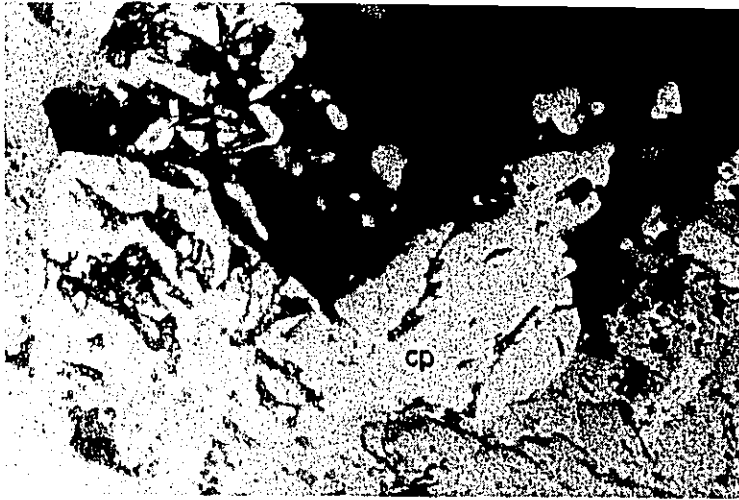
Location
DDH 4. 70.0m

cp : Chalcopyrite

bn : Bornite

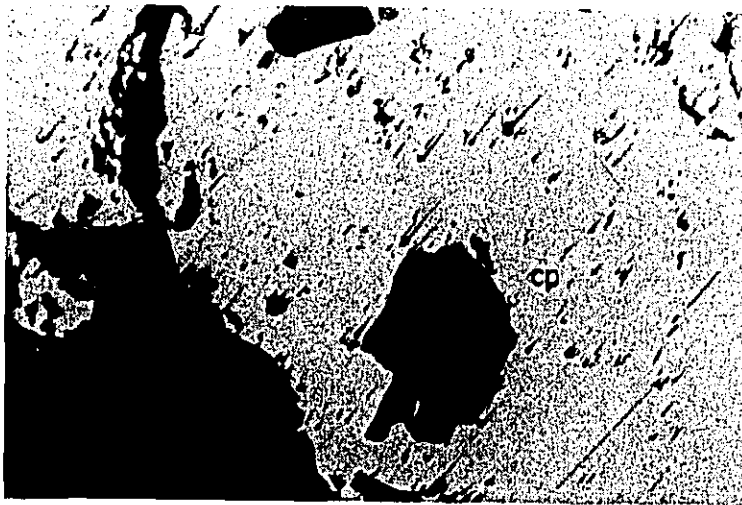
Scale

0.5 mm



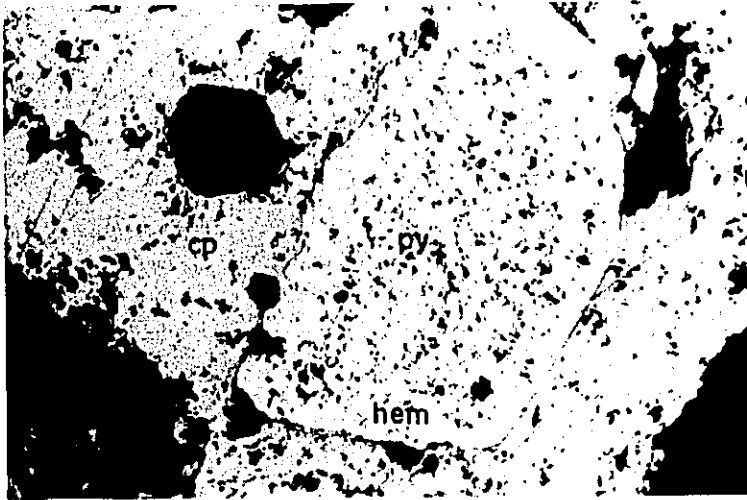
Sample No. 353
Rock name
Quartz monzonite
porphyry
Location
DDH 4. 166.3m
cp : Chalcopyrite

Scale 0.5 mm



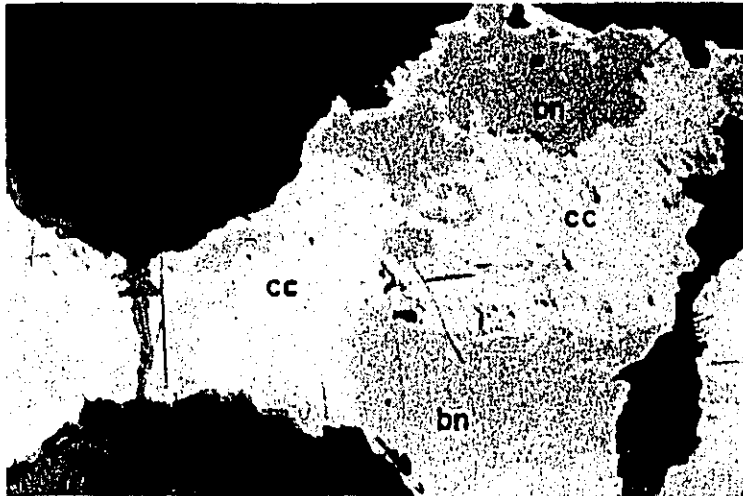
Sample No. 354
Rock name
Quartz monzonite
porphyry
Location
DDH 4. 177.3m
cp : Chalcopyrite

Scale 0.5 mm



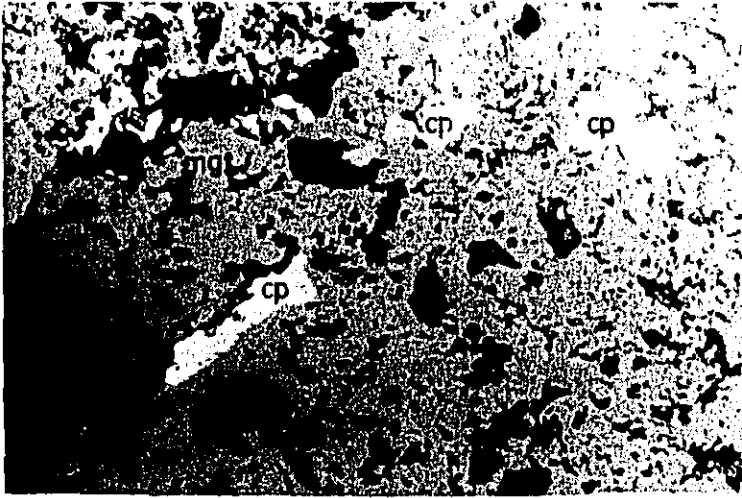
Sample No. 358
Rock name
Quartz monzonite
porphyry
Location
DDH 4. 220.0m
cp : Chalcopyrite
py : Pyrite
hem : Hematite

Scale 0.5 mm



Sample No. 362
Rock name
Meta gabbro
Location
DDH 5. 67.3
bn : Bornite
cc : Chalcocite

Scale 0.5 mm



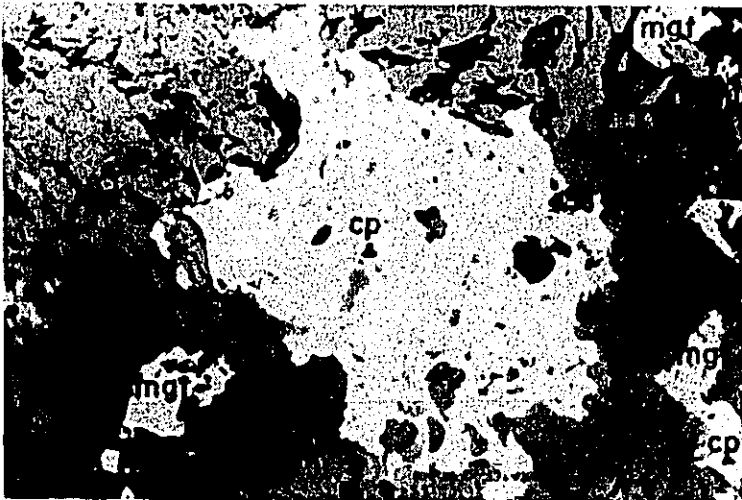
Sample No. 363

Rock name
Gabbro

Location
DDH 5. 84.5

cp : Chalcopyrite
mgt : Magnetite

Scale 0.5 mm



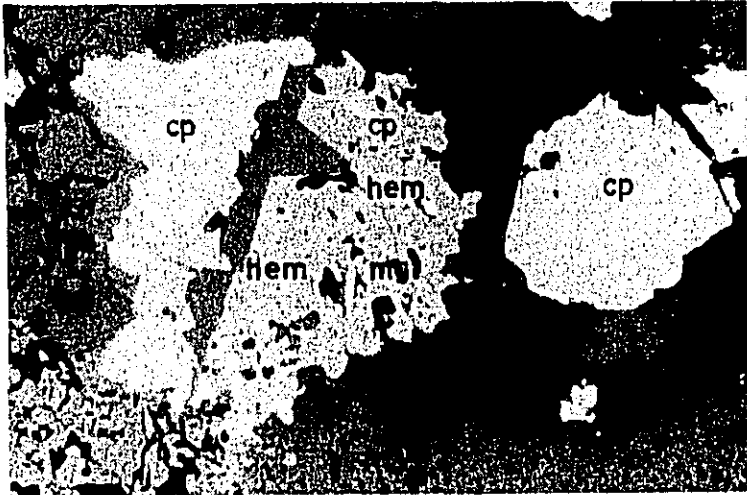
Sample No. 364

Rock name
Gabbro

Location
DDH 5. 98.5

cp : Chalcopyrite
mgt : Magnetite

Scale 0.5 mm



Sample No. 365

Rock name
Diorite

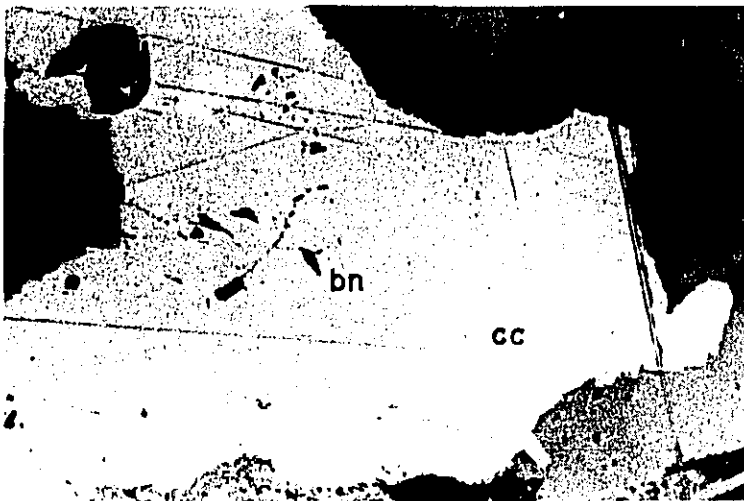
Location
DDH 5. 122.7m

cp : Chalcopyrite

hem : Hematite

mgt : Magnetite

Scale 0.5 mm



Sample No. 366

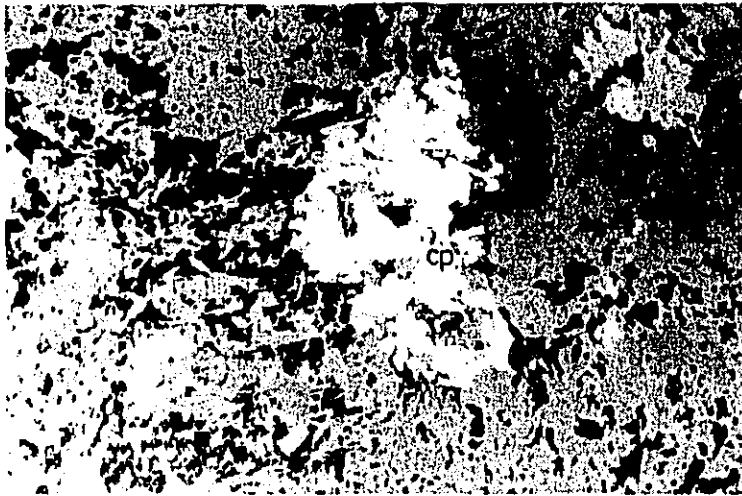
Rock name
Altered diorite

Location
DDH 5. 132.0m

bn : Bornite

cc : Chalcocite

Scale 0.5 mm



Sample No. 367

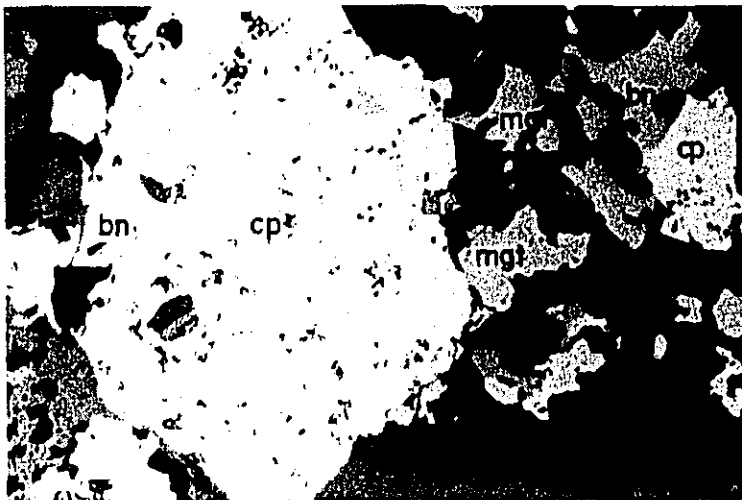
Rock name
Gabbro

Location
DDH 172.0m

cp : Chalcopyrite

Scale

0.5 mm



Sample No. 369

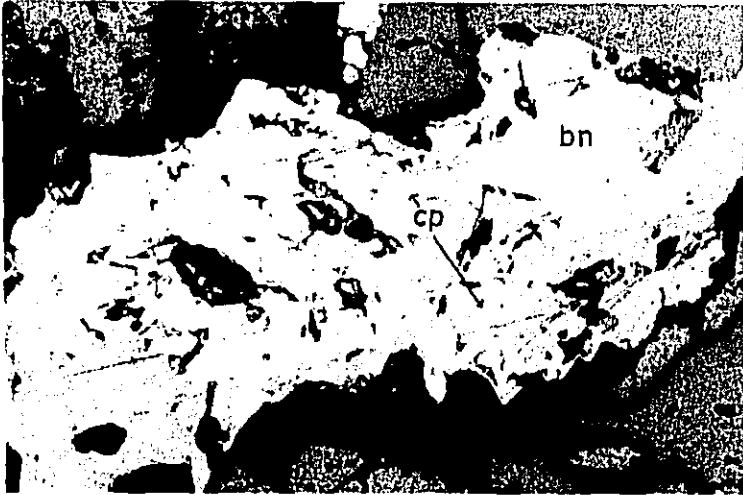
Rock name
Altered gabbro

Location
DDH 5. 188.9m

bn : Bornite
cp : Chalcopyrite
mgt : Magnetite

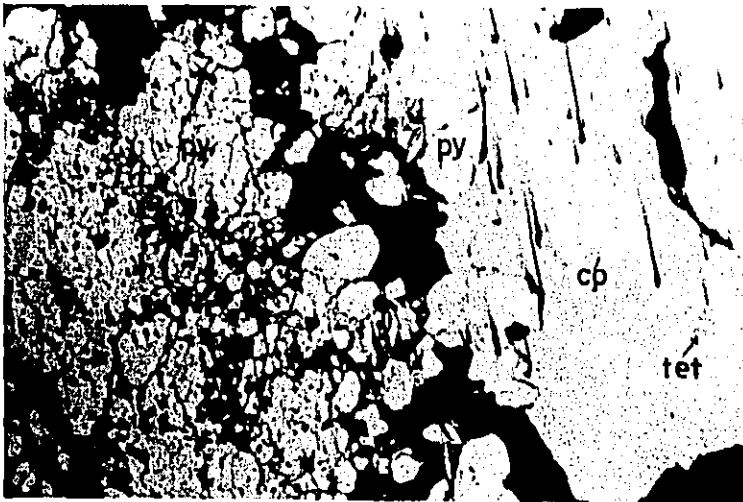
Scale

0.5 mm



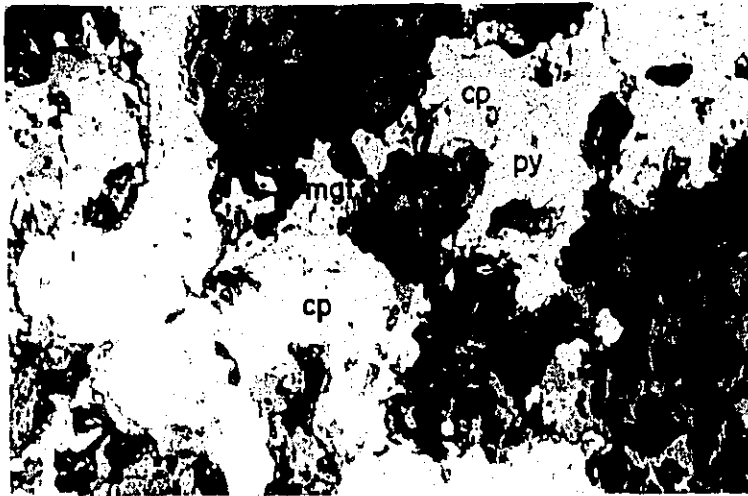
Sample No. 373
Rock name
Hornblende gabbro
Location
DDH 6. 31.0m
bn : Bornite
cp : Chalcopyrite

Scale _____ 0.5 mm



Sample No. 374
Rock name
Calcite vein
Location
DDH 6. 74.8m
cp : Chalcopyrite
tet : Tetrahedrite

Scale _____ 0.5 mm



Sample No. 375

Rock name
Altered diorite

Location
DDH 6. 80.5m

cp : : Chalcopyrite
py : : Pyrite
mgt : : Magnetite

Scale 0.5 mm



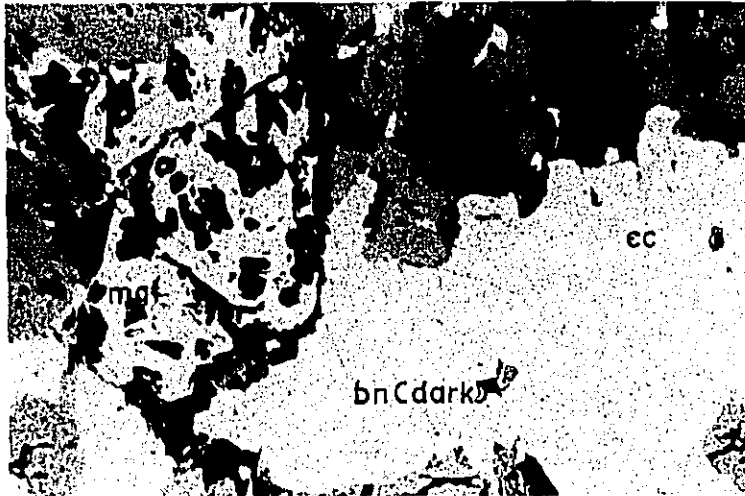
Sample No. 376

Rock name
Hornblende gabbro

Location
DDH 6. 93.3

cp : : Chalcopyrite
mgt : : Magnetite
hem : : Hematite

Scale 0.5 mm



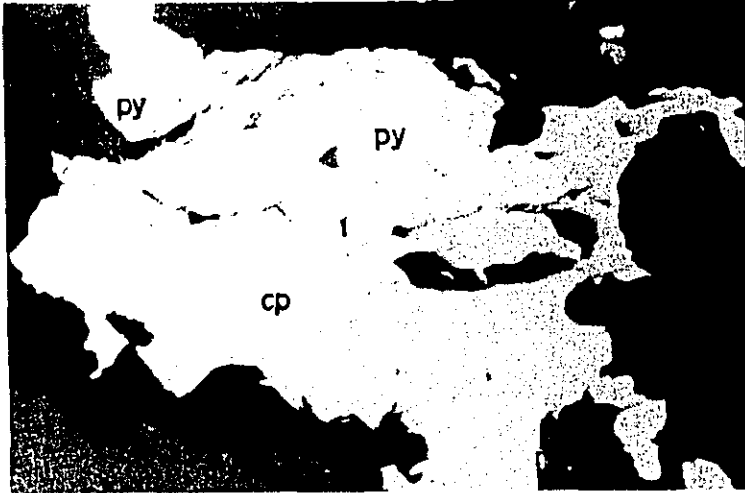
Sample No. 377
Rock name
Hornblende gabbro
Location
DDH 6. 97.0m
bn : Bornite
cc : Chalcocite
mgt : Magnetite

Scale 0.5 mm



Sample No. 379
Rock name
Hornblende gabbro
Location
DDH 6. 114.4m
bn : Bornite
cp : Chalcopyrite

Scale 0.5 mm



Sample No. 381

Rock name
Altered diorite

Location
DDH 6. 117.0m

cp : Chalcopyrite

py : Pyrite

Scale

0.5 mm



Sample No. 385

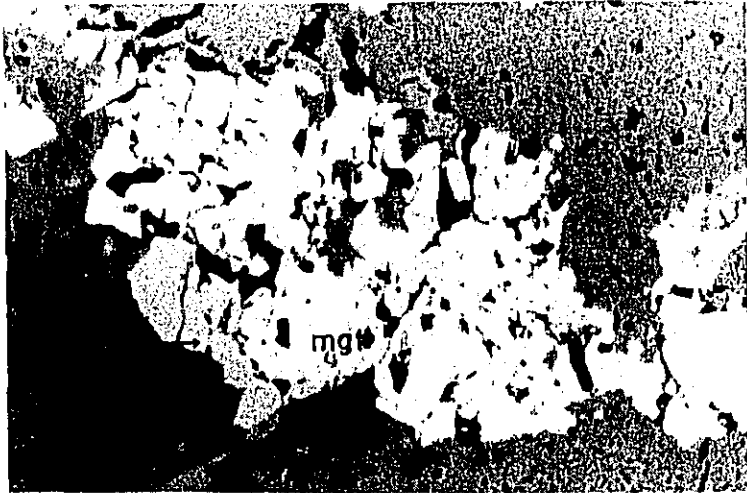
Rock name
Gabbro

Location
DDH 6. 234.0m

cp : Chalcopyrite

Scale

0.5 mm

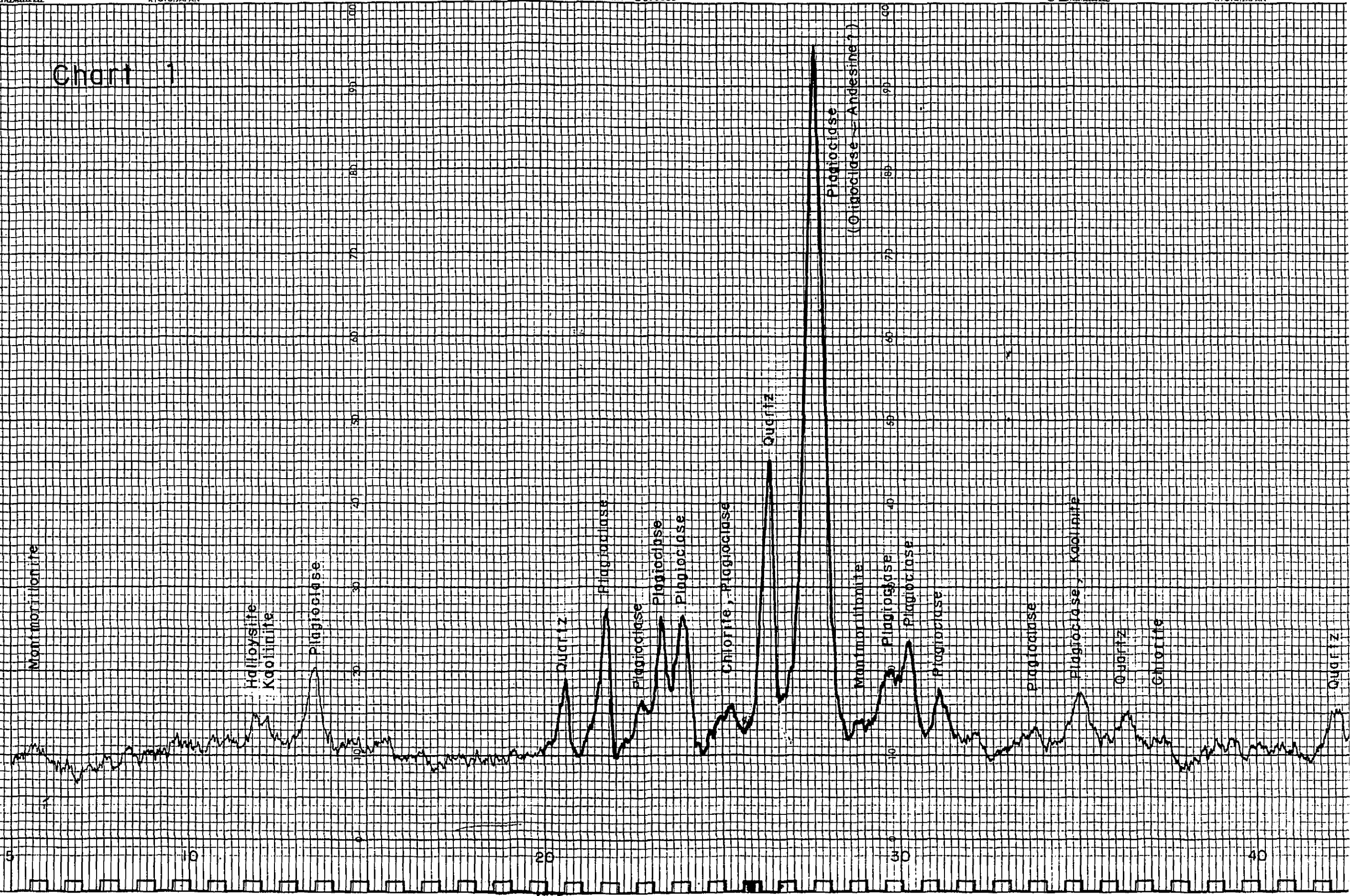


Sample No. 388
Rock name
Hornblende gabbro
Location
DDH 6. 250.3
mgt : Magnetite

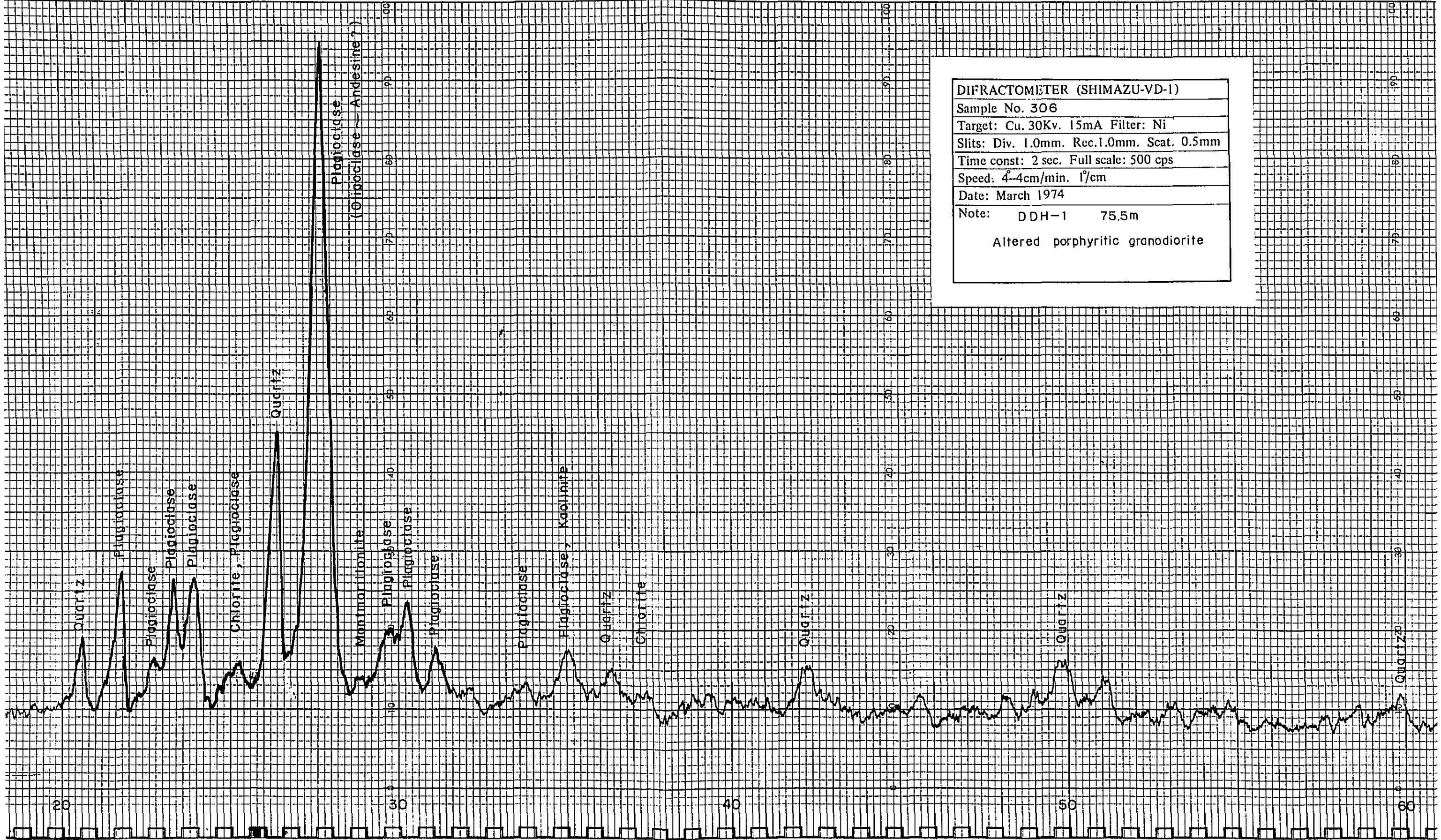
Scale 0.5 mm

Table I-12 chart of X-ray Diffractive Analysis

Chart 1



DIFRACTOMETER (SHIMAZU-VD-1)
Sample No. 306
Target: Cu. 30Kv. 15mA Filter: Ni
Slits: Div. 1.0mm. Rec. 1.0mm. Scat. 0.5mm
Time const: 2 sec. Full scale: 500 cps
Speed: 4-4cm/min. 1°/cm
Date: March 1974
Note: DDH-1 75.5m
Altered porphyritic granodiorite



DIFRACTOMETER (SHIMAZU-VD-1)
 Sample No. 306
 Target: Cu. 30Kv. 15mA Filter: Ni
 Slits: Div. 1.0mm. Rec.1.0mm. Scat. 0.5mm
 Time const: 2 sec. Full scale: 500 cps
 Speed: 4-4cm/min. 1°/cm
 Date: March 1974
 Note: DDH-1 75.5m
 * Altered porphyritic granodiorite

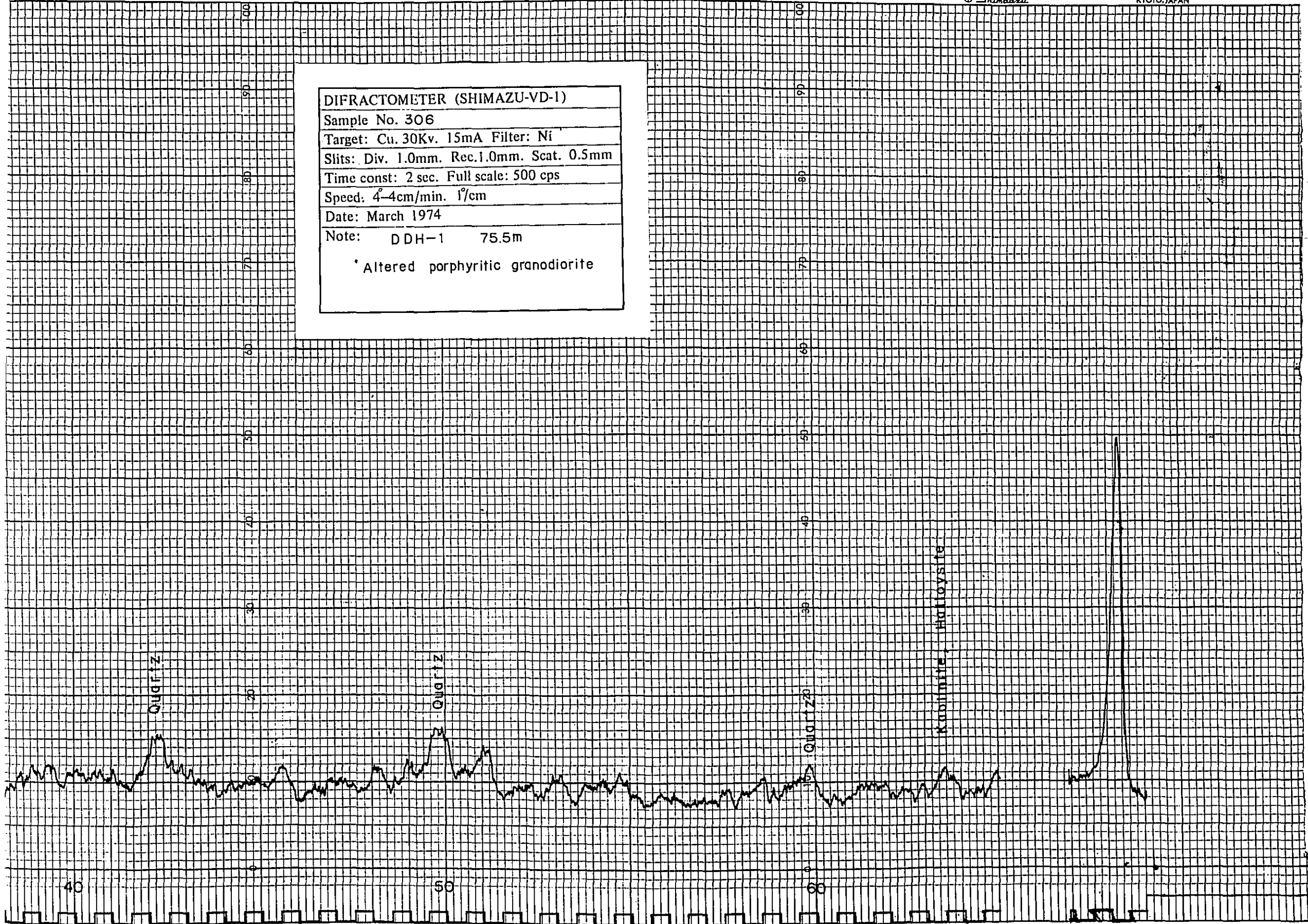
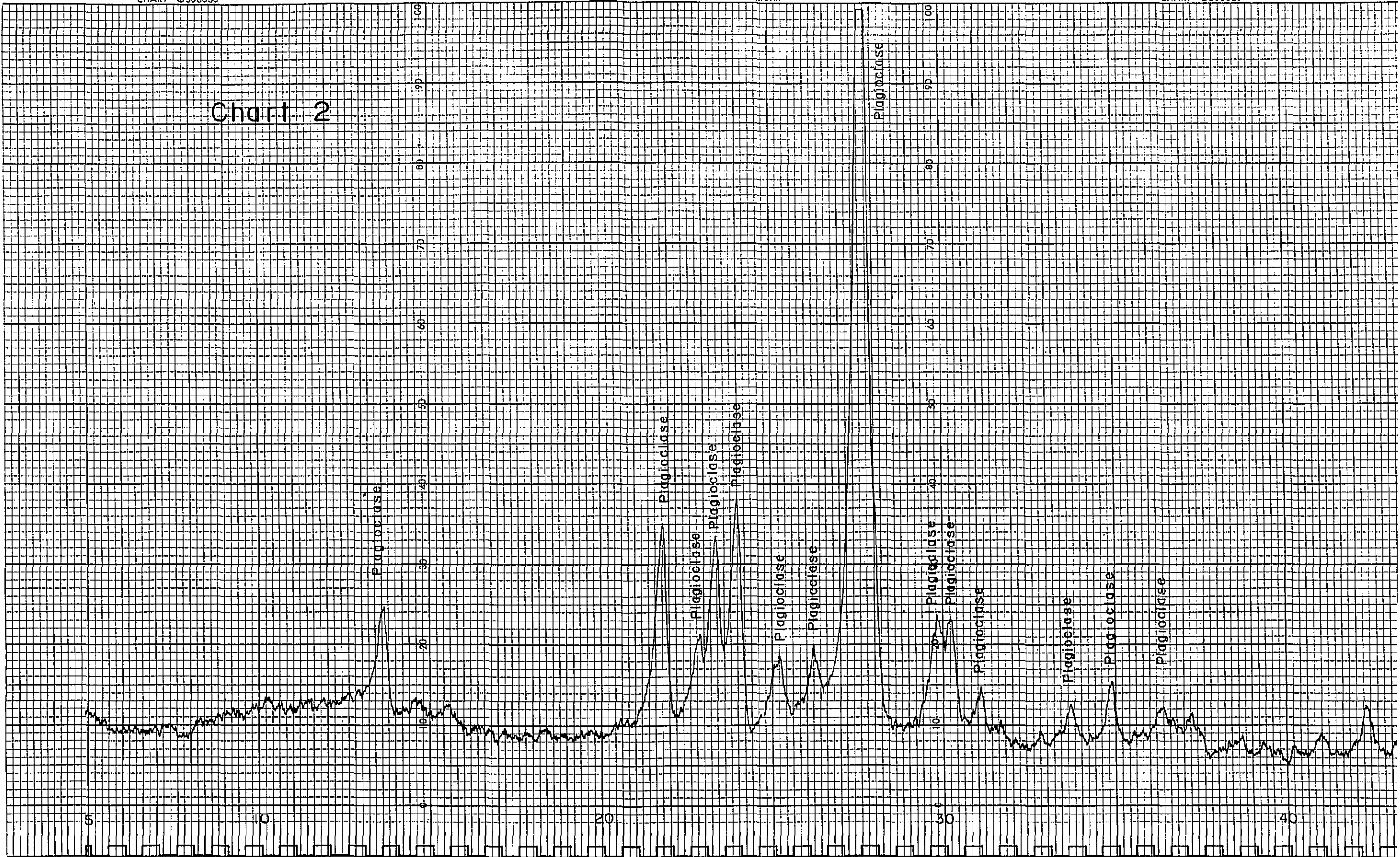


Chart 2



DIFRACTOMETER (SHIMAZU-VD-1)
Sample No. 313
Target: Cu. 30Kv. 15mA Filter: Ni
Slits: Div. 1.0mm. Rec.1.0mm. Scat. 0.5mm
Time const: 2 sec. Full scale: 500 cps
Speed: 4°-4cm/min. 1°/cm
Date: March 1974
Note: DDH-2 60.5m
Salic phenocrysts of porphyritic
granodiorite

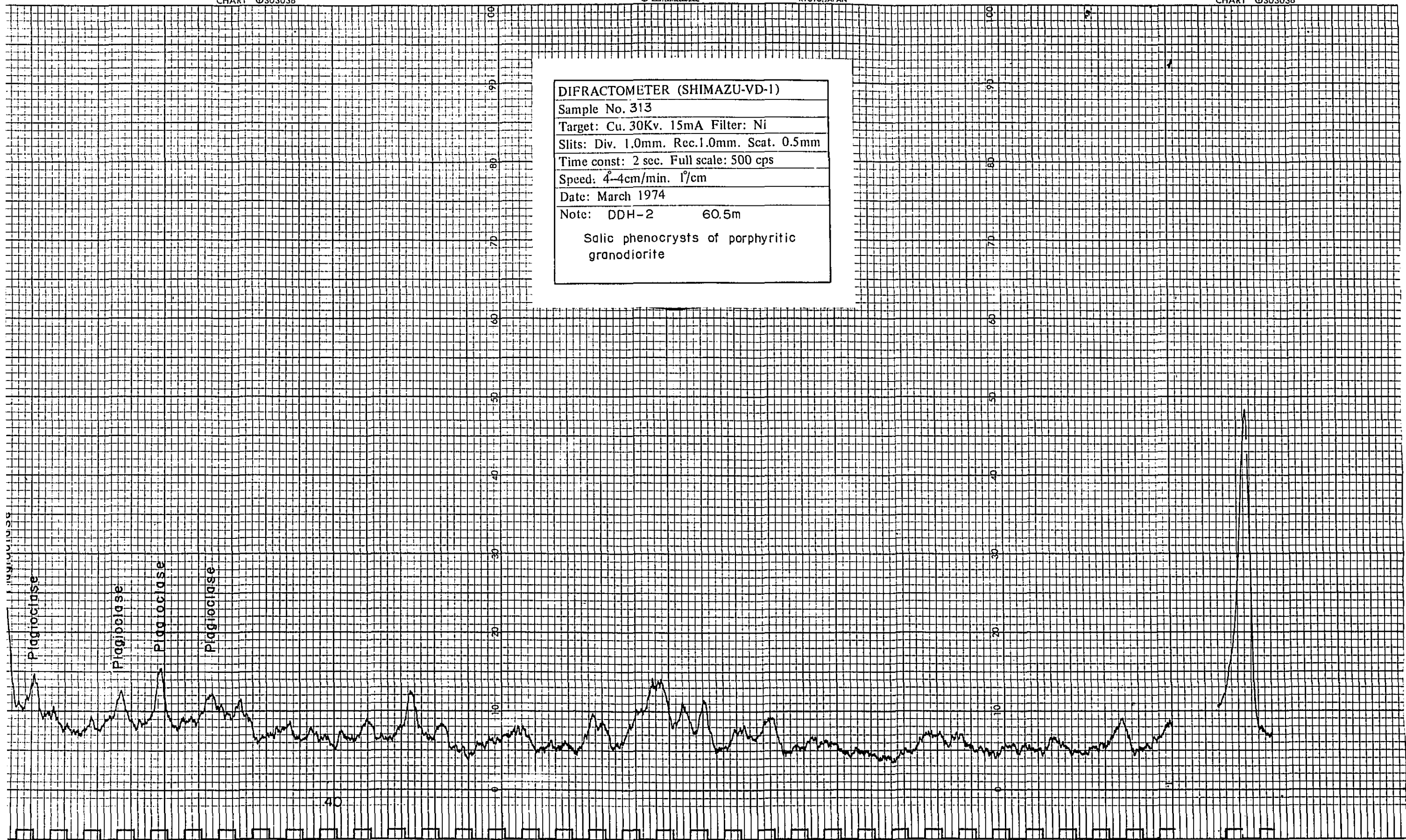


Chart 3

DIFRACTOMETER

Sample No. 328

Target: Cu. 30Kv.

Slits: Div. 1.0mm.

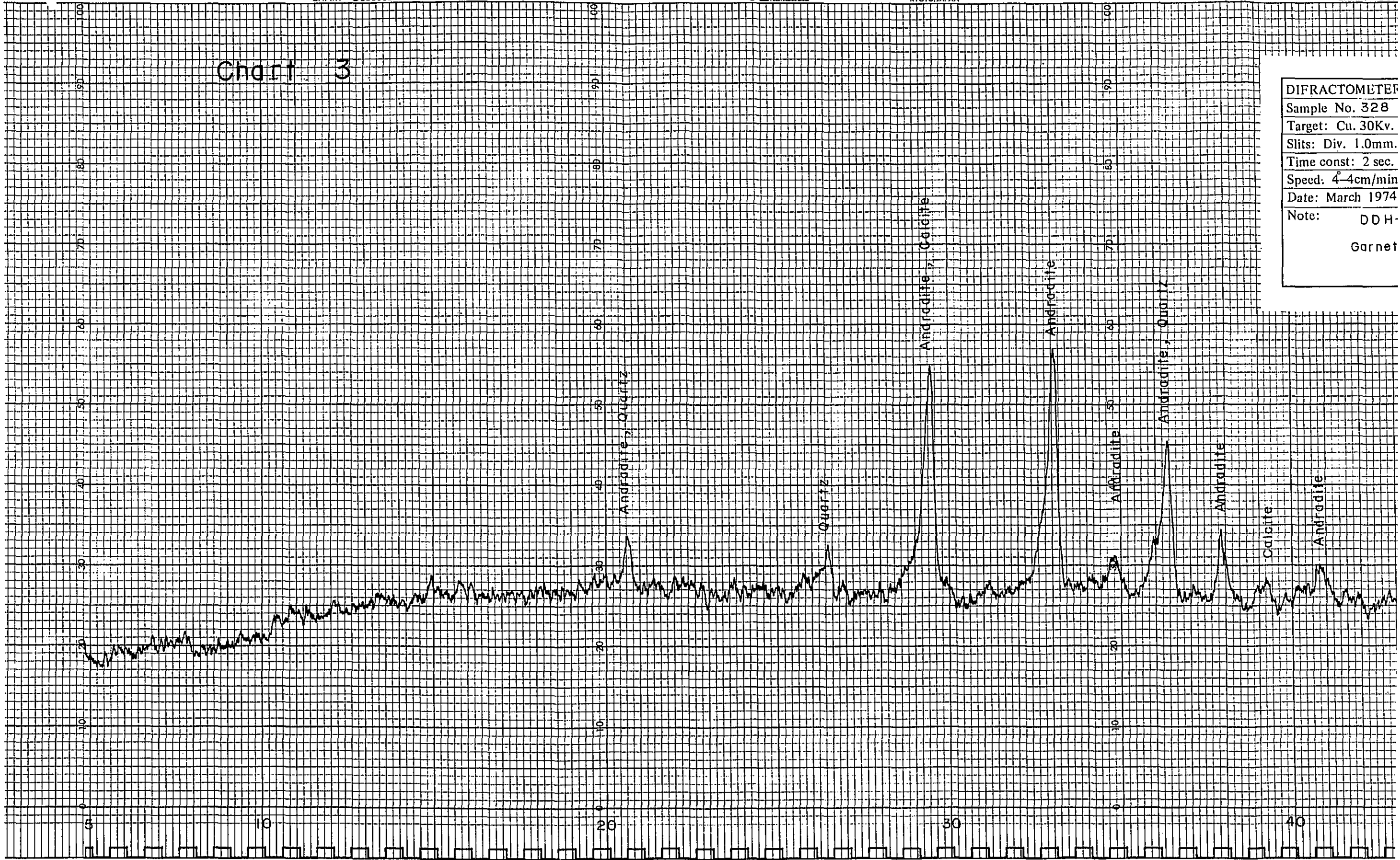
Time const: 2 sec.

Speed: 4°-4cm/min

Date: March 1974

Note: DDH-

Garnet



DIFRACTOMETER (SHIMAZU-VD-1)	
Sample No. 328	
Target: Cu. 30Kv. 15mA Filter: Ni	
Slits: Div. 1.0mm. Rec.1.0mm. Scat. 0.5mm	
Time const: 2 sec. Full scale: 500 cps	
Speed: 4-4cm/min. 1°/cm	
Date: March 1974	
Note:	DDH-3 120.0m
	Garnet skarn after limestone

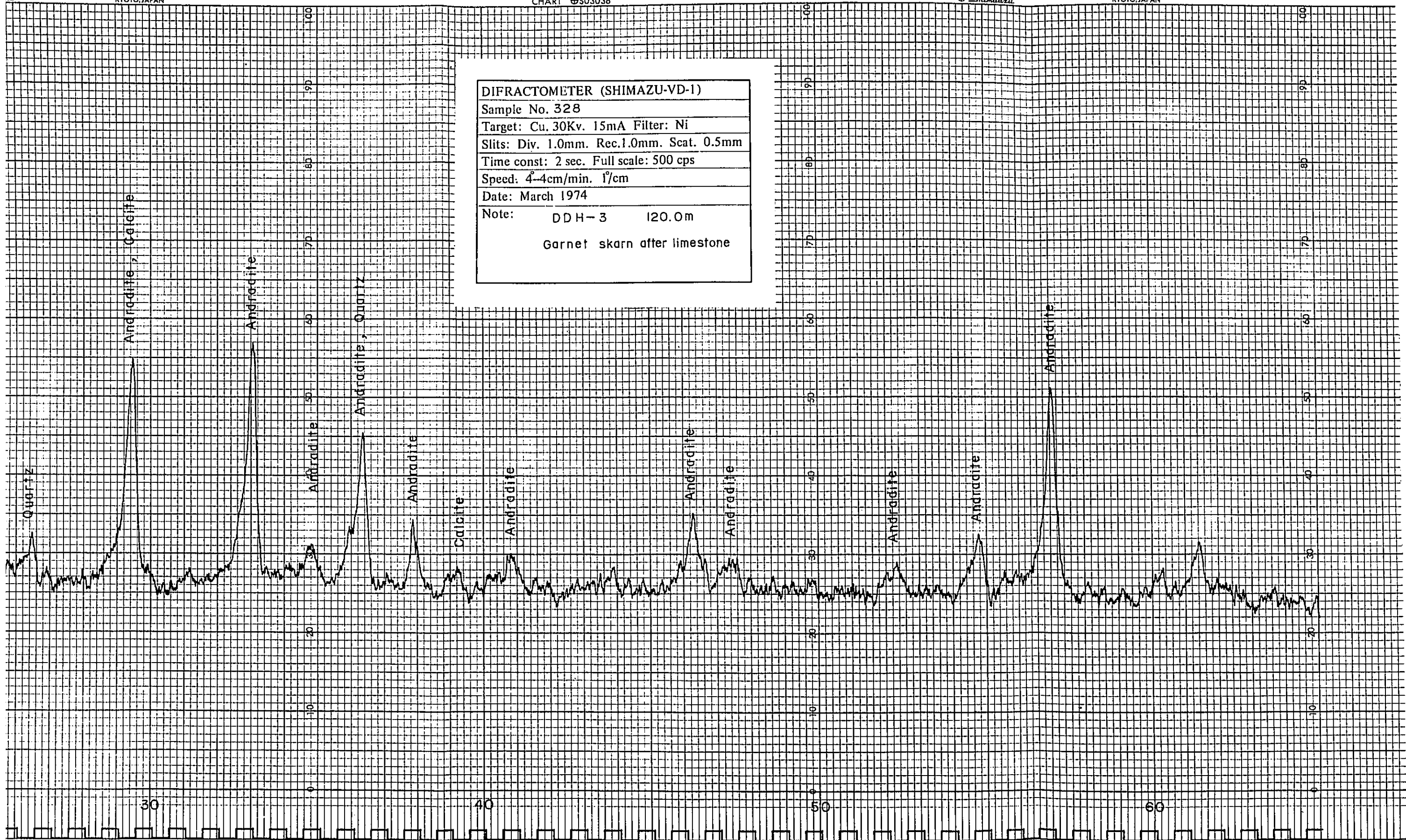
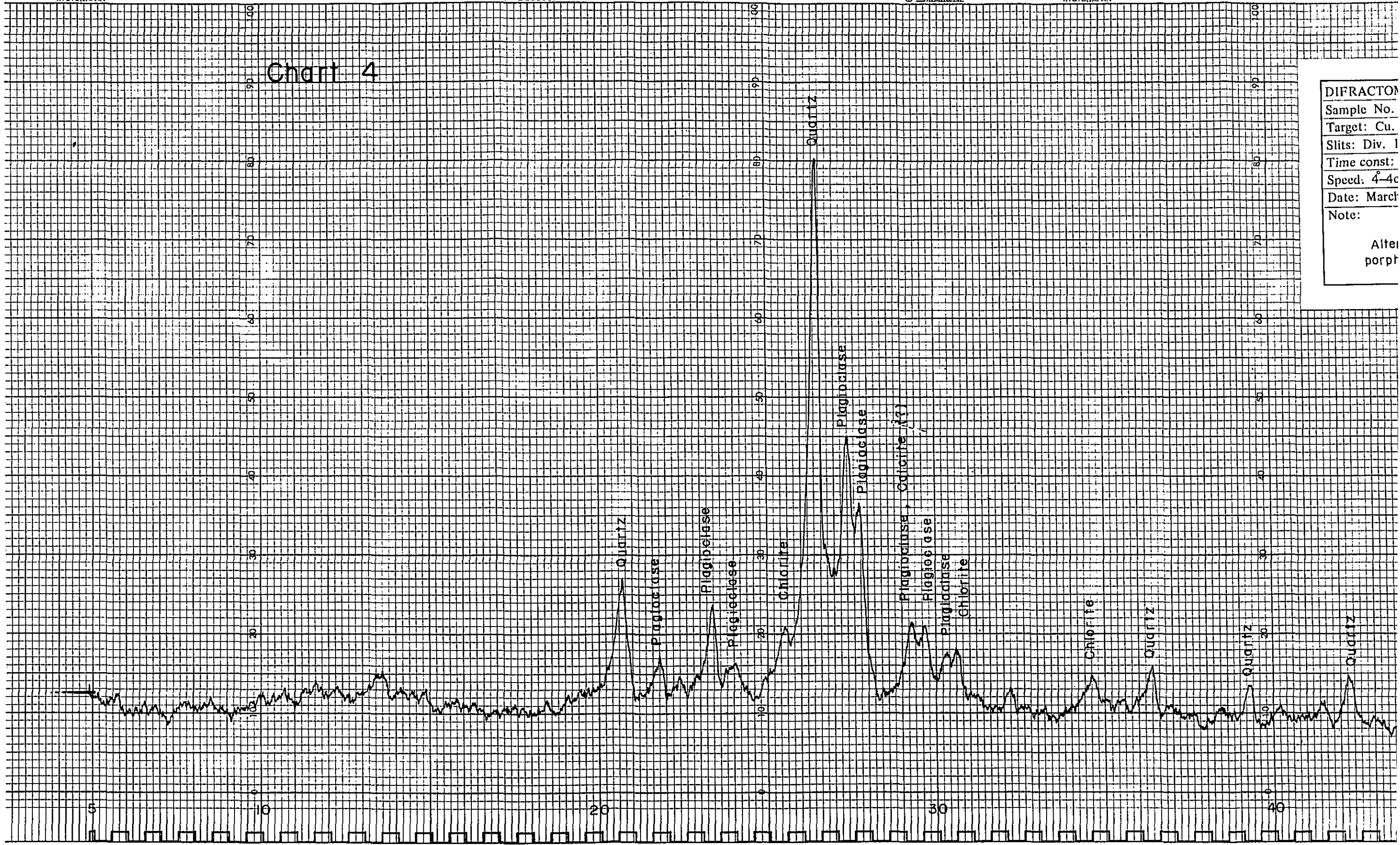


Chart 4

DIFRACTOM
 Sample No.
 Target: Cu.
 Slits: Div. 1
 Time const:
 Speed: 4-4c
 Date: March
 Note:
 Alter
 porph



DIFRACTOMETER (SHIMAZU-VD-1)
 Sample No. 340
 Target: Cu. 30Kv. 15mA Filter: Ni
 Slits: Div. 1.0mm. Rec.1.0mm. Scat. 0.5mm
 Time const: 2 sec. Full scale: 500 cps
 Speed: 4°-4cm/min. 1°/cm
 Date: March 1974
 Note: DDH - 4 10.0m
 Altered quartz monzonite
 porphyry (mainly silicified)

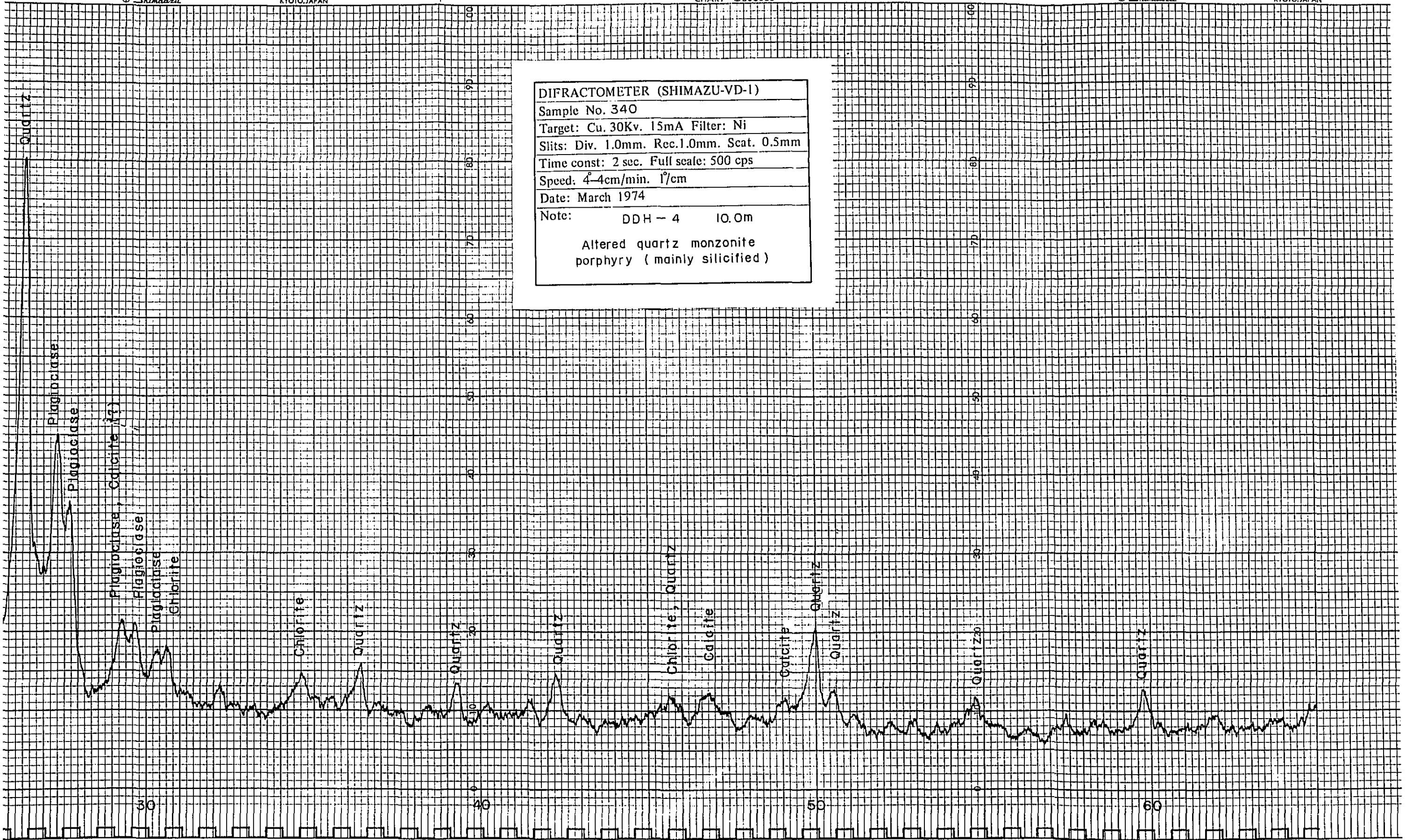
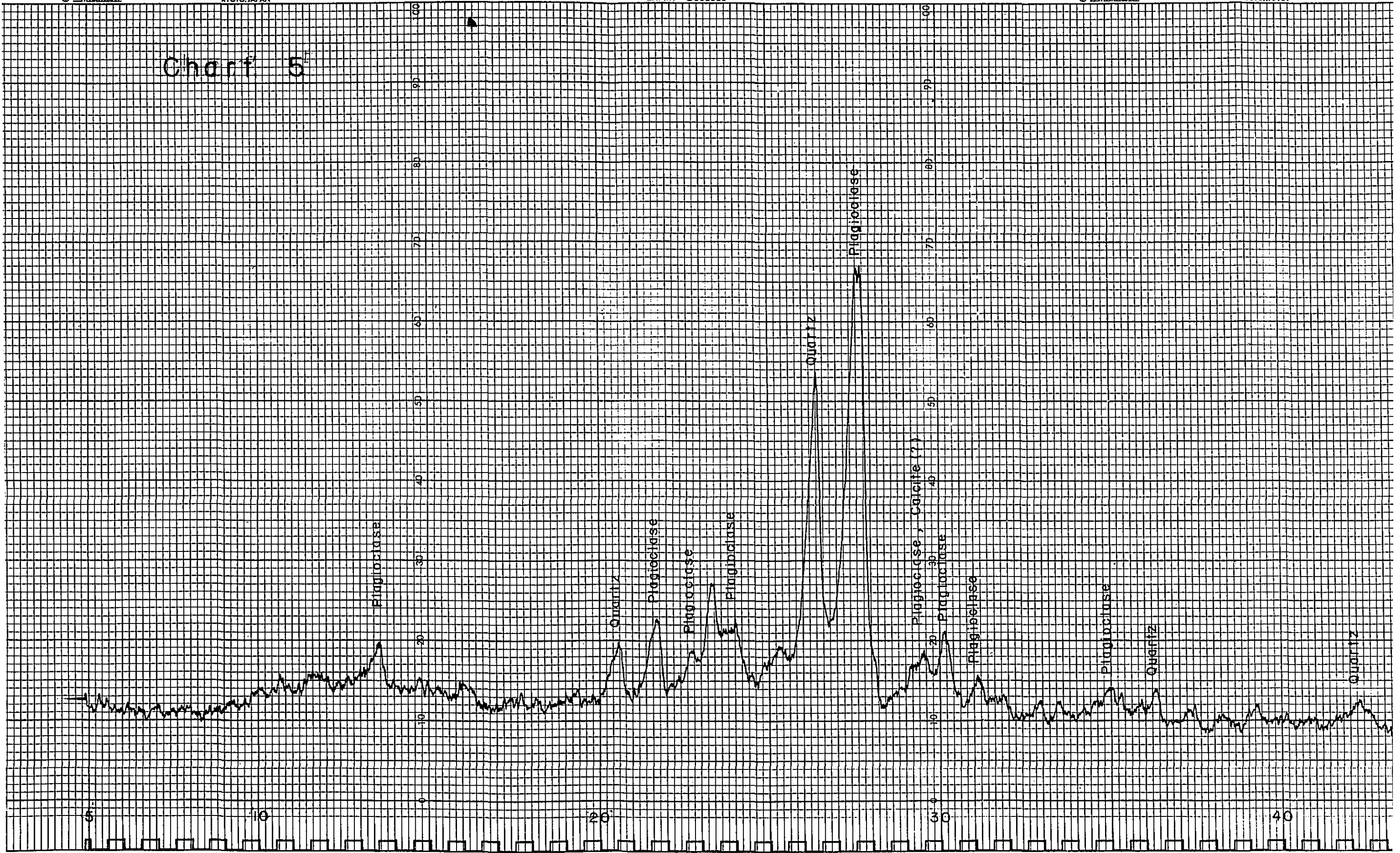


Chart 5



DIFRACTOMETER (SHIMAZU-VD-1)

Sample No. 343

Target: Cu. 30Kv. 15mA Filter: Ni

Slits: Div. 1.0mm. Rec.1.0mm. Scat. 0.5mm

Time const: 2 sec. Full scale: 500 cps

Speed: 4-4cm/min. 1°/cm

Date: March 1974

Note: DDH-4 40m

Silicified quartz monzonite porphyry

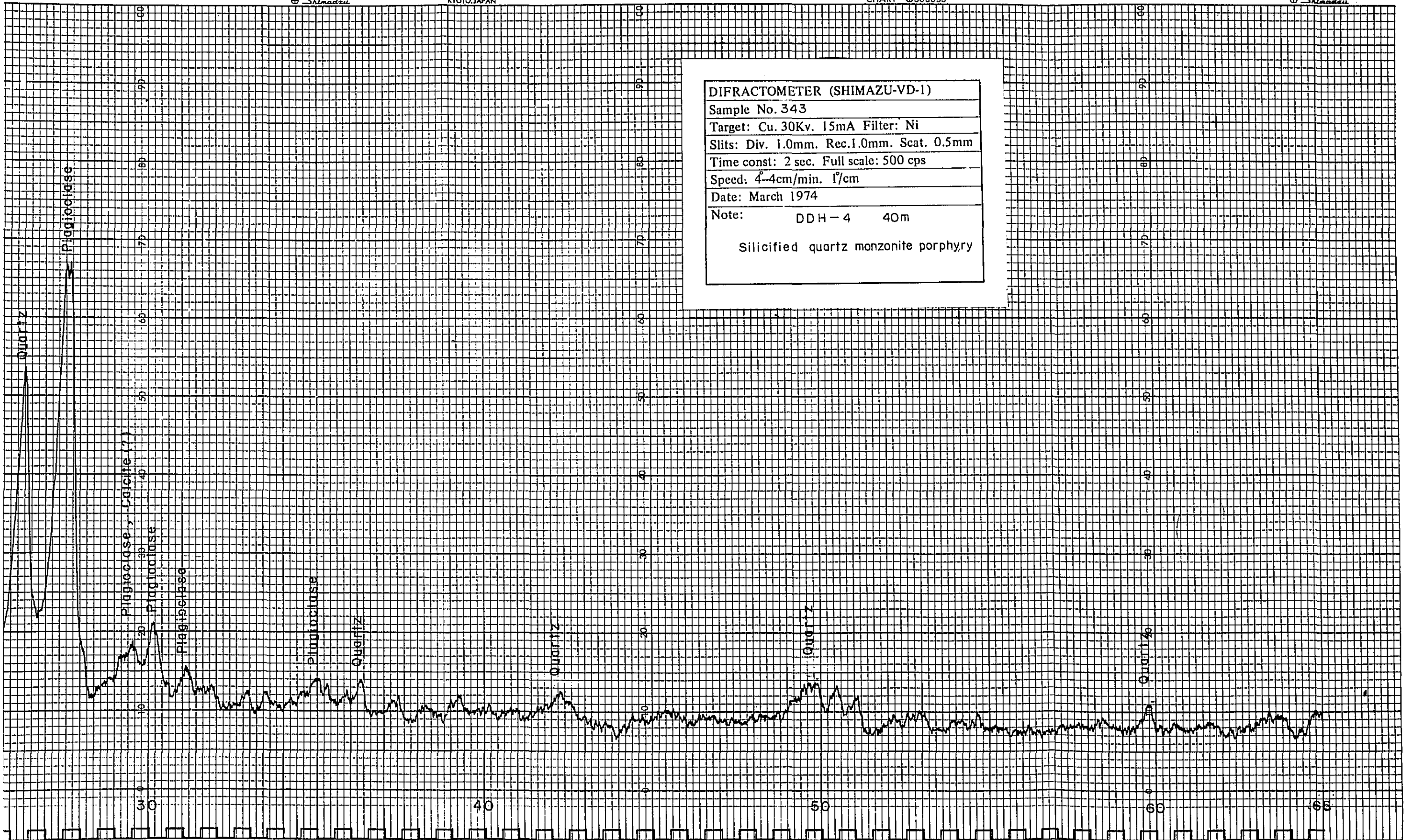
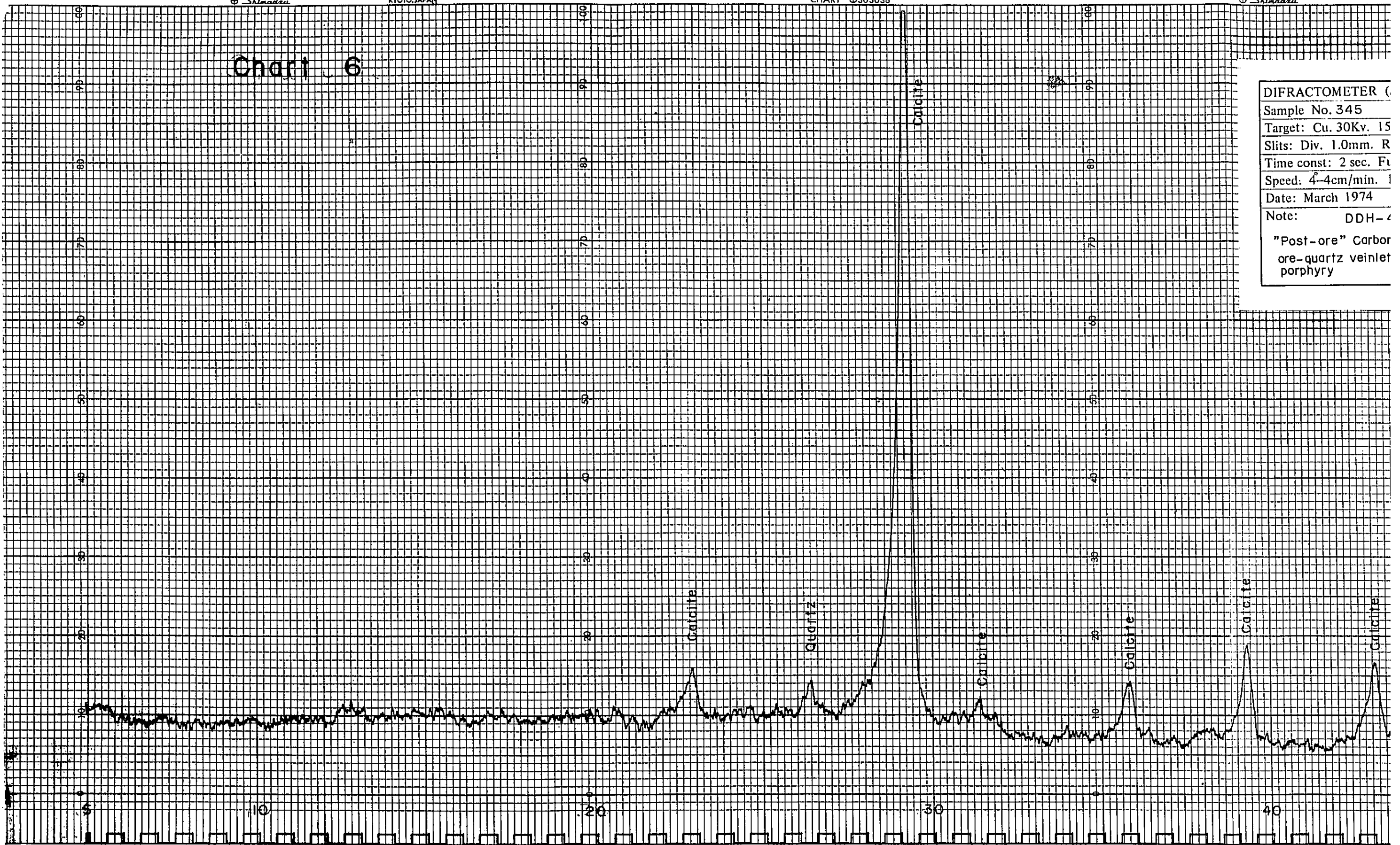


Chart 6

DIFRACTOMETER ()
 Sample No. 345
 Target: Cu. 30Kv. 15
 Slits: Div. 1.0mm. R
 Time const: 2 sec. Fu
 Speed: 4-4cm/min. 1
 Date: March 1974
 Note: DDH-4
 "Post-ore" Carbon
 ore-quartz veinlet
 porphyry



DIFRACTOMETER (SHIMAZU-VD-1)	
Sample No. 345	
Target: Cu. 30Kv. 15mA Filter: Ni	
Slits: Div. 1.0mm. Rec.1.0mm. Scat. 0.5mm	
Time const: 2 sec. Full scale: 500 cps	
Speed: 4°-4cm/min. 1°/cm	
Date: March 1974	
Note: DDH-4 53.2 m	
"Post-ore" Carbonate vein cutting ore-quartz veinlets in quartz monzonite porphyry	

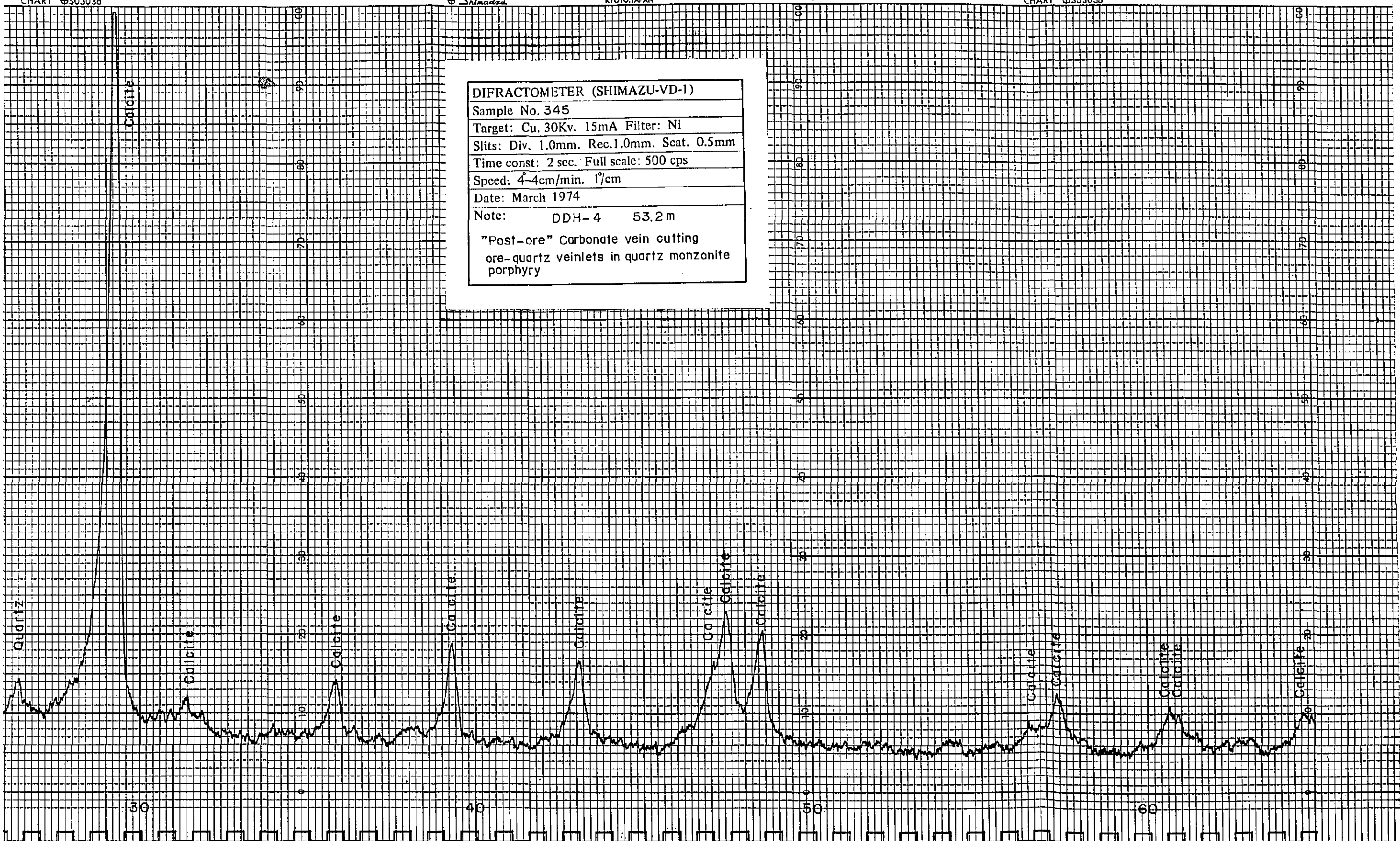
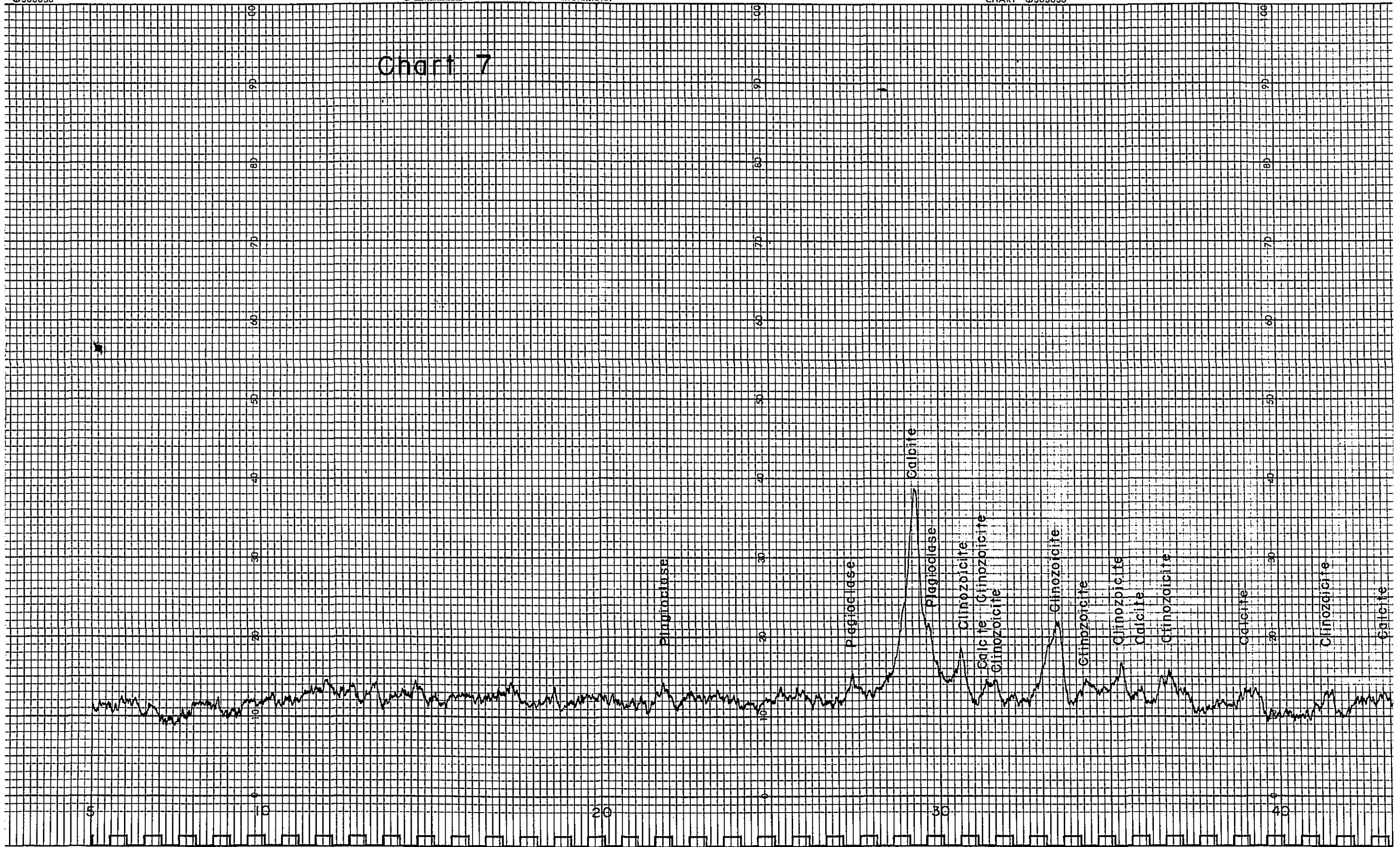


Chart 7



DIFRACTOMETER (SHIMAZU-VD-1)
 Sample No. 356
 Target: Cu. 30Kv. 15mA Filter: Ni
 Slits: Div. 1.0mm. Rec.1.0mm. Scat. 0.5mm
 Time const: 2 sec. Full scale: 500 cps
 Speed: 4-4cm/min. 1/cm
 Date: March 1974
 Note: DDH-4 140m
 Altered quartz monzonite porphyry
 (propylitic alteration)

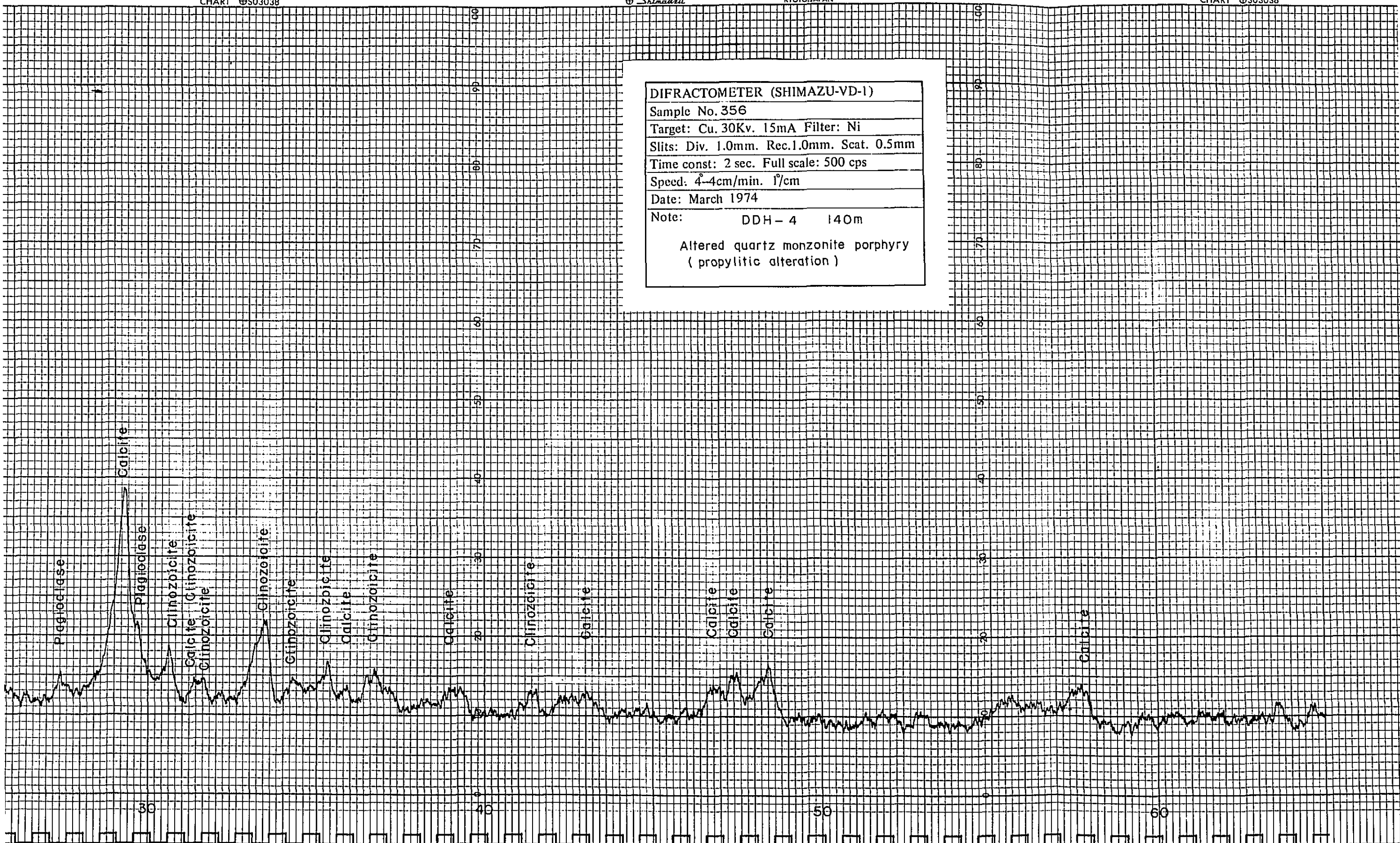


Chart 8

5

Montmorillonite

Montmorillonite

Quartz

Quartz

Pyroclase

Pyroclase

Montmorillonite

Quartz

DIFRACTOMETER (SHIMAZU-VD-1)

Sample No. 361

Target: Cu. 30Kv. 15mA Filter: Ni

Slits: Div. 1.0mm. Rec.1.0mm. Scat. 0.5mm

Time const: 2 sec. Full scale: 500 cps

Speed: 4-4cm/min. 1°/cm

Date: March 1974

Note: DDH-5 45.6m

Clay-quartz veinlet in altered gabbroic rock

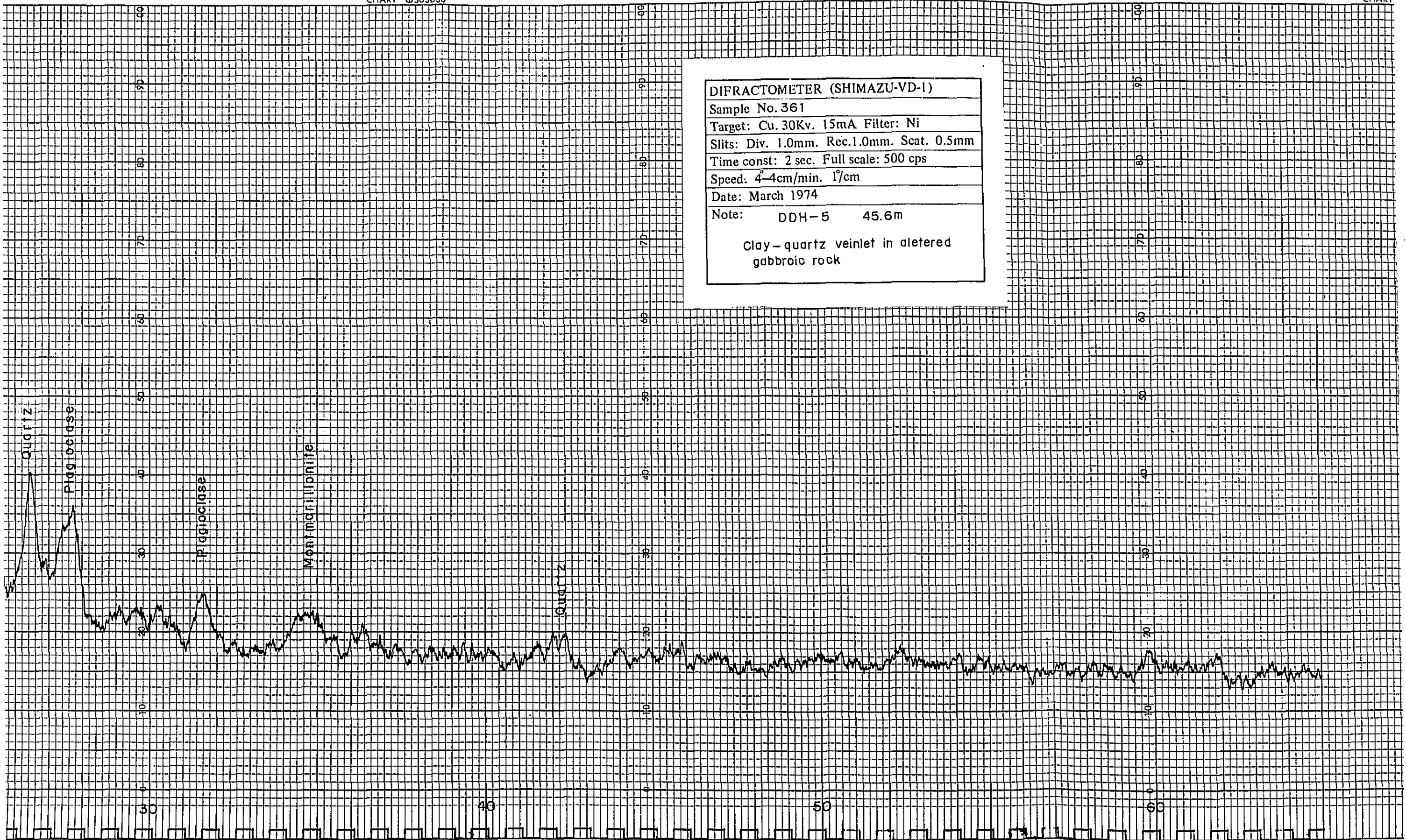
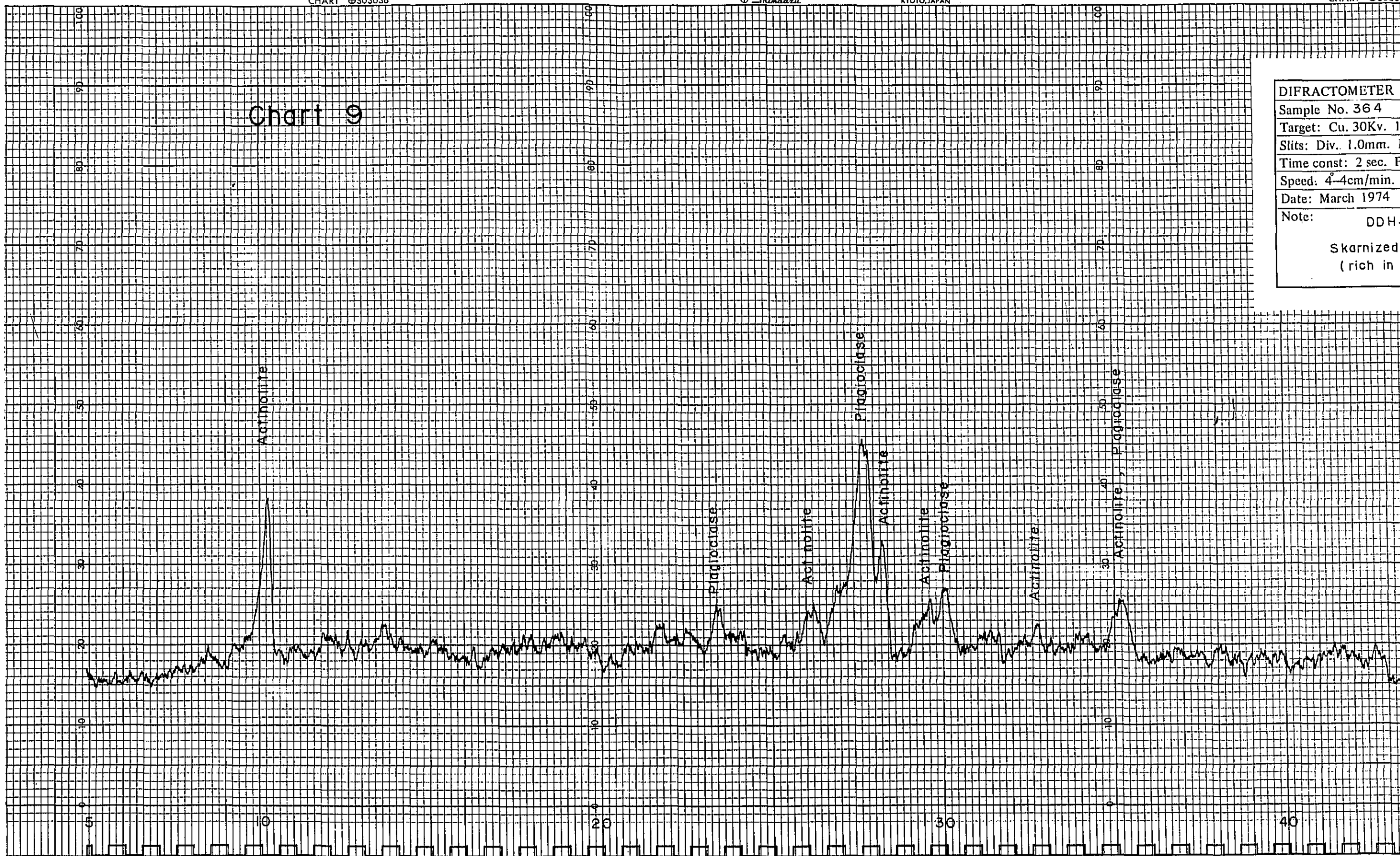


Chart 9

DIFRACTOMETER (C
 Sample No. 364
 Target: Cu, 30Kv, 15
 Slits: Div. 1.0mm, R
 Time const: 2 sec. Fu
 Speed: 4°-4cm/min.
 Date: March 1974
 Note: DDH-
 Skarnized
 (rich in g



DIFRACTOMETER (SHIMAZU-VD-1)
Sample No. 364
Target: Cu, 30Kv, 15mA Filter: Ni
Slits: Div. 1.0mm. Rec. 1.0mm. Scat. 0.5mm
Time const: 2 sec. Full scale: 500 cps
Speed: 4-4cm/min. 1°/cm
Date: March 1974
Note: DDH- 5 98.5m
Skarnized gabbroic rock (rich in green skarn)

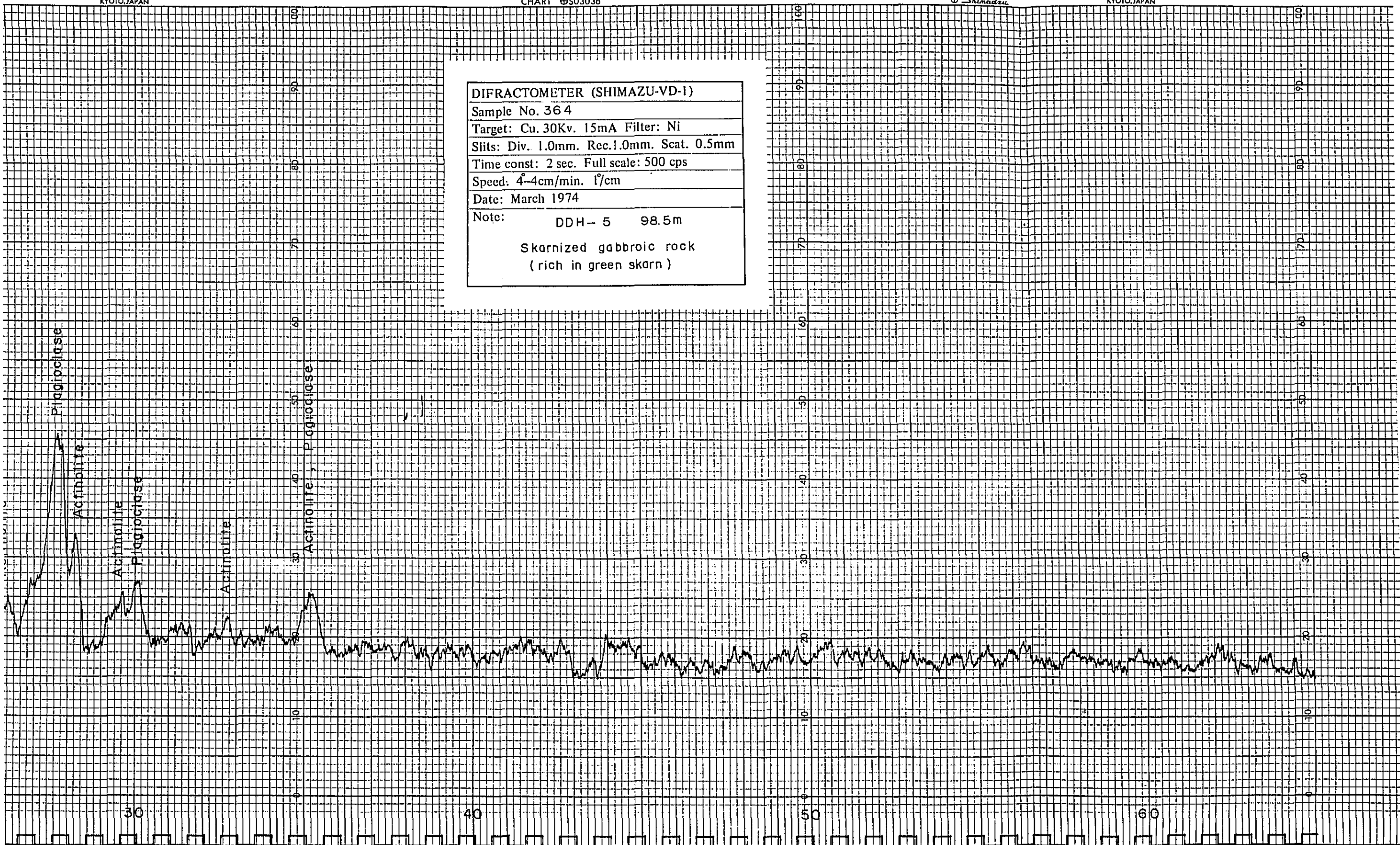
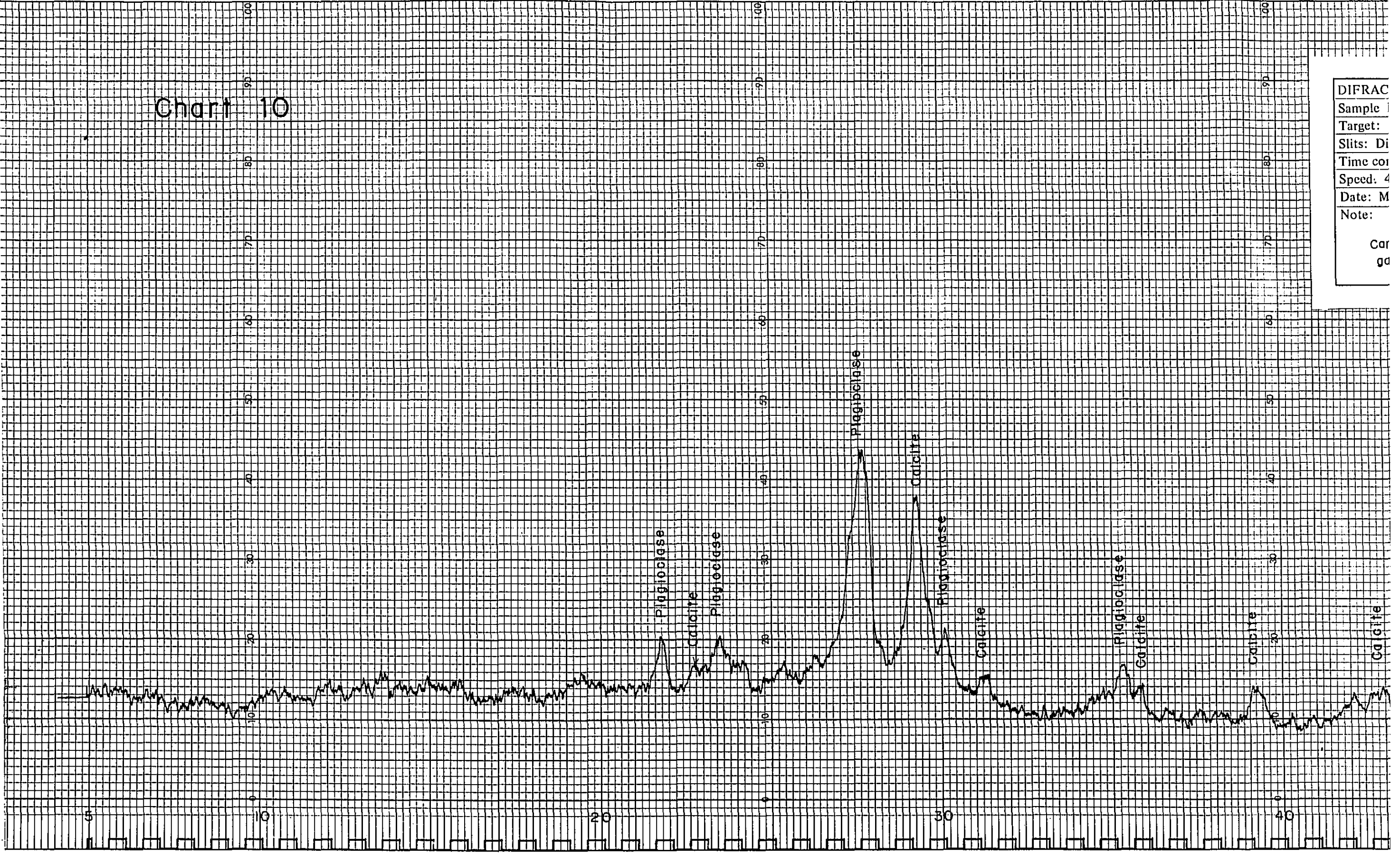


Chart 10

DIFRAC
Sample
Target:
Slits: Di
Time cor
Speed: 4
Date: M
Note:
Car
gd



DIFRACTOMETER (SHIMAZU-VD-1)	
Sample No. 368	
Target: Cu. 30Kv. 15mA Filter: Ni	
Slits: Div. 1.0mm. Rec.1.0mm. Scat. 0.5mm	
Time const: 2 sec. Full scale: 500 cps	
Speed: 4°-4cm/min. 1°/cm	
Date: March 1974	
Note: DDH-5 178.8m	
Carbonate veinlets in altered gabbroic rock	

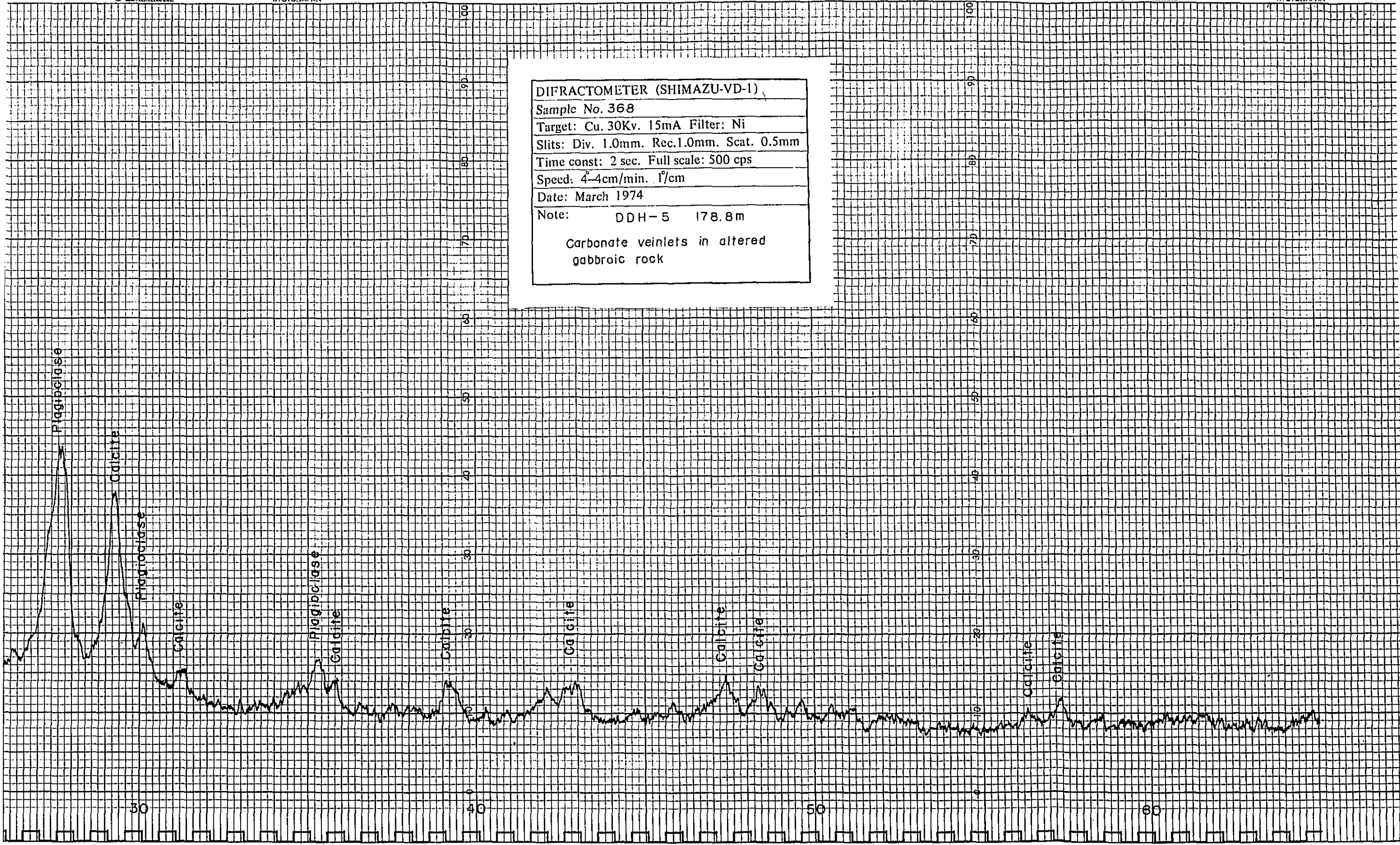
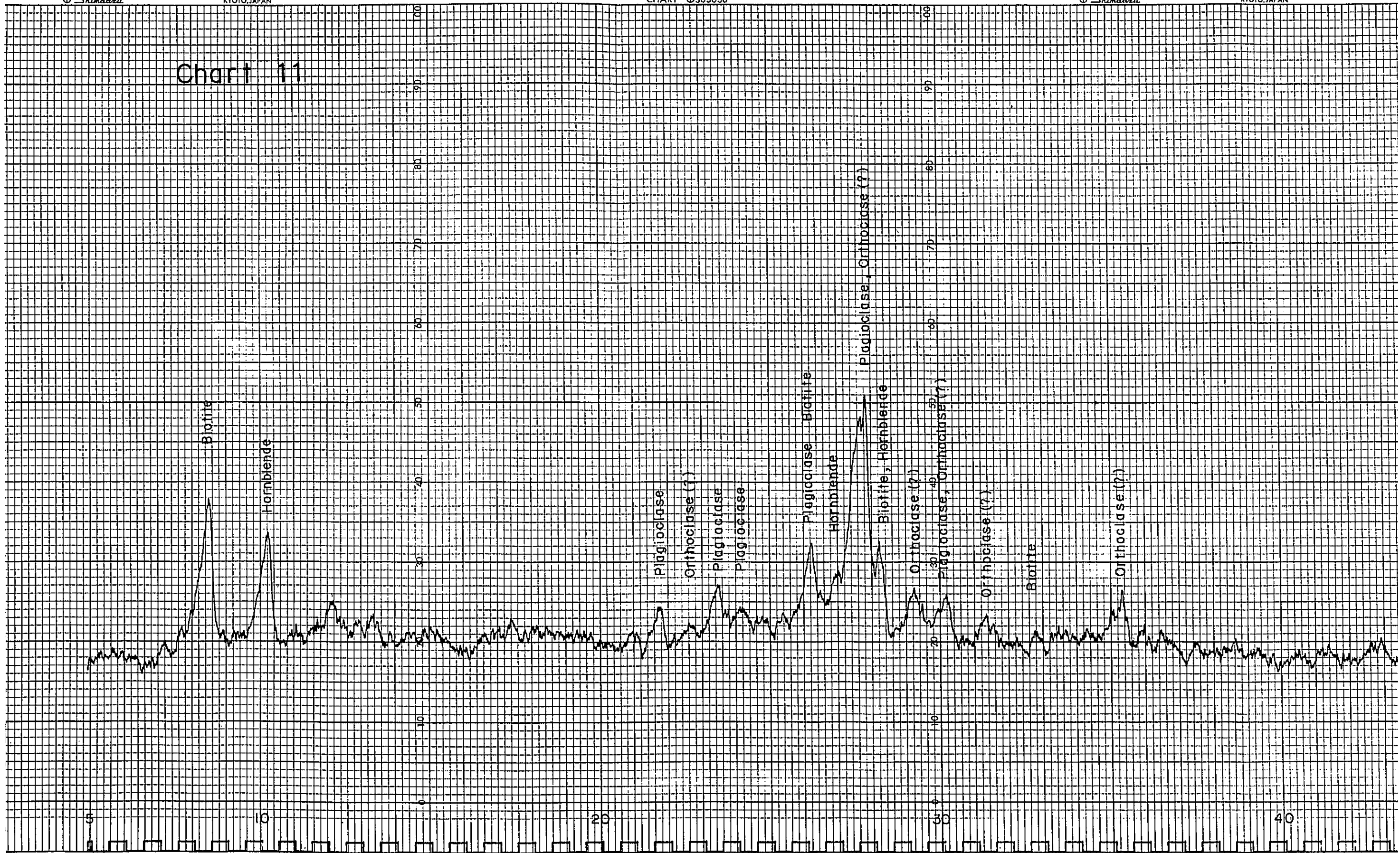


Chart 11



DIFRACTOMETER (SHIMAZU-VD-1)	
Sample No. 375	
Target: Cu. 30Kv. 15mA Filter: Ni	
Slits: Div. 1.0mm. Rec.1.0mm. Scat. 0.5mm	
Time const: 2 sec. Full scale: 500 cps	
Speed: 4°-4cm/min. 1°/cm	
Date: March 1974	
Note:	DDH - 6 80.0m
	Altered gabbro

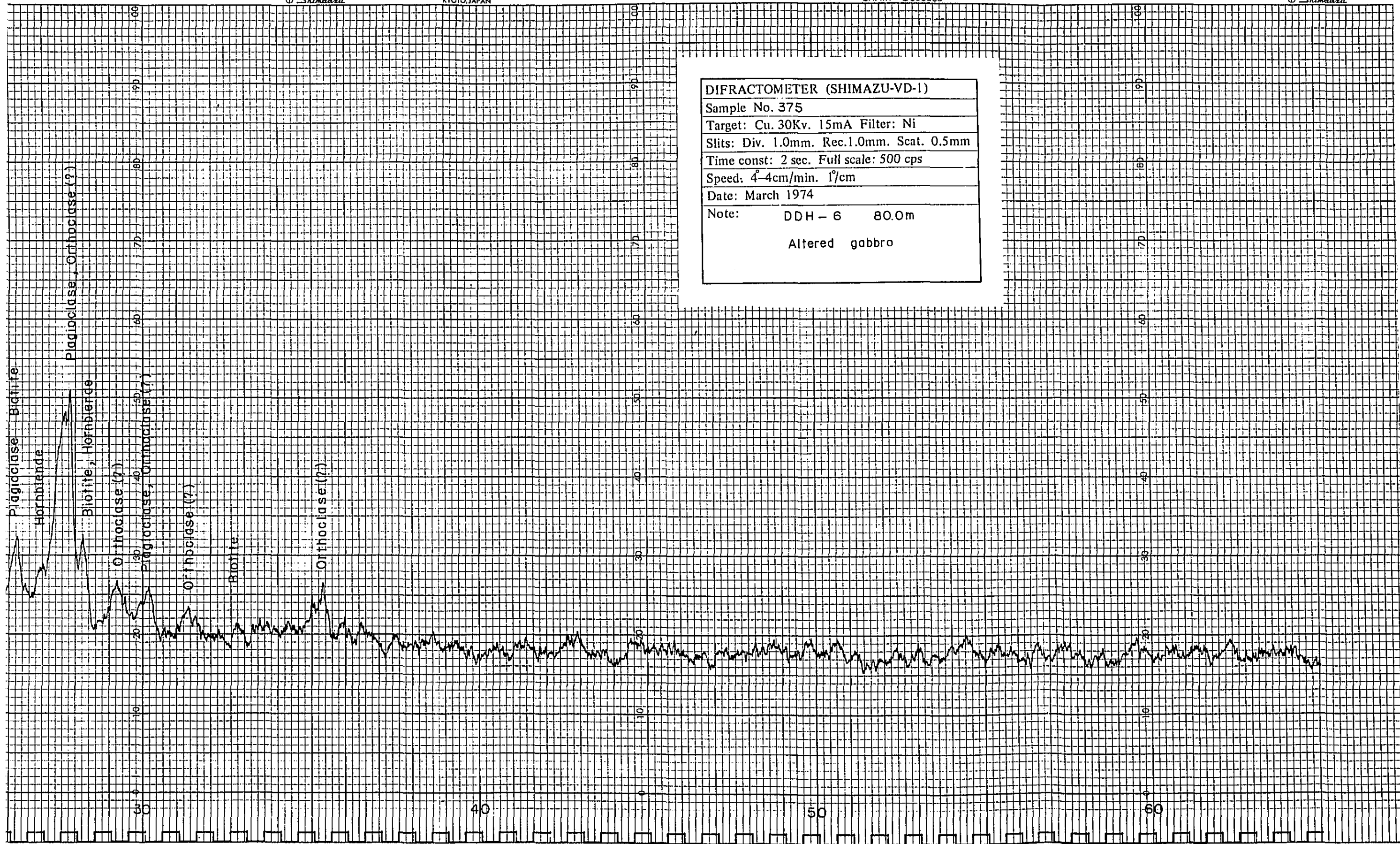
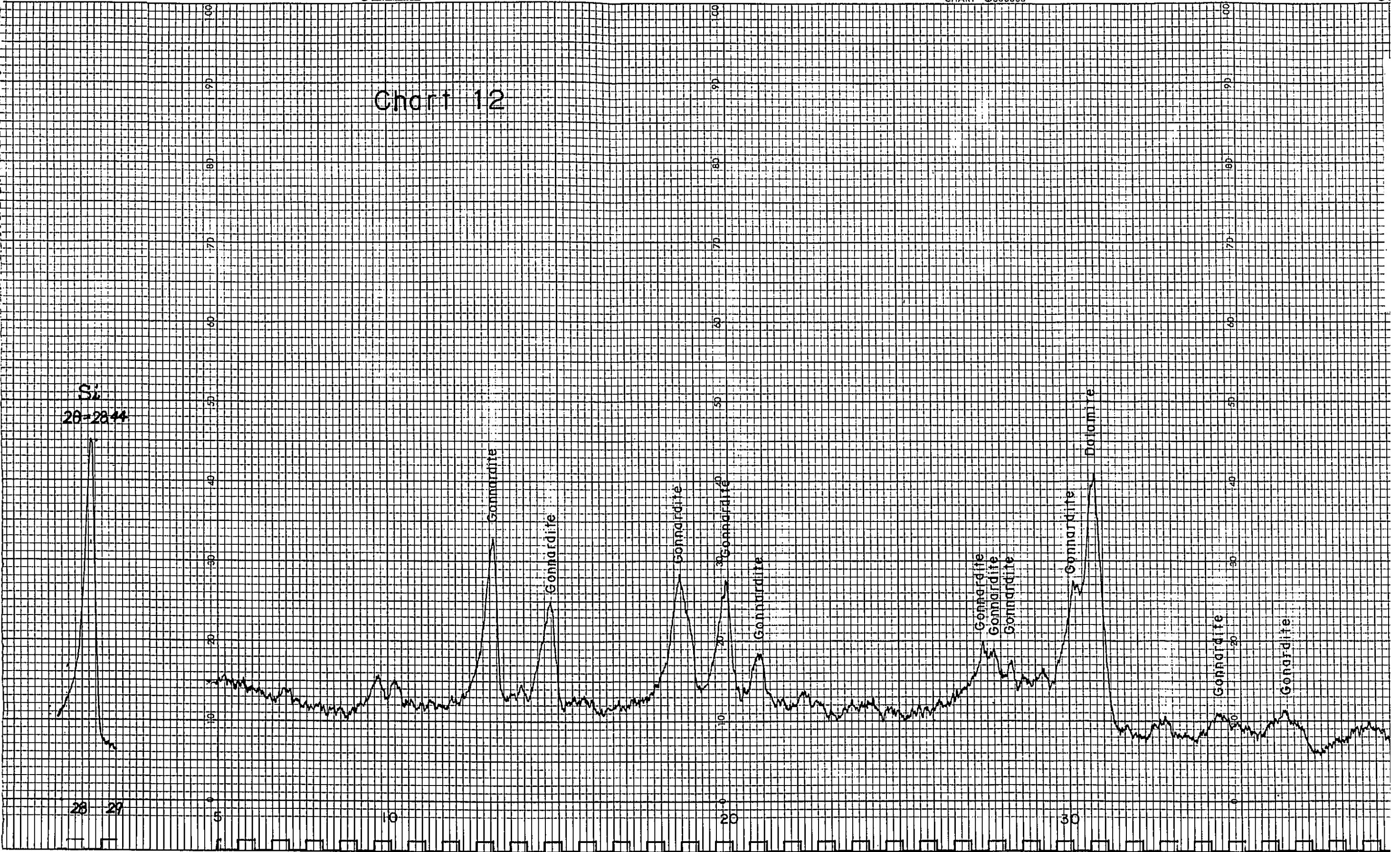
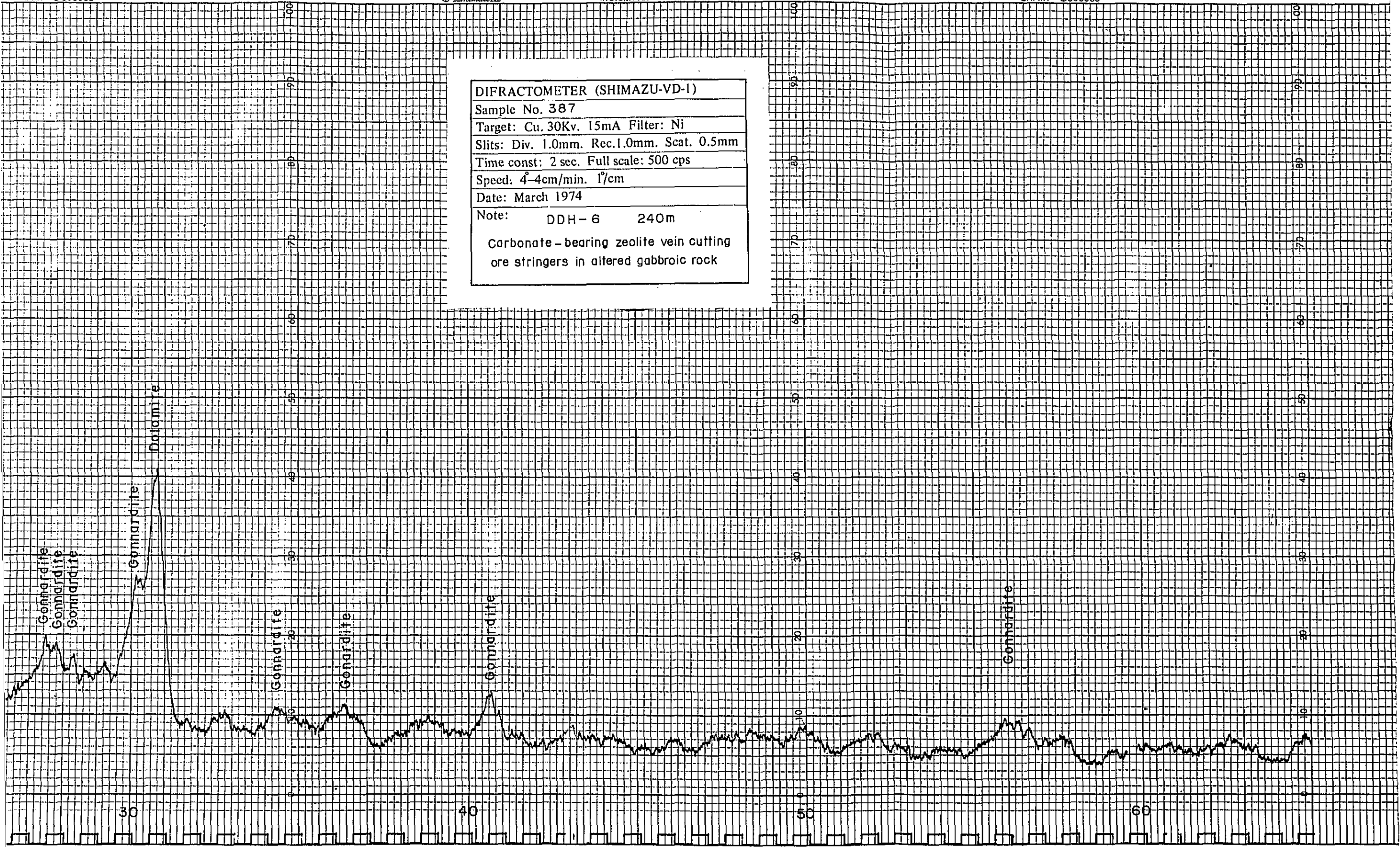


Chart 12

Si
28-2844



DIFRACTOMETER (SHIMAZU-VD-1)
 Sample No. 387
 Target: Cu, 30Kv, 15mA Filter: Ni
 Slits: Div. 1.0mm. Rec.1.0mm. Scat. 0.5mm
 Time const: 2 sec. Full scale: 500 cps
 Speed: 4-4cm/min. 1°/cm
 Date: March 1974
 Note: DDH-6 240m
 Carbonate-bearing zeolite vein cutting
 ore stringers in altered gabbroic rock



**APPENDICES
(DRILLING DATA)**

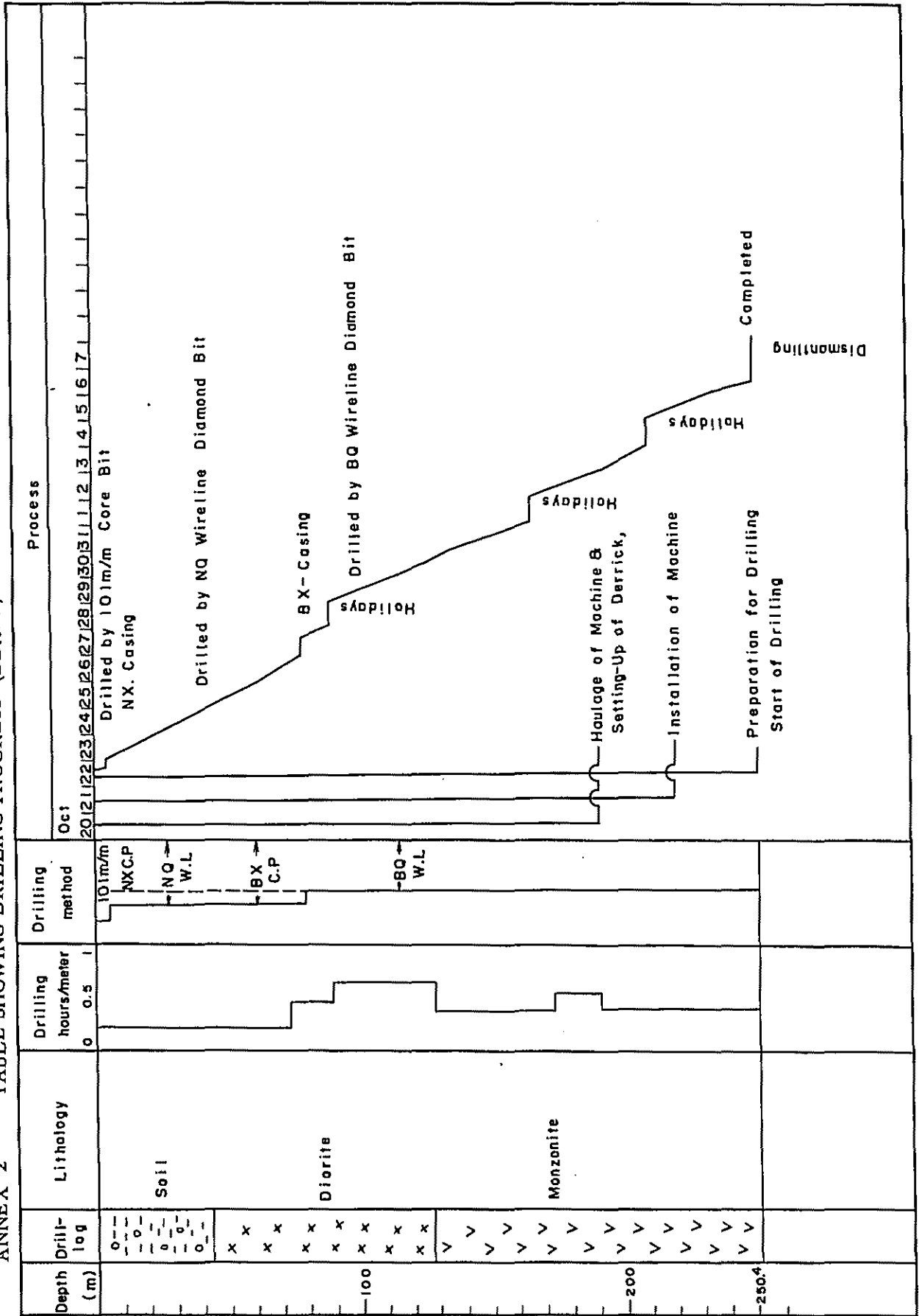
ANNEX 1

SPECIFICATIONS DIAMOND BITS REAMING SHELLS

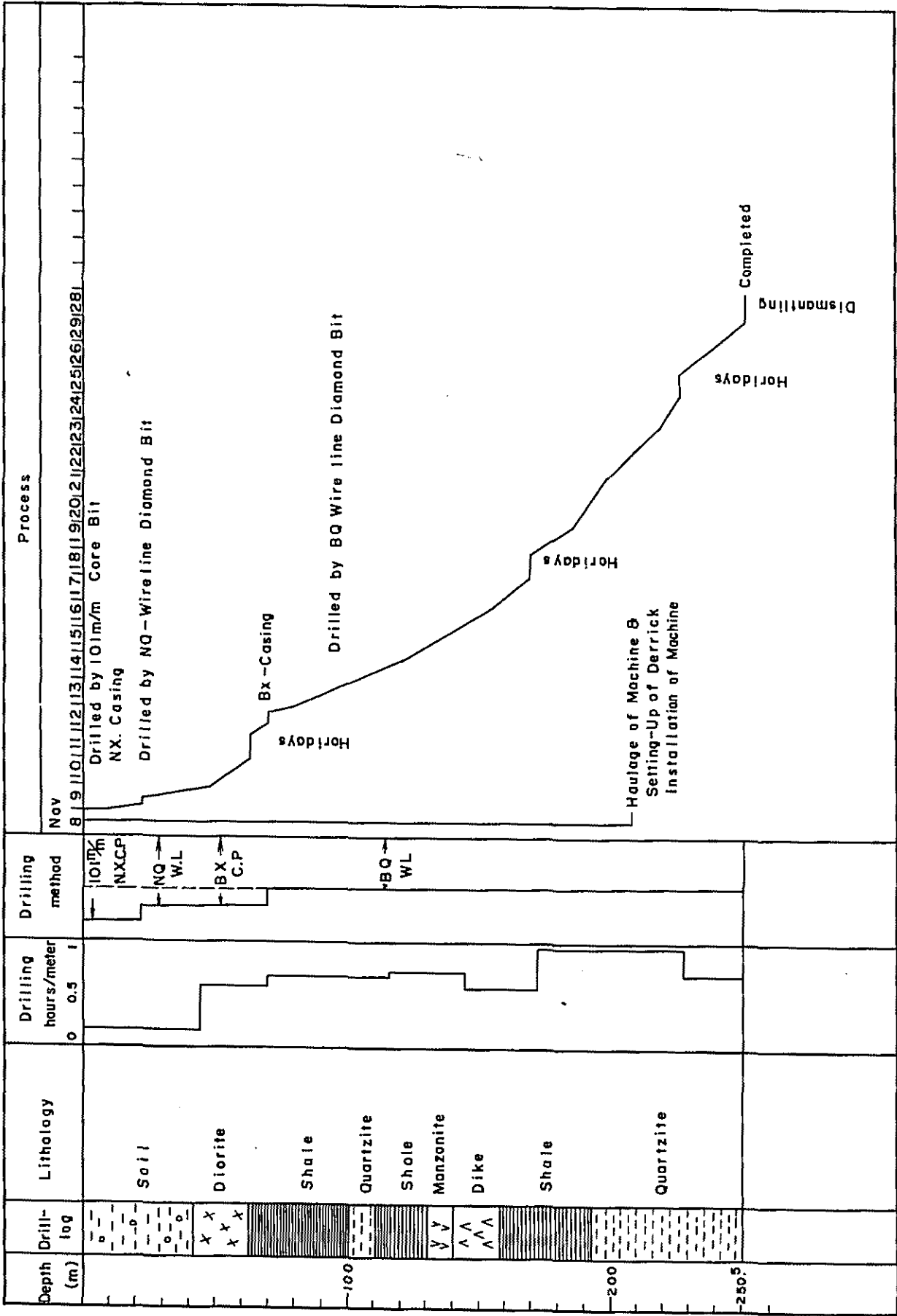
ITEM	SIZE	TYPE	No.	DRILL HOLES						TOTAL
				DDH-1	DDH-2	DDH-3	DDH-4	DDH-5	DDH-6	
Metal Bit	101 m/m		10	4.50 ^m						4.50 ^m
	"		11			6.30				6.30
	"		12		22.50					22.50
	"		16				6.00			6.00
	"		20					7.50		7.50
	"		30						6.50	6.50
Diamond Bit	NX-WL	NQ-WL	585						31.20	31.20
	"	"	592					54.30	0.70	55.00
	"	"	651						58.60	58.60
	"	"	710						42.20	42.20
	"	"	711						23.80	23.80
	"	"	5265			42.50				42.50
	"	"	5266			58.20		2.90		61.10
	"	"	5267	45.50						45.50
	"	"	5269					40.30		40.30
	"	"	5271				39.50			39.50
	"	"	5272				1.20			1.20
	"	"	5273		47.50					47.50
	"	"	5294	4.00			32.30			36.30
	"	"	6268	24.00						24.00
	BX-WL	BQ-WL	606					59.10		59.10
	"	"	609		5.10					5.10
	"	"	610					37.50		37.50
	"	"	618					27.60		27.60
	"	"	620					21.90		21.90
	"	"	1920		8.40					8.40
	"	"	2227		2.00					2.00
	"	"	2228		0.70					0.70
	"	"	2254		6.90					6.90
	"	"	2580		2.60					2.60
	"	"	3278	21.60	8.20					29.80
	"	"	3450					27.60		27.60
	"	"	3451					60.50		60.50
	"	"	5500		2.30					2.30
	"	"	5503	38.25						38.25
	"	"	5505	36.70						36.70
	"	"	5507		28.60					28.60
	"	"	5508		2.00					2.00
	"	"	5510				47.00			47.00
	"	"	5512		11.30					11.30
	"	"	5513	13.75						13.75
	"	"	5514		0.50	111.60				112.10
	"	"	5515		17.00					17.00

ITEM	SIZE	TYPE	No.	DRILL HOLES						TOTAL
				DDH-1	DDH-2	DDH-3	DDH-4	DDH-5	DDH-6	
Diamond Bit	BX-WL	BQ-WL	5516		3.20					3.20
"	"	"	5517				43.90			43.90
"	"	"	5518		26.70					26.70
"	"	"	5520		17.90					17.90
"	"	"	5275		15.50					15.50
"	"	"	5277		2.20					2.20
"	"	"	5279				44.40			44.40
"	"	"	5283	62.10						62.10
"	"	"	5284		6.20					6.20
"	"	"	5285			31.60				31.60
"	"	"	5286		13.20		36.00			49.20
	Total		(M6) 54	250.40	250.50	250.20	250.30	251.10	251.10	1503.60
Metal Reamer			14	4.50	22.50					27.00
			15			6.30	6.00			12.30
			25					7.50		7.50
			28						6.50	6.50
Diamond Reamer	NX-WL	NQ	260	73.50						73.50
"	"	"	331					90.50		90.50
"	"	"	410					66.00		66.00
"	"	"	1331					97.50		97.50
"	"	"	5261			100.70	73.00			173.70
"	"	"	5262		47.50					47.50
	BX-WL	BQ	502	172.40						172.40
"	"	"	508					88.10		88.10
"	"	"	5288		180.50	143.20				323.70
"	"	"	6600				171.30			171.30
"	"	"	6601					131.70		131.70
"	"	"	6625					14.40		14.40
	Total		(M4) 16	250.40	250.50	250.20	250.30	251.10	251.10	1503.60

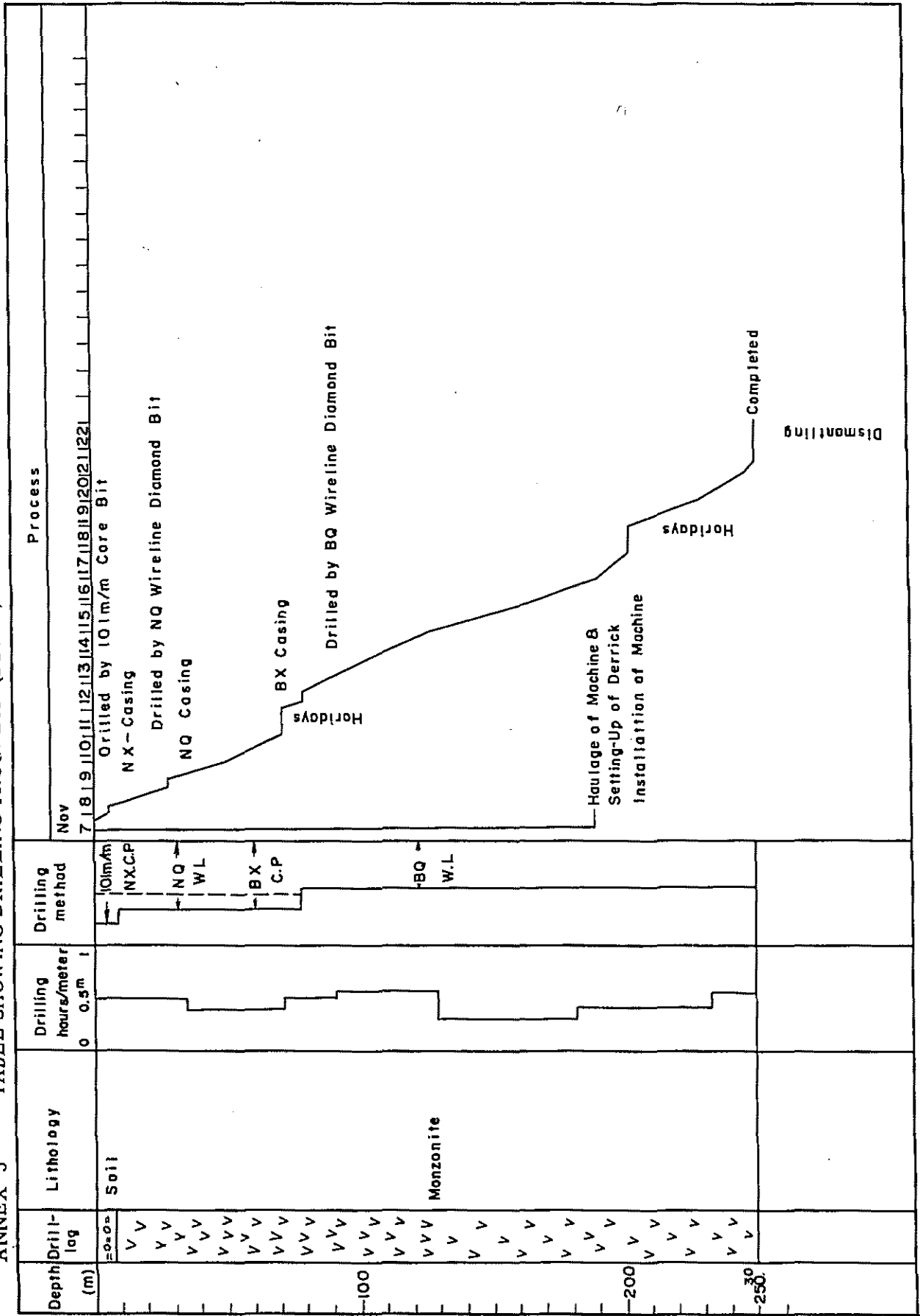
ANNEX 2 TABLE SHOWING DRILLING PROGRESS (DDH-1)



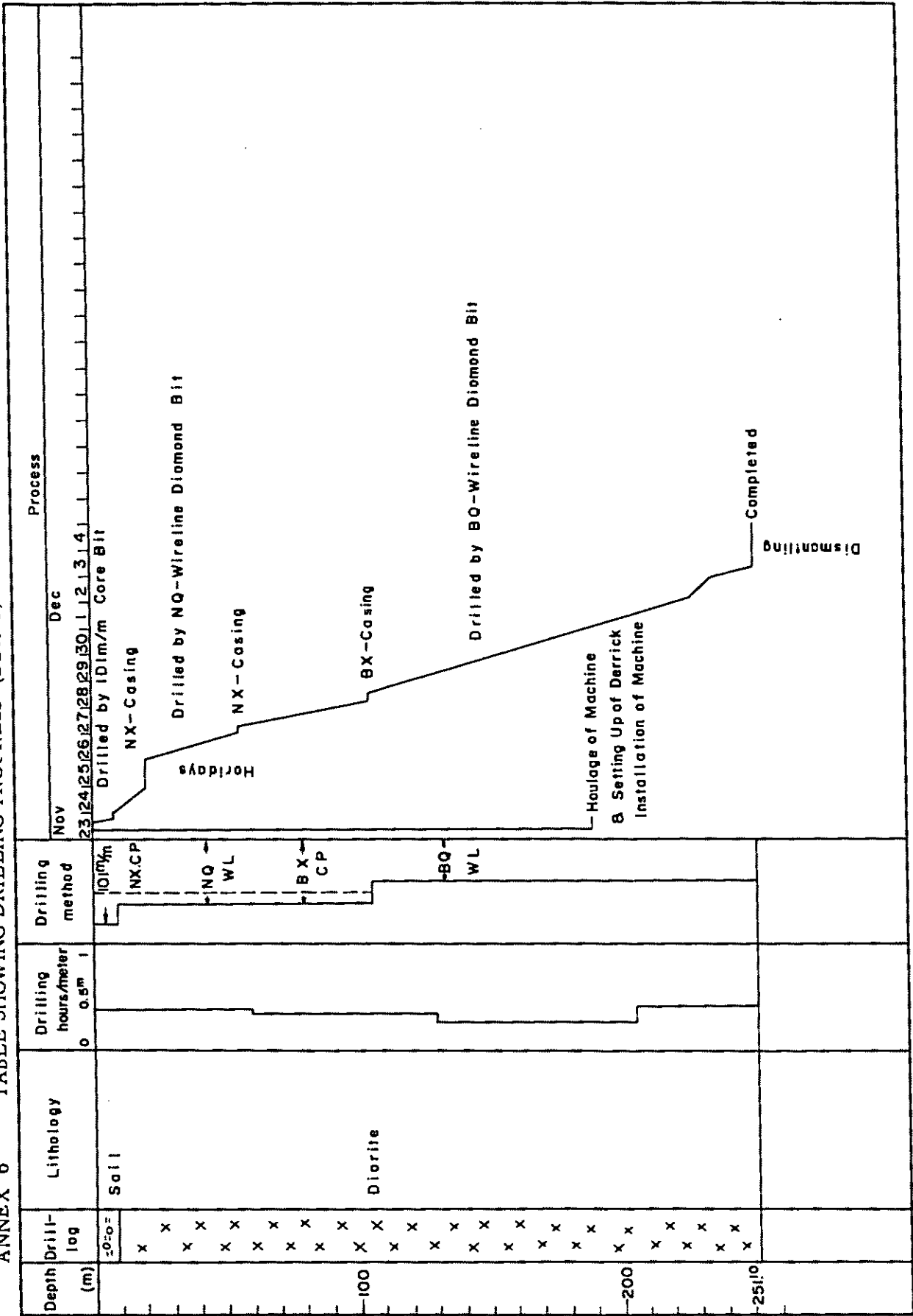
ANNEX 3 TABLE SHOWING DRILLING PROGRESS (DDH-2)



ANNEX 5 TABLE SHOWING DRILLING PROGRESS (DDH-4)



ANNEX 6 TABLE SHOWING DRILLING PROCESS (DDH-5)



ANNEX 7 TABLE SHOWING DRILLING PROGRESS (DDH-6)

